UNIVERSITY OF LONDON THESIS

Degree PhD Year 2007 Name of Author WORTHAM, Noel Christopher

Functional Genetics of Hereditary and Sporadic Uterine Leiomyomas

Noel Christopher Wortham

A thesis submitted for the degree of Doctor of Philosophy at the University of London

Supervisor: Prof Ian Tomlinson

Cancer Research UK

December 2006

ProQuest LLC
789 East Eisenhower Parkway
P.O. Box 1346
Ann Arbor, MI 48106-1346

Abstract

Uterine leiomyomas (fibroids) are common benign neoplasms arising from the smooth muscle layer of the uterus, the myometrium. Despite their prevalence in reproductive age women, little is understood of their pathobiology. The work in this thesis examined genetic and functional factors involved in the aetiology of sporadic leiomyomas, those in the hereditary leiomyomatosis and renal cell cancer syndrome, and leiomyomas from patients of African/Afro-Caribbean ethnicity, who develop more severe tumours at an earlier age. Work was carried out studying: the role of apoptosis in the tumours; mutations in the *FH* gene and mtDNA; and copy number change by microarray CGH.

The findings of this work demonstrated further differences between the pathobiology of HLRCC leiomyomas, compared to sporadic lesions, particularly with regard to the mechanisms of resistance to apoptosis of each tumour type. Furthermore, germline *FH* mutations, which cause HLRCC, were excluded as a major cause of overall uterine leiomyoma prevalence in both sporadic cases, and in African/Afro-Caribbean women.

A 1Mb resolution microarray CGH screen demonstrated a number of novel regions of copy number change, not previously reported, that may harbour novel genes involved in leiomyoma development. Furthermore, this study identified a minimal region of 7q deletion of 3.82Mb. Progressing from this, a tiling-path resolution CGH microarray specific for chromosome 7q was constructed and a number of tumours from different ethnicities were tested. This array narrowed the minimal region of deletion to ~273kb on 7q22.2, a region containing 2 genes, *SRPK2* and *MLL5*, either of which could

potentially be involved in uterine leiomyoma aetiology. The results from this array also demonstrated a common overlap in the pathobiology of uterine leiomyomas from Caucasian and African/Afro-Caribbean women, who demonstrated equal frequencies of 7q deletion.

Declaration

I, Noel Christopher Wortham, confirm that the work presented in this thesis is my own. Where information has been derived from other sources, I confirm that this has been indicated in the thesis.

Dedication

To Naomi and Leah, I love you.

Acknowledgements

It has been a privilege to work alongside a fantastic group of people in the MPG lab in the past four years. But in particular I want to thank my supervisor, Ian Tomlinson, for his support and ideas. I am also indebted to those who have patiently taught me, in particular Andrew Rowan who has been a continual source of advice, and also Pat Gorman, Angela Jones, Rebecca Roylance, Kimberley Howarth, Emma Jaeger and Paddy Pollard for advice in different techniques. And also to Zoe Kemp, Sarah Spain and Luis Carvajal, the inhabitants of Corgi corner for their great friendship. I am grateful to all my collaborators: Zephne van der Spuy, Jacquie Greenberg, Mona El-Bahwary, Cordelia Langford, Oliver Dovey, Sakari Vanharanta, Bart Wagner; without whom so much of this work could not have progressed. And also to the histopathology group, particularly George Elia, and the equipment park at CRUK.

I'm also very grateful to my new colleagues in Dundee. In particular my new boss, Frances Fuller-Pace, and my lab mates, Hayley Moore and Sam Nicol, for their patience and support during the final stages of writing.

My family and friends, both at work and outside, have been such an amazing source of support throughout the past 4 years, and they've kept me going when I've hit slumps, and rejoiced when things have been flying.

Finally, I want to thank the One, without whom the intricacies of the cell and the joy of discovery would be meaningless.

Abbreviations used in this thesis

ATP	Adenosine triphosphate
BAC	Bacterial artificial chromosome
Bak	Bcl-2 antagonist/killer 1
Bax	Bcl-2 associated x-protein
Bcl-2	B-cell lymphoma protein 2
BHD	Birt-Hogg-Dube
BMI	Body mass index
BNIP3	Bcl-2/adenovirus E1B 19kDa interactin protein 3
CCD	Charge-coupled device
cDNA	Complementary DNA
CGH	Comparative genomic hybridisation
cIAP2	Cellular inhibitor of apoptosis 2
CNP	Copy number polymorphism
COL4A5	Alpha 5 type IV collagen
COL4A6	Alpha 6 type IV collagen
COMT	Catechol-O-methyltransferase
CUTL1	Cut-like homologue 1
Cy3	Cyanine-3
Cy5	Cyanine-5
CYP17	Cytochrome p450c17 alpha
D-loop	Displacement loop of mt-DNA
DMSO	Dimethyl-sulphoxide
DNA	Dexoxyribose nucleic acid
DOP-PCR	Degenerate oligonucleotide primer polymerase chain reaction

ECM	Extracellular matrix
E. coli	Escherichia coli
EDTA	Ethylene-diamine-tetraacetic acid
EGF	Epidermal growth factor
EGFR	Epidermal growth factor receptor
ERα	Estrogen receptor alpha
FBI	Federal Bureau of Investigation
FH	Fumarate hydratase
FISH	Fluorescence in situhybridisation
FSH	Follicle stimulating hormone
FumC	E. coli Fumarase C
GC content	Guanine and cytosine content
GnRH	Gonadotropin releasing hormone
HIF-1α	Hypoxia-inducible factor 1a
HLRCC	Hereditary leiomyomatosis and renal cell cancer
HMG	High mobility group
HPGL	Hereditary paragangliomatosis
H-strand	Purine-rich heavy strand of mtDNA
HVS	Hypervariable segment of mtDNA
IAP	Inhibitor of apoptosis
IGF-I	Insulin-like growth factor 1
IQR	Interquartile range
KRAS2	Kirsten ras 2
LINE	Long interspersed nuclear element
LH	Lutenising hormone

LOH	Loss of heterozygosity
Lowess	Locally weighted scatterplot smoothing
L-strand	Pyrimidine-rich light strand of mtDNA
LTR	Long terminal repeat
MAPH	Multiplex amplifiable probe hybridisation
MAPK	Mitogen-activated protein kinase
MCUL	Multiple cutaneous and uterine leiomyomatosis
MEN	Multiple endocrine neoplasia
MLL5	Mixed Leukaemia Lineage 5
MLPA	Multiplex ligation dependent probe amplification
mRNA	Messenger RNA
mtDNA	Mitochondrial DNA
mTOR	Mammalian target of rapamycin
NBF	Neutral buffered formalin
nDNA	Nuclear DNA
ORC5L	Origin recognition complex subunit 5
p	petit (short) chromosome arm, eg 1p"
P4H	Prolyl-4-hydroxylase
PBS	Phosphate buffered saline
PCNA	Proliferating cell nuclear antigen
PCOLCE	Procollagen C endopeptidase enhancer
PCR	Polymerase chain reaction
PDGF	Platelet-derived growth factor
PI3K	Phosphatidyl-inositol 3 kinase
PR	Progesterone receptor

PTEN	Phosphatase and tensin homologue
q	queue (long) arm of chromosome, eg 7q"
RCC	Renal cell carcinoma
rCRS	Revised Cambridge reference sequence
RFLP	Restriction fragment length polymorphism
ROS	Reactive oxygen species
rRNA	Ribosomal RNA
SDH	Succinate Dehydrogenase
SDS	Sodium Dodecyl Sulphate
SINE	Short interspersed nuclear element
SNP	Single nucleotide polymorphism
S-phase	DNA replication phase of the cell cycle
SRPK2	Serine Arginine protein kinase 2
SSCP	Single-stranded conformational polymorphism
TE	Tris-EDTA buffer
TGFß	Transforming growth factor β
TNFα	Tumour necrosis factor α
TP53	Tumour protein p53
tRNA	Transfer RNA
TSC2	Tuberous scelorsis complex 2
UTR	Untranslated region
UV	Ultraviolet light
VEGF	Vascular endothelial growth factor
VHL	von-Hippel Lindau protein
WHO	World Health Organisation

Units of measurement

°C	Degrees celcius
RT	Room temperature - approximately 23 degrees C
g	grams
mg	milligrams (10^{-3} g)
µg	micrograms (10^{-6} g)
ng	nanograms (10^{-9} g)
M	molar (1 mole/litre)
mM	millimolar (10^{-3} M)
µM	micromolar (10^{-6} M)
nM	nanomolar (10^{-9} M)
mm	millimetres (10^{-3} metres)
µm	micrometres (10^{-6} metres)
nm	nanometres (10^{-9} metres)
mins	minutes
rpm	revolutions per minute
g	1x earth's gravitational pull
bp	base pairs of DNA
kb	"kilo base pairs (1,000 bp)"
Mb	"Mega base pairs (1,000,000 bp)"
µm2	square micrometre
ml	millilitre (10^{-3} l)
µl	microlitre (10^{-6} litres)
IQR	Interquartile range

Amino acid code

A	Ala	Alanine	M	Met	Methionine
C	Cys	Cysteine	N	Asn	Asparagine
D	Asp	Aspartic acid	P	Pro	Proline
E	Glu	Glutamic acid	Q	Gln	Glutamine
F	Phe	Phenylalanine	R	Arg	Arginine
G	Gly	Glycine	S	Ser	Serine
H	His	Histidine	T	Thr	Threonine
I	Ile	Isoleucine	V	Val	Valine
K	Lys	Lysine	W	Trp	Tryptophan
L	Leu	Leucine	Y	Tyr	Tyrosine
			X	Stp	Stop codon

DNA alphabet

A	Adenine	M	A or C (aMino)
C	Cytidine	S	G or C (Strong – 3H-bonds)
G	Guanosine	W	A or T (Weak – 2H-bonds)
T	Thymidine	B	C, G or T (not A)
U	Uracil	D	A, G or T (not C)
R	A or G (puRine)	H	A, C or T (not G)
Y	C or T (pYrimidine)	V	A, C or G (not T)
K	G or T (Keto)	N	A, C, G or T (aNy)

Table of Contents

Table of Figures

Table of Tables

Chapter 1

Introduction – Uterine leiomyomata

1.1 Uterine leiomyomas

Uterine leiomyomas (WHO International Classification of Diseases, Tenth Revision, Code D25), more commonly known as fibroids, are benign tumours arising from the smooth muscle layer of the uterus, the myometrium. They are frequently occurring tumours in women of reproductive age characterised by myometrial smooth muscle cell proliferation, and fibrosis (Walker and Stewart 2005) .

1.1.1 Location and nomenclature

Uterine leiomyomas can occur throughout the myometrium, and are classified depending on their locality within the uterus. The most common form is the intramural form, where the tumour occurs within the wall of the uterus (Stewart 2001b). As the tumour grows, it may extend into the abdominal cavity, where it would then be classified as subserosal, or into the uterine cavity, where it would be classified as submucosal. Leiomyomas of the uterine cervix can also occur, but are uncommon (Wilkinson and Rollason 2001)(**Figure 1.1**). Pedunculated leiomyomas, where the tumour grows out from the myometrium, forming a polypoid structure, may also form from subserosal and submucosal leiomyomas (Stewart 2001b).

The location of a uterine leiomyoma influences the type of symptoms that affect a patient. For example, submucosal leiomyomas, which intrude into the uterine cavity, are most likely to cause menorrhagia due to interference with the endometrial lining. Submucosal leiomyomas are also associated with increased infertility, again due to the interference with the endometrial lining. Finally, pelvic pressure caused by an irregularly shaped, bulky uterus, can

cause different symptoms depending on leiomyoma location. For example, anterior leiomyomas put pressure on the bladder, resulting in urinary symptoms, whereas posterior leiomyomas can put pressure on the colorectum, leading to constipation (Stewart 2001b).

While the histology of uterine leiomyomas from different locations appears similar, a number of molecular differences have been observed. These differences, which will be more thoroughly dealt with later on, are suggestive of a number of different pathways involved in leiomyoma tumorigenesis, and are also reflective of structural differences within the myometrium (Brosens et al. 1998).

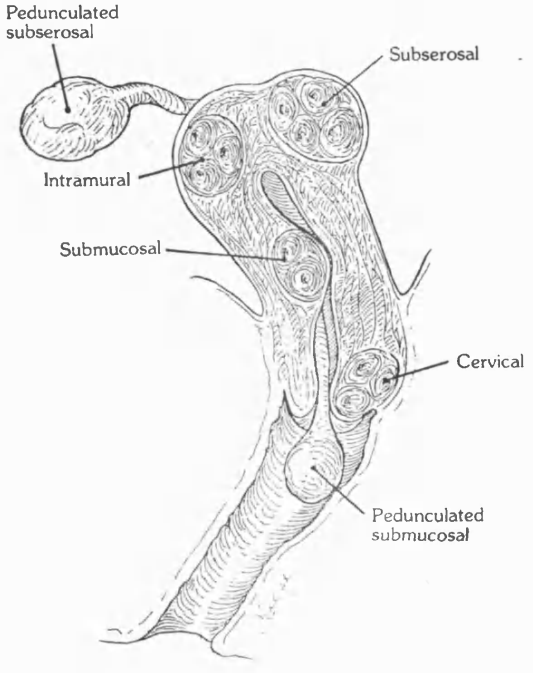

Figure 1.1 Classification of uterine leiomyomas depending on their position within the uterus (from (Brosens et al. 1998)).

1.1.2 Histology and ultrastructure

Grossly, uterine leiomyomas are firm, pale tumours. They are not encapsulated, but are well circumscribed by a pseudo-capsule of compressed smooth muscle (**Figure 1.2**a). They vary considerably in size. Symptomatic lesions can be as small as 10mm, but tumours greater than 20cm diameter are not uncommon (Walker and Stewart 2005). Leiomyomas consist of interlacing fascicles of uniform spindle cells. There is abundant eosinophilic fibrillar cytoplasm with blunt-ended, cigar-shaped nuclei of uniform size and little or no mitotic activity. The cells are embedded in an extensive, eosinophilic, collagen matrix (**Figure 1.2**b) (Stewart 2001b).

Other histological forms of uterine leiomyomas also exist (Wilkinson and Rollason 2001). These include: cellular leiomyomata, which are defined as being significantly more cellular than the myometrium, but retain the fascicular growth of usual leiomyomas (Wilkinson and Rollason 2001); bizarre leiomyoma, which contain multinucleated, monolobed or mononucleated giant cells with unusual smooth muscle differentiation (Wilkinson and Rollason 2001); and leiomyomblastoma, which contains immature smooth muscle cells that mimic foetal uterine myocytes (Watanabe et al. 2003).

Ultrastructural studies of uterine leiomyomas have demonstrated a number of features distinguishing the tumour cells from the myometrium. Common features of the tumour cells include: 6-7nm actin myofilaments present in the cytoplasm aligned with the cell axis; sparse rough endoplasmic reticulum; few mitochondria, with morphological aberrations including swelling; and clustering of organelles to the ends of the nucleus, which is itself

elongated along the long cell axis. The tumour cells are separated by variable-size masses of collagen, which have a diffuse and disorganised structure. An increase in the amount and aggregation of the intermediate filament protein desmin, has been observed in some leiomyoma cells (Eyden et al. 1992; Erlandson 1994; Richards et al. 1998; Eyden 2004).

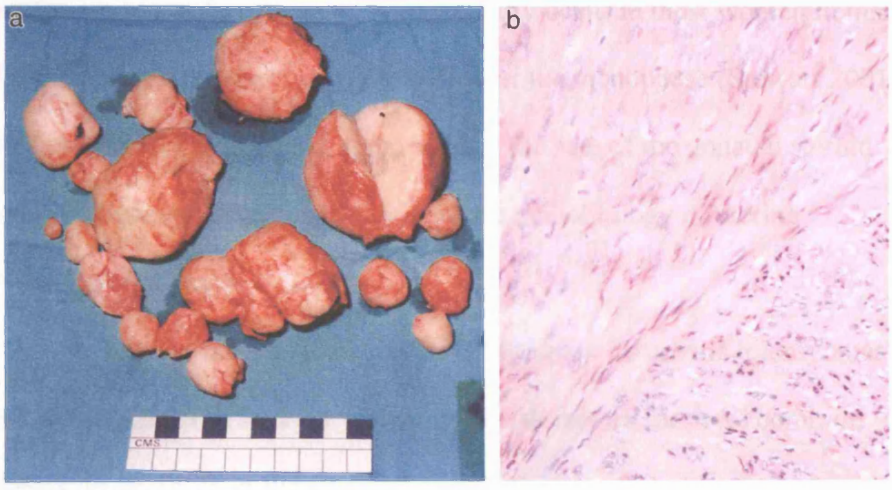

Figure 1.2 a) Uterine leiomyomas from a single patient following surgical removal. The tumours occur in a range of sizes, and are removed from a variety of locations within the uterus. b) Haematoxylin and eosin stained section of a uterine leiomyoma (Original magnification, 400x). The leiomyoma cells can be seen running longitudinally and transversely in the tumour. The nuclei are elongated and the cells sit in an extensive collagen extracellular matrix.

1.1.3 Epidemiology

Uterine leiomyomas are very common tumours, occurring in approximately 30% of reproductive-age women (Buttram and Reiter 1981). One study of serial sections of uteri has suggested that up to 77% of women have one or more uterine leiomyomas, albeit a majority asymptomatically(Cramer and Patel 1990). In the United States, uterine leiomyomas account for more than 26% of 650,000 hysterectomies annually (Pokras and Hufnagel 1988). The epidemiology of the tumours parallels the life-cycle changes in reproductive endocrinology. They have not been described in pre-pubescent girls, and generally occur in most women in their 30's to 40's. The symptoms are relieved after the menopause (Stewart 2001b). This has lead to a widespread acceptance of the role of the gonadal steroid hormones oestrogen and progesterone in the pathobiology of uterine leiomyomas (Maruo et al. 2004).

Several epidemiological studies of women with uterine leiomyomas have been carried out in order to determine risk factors for these common tumours. From these studies, a number of both hormonal and non-hormonal factors have been suggested to be associated with an increased risk of developing leiomyomas. Hormonal factors affect a woman's exposure to gonadal steroid hormones. These factors include early menarche (Faerstein et al. 2001a) (Marshall et al. 1998), increased menstrual cycle length (>30 days) (Chen et al. 2001), prolonged menstrual bleeding (>6 days) (Chen et al. 2001), and nulliparity (although this may be as a result of uterine leiomyoma-induced infertility) (Marshall et al. 1998; Chen et al. 2001).

The role of oral contraceptives has also been explored. Initially conflicting results were published, with some groups claiming an increase in leiomyoma prevalence (Samadi et al. 1996), and others claiming a decrease (Ross et al. 1986b). Subsequent stratification of the results discovered an increase in leiomyoma growth in women exposed to oral contraceptives between the ages of 13 and 16 (Marshall et al. 1998), and a decrease in prevalence in women exposed to oral contraceptives later on (Marshall et al. 1998). Conflicting results have also been obtained in studies examining the effects of increased body mass index (BMI), but it is generally thought that increased BMI leads to an increased risk of uterine leiomyomas (Ross et al. 1986b) due to increased oestrogen production by adipose tissue (Glass 1989). Smoking has also been shown to reduce the risk of uterine leiomyomas, which may be due to a smoking-associated lowering of endogenous estrogens (MacMahon et al. 1982).

In addition to these hormonal factors, a number of non-hormonal risk factors have also been identified. These include: any history of hypertension, particularly when requiring medication; pelvic inflammatory disease; *Chlamydia trachomatis* infection; and infectious complications resulting from the use of an intrauterine contraceptive device (Faerstein et al. 2001b).

Genetic factors also been shown to play a role in uterine leiomyoma pathogenesis. Despite the high prevalence of these tumours in reproductive age women, a number of studies have confirmed familial susceptibility. Familial clustering has been well documented and it is accepted that female relatives of a patient with uterine leiomyomas are at an increased risk (Gross and Morton 2001). Furthermore, retrospective twin studies using hysterectomy

data have shown that monozygotic twins have twice the twin-pair correlation for hysterectomy than dizygotic twins. While the data only examined the frequency of hysterectomies, the fact that uterine leiomyomas are the leading cause for hysterectomy was used to associate this with increased twin-pair correlation with familial effects of uterine leiomyomas (Treloar et al. 1992).

A number of Mendelian genetic syndromes have also been identified, in which uterine leiomyomas are a part of the tumour spectrum. These include hereditary leiomyomatosis and renal cell carcinoma (HLRCC) (Launonen et al. 2001), multiple endocrine neoplasia (MEN) (McKeeby et al. 2001) and Alport syndrome (Cochat et al. 1988). These will be discussed in greater depth later on.

Associations of fibroid prevalence with ethnicity have been observed. The most striking example occurs in patients of African or Afro-Caribbean ethnicity, who have been shown to develop uterine leiomyomas significantly more frequently, with greater multiplicity, at an earlier age of onset, and with an increased severity of disease, than Caucasian women or women of other ethnicities (Marshall et al. 1997). Prospective studies have demonstrated a three-fold greater frequency of leiomyomas in African and Afro-Caribbean women compared to white women (Kjerulff et al. 1993). A study by Marshall *et al* demonstrated that despite a higher prevalence of known risk factors in African and Afro-Caribbean women, these only accounted for a small proportion of the ethnicity-related differences in leiomyoma development (Marshall et al. 1997).

1.1.4 Treatment of uterine leiomyomas

A variety of treatments have been used for uterine leiomyoma patients. Surgical intervention is a common treatment and generally takes two forms: hysterectomy, the only genuinely curative treatment; and myomectomy, where individual leiomyomas are surgically removed and the uterus is left intact (Stewart and Nowak 1998). This latter treatment is preferential for younger patients who may still wish to have children. However, recurrence of the tumours is common following this latter procedure, with one study reporting a 10 year recurrence rate of 27% in a review of 622 patients (Candiani et al. 1991). Less invasive surgical techniques have also been used for patients with milder symptoms, including hysteroscopic resection for submucosal leiomyomas projecting into the uterine cavity (Brandner et al. 2000), and laparoscopic ("keyhole") myomectomy (Donnez et al. 1996).

A number of non-surgical treatments have also been used. The two major treatments are uterine artery embolization and Gonadotropin-releasing hormone (GnRH) analogue treatment. Both of these interventions are used prior to surgery to shrink tumours (Stewart 2001b). Uterine artery embolization involves blocking the blood supply to the tumour by injecting small particles which block the arteriole branches into the leiomyoma (Smith 2000). While the technique itself is modern, the principles of blocking the tumour blood supply to the tumour were described in 1906 in the textbook *Operative Gynaecology* in which the use of selective artery ligation was a complement to surgical myomectomy and hysterectomy (Kelly 1906).

GnRH analogues, such as leuprolide acetate and goserelin acetate, work by targeting the pituitary gland, which releases luteinising hormone (LH)

and follicle stimulating hormone (FSH), which are responsible for the release of oestrogen and progesterone from the ovaries. GnRH analogues work by constitutively binding to GnRH receptors in the pituitary gland. Initially this causes an increase in LH and FSH release, but chronic treatment results in receptor desensitisation, inducing a pseudomenopausal state characterised by decreased oestrogen and progesterone (Flake et al. 2003). This results in shrinkage of uterine leiomyomas. GnRH analogues have been used extensively in the study of the molecular pathways of leiomyoma pathogenesis, more of which will be discussed later.

1.2 Pathobiology of Uterine Leiomyomas

The epidemiology of uterine leiomyomas provides some clues as to their pathogenesis, particularly with respect to the reliance of tumorigenesis on the presence of the sex hormones oestrogen and progesterone (Gross and Morton 2001). However, beyond this, little is understood of the pathobiology of the tumours, and many questions, such as why do they occur so frequently, and how do the tumours arise in the first place, remain unanswered.

Further molecular clues to leiomyoma pathobiology have been identified through a vast number of molecular and genetic studies. However, despite the vast array of data, to date no complete picture of the mechanism of leiomyoma growth has emerged. Instead, diverse groups of involved cellular processes have been implicated.

It has been suggested that there are two distinct components to uterine leiomyoma development (Stewart 2001b): the transformation of normal myometrial smooth muscle cells into leiomyoma cells; and subsequent growth of these cells into clinically apparent tumours. The initial transformation is a common event, demonstrated by the high prevalence of microscopic leiomyomas (Cramer and Patel 1990; Kjerulff et al. 1993). Subsequent clonal expansion leads to the development of symptomatic leiomyomas (Stewart 2001a).

1.2.1 A genetic basis for uterine leiomyoma development

A number of studies have identified an inherited basis for uterine leiomyoma pathogenesis in some patients (Ligon and Morton 2001). Many of the key players have been identified through genetic studies, either of

inherited syndromes characterised by uterine leiomyomas, or through cytogenetic studies of somatic tumours.

1.2.1.1 Inherited uterine leiomyoma syndromes

As discussed above, strong evidence exists for inherited forms of uterine leiomyoma, starting from the observation of familial clustering (Gross and Morton 2001). Within the overall genetic contribution to uterine leiomyomas, several known inherited syndromes exist in humans and animals for which these tumours are a defined part of the clinical presentation. In a number of these syndromes, there is also associated renal disease, including cancers. This may reflect the fact that the uterus and kidneys both arise from the intermediate mesoderm (Strachan and Read 2004).

1.2.1.1.1 Hereditary Leiomyomatosis and Renal Cell Cancer

In 1958, Kloepfer and colleagues described a family with several members with cutaneous leiomyomas, benign tumours of the skin erector pili muscle, demonstrating autosomal dominant inheritance with incomplete penetrance (Kloepfer et al. 1958). These data were supported by the identification of other families with a similar condition (Rudner et al. 1964; Berendes et al. 1971). Reed and colleagues described a multiple uterine leiomyomas associated with the skin leiomyomas previously described (Walker and Reed 1972). Finally, Launonen *et al* described Finnish families with this condition and an increased risk of aggressive renal cancers of rare pathology (Launonen et al. 2001). The latter group named this condition Hereditary Leiomyomatosis and Renal Cell Cancer (HLRCC) .

A large study of a number of families with this condition lead to the discovery of linkage to chromosome 1q42.3-q43 (Alam et al. 2001), and the subsequent identification of germline inactivating mutations in the *FH* gene, encoding the Krebs' cycle enzyme fumarate hydratase (FH) (Tomlinson et al. 2002). Subsequent activity assays of patient lymphoblastoid cell lines confirmed a reduction in FH activity in heterozygous patients, implying that loss of the wild-type copy of the gene would result in a loss of FH activity in the cell, and cessation of the Krebs cycle (Alam et al. 2003).

1.2.1.1.1.1 Pathogenic effects of *FH* mutations

The role of *FH* as a tumour suppressor gene suggested an apparent paradox of loss of energy production resulting in tumour growth. Several theories were initially proposed as to how tumorigenesis could come about including: i) pseudo-hypoxic drive, where hypoxia related signalling pathways are activated by the cessation of oxidative metabolism; ii) defective apoptosis caused by altered mitochondrial function; iii) stress pathway activation; iv) increased mutagenesis by the accumulation of reactive oxygen species (ROSs); and v) anabolic drive, where cessation of the Krebs cycle leads to an accumulation of biosynthetic building blocks, such as amino acids, fooling the cell into thinking it is in a nutrient-rich state and inducing proliferation (Pollard et al. 2003; Pollard et al. 2005a). These mechanisms may not be mutually exclusive.

The first clues as to the tumorigenic mechanism of HLRCC came through the discovery of increased microvessel density in HLRCC leiomyomas, with increased expression of pro-angiogenic vascular endothelial growth factor, and decreased expression of anti-angiogenic thrombospondin.

The Bcl-2/adenovirus E1B 19kD protein interacting protein (BNIP3), which contains a hypoxia response element in its promoter, was also found to be upregulated in HLRCC leiomyomas (Pollard et al. 2005a). Thus, pseudo-hypoxia was beginning to emerge as a candidate mechanism.

Subsequent *in vitro* work by Selak *et al* demonstrated that accumulation of succinate, the metabolite immediately preceding fumarate in the Krebs cycle, resulted in the stabilisation of Hypoxia inducible factor 1α (HIF1α) through the direct product inhibition of the HIF prolyl-hydroxylase enzyme, which hydroxylates proline 402 or 564 of HIF1α, targeting it for ubiquitylation and degradation by the proteasome (Selak et al. 2005). This mechanism was confirmed *in vivo* by the demonstration of accumulation of succinate and increased expression of HIF1α in HLRCC tumours (Pollard et al. 2005c).

1.2.1.1.1.2 The Krebs cycle and tumorigenesis

HLRCC is not the only inherited tumour condition resulting from mutations in Krebs cycle enzymes. Hereditary paragangliomatosis and pheochromocytoma (HPGL), typified by carotid body tumours, is caused by mutations in 3 of the 4 genes encoding succinate dehydrogenase (SDH), the enzyme preceding FH in the Krebs cycle (Baysal et al. 2000). Mutations in this gene cause loss of enzyme activity and subsequent accumulation of succinate following loss of heterozygosity (Selak et al. 2005). The pathogenic mechanism of these tumours has been shown to be very similar to that of HLRCC (Pollard et al. 2005b).

1.2.1.1.2 Multiple Endocrine Neoplasia type 1

Multiple endocrine neoplasia type 1 (MEN1) is an autosomal dominant tumour syndrome resulting in multiple tumours in the parathyroid and anterior pituitary glands and the enteropancreatic endocrine tissues. MEN1 is caused by germline mutations in the *MEN1* gene on chromosome 11q13 (Chandrasekharappa et al. 1997). MEN1 patients have also been shown to develop multiple leiomyomas of the lungs, oesophagus and uterus (McKeeby et al. 2001).

The *MEN1* gene encodes the menin protein, which plays a role in transcriptional regulation. It has been shown to interact with the transcription factor JunD, and loss of menin antagonises transforming growth factor β (TGFβ) mediated cell growth inhibition (Kaji et al. 2001). As will be discussed later, the TGFβ pathway plays an important role in uterine leiomyoma pathogenesis, and menin may cause uterine leiomyomas through that pathway.

1.2.1.1.3 Alport syndrome

The Alport syndrome is an X-linked condition resulting in renal failure due to mutations in collagen IV that affect the structure of the glomerular basement membrane. Alport syndrome has also been associated with diffuse leiomyomatosis, particularly of the vulva and oesophagus (Cochat et al. 1988). Alport syndrome with diffuse leiomyomatosis arises due to a large germline deletion encompassing the *COL4A5* and *COL4A6* genes on Xq22, encoding two collagen type IV isoforms which form an integral part of the basement membrane. Alport syndrome without leiomyomatosis results from mutations

in the *COL4A5* gene only (Heidet et al. 1995). Therefore, it has been proposed that *COL4A6* plays a role in smooth muscle differentiation (Zhou et al. 1993).

1.2.1.2 Animal models of uterine leiomyomas

Several animal models of uterine leiomyomas have also been described. These have proved useful in functional studies of uterine leiomyomas, and the evaluation of novel therapies. Furthermore, the genes involved have provided new insights into uterine leiomyoma pathogenesis.

1.2.1.2.1 The Eker Rat

The Eker rat was a naturally arising model that was initially studied as one of the earliest autosomal dominant models of renal cancers (Eker et al. 1981). They were used by Knudson to confirm his two-hit hypothesis (Yeung et al. 1994). Further breeding and pathology studies demonstrated frequent development of uterine leiomyomas and splenic hamengiosarcomas (Howe et al. 1995). The mutation that resulted in this phenotype was found to be a retroviral insertion disrupting the rat tuberous sclerosis complex 2 (*Tsc2*) gene, and loss or disruption of the wild-type copy has been demonstrated in virtually all uterine leiomyomas in this model (Yeung et al. 1995). Expression of the *TSC2* gene product, Tuberin, has also been found to be decreased in human uterine leiomyomas (Wei et al. 2005). This gene is mutated in the human disease Tuberous Sclerosis, a hamartoma condition in which patients develop tuber-like growths on the brain and may also develop renal carcinoma and giant cell astrocytoma (Au et al. 1999).

Tumour samples and cells lines derived from Eker rat leiomyomas have been used as a model system analogous to human leiomyomas in a number of studies. The tumours have a similar steroid hormone response to human leiomyomas, and also appear to be affected by similar factors, such as the protective effect of pregnancy on tumour onset (Walker et al. 2003). In addition, a number of molecular similarities have been observed, in particular aberrant expression of the High Mobility Group protein HMGA2, which, as will be discussed later, is of importance in the pathobiology of human uterine leiomyomas (Walker et al. 2003).

1.2.1.2.2 Birt-Hogg-Dubé syndrome

Canine hereditary multifocal cystadenocarcinoma and nodular dermatofibrosis (RCND) is a naturally occurring inherited cancer syndrome first described in German Shepherd dogs. In addition to bilateral, multifocal kidney tumours, affected dogs also develop firm collagenous dermal nodules, and all affected females develop uterine leiomyomas (Jonasdottir et al. 2000). Linkage analysis identified a region on canine chromosome 5 which contained the orthologue to the human *BHD* gene, encoding the protein folliculin, mutations of which cause the human renal cancer syndrome Birt-Hogg-Dubé (Lingaas et al. 2003). In humans, this syndrome also results in hair follicle hamartomas and benign lung cysts (Nickerson et al. 2002).

A recent study demonstrated identified the folliculin interacting protein 1 (FNIP1) and an interaction with AMP-activated protein kinase (AMPK), a member of the mammalian target of rapamycin (mTOR) signalling pathway, which also involves the TSC2 protein that is mutated in the Eker rat (Baba et al. 2006). The mTOR pathway has also been shown to stimulate the

translation of HIF1α, and so the mechanisms in these animal models of uterine leiomyoma and HLRCC may converge (King et al. 2006).

1.2.1.3 Other inherited components in uterine leiomyoma pathogenesis

In addition to defined single-gene syndromes with high penetrance, familial clustering and ethnicity studies suggest that there are further genetic variants within the general population that increase the risk of developing uterine leiomyomas.

1.2.1.3.1 Prevalence of uterine leiomyomas in African/Afro-Caribbean women

The clearest association of any factor with increased prevalence of uterine leiomyomas has been shown to be African or Afro-Caribbean ethnicity (Marshall et al. 1997). Even after taking into account a high level of uterine leiomyoma risk factors, such as increased BMI, reproductive history and age of oral contraceptive use, ethnicity alone still imparted a relative risk of 3.25 for the development of uterine leiomyomas (Marshall et al. 1997). This increased prevalence on the basis of ethnicity implies that an underlying genetic element results in this increased susceptibility.

In the past few years, a number of association studies have attempted to elucidate the underlying genetic elements causing this ethnic prevalence. Several studies have focused on the oestrogen receptor α gene. Sadan *et al* examined the variation of oestrogen and progesterone receptor levels in myometrium and leiomyomas of Caucasian and Negroid patients. They found no difference in receptor content between leiomyomas from the two ethnic

groups, but they demonstrated decreased expression of both receptors in myometrium from the Negroid group (Sadan et al. 1988). However, a similar study by Amant *et al* failed to identify this change in expression (Amant et al. 2003).

More recently, intronic polymorphisms of the oestrogen receptor α (ERα) gene have been associated with increased prevalence of leiomyomas in African and Afro-Caribbean patients (Al-Hendy and Salama 2006b). They examined the distribution of a *PvuII* RFLP site within intron 1 close to the start of exon 2 of the ERα gene in 198 cases and 229 controls and determined that patients homozygous for an absence of this restriction site were 6.42 times more likely to develop uterine leiomyomas than patients of other genotypes (Confidence limits 2.04-20.16). This genotype, termed the PP genotype, was found to be more prevalent in African and Afro-Caribbean women (35%) than Caucasian (13%) or Hispanic (16%) women. Finally, they demonstrated that myometrial cells from women with the PP genotype exhibited greater proliferation in response to oestrogen stimulation than cells from other genotypes (Al-Hendy and Salama 2006b).

Other genetic loci have also been associated with uterine leiomyomas in African and Afro-Caribbean women. The Val138Met coding polymorphism in the gene encoding Catechol-O-Methyltransferase (COMT), an important enzyme in oestrogen biosynthesis, was investigated and patients homozygous for the Val allele were found to have a 2.5 fold increased risk of uterine leiomyomas through increased activity of the enzyme (Confidence limits 1.017-6.151). Again this genotype was more prevalent in African and Afro-Caribbean women (Al-Hendy and Salama 2006a).

Polymorphisms of the promoter of the p450c17α gene (CYP17), another oestrogen biosynthetic enzyme, have also been investigated as a possible important variant (Amant et al. 2004). This polymorphism is suspected to alter transcription of the gene, with the associated variant increasing expression. Results of this pilot study suggested that an association was present, and suggested the study be expanded to increase power.

1.2.1.3.2 Other genetic associations with uterine leiomyomas

Studies of genetic variants have also been carried out in women of other ethnicities in order to determine genetic factors that may increase susceptibility to uterine leiomyomas. In addition to its apparent role in ethnic determination of leiomyoma prevalence, the ERα gene has also been a target of association studies in other ethnic groups. A number of associations between polymorphisms of this gene and increased susceptibility to uterine leiomyomas have been described. For example, Hsieh *et al* identified an association between different lengths of a TA dinucleotide repeat upstream of the *ESR1* gene (encoding ERα), demonstrating an increased prevalence of leiomyomas with shorter repeat lengths (Hsieh et al. 2003; Hsieh et al. 2006). However, several studies have shown no association of the same alleles with uterine leiomyomas (Massart et al. 2001; Denschlag et al. 2006). The general functional effect of the reportedly disease-associated alleles of the ERα gene is to increase sensitivity of a cell to oestrogen signalling, be it through increased receptor expression, or a coding polymorphism that alters ligand binding affinity. This increased sensitivity has been shown for at least one of

these alleles *in* vitro (the PP allele, described above (Al-Hendy and Salama 2006b)).

Other allele associations have also been studied, including alleles of the CYP17 and COMT genes tested for ethnic association. Whereas associations of certain alleles of these had been identified in African and Afro-Caribbean patients, as described above (Amant et al. 2004; Al-Hendy and Salama 2006a), Denschlag *et al* identified no such association in either gene (Denschlag et al. 2006).

Polymorphisms have also been studied in p53, where one study identified associations of uterine leiomyomas with the proline variant of the Arg72Pro polymorphism (Denschlag et al. 2005), whereas a separate group failed to identify an association of the same polymorphism (Hsieh et al. 2004), but did identify an association with a promoter polymorphism of tumour necrosis factor α (Hsieh et al. 2004).

Many other such associations have been made in the literature, often with conflicting results. This may derive from the high frequency of uterine leiomyomas in the general population. Potentially, a large, genome-wide association study with careful selection of controls may provide a more valid insight into genetic elements increasing the risk of uterine leiomyomas.

1.2.1.4 Somatic Genetics of uterine leiomyomas

Uterine leiomyomas frequently arise sporadically, and have been determined to occur asymptomatically in as many as 70% of reproductive age women (Cramer and Patel 1990). Tumour clonality has been determined by analysis of the X-linked polymorphic loci of glucose-6-phosphate (Linder and

Gartler 1965) and the human androgen receptor (Fujimoto et al. 2000), which have both shown that uterine leiomyomas arise from a single cell or clone of cells. The somatic genetics of uterine leiomyomas have been extensively studied and both cytogenetic and sequence aberrations have been identified.

1.2.1.4.1 Cytogenetic aberrations

The most frequently described genetic changes in uterine leiomyomas are cytogenetic aberrations, where chromosomal structure is altered. Such changes have been observed in approximately 40% of studied tumours (Ligon and Morton 2001). A wide variety of changes have been observed, including: copy number changes, where regions of chromosomes are deleted or amplified; translocations, where two chromosomes break and are fused together; and other changes such as inversions or the presence of marker chromosomes (Ligon and Morton 2001).

While cytogenetic changes involving almost every chromosome have been reported, several relatively frequent, non-random changes have been extensively studied in order to provide clues to their role in leiomyoma pathogenesis. The most frequent of these changes are interstitial deletions of chromsome 7q, translocations between chromosomes 12 and 14, and rearrangements of 6p21 (Ligon and Morton 2001).

One study identified a difference in the frequency of chromosomal abnormalities in uterine leiomyomas depending on their location (Brosens et al. 1998). Submucosal leiomyomas had fewer abnormalities than subserosal and intramural leiomyomas. This difference could be explained by an apparent difference in hormonal regulation of submucosal leiomyomas. Higher levels of progesterone and oestrogen receptors have been reported in submucosal

leiomyomas (Marugo et al. 1989), and the embryonic development of oestrogen receptors in the subendometrial myometrium also differs from the rest of the myometrium (Glatstein and Yeh 1995). Submucosal leiomyomas are also more effectively treated by GnRH analogues (Donnez et al. 1989). Therefore, it was suggested that leiomyomas with cytogenetic aberrations exhibited loss of dependency on sex hormones for growth (Brosens et al. 1998), and the genes affected by these aberrations confer that growth independence.

1.2.1.4.1.1 The del(7q) group

Interstitial deletions of chromosome 7q, particularly involving bands q22-q32, are a frequently observed cytogenetic aberration in uterine leiomyomas, occurring in approximately 17% of karyotypically abnormal lesions (Xing et al. 1997). The high frequency and specificity of deletions in this region has lead to widespread speculation that a novel leiomyoma tumour suppressor gene is present there.

Observations of 7q deletions have frequently shown tumours to be mosaics, containing a number of karyotypically normal cells (Xing et al. 1997). Clonality studies have shown that all the cells in these mosaic tumours arose from the same cells (Xing et al. 1997). This has lead to speculation that deletions of 7q are a secondary event in leiomyoma pathogenesis, potentially an event that occurs as a later part of tumour progression (Xing et al. 1997).

7q deletions can occur as the sole abnormality, or in conjunction with other chromosomal changes. Leiomyomas with 7q deletions are smaller than those with other karyotypic abnormalities, such as t(12;14), and have been reported to be smaller than karyotypically normal leiomyomas (Rein et al.

1998). Furthermore, cultures of leiomyomas with del(7q) grow particularly poorly and frequently become enriched for karyotypically normal cells (Xing et al. 1997). The combination of decreased tumour size and poor *in vitro* growth has lead to speculation that a tumour suppressor gene on 7q22 may be involved in the regulation of cell growth, and deletion of this gene may inhibit cell growth (Xing et al. 1997). However, the possibility also exists that while deletion of this gene may inhibit cell growth, it may promote cell survival, although one study examining the effectiveness of GnRH analogue therapy on uterine leiomyomas with 7q LOH failed to find a protective effect (Takahashi et al. 2001a).

In addition to deletion, involvement of 7q22 has been reported in other cytogenetic abnormalities in leiomyomas, including inversions (Fan et al. 1990) and translocations (Sargent et al. 1994), thus implicating this band as the important region in these rearrangements. Uterine leiomyomas are the only solid tumour where 7q22 rearrangements occur consistently, although deletions are frequently observed in acute leukaemias (Flake et al. 2003) and translocations and deletions involving 7q22 have been described in other benign mesenchymal tumours, such as lipomas (Mandahl et al. 1988; Dal Cin et al. 1997).

The q22 band of chromosome 7 is a gene-dense region (Xing et al. 1997). A number of genes in the 7q22 band have been studied as candidate tumour suppressors. The Cut-like homeobox gene (*CUTL1*) was found to be deleted and to have reduced expression in del(7q22) leiomyomas (Zeng et al. 1997). This was an intriguing candidate since it encodes a transcriptional repressor that down-regulates the expression of the c-myc oncogene (Higgy et

al. 1997). However, a later study by the same authors identified overexpression of N-terminally truncated versions of CUTL1 in leiomyomas, and so concluded that it was unlikely to be the candidate tumour suppressor (Moon et al. 2002). Other genes have also been studied, including pro-collagen carboxy-terminal proteinase enhancer protein (*PCOLCE*), although no change in expression was identified (Ligon et al. 2002), and laminin B1 (*LAMB1*) (Saito et al. 2005). However, no strong candidate gene has been identified.

Other studies have attempted to minimise the region of deletion in order to identify the predicted tumour suppressor. One study used a combination of karyotyping and loss of heterozygosity (LOH) analysis to minimise the region (Ishwad et al. 1995). They reported a minimal region of deletion between the markers D7S518 and D7S471, a region of approximately 10Mb. A later study by the same group claimed to have further refined this region surrounding the marker D7S666 (Ishwad et al. 1997). However, the LOH map in this paper did not appear to support their conclusions, with LOH occurring in samples outside their minimum defined region in the samples used to define that region.

Another study also used LOH analysis to refine the deleted region to an approximately 1.5Mb region (van der Heijden et al. 1998), 4Mb distal from the region identified in the previous studies (Ishwad et al. 1997). A fluorescence *in situ* hybridisation (FISH) based study refined the region to approximately 11Mb (Vanni et al. 1999). More recently, Sell *et al* identified LOH at a single marker, D7S2446, giving a supposed minimal region of less than 500kb and containing 2 genes, Origin recognition complex subunit 5

(*ORC5L*) and Lipoma HMGIC fusion partner-like 3 (*LHFPL3*) (Sell et al. 2005). Again, however, this region differed from the locations of other minimal regions.

1.2.1.4.1.2 The t(12;14) group

Translocations involving chromosomes 12q14-15 are also a frequently reported aberration, occurring in approximately 20% of karyotypically abnormal leiomyomas (Heim et al. 1988; Ligon and Morton 2001). The most frequent translocation partner is chromosome 14q24 (Ligon and Morton 2001). Mapping of the chromosome 12 breakpoint revealed the high mobility group gene *HMGI-C* (more recently called *HMGA2*) as the translocation partner (Schoenmakers et al. 1995). The involved gene on chromosome 14q24 was identified as the DNA repair gene *RAD51L* (Schoenmakers et al. 1999). This translocation has been shown to fuse the two genes and produce an in-frame fusion transcript (Takahashi et al. 2001b). However, fusion transcripts do not occur in all leiomyomas with t(12;14) (Quade et al. 2003) and it is thought that they are not the principal means of pathogenesis occurring from this rearrangement.

Uterine leiomyomas with t(12;14) have been shown to be significantly larger (Rein et al. 1998) and less responsive to GnRH analogue therapy (Takahashi et al. 2002) than karyotypically normal tumours, and those with 7q deletions. Thus it appears that leiomyomas with this karyotype attain independence from sex hormones.

HMGA2 has also been shown to translocate with other chromosomes in uterine leiomyomas, and a number of other fusion partners have been described, including: cytochrome c oxidase subunit 6C (*COX6C*) on

chromosome 8q22-23 (Kurose et al. 2000); homo sapiens enhancer of invasion 10 (*HEI10*) on chromosome 14q11 (Mine et al. 2001); and the aldehyde dehydrogenase gene (*ALDH2*) on 12q24 as the result of an inversion (Kazmierczak et al. 1995). There is also a suspected fusion partner on chromosome 5q22 in uterine lipoleiomyomas (Havel et al. 1989). Furthermore, *HMGA2* has also been involved in translocations observed in other benign mesenchymal tumours including lipomas, hamartomas and endometrial polyps (Tallini et al. 2000).

Expression of the HMGA2 protein is normally associated with foetal tissues, and its expression is switched off in adult tissues, bar the lung and kidney (Gattas et al. 1999). Analysis of HMGA2 expression in uterine leiomyomas demonstrated an increase in expression compared to matched myometrium, but only in samples with t(12;14) (Gross et al. 2003). HMGA2 expression has also been shown to be increased in uterine leiomyomas from the Eker rat (Hunter et al. 2002) Therefore, it has been suggested that disruption of the *HMGA2* gene exerts a pathogenic effect by increasing HMGA2 expression. This increased expression may come about because of mRNA truncation resulting from the translocation. It has been shown that the 3'-UTR of the HMGA2 gene is responsible for controlling translation of the mRNA. Removal of the 3'-UTR, which occurs in uterine leiomyomas with t(12;14) results in an increase in levels of translated protein (Borrmann et al. 2001).

Very recently, a series of novel transcripts were identified within the *HMGA2* gene transcribed from the complementary strand (Ingraham et al. 2006). Expression of these novel transcripts was also found to be upregulated

in uterine leiomyomas. Their role is as yet undefined, although they are suspected of being non-coding RNA molecules, potentially with regulatory capacity.

HMGA2 is a nuclear phosphoprotein containing 3 DNA binding domains, and is thought to be an architectural transcription factor. It was originally discovered as a protein expressed at high levels following transformation of fibroblasts with an oncogenic virus (Giancotti et al. 1987). It has recently been shown that HMGA2 overexpression results in pituitary tumorigenesis through interaction with the retinoblastoma tumour suppressor gene product pRB. It displaces the histone deacetylase HDAC1 from the DNA bound pRB/E2F1, resulting in local histone and E2F1 acetylation, which switches on the expression of S-phase genes (Fedele et al. 2006). A similar mechanism may occur in leiomyoma cells with t(12;14).

1.2.1.4.1.3 The 6p21 group

Identification of the *HMGA2* gene as the translocation partner involved in t(12;14) and the frequency of rearrangements of 6p21 in uterine leiomyomas and other benign mesenchymal tumours lead to the study of the known *HMGA1* gene in this region. A single PAC clone containing *HMGA1* was found to span breakpoints in this region (Kazmierczak et al. 1996). Rearrangements of this region include t(6;10)(p21;q22) (Gross et al. 2004), and t(1;6)(q23;p21) and t(6;14)(p21;q24) (Ligon and Morton 2001). HMGA1 expression has been shown to be increased in uterine leiomyomas with rearrangements of 6p21 (Tallini et al. 2000).

The mechanism of HMGA1-associated tumorigenesis is likely to be similar to that of HMGA2. Indeed, overexpression of truncated HMGA1 in

mouse pre-adipocytes induced proliferation with increased E2F1 activity (Tallini et al. 2000), implying that HMGA1 and HMGA2 may have a similar effect on inducing cell proliferation through interaction with pRB.

1.2.1.4.1.4 Other cytogenetic aberrations

A whole host of other cytogenetic aberrations have been described in uterine leiomyomas. Many of these are recurrent changes, though not at the frequency of those described above. These include deletions of 3p13-14 (Hu and Surti 1991), and rearrangements of the X chromosome such as inv(X)(p22;q13) (Ozisik et al. 1992) and del(X)(p11) (Turc-Carel et al. 1988). Marker chromosomes, such as ring chromosome 1, have also been observed in leiomyomas, although always where other abnormalities are present (Nilbert et al. 1988).

A translocation of chromosomes 10 and 17 was shown to disrupt the histone deacetylase MORF (Moore et al. 2004). Disruption of this gene may be related to HMGA pathogenesis due to the involvement of histone acetylation. Deletions have also been observed of 1q42.3, the cytogenetic location of the *FH* gene, indicating that this gene might have a role to play in sporadic leiomyma development (Gattas et al. 1999).

1.2.1.4.2 Somatic mutations in uterine leiomyomas

Screening for somatic sequence variants has also been carried out in a number of genes, including *FH*, *TP53*, *MDM2*, *KRAS*, and *CUTL1* (Hall et al. 1997; Barker et al. 2002; Kiuru et al. 2002; Patrikis et al. 2003).

Some *FH* mutations were observed in sporadic uterine leiomyomas but at a very low frequency (Kiuru et al. 2002). Activating *KRAS* mutations were observed in 3/20 uterine leiomyomas screened in one study (Hall et al. 1997), but none were found in the other (Patrikis et al. 2003). No somatic mutations were identified in any of the other genes screened.

1.2.2 Mechanisms and pathways of leiomyoma growth

In addition to the genetic studies carried out on uterine leiomyoma patients, numerous studies have been carried out in an attempt to elucidate the mechanisms and signalling pathways involved in leiomyoma pathogenesis in order to identify targets for clinical intervention. A variety of cell signalling pathways and associated growth factors have been implicated in uterine leiomyoma pathogenesis (Maruo et al. 2004). Strong evidence exists for the roles of oestrogen, progesterone, transforming growth factor β (TGFβ), platelet-derived growth factor (PDGF), epidermal growth factor (EGF) and vascular endothelial growth factor (VEGF) among others (Maruo et al. 2004). These pathways have effects on a number of mechanisms important to leiomyoma pathogenesis, including cell proliferation, extracellular matrix deposition, resistance to apoptosis and angiogenesis (Maruo et al. 2004).

1.2.2.1 Sex hormone signalling

As is eluded to above, the epidemiology of uterine leiomyomas suggests a strong, if not essential involvement of the female sex hormones oestrogen and progesterone in tumour formation, particularly due to the observed regression of the tumours following the menopause, and the successful use of GnRH analogues, which induce a hormonally pseudomenopausal state, in shrinking uterine leiomyomas prior to surgery (Stewart 2001b).

The levels of oestrogen and progesterone vary with the stage of the 28 day menstrual cycle. In the follicular phase of the cycle, from day 0 to day 13, progesterone and oestrogen levels are initially low during menstruation. The

level of oestrogen begins to accumulate before peaking approximately 1 day prior to ovulation before regressing slightly. Following ovulation, the cycle enters the luteal phase. Levels of both progesterone, produced by the corpus luteum in the ovary, and oestrogen begin to rise, peaking at approximately 5-7 days following ovulation. The levels of both hormones then regress back to the basal level on about day 28 as the menstruation begins to occur (Hacker and Moore 1998). Leiomyomas have been shown to be most proliferative in the luteal phase of the cycle, when there is abundant oestrogen and progesterone (**Figure 1.3**) (Walker and Stewart 2005).

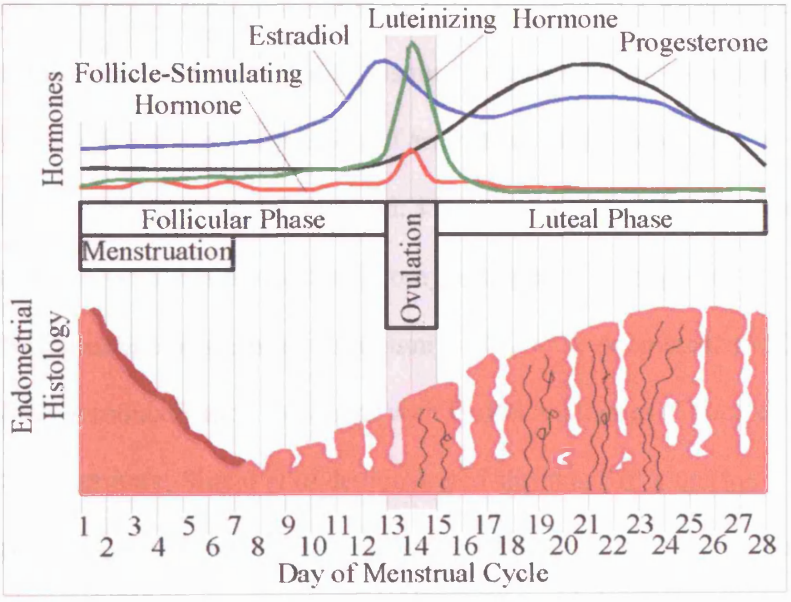

Figure 1.3 Hormone levels and endometrial histology during the menstrual cycle. (Adapted from https://webapp.walgreens.com/cePharmacy/programsHTML/reproductive.html, Figure 3)

1.2.2.1.1 Oestrogen signalling

Oestrogen has been shown to act on two receptors, ERα and ERβ. Both receptors are expressed in the myometrium and leiomyoma, with ERα being the more prevalent form. Expression of both receptors has been shown to be increased in uterine leiomyomas compared to the host myometrium at the mRNA level (Benassayag et al. 1999), with the increase in ERα expression more notable. This increased expression would increase the sensitivity of a leiomyoma cell to oestrogen signalling.

Levels of circulating oestrogen do not differ between women with and without uterine leiomyomas, nor are leiomyomas associated with conditions resulting in elevated oestrogen, such as polycystic ovarian syndrome (Buttram 1986). However, local oestrogen levels may be elevated since several studies have identified increased expression of aromatase p450, an oestrogen synthetase, in leiomyomas (Bulun et al. 1994; Shozu et al. 2002). Therefore, *in situ* oestrogen synthesis may affect leiomyoma growth through an autocrine/paracrine mechanism (Sumitani et al. 2000). Aromatase p450 expression is reduced upon treatment with GnRH analogues (Shozu et al. 2001). Furthermore, Shozu *et al* demonstrated shrinkage of a uterine leiomyoma upon treatment with the aromatase inhibitor, Fadrazole, reporting a 71% loss in tumour volume in 8 weeks (Shozu et al. 2003).

Barbarisi *et al* examined the effects of oestrogen signalling on cultured leiomyoma cells (Barbarisi et al. 2001). They found that oestrogen triggers a rapid and transient activation of the mitogen-activated protein kinase (MAPK) pathway. Furthermore, tyrosine phosphorylation of some intracellular pathways, including phosphoplipase C γ (PLCγ), phosphatidyl-inositide-3-

kinase (PI-3-K) and the GTPase activating protein (GAP) was observed, indicative of activation of a transmembrane receptor tyrosine kinase. The activating ligand was discovered to be platelet derived growth factor (PDGF) (Barbarisi et al. 2001). Further details of this will be discussed later.

A number of oestrogen regulated genes have been reported as being overexpressed in uterine leiomyomas, including collagens I and III, and the progesterone receptor (Maruo et al. 2004). Oestrogen is also thought to induce the expression of other growth factors in leiomyoma cells including IGF-I and its receptor, the epidermal growth factor receptor (EGFR) and prolactin (Watters et al. 2000). It has also been shown to alter the expression of a number of other important cell factors, including downregulation of the p53 tumour suppressor (Gao et al. 2002), and upregulation of the proliferative marker proliferating cell nuclear antigen (PCNA) (Maruo et al. 2003).

1.2.2.1.2 Progesterone signalling

The effects of progesterone signalling in leiomyomas are less clear, and studies have produced conflicting results. Although two peaks of oestrogen production occur during the menstrual cycle, the greatest level of proliferation is observed in the luteal phase, when not only oestrogen, but also progesterone levels peak (Hacker and Moore 1998; Walker and Stewart 2005). Progesterone receptor (PR) expression is also increased in uterine leiomyomas (Sadan et al. 1987), and several studies have been published implicating progesterone in uterine leiomyoma pathogenesis. The progesterone analogue medroxyprogesterone acetate significantly increases mitotic activity in leiomyomas (Tiltman 1985), and the progesterone antagonist RU-486 reduces the size of leiomyomas and PR expression (Murphy et al. 1995). Progestins

have also been shown to inhibit the therapeutic effects of GnRH analogues(Friedman et al. 1988). To confuse matters, progestins have been demonstrated to transdominantly suppress ER signalling in Eker rat leiomyomas, resulting in down regulation of oestrogen-induced PR expression (Hodges et al. 2002).

PR, like ER, exists in two forms, PR-A and PR-B, each of which possesses a distinct biological function. PR-B is a transcriptional activator of progesterone responsive genes, whereas PR-A is a repressor of PR-B transcriptional activity in certain cell contexts. Expression of both PRs is higher in leiomyomas than myometrium, with a dominance of PR-A over PR-B (Viville et al. 1997; Nisolle et al. 1999), although one of these studies failed to find an increase in mRNA level. Another study demonstrated relative overexpression of PR-B on the cell surface (Fujimoto et al. 1998). This pattern of expression may represent a proliferating phenotype for leiomyoma growth, allowing a majority of progesterone to be bound by the transcription-activating PR-B, before it reaches the intracellular PR-A.

The more specific downstream effects of progesterone in uterine leiomyomas have also been studied. Maruo *et al* studied the effects of progesterone on growth factor expression in cultured leiomyoma cells. They demonstrated an increase in the expression of EGF, which complemented the increase in EGFR by oestrogen signalling. They also demonstrated an increase in PCNA expression which, *in vivo*, is most highly expressed in the progesterone dominated luteal phase of the menstrual cycle, and is also upregulated by oestrogen (Maruo et al. 2003). The expression of IGF-I, which induces proliferation, was also examined in this study. The results showed a

significant decrease in IGF-I mRNA upon treatment with progesterone or combined progesterone and oestrogen treatment, with no effect on expression caused by oestrogen alone (Maruo et al. 2003). This finding differs from the results of Burroughs *et al* in studies using Eker rat leiomyomas, who demonstrated a 7.5-fold increase in IGF-I mRNA upon treatment with oestrogen (Burroughs et al. 2002).

The progesterone response of the expression of two apoptosis-related proteins, the apoptosis inducing tumour necrosis factor α (TNFα), and the anti-apoptotic B-cell lymphoma 2 (Bcl-2), has also been studied. These studies have identified increased expression of Bcl-2 (Matsuo et al. 1997), and decreased expression of TNFα (Kurachi et al. 2001) in response to progesterone. This implies that progesterone is a pro-survival signal for leiomyoma cells, but also has an anti-proliferative effect.

This anti-proliferative effect of progesterone may explain why uterine leiomyomas very rarely grow during pregnancy, but remain the same size or shrink over the course of the pregnancy (Phelan 1995), since progesterone concentrations increase throughout the course of the pregnancy to levels higher than observed during the menstrual cycle (Hacker and Moore 1998).

Overall there appears to be complex interplay between oestrogen and progesterone signalling in uterine leiomyomas. Ultimately, the two hormones almost certainly exhibit a combined effect, resulting in leiomyoma growth. However, the exact mechanism of how this occurs has yet to be fully discovered.

1.2.2.2 Platelet-derived growth factor signalling

Platelet-derived growth factor (PDGF) is a potent smooth muscle cell mitogen, acting through a receptor tyrosine kinase to activate the MAPK pathway, resulting in increased DNA synthesis and cell proliferation (Ross et al. 1986a). Expression of PDGF and its receptor has been described in leiomyoma cells, suggesting an autocrine/paracrine signalling mechanism (Palman et al. 1992). As described above, PDGF expression in leiomyoma cells is stimulated by oestrogen, and it appears that expression of PDGF by these cells is at least one of the means by which oestrogen induces cell proliferation (Barbarisi et al. 2001). In cultured cells, treatment with oestrogen induces PDGF expression and cell proliferation. Addition of antibodies against PDGF to the culture media to sequester secreted PDGF inhibited oestrogen-induced cell proliferation (Barbarisi et al. 2001). In addition, PDGF expression is downregulated by GnRH analogues, implying an *in vivo* relationship between the sex hormones and PDGF expression (Di Lieto et al. 2005). The PDGF-R receptor is overexpressed in cultured leiomyoma cells compared to myometrium, but has a lower affinity for the ligand (Fayed et al. 1989).

PDGF expression has also been shown to be modulated by TGFβ-1. In smooth muscle cells, low levels of TGFβ-1 stimulate PDGF secretion, whereas at higher concentrations it down-regulates PDGF-R expression. This bimodal effect is also observed in leiomyoma cells, where low levels of TGFβ-1 induces cell proliferation, but increasing levels remove this stimulatory effect (Battegay et al. 1990; Arici and Sozen 2003).

PDGF consists of two polypeptide chains, A and B, and can exist as a heterodimer, or as a homodimer of either chain. The activity of PDGF is dependent on which dimer is formed (Ross et al. 1986a). Differing reports exist in the literature as to which dimer is dominant in uterine leiomyomas, with one study showing an increase in PDGF-A mRNA expression in leiomyoma cells, (Mendoza et al. 1990) whereas two other studies show no difference in the expression of PDGF-A and PDGF-B between myometrium and leiomyomas (Boehm et al. 1990; Mangrulkar et al. 1995).

1.2.2.3 Epidermal growth factor signalling

Epidermal growth factor (EGF) is also a mitogenic factor that has been shown to play an important role in leiomyoma growth. Stimulation of cultured leiomyoma cells with either oestrogen or EGF results in an increase in cell proliferation, but treatment with both factors is not additive (Maruo et al. 2004). This indicates that, as is the case for PDGF, EGF expression may be a downstream effect of oestrogen signalling. This turns out to be the case since, as is described above, oestrogen and progesterone are responsible for increased expression of EGF-R and EGF respectively in uterine leiomyoma cells (Watters et al. 2000). Since both EGF and its receptor are expressed in leiomyomas, an autocrine/paracrine signalling mechanism again appears to be involved (Maruo et al. 2004).

EGF again acts through a classical MAPK pathway to induce cell proliferation (Shushan et al. 2004). It has been shown to stimulate expression of PCNA (Shimomura et al. 1998), which correlates with increased expression of PCNA in the luteal phase of the menstrual cycle (Zaslawski et al. 2001). In addition, the EGF receptor antagonist AG1478 has been shown to suppress

leiomyoma cell growth, further indicating an important role of this growth factor in leiomyoma pathogenesis (Shushan et al. 2004).

1.2.2.4 Transforming Growth Factor β signalling

Uterine leiomyomas are fibrotic tumours with increased levels of extracellular matrix and therefore studies of the transforming growth factor β (TGFβ) pathway have been carried out, since this pathway has been shown to increase the expression of ECM proteins such as collagen (Lee and Nowak 2001). The TGFβ pathway has been shown to be involved in a variety of cellular roles, including stimulation or inhibition of cell growth, differentiation, and the aforementioned increase in ECM deposition (Lee and Nowak 2001). Due to this latter role, TGFβ plays an important role in wound healing. However, excessive TGFβ production or signalling has been shown to result in tissue fibrosis. In particular, TGFβ may be involved in keloid formation (Liu et al. 2004).

Three isoforms of TGFβ, (TGFβ-1, TGFβ-2 and TGFβ-3) have been detected in human myometrium and leiomyomas, as well as the 3 receptors (TGFβR-1, TGFβR-2, and TGFβR-3), although TGFβ-2 is the least abundant (Maruo et al. 2004). Increased expression of TGFβ-3 has been reported in uterine leiomyomas (Lee and Nowak 2001), whereas changes in expression of TGFβ-1 are less clear, with 3 different reports providing 3 different results (Lee and Nowak 2001; Arici and Sozen 2003; Chegini et al. 2003). The highest levels of TGFβ-3 have been observed in mid-luteal phase, and *in vitro* experiments have demonstrated both oestrogen and progesterone-induced TGFβ-3 expression (Arici and Sozen 2003).

Binding of a TGFβ ligand to its receptor results in phosphorylation of the Smad proteins Smad2 or Smad3, which then translocate to the nucleus, resulting in altered gene transcription. The inhibitory Smad, Smad 7, helps to modulate signalling. As well as Smad activation, TGFβ can also activate the MAPK pathway (Chegini et al. 2003). Stimulation of cultured myometrium cells with TGFβ-1 and TGFβ-3 results in inhibition of cell proliferation (Lee and Nowak 2001). However, in cultured leiomyoma cells, TGFβ-3 resulted in an increase in cellular proliferation (Lee and Nowak 2001). This proliferation is reduced following treatment with GnRH analogues, suggesting that oestrogen signalling may be closely tied in with TGFβ signalling (Lee and Nowak 2001). In addition, expression of Smad3, phosphorylated Smad3, TGFβR-1 and TGFβR-3 are increased in leiomyomas compared to normal myometrium (Chegini et al. 2003). GnRH analogue treatment results in a reduction of the expression of these proteins in both myometrium and leiomyoma cells, with a concurrent increase in inhibitory Smad7 (Chegini et al. 2003). In addition to the increased cell proliferation, TGFβ-1 and -3 both increase fibronectin mRNA levels in cultured leiomyoma cells (Arici and Sozen 2000).

A recent study used a microarray-based approach to examine the effects of TGFβ-1 stimulation on cultured leiomyoma and myometrium cells. Grouping of differentially expressed genes by gene ontology demonstrated that a majority of genes with altered expression were involved in transcriptional regulation, cell cycle regulation, extracellular matrix and signal transduction (Luo et al. 2005).

TGFβ-1 may also be involved in the regulation of other growth factors involved in leiomyoma pathogenesis, such as the regulation of PDGF expression described above (Battegay et al. 1990; Arici and Sozen 2003). Therefore, it appears that TGFβ has several roles in leiomyoma pathogenesis: the stimulation of cell proliferation; increased ECM synthesis; and the regulation of other mitogenic growth factors.

The role of TGFβ may be important in relation to the increased prevalence of uterine leiomyomas in African and Afro-Caribbean women. A recent study identified decreased expression of the collagen binding protein dermatopontin in uterine leiomyomas. Reduced expression of dermatopontin is also observed in keloids, a fibrotic disease that occurs 3 times more frequently in African and Afro-Caribbean women than Caucasian women. Dermatopontin interacts with TGFβ to downregulate its growth-inhibitory action (Catherino et al. 2004)

1.2.2.5 Insulin-like growth factor I signalling

Another implicated growth factor in leiomyoma pathogenesis is the insulin-like growth factor I (IGF-I). This is an anabolic growth factor, responsible for cell growth and differentiation. Studies using the Eker rat model demonstrated a 7.5-fold increase in IGF-I expression in leiomyomas compared to normal tissue, but an inverse change in IGF-I receptor expression (Burroughs et al. 2002). Increases in IGF-I and IGF-II expression have been reported in human leiomyomas (Boehm et al. 1990). However, unlike the Eker rat, human leiomomyas have shown an increase in IGF-I receptor expression in leiomyomas (Chandrasekhar et al. 1992). Again an autocrine/paracrine mechanism appears to be apparent.

Studies in cultured cells have further refined the role of IGF-I, demonstrating an increase in cell numbers and proliferation rate. An increase in PCNA expression was observed upon treatment with IGF-I (Gao et al. 2001). Furthermore, IGF-I also increases expression of anti-apoptotic Bcl-2 and reduces the cell's susceptibility to apoptosis (Gao et al. 2001).

The expression of IGF-I is related to the signalling by sex hormones. As described above, oestrogen induces the expression of both IGF-I and its receptor, whereas progesterone reduces IGF-I expression (Maruo et al. 2003; Maruo et al. 2004). In addition, GnRH analogue treatment results in a decrease in IGF-I and IGF-I receptor expression (Maruo et al. 2004). It has been shown that IGF-I mediates oestrogen action in the animal uterus (Burroughs et al. 2002), and it has been demonstrated that it can replicate the mitogenic and PR expression responses exerted by oestrogen (Murphy et al. 1987).

1.2.2.6 The mTOR pathway

The mTOR pathway has been heavily implicated in leiomyoma pathogenesis, particularly due to the Eker rat model and Birt-Hogg-Dube syndrome (Walker et al. 2003; Baba et al. 2006). Expression of the *TSC2* gene, mutations of which cause the Eker rat phenotype, is decreased in approximately half of sporadic leiomyomas, (Wei et al. 2005), and has been associated with up-regulation of EGF (Wei et al. 2006a). Another member of this pathway, Akt/protein kinase B, was also up-regulated and found to be phosphorylated during the luteal phase of the cycle (Kovacs et al. 2003). Inactivating phosphorylation of the PTEN tumour suppressor, which is also a member of this pathway, occurs in uterine leiomyomas in the luteal phase (Kovacs et al. 2006). These results imply that the mTOR pathway is being

activated during the luteal phase of the cycle. PDGF expression leads to activation of PI3K, which is at the head of the mTOR pathway (Barbarisi et al. 2001). One of the effects of this pathway is the stimulation of the translation of HIF1α (King et al. 2006), therefore, leiomyomas with activation of this pathway could follow a similar pathogenic route to HLRCC, Eker rat and BHD uterine leiomyomas.

1.2.2.7 Resistance to apoptosis

Deficiency in apoptosis has been described as one of the fundamental features of a tumour cell (Hanahan and Weinberg 2000), and this has also been observed to be true for uterine leiomyomas. A number of studies have identified aberrant expression of apoptosis-related proteins in uterine leiomyomas. Of particular focus has been the role of Bcl-2 family members. Members of this family of homologous proteins are responsible for the regulation of mitochondrial apoptosis (Kirkin et al. 2004). They can be divided into two groups: the anti-apoptotic proteins, such as Bcl-2, Mcl-1 and Bcl-x_L; and the pro-apoptotic members, such as Bax, Bak and Bad. These proteins act to control the integrity of the outer mitochondrial membrane. In response to apoptotic stimuli, factors such as cytochrome c and Smac/Diablo are released into the cytoplasm, resulting in caspase activiation and apoptosis (Kirkin et al. 2004).

As is mentioned above, Bcl-2 expression is upregulated in leiomyoma cells in response to progesterone stimulation (Maruo et al. 2004). Immunohistochemical studies have also identified increased levels of Bcl-2 protein *in vivo*, particularly in the luteal phase, but also in the follicular phase of the menstrual cycle (Matsuo et al. 1997; Dixon et al. 2002; Wu et al. 2002;

Kovacs et al. 2003). This increase in Bcl-2 levels was only observed in leiomyomas from pre-menopausal women (Wu et al. 2002). Increased expression of Bcl-2 has been shown to be sufficient to inhibit apoptosis (Kirkin et al. 2004). Studies examining the expression of pro-apoptotic Bax have produced conflicting results; some studies have demonstrated a decrease in Bax expression in leiomyomas (Dixon et al. 2002; Zhang et al. 2005), while others have shown no change (Kovacs et al. 2003) or increases in Bax expression (Wu et al. 2002). The role of other Bcl-2 family members has also been examined in uterine leiomyomas. No changes in expression have been observed in expression of anti-apoptotic Bcl-x and Mcl-1, or in pro-apoptotic Bak (Wu et al. 2002).

The expression of other apoptosis-related factors has also been studied. Expression of tumour necrosis factor α (TNFα) was decreased in cultured leiomyoma cells following progesterone stimulation (Matsuo et al. 1999). However, TNFα expression is higher in leiomyoma cells than myometrium cells (Kurachi et al. 2001), and therefore, the increased expression of Bcl-2 may be important in protecting leiomyoma cells from apoptosis.

The p53 tumour suppressor protein is a frequent target of mutation and inactivation in tumour cells, given its pivotal role in regulation of the cell cycle, particularly in response to DNA damage (Meek 2004). p53 content in leiomyomas is greater in the follicular phase than the luteal phase of the menstrual cycle, and has been shown to be decreased by oestrogen in leiomyoma cells (Gao et al. 2002), but no difference in p53 content has been observed between myometrium and leiomyoma. GnRH analogue treatment

was shown to up-regulate p53 in leiomyomas, possibly as a result of oestrogen depletion (Gao et al. 2002).

1.2.2.8 Angiogenesis

The role of angiogenesis in uterine leiomyomas also appears to be important. As discussed above, *FH* mutations in HLRCC patients initiate a pseudo-hypoxic response, resulting in the upregulation of vascular endothelial growth factor (VEGF) expression, and increased microvessel density in uterine leiomyomas from these patients compared to their host myometrium (Pollard et al. 2005a). However, vessel density in non-syndromal leiomyomas has been found to be lower than in the myometrium (Poncelet et al. 2002; Pollard et al. 2005a).

Despite this decreased vessel density, the successful treatment of uterine leiomyomas by uterine artery embolisation suggests that the vascular structure of the leiomyoma is vital for growth of the tumour and the provision of nutrients and oxygen (Stewart and Nowak 1998).

VEGF expression has been studied in uterine leiomyomas and the myometrium. VEGF mRNA and immunoreactivity has been identified in both myometrium and leiomyoma. In the myometrium, VEGF expression is slightly higher in the follicular phase, presumably as a part of the new formation of endometrium. However, no menstrual cycle related changes are observed in leiomyomas. VEGF levels were found not to differ between myometrium and leiomyomas, nor are they affected by GnRH analogues, suggesting that VEGF expression is not mediated by sex hormones (Harrison-Woolrych et al. 1995).

Expression of the anti-angiogenic factor thrombospondin was also found to be downregulated in HLRCC leiomyomas (Pollard et al. 2005a). Microarray expression studies of sporadic uterine leiomyomas have found a similar result (Tsibris et al. 2002).

1.3 Aims of this thesis

The work in this thesis is intended to tackle several genetic and functional issues related to both inherited and sporadic uterine leiomyomata. The first part examines the pathobiology of HLRCC uterine leiomyomas. The frequency and spectrum of germline *FH* mutations in uterine leiomyoma patients was determined, and *in silico* methods were used to analyse their functional effects on protein structure. Studies were also undertaken on two of the potential mechanisms of HLRCC pathogenesis, by examining defects in apoptosis and aberrant ultrastructural features in HLRCC uterine leiomyomas. The potential role of ROS-driven mutagenesis was also studied by examining the frequency of mutations in the vulnerable mitochondrial genome (mtDNA).

The second part of the thesis examines genetic factors in the pathogenesis of sporadic uterine leiomyomas. Initially, the role of germline *FH* variants in predisposition to leiomyomas in the general population was determined. Then the focus shifted on to the identification of large-scale somatic genetic changes in sporadic uterine leiomyomas, with particular emphasis on deletions of chromosome 7q. Finally, the possible role of somatic mtDNA mutations in uterine leiomyoma pathogenesis was assessed.

Chapter 2

Materials and Methods

2.1 Study Samples

The different samples used in this study came from a number of different centres depending on the study. All samples were obtained with full ethical consent.

2.1.1 Hereditary Leiomyomatosis and Renal Cell cancer Samples

HLRCC samples were obtained as a part of the ongoing study into this condition. Samples were obtained from a number of clinical collaborators and consisted of blood or DNA samples in all cases, and archival pathology blocks in a number of cases. For one patient, surgery was attended and fresh frozen samples of uterine leiomyomas, as well as tissue fixed for paraffin embedding, were obtained.

As a study sample for the frequency of *FH* gene mutations in uterine leiomyoma patients, 100 blood samples were collected from patients attending the uterine leiomyoma clinic at St. Mary's hospital, Paddington, London.

2.1.2 Sporadic Uterine leiomyomas samples

Frozen sporadic uterine leiomyoma tissue samples were collected from the tissue banks at the Addenbrookes Hospital, Cambridge and the Hammersmith Hospital, London. Where possible, ethnicity and age data were collected. Samples were also collected from the North Middlesex Hospital in London in collaboration with Mr Stanley Okolo, and archival paraffin-embedded tissue samples of sporadic uterine leiomyomas were supplied by Dr Sanjiv Manek at the John Radcliffe Hospital, Oxford. All samples were anonymised.

2.1.3 South African Uterine leiomyoma samples

In collaboration with Prof Zephne van der Spuy at the University of Cape Town, South Africa, blood and tissue samples from sporadic uterine leiomyoma patients was collected. DNA was extracted from blood and tissue samples by Dr Jacquie Greenberg of the Division of Human Genetics at the University of Cape Town. Clerking sheets supplied with each sample gave details of ethnicity, age of onset, family history, and diagnosis, but without details of patient names.

2.2 Nucleic acid extraction

2.2.1 Fresh tissue and cell line DNA extraction

DNA extraction was carried out using the Qiagen QIAamp DNA mini kit (Qiagen, Crawley, UK) as per the manufacturer's instructions. DNA was extracted from 30mg of fresh frozen tissue and resuspended in 400µl TE buffer.

2.2.2 Genomic DNA extraction from whole blood

DNA was extracted from whole blood taken into EDTA vacutainer tubes (BD, Oxford, UK) by two methods. Automatic extraction of DNA was carried out by using charged magnetic beads, using the Chemagen blood DNA extraction kit and magnetic robot as per the manufacturer's instructions (Chemagen, Germany).

Manual extraction of DNA was carried out using an ammonium acetate extraction method. Blood samples (~10ml) were transferred into a 50ml falcon tube. Ice cold water was added to a final volume of 50ml to osmotically lyse cells. The tubes were spun at 2300 rpm in a Jouan CR412 centrifuge (Thermo-Scientific, Waltham, MA, USA) for 20 mins at 4°C, and the supernatant was discarded into Virkon, leaving a white nuclear pellet. The pellet was washed with 0.1% Nonidet P-40 in water and centrifuged at 2300 rpm for 20 mins at 4°C. The supernatant was discarded and 3ml nuclei lysis buffer (10mM Tris-HCl, 400mM NaCl, 2mM EDTA, autoclaved) was added to the pellet, which was subsequently resuspended by vortexing. 200µl of 10% SDS and 600µl Proteinase K solution (2mg/ml proteinase K in 2mM EDTA,

1% SDS (Autoclaved before addition of proteinase K)) was added to the tube, which was mixed by inversion and incubated overnight at 55°C to digest nucleosomal protein.

The following day, 1ml saturated ammonium acetate was added to the tube to precipitate remaining protein. The tube was then mixed by vigorous shaking for 15s, and left to stand at RT for 10-15 mins before centrifugation at 2300 rpm for 20 mins at RT. The supernatant was transferred to a new tube, taking care not to transfer any of the precipitated protein. The DNA was precipitated by the addition of 2 volumes of 100% ethanol and spooled out of solution using an inoculation loop into 80% ethanol, where it was washed for 1 hour at room temperature. The DNA was then spooled out of the 80% ethanol and dissolved in 300µl TE buffer.

2.2.3 DNA extraction from cell pellets

DNA was extracted from cell pellets using a high-salt method. $3x10^7$ cells were pelleted into a 50ml falcon tube by centrifugation at 1000 rpm in a Jouan CR412 centrifuge. The cell pellet was resuspended in 2ml SE buffer (75mM NaCl, 25mM EDTA, 1% SDS, filter sterilised) per 10^7 cells. 20µl of RNase A (10mg/ml, Qiagen) was added to the cells, which were then incubated at 37°C for 1hr. Proteinase K was then added to a final concentration of 200µg/ml (10µl of a 20mg/ml stock per 1ml SE buffer used) and incubated overnight at 55°C. Prewarmed 5M NaCl was added to a final concentration of 1.5M (300µl 5M NaCl per 1ml SE buffer used). One volume of chloroform was added and mixed for 30 mins at RT with rotation, followed by centrifugation at 2000 rpm for 10 minutes at RT. The top layer was

transferred to a new 50ml tube using a wide bore pipette, and an equal volume of isopropanol was added to precipitate the DNA. The DNA was spooled into 80% ethanol and washed for 1hr at RT. The DNA was removed from the 80% ethanol and dissolved in TE buffer.

2.2.4 BAC DNA extraction

Stabs of BAC clones were obtained from BACPAC resources (Childrens's hospital, Oakland, CA, USA). Clones were streaked onto LB-Agar plates containing 25μg/ml Chloramphenicol and grown overnight at 37°C. A single clone was picked and grown overnight in 5ml LB containing 25μg/ml chloramphenicol at 37°C in a shaking incubator. The culture was centrifuged at 3000 rpm for 10 mins and the supernatant was discarded. The pellet was resuspended in 300μl buffer P1 (See 2.12) and transferred to a 1.5ml microfuge tube. 300μl buffer P2 was added followed by gentle shaking and incubation at room temperature for 5 mins to lyse the bacteria. 300μl buffer P3 was added and mixed to precipitate bacterial genomic DNA and protein. The tubes were incubated on ice for 5 mins.

The lysate was centrifuged at 10,000 rpm for 10 mins at 4°C to pellet the precipitated DNA and protein. The supernatant was then transferred to a new tube and the BAC DNA was precipitated by adding 800μl of ice-cold isopropanol. The tube was incubated on ice for 5 mins and the precipitated DNA was pelleted by centrifugation at maximum speed (13,000 rpm) for 15 mins. The supernatant was discarded and the pellet was washed with 500μl 70% ice-cold ethanol and centrifuged at maximum speed for 5 mins. The

supernatant was discarded and the pellet allowed to air dry before being resuspended in 50µl UV-treated TE buffer.

2.2.5 DNA quantification

DNA was quantified by Spectrophotometry at 260 and 280nm blanked against the buffer in which the DNA sample was dissolved using a nanodrop instrument (Nanodrop technologies, Wilmington, DE, USA). In order to calculate the concentration, the absorbance at 260nm was multiplied by 500 to give the concentration in ng/µl. The ratio of absorbance at 260/280 nm was used to calculate the purity of the DNA. A ratio of 1.8-1.9 indicated clean DNA; a ratio below this indicated protein contamination, and a ratio above this indicated, amongst other contaminants, RNA contamination.

2.3 Polymerase Chain Reaction (PCR)

The polymerase chain reaction (PCR) is a means of amplifying fragments (amplimers) of DNA from a template. The amplimer is determined by oligonucleotide primers specific to the each end of the region to be amplified (Strachan and Read 2004). Work in this thesis used standard PCR and two specialised PCR protocols for microarray construction: Degenerate oligonucleotide primer (DOP) PCR, and aminolinking PCR.

2.3.1 Primer design

Primer design was carried out using the Primer3 program (Rozen and Skaletsky 2000). Primers were ordered from Sigma-Genosys. Primer sequences for genomic microsatellite markers were obtained from the UCSC genome browser (Hinrichs et al. 2006). All primer stocks were diluted to 20μM in UV-treated water.

2.3.2 Standard PCR

For products for mutation analysis and sequencing, which involved PCR products of less than 1kb, a standard PCR protocol was used. A typical PCR reaction mixture is shown in **Table 2.1**. Dimethylsulfoxide (DMSO) was included in the reaction mixture to reduce template and primer secondary structure. Thermal cycling was carried out on an MJ research Tetrad thermal cycler in 96 or 48-well plates.

Table 2.1 Standard PCR reaction mix

Component	Volume in 25µl reaction	Final concentration
Promega PCR Buffer (10x)	2.5µl	1x
dNTPs (2.5mM dATP, dCTP, dGTP, dTTP)	2µl	0.2mM of each dNTP
$MgCl_2$ (25mM)	1.5µl	1.5mM
DMSO	1.25µl	5%
Forward primer (20µM)	0.25µl	200nM
Reverse primer (20µM)	0.25µl	200nM
Taq polymerase (5U/µl)	0.25µl	1.25U/reaction
DNA template	25ng	1ng/µl
Water	To 25µl	-

2.3.2.1 Standard PCR thermal cycler programs

All thermal cycler programs were carried out on an MJ Research Tetrad thermal cycler. Two standard programs were used for PCR, EJ55 and AR55. All primer pairs worked with these cycling conditions.

EJ55

Temperature	Time (mins)	Cycles
94°C	5:00	1x
94°C	0:30	35x
55°C	0:30	
72°C	0:30	
72°C	7:00	1x
4°C	Hold	1x

AR55

Temperature	Time (mins)	Cycles
94°C	5:00	1x
94°C	1:00	35x
55°C	1:00	
72°C	1:00	
72°C	7:00	1x
4°C	Hold	1x

2.3.3 Degenerate oligonucleotide PCR (DOP-PCR)

Degenerate oliogonucleotide PCR (DOP-PCR) is the amplification of whole genomic, or BAC clone DNA using a degenerate primer containing a specific hexamer, a random hexamer, and a restriction-site linker sequence (Telenius et al. 1992). In this thesis, it was used for the amplification of BAC clones in the construction of the 7q tiling path array. Three DOP primers were used, designed to preferentially amplify human genomic DNA over background *E.coli* DNA contaminating the BAC from the purification procedure (Fiegler et al. 2003) (**Table 2.2**).

Table 2.2 DOP-PCR and aminolink primer sequences (From (Fiegler et al. 2003))

Primer Name	Primer Sequence
DOP-1	CCGACTCGAGNNNNNNCTAGAA
DOP-2	CCGACTCGAGNNNNNNTAGGAG
DOP-3	CCGACTCGAGNNNNNNTTCTAG
Aminolink	GGAAACAGCCCGACTCGAG*

*This primer has a C6-aminolinker at the 5' end

The DOP-PCR reaction was carried out using a different buffer (10x buffer = 100mM Tris-HCl (pH 8.4), 20mM NaCl, 500mM KCl, 1mg/ml Gelatin) and different conditions to standard PCR. All plastics, buffers and water were UV sterilised before the reaction was set up due to the sensitivity of the procedure to contamination. The reaction mix was set up as below, one reaction was carried out for each DOP primer:

DOP-PCR reaction mix

Component	Volume (50µl reaction)	Final Concentration
10x DOP Buffer	5µl	1x
dNTPs (As above)	4µl	0.2mM each
$MgCl_2$ (25mM)	5µl	2.5mM
W1 (1% stock)	2.5µl	0.05%
Primer (20µM stock)	5µl	2µM
Taq polymerase (5U/µl)	0.5µl	2.5U/50µl
DNA (1ng/µl)	2.5µl	-
Water	To 50µl	-

The thermal cycling conditions were as below:

Temperature	Time (mins)	Cycles
94°C	3:00	1x
94°C	1:30	10x
30°C	2:30	
72°C	3:00	
94°C	1:00	30x
62°C	1:30	
72°C	2:00	
72°C	8:00	1x
15°C	Hold	1x

2.3.4 Aminolinking PCR

Aminolinking PCR was carried out using the DOP-PCR products to attach a C6-aminolink moiety to allow the amplified products to attach to the Codelink slides. A different buffer (10x aminolink buffer = 500mM KCl, 25mM $MgCl_2$, 50mM Tris-HCl (pH 8.5)) was used for this reaction, and the same UV sterilisation procedures were used prior to setting up this reaction. The reaction mix is shown below, this protocol is taken from (Fiegler et al. 2003):

Component	**Volume (60µl reaction)**	**Final Concentration**
10x Aminolink buffer	6µl	1x
dNTPs (2.5mM each)	6µl	0.25mM each
Aminolink primer (200ng/µl)	3µl	4ng/µl
Taq polymerase (5U/µl)	0.6µl	3U/60µl
Water	42.4µl	-
Pooled DOP-PCR products	2µl	-

And the thermal cycling conditions were as follows:

Temperature	**Time (mins)**	**Cycles**
95°C	10:00	1x
95°C	1:00	35x
60°C	1:30	
72°C	7:00	
72°C	10:00	1x
10°C	Hold	1x

2.4 Electrophoresis

Electrophoresis of DNA, RNA and protein samples allows the separation of molecules on the basis of size. This separation is useful for analytical purposes, for example, ensuring a PCR reaction is successful and the product is the correct size, and for extraction of specific samples, for example gel purification of DNA fragments for cloning. Analysis of DNA samples in this thesis was carried out by agarose gel electrophoresis.

2.4.1 Agarose gel electrophoresis

Analytical electophoresis was carried out using agarose gels prepared with 1x Tris-Borate-EDTA (TBE), and run in the same buffer. Different percentages of gels were used for different product lengths. Typically, a 2% gel was used for products of between 150 and 1000bp; a 1% gel was used for product lengths up to 3kb; a 0.8% gel was used for very long products; and a 3% gel was used for products under 150bp.

Gels were prepared by boiling agarose powder in 1x TBE buffer until it was dissolved. The gel was allowed to cool to approximately 60°C before addition of ethidium bromide to a concentration of 100ng/ml. Gels were cast and run using the Biorad mini-sub cell electrophoresis system. 10µl of PCR product was mixed with 2µl of 5x Orange G loading buffer (50% Glycerol, 50mM EDTA, 0.2% Orange G), which migrates at approximately 50bp.

Gels over 1% were run at 120V, with the time dependent on the size of the product, typically 20 minutes for 300bp. Gels of 1% and under were run at 100V, again with the length of time dependent on the size of the product. Gels

were visualised under UV light using a UVP transilluminator and captured using a CCD camera coupled to Labworks software (UVP, Cambridge, UK).

2.5 Mutation screening techniques

2.5.1 Single stranded conformational polymorphism analysis (SSCP)

SSCP analysis detects alterations in the electrophoretic mobility of single strands of DNA, which have a tendency to fold into complex structures stabilised by hydrogen bonding (Strachan and Read 2004). The difference in mobility of these structures can be indicative of single base mutations in a DNA sample. For SSCP analysis, PCR products to be screened were amplified using both forward and reverse labelled primers using a standard PCR protocol. These products were then denatured and snap-cooled to produce single-strand structures. The products were detected by capillary electrophoresis using an ABI 3100 genetic analyser (Applied Biosystems) and analysed using GENESCAN and GENOTYPER software (Applied Biosystems).

2.5.2 Melting curve analysis

Another means of mutation detection used was meltpoint analysis using LCgreen (Wittwer et al. 2003). The basis of this method is the analysis of the melting profile of a DNA molecule. The LCgreen dye (Idaho technology), which is incorporated into the PCR reaction mixture, binds to double stranded DNA and fluoresces. As the DNA is slowly melted over a temperature gradient, the LCgreen dissociates from the now single-stranded DNA and no longer fluoresces. The melting curve produced by this

dissociation is dependent upon the sequence of the PCR product, and differences in melting curves are indicative of DNA variants.

Melting curve analysis was carried out by amplifying DNA using unlabelled primers in a 10μl standard PCR protocol, with the addition of 1μl of 10x LCgreen reagent, layered with mineral oil in an opaque PCR plate. The melting curves of the samples were analysed using the Lightcycler instrument (Idaho technologies). Samples with differences in the melting curve, visualised with the instrument's software, were selected for sequencing.

2.6 DNA sequencing

DNA sequencing was carried out using the Big Dye Terminator kit v3.1 (Applied Biosystems). 5µl of PCR product amplified using unlabelled primers was treated with 2µl ExoSap-IT (GE) to remove single-stranded DNA from the first PCR reaction as per the manufacturer's instructions. Samples were then diluted to approximately 2.5ng/ul, estimated using the gel run for the PCR reaction. 4µl of diluted PCR product was used in a sequencing reaction mix as follows:

Component	**Volume**
BDT v3.1	8µl
Primer (20µM)	1µl
Water	7µl
Diluted PCR product	4µl

Using the following thermal cycler conditions

Temperature	**Time (mins)**	**No. Cycles**
96°C	1:00	1x
96°C	0:10	25x
30°C	0:05	
60°C	4:00	
4°C	Forever	1x

The sequencing reaction was cleaned up using Dye-Ex columns (Qiagen) and analysed using an ABI 3730 genetic analyser (Applied Biosystems). Sequences were analysed using 4peaks software (Netherlands Cancer Institute).

2.7 Microsatellite Loss of heterozygosity analysis

Loss of heterozygosity (LOH) analysis was carried out by PCR amplification of labelled markers using a short-range PCR protocol. Primer sequences and conditions for each marker are detailed in the relevant chapter. Dye-labelled PCR products were detected on an ABI 3100 genetic analyser (Applied biosystems) and analysed using GENESCAN and GENOTYPER software (Applied Biosystems). In order to assess LOH, the ratio of the areas under the peak were calculated. LOH was called if the ratio of the areas under the peaks in one sample were greater than 2x or less than 0.5x the ratio of the areas in the control. Where a single peak was observed in the normal sample, the marker was deemed non-informative for that sample.

2.8 Histology and Immunohistochemistry

2.8.1 Fixation and paraffin embedding of tissue samples

Tissue samples were collected and fixed in neutral buffered formalin (NBF) overnight at room temperature. Samples were then transferred to 70% ethanol before paraffin embedding. Embedding of samples and cutting of sections was carried out by the Cancer Research UK histopathology unit. Briefly, samples were placed in a histology cassette and dehydrated by taking through 3 changes of 70%, 80%, 95% and 100% ethanol, followed by 3 changes of xylene, and finally 4 changes of paraffin wax. The tissue was embedded in paraffin wax and allowed to set overnight.

Serial 4μm sections were cut using a microtome and mounted onto plain glass slides. One section from each block was dewaxed and rehydrated by two 10 minute washes in xylene, followed by 10 minute washes in 100%, 90% and 70% ethanol, and water. Sections were stained using haemotoxylin and eosin, and dehydrated through graded alcohols and xylene. Coverslips were mounted using DepEx.

2.8.2 Immunohistochemistry

Immunohistochemistry was carried out on 4μm cut sections mounted onto glass slides. Sections were dewaxed and dehydrated by two 10 minute washes in xylene, followed by 10 minute washes in 100%, 90% and 70% ethanol before being transferred to water. Endogenous peroxidase activity was blocked by incubation in 3% hydrogen peroxide in methanol for 30 minutes.

Antigen retrieval was carried out by pressure cooking the slides at 16psi in 0.01M sodium citrate buffer (10mM) for 3 minutes, and were subsequently transferred to PBS.

Sections were pre-blocked using 1.5% serum in PBS for 30 minutes. The serum used depended on the source of the secondary antibody used. For mouse derived primary antibodies, whole horse serum was used; and for rabbit derived primary antibodies, whole goat serum was used. The sections were then incubated with the primary antibody at an appropriate dilution in PBS for 1 hour at room temperature, before being washed twice with PBS. Antibody-antigen binding was detected using biotinylated secondary antibodies at a dilution of 1:200 in PBS for 30 minutes at room temperature. Goat-derived anti-rabbit IgG (BA-1000, Vector laboratories) was used for rabbit-derived primary antibodies, and horse-derived anti-mouse IgG (BA-2080, Vector laboratories) was used for mouse-derived primary antibodies. Sections were again washed twice in PBS and were incubated with a streptavidin-horseradish peroxidase complex (Dako), diluted 1:200 in PBS, for 30 minutes. Following this, the sections were washed twice more in PBS.

Sites of peroxidase activity were detected by incubation with 3-3'-diaminobenzidine (Dab, Sigma-Aldrich) for 5 minutes. The reaction was quenched by flushing the sections with water. Slides were subsequently counterstained for 15 seconds in Mayer's haematoxylin before being dehydrated through 2 minute washes in 70%, 90% and 100% ethanol, and xylene. Coverslips were mounted using DepEx.

Patterns of staining were evaluated as absent (-), weak (+), moderate (++), strong (+++) and very strong (++++) by semi-quantitative observation of

20 high power fields for all antibodies with cytosplasmic staining. Staining of nuclear markers, such as PCNA, was assessed by percentage of stained nuclei: <10% (-), 10-25% (+), 25-50% (++), 50-75% (+++), and >75% (++++). Scoring was undertaken blind by two independent observers under the guidance of histopathologists.

2.9 Electron Microscopy

All electron microscopy procedures, including tissue preparation, staining and electron microscopy, were carried out by Mr Bart Wagner at the Northern General Hospital, Sheffield, UK.

Samples were collected fresh from surgery and fixed in 2.5% (v/v) glutaraldehyde in phosphate buffer (pH7.4). Fixed samples were diced into $1mm^3$ cubes, rinsed in distilled water, transferred into 1% aqueous osmium tetraoxide and embedded in TAAB Emix resin. Sections of 0.6μm were cut, mounted on glass slides, and stained in 1% toluidine blue in 1% sodium tetraborate for 30s on a hot plate at 140°C. After checking the histology of the samples, they were sectioned with a diamond knife in a Leic Ultracut E ultramicrotome, with interference colour gold of approximately 95nm. Sections were stained by immersion for 3 min in 99% alcoholic saturated uranyl water, 3 min in Reynolds lead citrate and thres washes in distilled water, and examined by a Philips 400 transmission electron microscope.

2.10 Fluorescent in-situ hybridisation (FISH)

Probe was prepared from isolated BAC DNA (2.2.4) and labelled using the Invitrogen Nick Translation kit. 500ng of DNA was diluted to a total volume of 17µl in nuclease free water. This was mixed with 2.5µl of 10x dNTP (low dUTP) mix from the kit, and 0.5µl dUTP-Rhodamine (red) or dUTP-Fluorescein (green) (Roche) and 5µl of Nick Translationenzyme mix. The reaction was incubated at 16°C for 2hrs and stopped with 2.5µl stop buffer.

The probe was then precipitated by combining 10µl of the labelling reaction mixture with 5µl C_0t-1 DNA (1mg/ml, Roche), 2µl Salmon sperm DNA (10mg/ml), 2µl of 3M sodium acetate (pH 5.2) and 50µl of cold ethanol. The probe was left to precipitate overnight at -20°C.

Purchased normal metaphase spread slides were prepared for hybridisation by incubation in 70% deionised formamide/2xSSC at 65°C for 2 mins, followed by a wash in 70% ice-cold ethanol for 3 mins and subsequent 3 min washes in 90% and 100% ethanol at room temperature. The slide was then allowed to air dry.

The precipitated probe was pelleted by centrifugation at top speed in a microcentrifuge at 4°C for 15 mins. The supernatant was removed and the pellet allowed to air dry before resuspension in 5µl hybridisation buffer (50% deionised formamide, 10% Dextran sulphate, 0.1% Tween-20, 2x SSC, 10mM Tris (pH 7.4)). The hybridisation mixture was vortexed to mix and incubated at 70°C for 5 mins, with occasional vortexing to resuspend the pellet. The probe was then placed at 37°C for ½ hr to compete.

Following this incubation, 5µl of rhodamine-labelled probe was spotted onto one half of the metaphase slide, followed by 5µl of fluorescein-labelled probe on top (the other half was used for a different pair of probes). A 22x22mm cover slip was gently dropped onto the hybridisation mix and the edges were sealed with rubber cement. The slide was placed in a box humidified with 50% formamide/2xSSC overnight at 37°C.

Washing of the slide was carried out the following day. All washing steps were carried out at 42°C using solutions pre-warmed to that temperature. The cover slip was carefully removed from each slide, and the slide was washed 3 times for 5 mins each in 50% formamide/2xSSC, followed by 3 x 5 mins washes in 2xSSC. The slides were then washed in 1xPBS/0.1% Tween-20 at room temperature for 5mins. Finally, the slides were washed in 70%, 90% and 100% ethanol at room temperature for 3 mins each, before being allowed to air dry. The slides were counterstained with DAPI and captured using a cooled CCD camera (Photometrics) attached to a Zeiss Axioplan 2 Imaging microscope and SmartCapture 2 software (Applied Imaging).

2.11 Microarray techniques

2.11.1 Microarray CGH

2.11.1.1 Microarrays

Two different CGH arrays were used in experiments in this thesis. The first was a 1Mb resolution array designed by Nigel Carter's group at the Wellcome Trust Sanger Centre in Cambridge. This array consisted of 3125 human Bacterial Artificial Chromosome (BAC) clones, amplified by degenerate oligonucleotide primer PCR (DOP-PCR) and printed in duplicate on to glass slides. In addition, 6 BAC clones from *Drosophila melanogaster* were also printed onto the array as a control for background hybridisation.

The BAC clones were selected from the Golden Path at a spacing of approximately 1Mb, excluding the short arms of the acrocentric chromosomes. Clones FISH-mapped to a single location or localised to known oncogenes and tumour suppressors were preferred, but the selection was arbitrary in a majority of cases (Fiegler et al. 2003).

The second microarray used was a tile-path resolution array for chromosome 7q, designed and prepared as described in Chapter 7.

2.11.1.2 Array printing and preparation

Array printing was carried out by Cordelia Langford at the Wellcome Trust Sanger Centre in Cambridge. Aminolinked PCR products were diluted into 1x printing buffer (250mM Sodium Phosphate pH 9.0, 0.000001% N-Laurylsarcosine) and filtered through 0.22μm filter plates (Millipore), before

re-arraying into 384-well plates. The DNA products were printed onto Codelink™ activated slides (GE healthcare) using a Microgrid II array spotter (Biorobotics).

Printed slides were transferred to a humid chamber at room temperature for 72 hours to drive the covalent attachment of the DNA to the slides. They were then immersed in 1% w/v ammonium hydroxide for 5 min, 0.1% sodium dodecyl sulphate for 5 min, and rinsed in water. The bound DNA was denatured by immersing the slides in water at 95°C for 2 min, before being rinsed in ice-cold water and dried by centrifugation.

2.11.1.3 DNA labelling and purification

500ng of normal ('Reference') and tumour ('Test') DNAs were labelled using Cy3-dCTP and Cy5-dCTP (Amersham) respectively, using the Bioprime array CGH labelling kit (Invitrogen), according to the manufacturer's instructions. Briefly, DNA was diluted to a volume of 21μl in nuclease-free water and combined with 20μl random octamer primers in 2.5x buffer (125mM Tris-Hcl (pH 6.8), 12.5mM $MgCl_2$, 25mM β-mercaptoethanol, 750μg/ml random octamers). The sample was incubated at 100°C for 10 minutes and immediately cooled on ice. 5μl of dNTP mix (1.2mM dATP, dGTP and dCTP, 0.6mM dCTP), 3μl of Cy3- or Cy5-dCTP (1μM) and 1μl of Exo-Klenow fragment (40U/μl) were mixed with the cooled sample. The samples were incubated overnight at 37°C. Reactions were stopped by the addition of 5μl 0.5M EDTA.

Labelled DNA was purified using Microspin G-50 columns (Amersham) according to the manufacturer's protocol. DNA samples were run on a 2% TBE-agarose gel at 120V for 20mins to check DNA labelling. Successfully labelled samples produced a low-molecular weight smear (~50-200bp) when viewed under UV light.

2.11.1.4 DNA precipitation and hybridisation

A seal was formed around the edge of the arrayed area on printed slides using 2 layers of adhesive PCR film (ABgene, cat no. AB-0558), cut with reference to a 'dummy' printed slide.

Labelled test and reference DNA samples were combined and precipitated with 135μg C_0t-1 DNA (Roche) in 0.1 volumes 3M sodium acetate (pH 5.2) and 2.5 volumes of ice-cold ethanol at -80°C for 30 minutes. Concurrently, 10μg of Herring sperm DNA was precipitated with 135μg C_0t-1 DNA. Precipitated DNA was pelleted by centrifugation at 16,000g for 15 minutes. The resultant pellet was washed with 80% ice-cold ethanol and re-pelleted at 16,000g for 5 minutes. The supernatant was removed and the pellet dried.

The labelled pellet was re-suspended in 80μl hybridisation buffer (50% deionised formamide, 10% Dextran sulphate, 0.1% Tween-20, 2x SSC, 10mM Tris (pH 7.4)) and 8μl yeast tRNA (100μg/μl, Invitrogen). The herring-sperm pellet was re-suspended in 180μl hybridisation buffer. Both samples were heated at 80°C and frequently mixed by vortex until the pellets were re-suspended. The labelled DNA sample was then placed at 37°C for 1 hour to

allow the labelled samples to compete with the C_0t-1 DNA, blocking repetitive sequences. The re-suspended herring sperm DNA mixture was carefully pipetted onto the prepared slide to pre-hybridise for 1 hour at 37°C in a humid chamber formed of a slide box containing 3MM paper (Whatman) soaked in 40% formamide/2x SSC.

Following competition, the labelled DNA sample was added to the pre-hybridised array. The humidity chamber was sealed with electrical tape and the array was incubated at 37°C with gentle rocking for 48 hours.

2.11.1.5 Array washing and scanning

All wash stages were carried out in reduced lighting. Arrays were removed from the humidity chamber and placed in wash buffer 1 (2x SSC/0.1% Tween-20) in a coplin jar at room temperature. The seal was carefully removed after about 30 seconds. The arrays were washed in this solution with rocking for 5 minutes. Arrays were then washed in wash buffer 1 at 65°C for 5 mins before being transferred to wash buffer B (0.2x SSC). Arrays were washed 4 times in wash buffer 2 (1x 2min, 3x 20mins) at room temperature before being transferred to wash buffer 3 (1x PBS, 0.1% Tween-20), for 5 minutes, then wash buffer 4 (1x PBS) for 5 minutes, and a final brief wash in ddH_2O. The arrays were dried by centrifugation at ~500g for 5 minutes in slide boxes lined with bleach-free paper towels and stored at room temperature in black boxes before scanning.

Arrays were scanned using a Scanarray confocal scanner and software (Perkin-Elmer). Each array was pre-scanned to and settings adjusted to ensure even signal from both the Cy3 and Cy5 channels. Arrays were then scanned at

10μm resolution, and TIFF image files of each channel saved for analysis.

Details of downstream analysis of image files can be found in 2.13.2.

2.11.2 Mitochondrial DNA resequencing array

The mtDNA resequencing array allows a complete mtDNA sequence to be derived from high-quality DNA samples. The arrays are able to identify heteroplasmy, and are over-tiled to take into account common variants, identified on the FBI mtDNA database. The resequencing protocol was divided into three sections: the first involved PCR amplification of specific mtDNA fragments; the second involved the labelling of samples, hybridisation and washing of the arrays; and the final stage involved scanning and data analysis.

2.11.2.1 PCR amplification of mtDNA fragments.

The mitochondrial genome of each sample was amplified into two long fragments, using specific primers designed by Affymetrix (**Table 2.3**). Amplification was carried out using TaKaRa LA Taq by a modified procedure. In addition to the test DNA sample, a 7.5kb control PCR and a negative control for each primer set were also run.

All PCR preparation procedures were carried out on ice after UV sterilisation. Primer stocks were diluted to 100μM in 0.1x TE. A primer pair stock was created by diluting 100μl of forward and reverse primer in 800μl of 0.1x TE, giving a final concentration of 10μM for each primer. For each reaction, 6μl of primer pair stock was diluted in 14μl of molecular biology grade water. 100ng of genomic DNA sample was diluted to 5ng/μl in molecular biology grade water, giving a total volume of 20μl. This was combined with the 20μl primer pair mix. A 100μl reaction volume was prepared with final concentrations of 1x LA PCR buffer, 2.5mM $MgCl_2$,

400μM dNTPs and 5U LA Taq enzyme. The reaction was run to the cycle shown in **Table 2.4**, and resulting products analysed on a 0.8% TBE-agarose gel run for 1 hour at 100V.

Table 2.3 Primers for amplification of mtDNA fragments.

Primer Name	**Forward Primer**	**Fragment Size**
Mito1-2F	ACATAGCACATTACAGTCAAATCCCTTCTCGTCCC	9307bp
Mito1-2R	ATTGCTAGGGTGGCGCTTCCAATTAGGTGC	
Mito3F	TCATTTTTATTGCCACAACTAACCTCCTCGGACTC	7814bp
Mito3R	CGTGATGTCTTATTTAAGGGGAACGTGTGGGCTAT	

Table 2.4 Thermal cycler program for mtDNA fragment amplification.

Temperature	**Time**	**Cycles**
94°C	2 minutes	1x
94°C	15 seconds	30x
68°C	1 minute/kb product size	
68°C	5 minutes + 1 minute/kb	1x
4°C	HOLD	

2.11.2.2 PCR product quantification, pooling, fragmentation, labelling and hybridisation

PCR products were purified using the Qiaquick PCR purification kit (Qiagen), and eluted in 30µl buffer EB. The concentration of each fragment, including the positive control, was calculated as described (2.2.5). Each fragment, including the positive control was diluted to a final concentration of 250pM and combined. Subsequent steps, including fragmentation, labelling, and hybridisation were carried out by the manufacturer's recommended protocol.

2.11.2.3 Array washing, scanning and data analysis.

Hybridised arrays were washed and scanned by the manufacturers protocol using an Affymetrix fluidics station and scanner. Sequence data was derived using the software GSEQ (Affymetrix). Analysis was carried out as an overall batch analysis of every array run from a manufactured batch using a diploid data analysis model in order to detect heteroplasmy. Data was exported as FASTA DNA sequence files, and a delimited file detailing identified changes.

2.12 Formulation of standard media and solutions

2.12.1 Buffers and saline

2.12.1.1 Phosphate Buffered Saline (1x)

Component	Mass for 1l (Conc)	Notes
NaCl	8g (137mM)	Check pH = 7.4 Autoclave
KCl	0.25g (2.7mM)	
Na_2HPO_4	1.43g (Total 10mM PO_4)	
KH_2PO_4	0.25g	

2.12.1.2 1M Tris (Various pH values)

Component	Mass for 1l (1M)	Notes
Tris base	121.14g	pH as desired using HCl Autoclave

2.12.1.3 0.5M EDTA (pH 8.0)

Component	Mass for 1l (0.5M)	Notes
Na-EDTA	184.1g	pH to 8.0 with 1M NaOH Autoclave

2.12.1.4 TE Buffer (1x)

Component	Vol for 1l (Conc)	Notes
1M Tris (pH 8.0)	10ml (10mM)	0.2μm filter and UV sterilise for 15min
0.5mM EDTA (pH 8.0)	2ml (1mM)	

2.12.1.5 SSC Buffer (20x)

Component	Mass for 1l (Conc)	Notes
NaCl	175.32g (3M)	pH to 7.0 with 1M NaOH
Na-Citrate	88.23g (0.3M)	Autoclave

2.12.1.6 TBE Buffer (10x)

Component	Mass for 1l (Conc)	Notes
Tris base	108g (0.89M)	pH should be 8.3, requiring
Boric Acid	55g (0.89M)	no adjustment
Na-EDTA	9.3g (0.02M)	Autoclave

2.12.2 Bacteriological Media

2.12.2.1 L-Broth

Component	Mass for 1l	Notes
Bacto-tryptone	10g	Autoclave
Yeast Extract	5g	
NaCl	10g	

2.12.2.2 L-Broth Agar (For 1 litre)

As for L-Broth, add 15g agar per litre.

2.12.2.3 Buffers for BAC DNA extraction

P1

Component	Volume for 1l (Conc)	Notes
1M Tris (pH 8.0)	50mls (50mM)	Filter sterilise, store at 4°C
0.5M EDTA (pH 8.0)	20mls (10mM)	
RNase A (10mg/ml)	10mls (100μg/ml)	

P2

Component	Volume for 1l (Conc)	Notes
1M NaOH	200mls (0.2M)	Filter sterilise, store at RT
20% SDS	50mls (1%)	

P3

Component	Mass for 1l (Conc)	Notes
Potassium Acetate	294.5g (3M)	pH to 5.5, autoclave, store at 4°C

2.13 Data Analysis

2.13.1 Statistical Analysis

Statistical analysis was carried out using the software R (Team 2006). This provides a framework to carry out a number of statistical calculations. Individual significance values and tests utilised are described in each chapter.

2.13.2 Microarray CGH data analysis

2.13.2.1 Rationale

All microarray based experiments produce large quantities of data, which must be dealt with in a robust manner in order to obtain valid and significant results. Probably the two most important issue facing researchers in this field are: 1) Normalisation of the data, where raw ratios are transformed to a defined baseline, accounting for artefacts of the experimental procedure, such as uneven hybridisations or differences in the brightness of individual images; and 2) The selection of significant regions of change for further study. The approaches used for both of these issues are described below, along with the additional data analysis steps.

2.13.2.2 Data analysis

Fiegler *et al* broke down array data analysis into several individual stages (Fiegler et al. 2003):

i) Overlaying image files and data-point quantification: Individual output files for each fluorescent dye channel are overlaid, and the intensity of individual spots is calculated.

ii) Data rejection: Individual spots are accepted or rejected on the basis of spot quality and the level of background hybridisation. Data is then normalised to the number of copies of test genome per copy of reference genome.

iii) Normalisation: Accepted data values are normalised across the array to give a ratio of the number of test genomes per copy of the reference genome.

iii) Duplicate rejection: Variability of data for duplicated spots of clones is compared, and excessively variable data is rejected.

iv) Identification of significant changes: Final calculated log2 ratios are used to identify regions of altered copy number in the test DNA sample with respect to the reference sample.

2.13.2.2.1 Overlaying Image Files

Scanned microarrays were overlaid and quantified using the freeware Spot (Jain et al. 2002). The software overlays the Cy3 and Cy5 array images, and calculates intensity values for each spot on the array using a local histogram method. This method takes into account non-circular spot morphologies, which may occur as a result of printing, providing accurate intensity values for each spot.

2.13.2.2.2 Drosophila clone-based rejection

In addition to the human BAC clones, the array contains 6 clones from *Drosophila melanogaster.* These clones were known not to hybridise to human DNA, and so were used as a measure of non-specific hybridisation. Individual spots were accepted or rejected after comparison with the *Drosophila* clone values. For an individual spot to be accepted, the reference (Cy3) intensity was required to be greater than twice the median reference

intensity of the *Drosophila* clones. This stage of rejection was only carried out using the reference intensities, since in the case of a homozygous deletion of a particular region, the test (Cy5) intensity would be expected to be at the level of background hybridisation, thus additional rejection on the basis of this parameter could lead to the exclusion of particularly interesting data.

2.13.2.2.3 Normalisation

The process of normalisation adjusts for systematic differences in the relative intensity of each channel, such that the normalised ratio identifies the number of test genomes per single copy of the reference genome. In early experiments using the arrays, data analysis was carried out in a Microsoft Excel spreadsheet written by Heike Fiegler in Nigel Carter's group at the Wellcome Trust Sanger Institute. (Fiegler et al. 2003)

This method of analysis normalised the data by block, or print-tip normalisation. The median of the accepted test/reference ratios for each block was calculated, and each ratio was divided by this median. As a comparison, a global normalisation, using the median accepted ratio for the whole array, was carried out. The use of block normalisation accounted for local differences on the array, which global normalisation could not account for, and hence reduced the spread of data and made changes more pronounced (**Figure 2.1**).

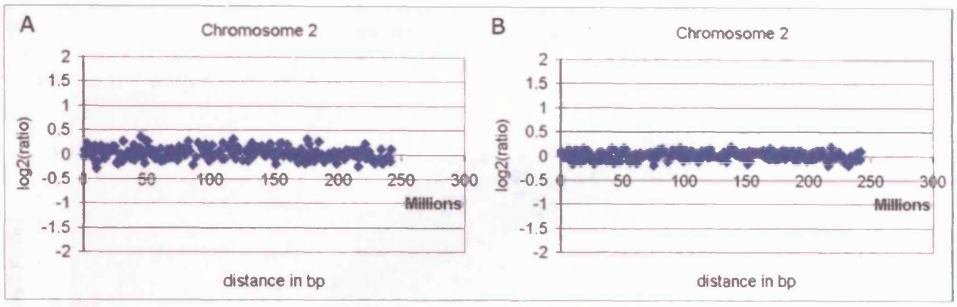

Figure 2.1 Comparison of global and block normalisation of array CGH data. In this example output of chromosome 2, block normalised data (B) demonstrates less spread than globally normalised data (A). This allows genuine changes to be more easily identified.

A study of published literature regarding microarray normalisation revealed a further factor found to affect data in cDNA expression array experiments (Yang et al. 2002). Variation between the Cy3 and Cy5 channels was found to not always be constant, but to change as a function of signal intensity. To see if this was the case for BAC-based CGH arrays, an MA plot was drawn (**Figure 2.2**a), whereby the spot intensity ($A = \log_{10}(Test*Ref)$, where *Test* and *Ref* are the raw signal intensities of the Cy5 and Cy3 channels respectively) is plotted against the raw log2 ratios ($M = \log_2(Test/Ref)$). An MA plot was also drawn to compare the intensity to block normalised log2 ratios (**Figure 2.2**b). In a number of samples, particularly those with a broad spread of data, a distinctive curve pattern of data was observed. As the intensity of a spot increased, so did the log2 ratio. Even after block normalisation, this pattern remained. Therefore, an alternative form of normalisation to overcome this effect was necessary.

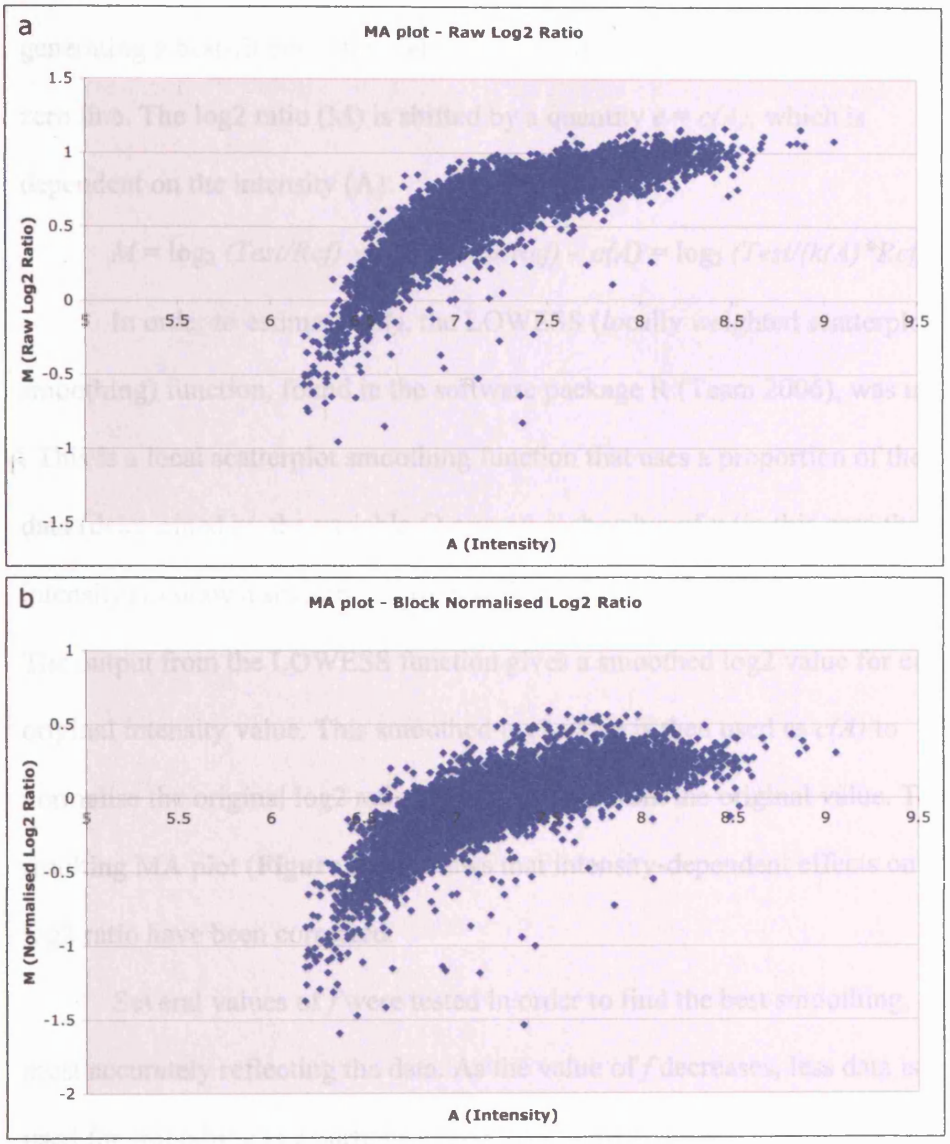

Figure 2.2 MA plots of array CGH data. Plotting intensity (A) against raw log2 ratios (M) shows a distinctive curve pattern indicative of intensity-dependent effects on the log2 ratios (a). This curved pattern remains even after block median normalisation (b).

Intensity dependent effects on log2 ratios can be corrected by generating a best-fit curve through the data and treating this curve as the new zero line. The log2 ratio (M) is shifted by a quantity $c = c(A)$, which is dependent on the intensity (A):

$$M = \log_2 (Test/Ref) \rightarrow \log_2 (Test/Ref) - c(A) = \log_2 (Test/(k(A)*Ref)$$

In order to estimate $c(A)$, the LOWESS (*lo*cally *we*ighted *s*catterplot *s*moothing) function, found in the software package R (Team 2006), was used . This is a local scatterplot smoothing function that uses a proportion of the data (determined by the variable f) around each value of x (in this case the intensity) to draw a smooth line of best fit through the data (Cleveland 1981). The output from the LOWESS function gives a smoothed log2 value for each original intensity value. This smoothed log2 value is then used as $c(A)$ to normalise the original log2 ratios by subtraction from the original value. The resulting MA plot (**Figure 2.3**b) shows that intensity-dependent effects on the log2 ratio have been corrected.

Several values of f were tested in order to find the best smoothing, most accurately reflecting the data. As the value of f decreases, less data is used for smoothing at a particular point. While this can lead to more accurate smoothing, local outliers can affect the smoothed data. A value of 0 (orange line in **Figure 2.3**a), did not use enough local data and gave a rough line affected by local outliers in the data, whereas higher values of f, such as 0.3 and 0.4 (green and blue lines in **Figure** 2.3a respectively) gave a smooth line, but did not reflect the fit of the data at intensities with sparse data, in this case at lower spot intensities. The best fit for global lowess correction was obtained

using a value for *f* of 0.2 (red line in **Figure 2.3**a), which produced a smooth line, unaffected by outliers, which reflected the data at lower intensities.

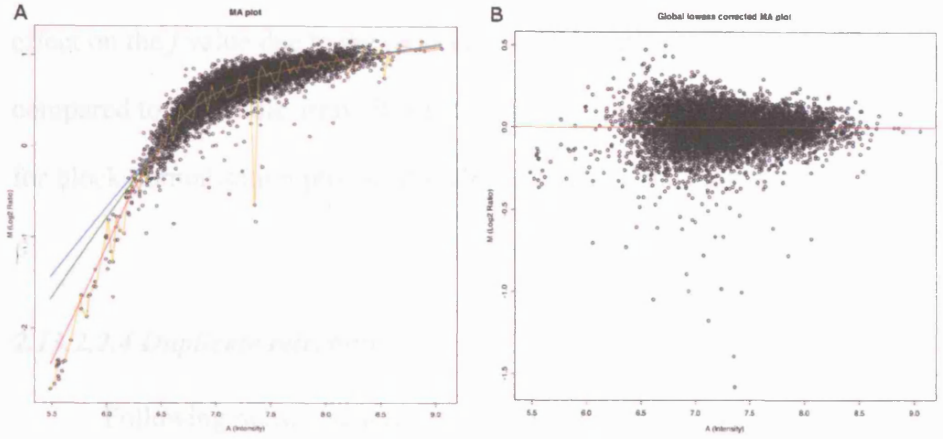

Figure 2.3 Global lowess correction of 1Mb array CGH data. (A) Raw MA plot with lowess smoothed lines using different values of *f*: 0=orange; 0.2=red; 0.3=green; 0.4=blue. The lowest value of *f* gives a rough line skewed by outliers, whereas the higher values do not accurately reflect the data at a lower intensity value. A value of 0.2 gave the most accurate smoothing. After normalisation by subtraction (B), the corrected MA plot shows that intensity dependent effects on the log2 ratio have been removed.

As for the median ratio-based method of normalisation (Fiegler et al. 2003), it was decided to normalise each block on the array individually. This would account for differences in hybridisation across the array. A separate lowess line was calculated for each block, and used to normalise log2 ratios within that block. This method reduced the spread of the normalised data compared to lowess normalisation across the entire array. For example, in the dataset used in **Figure 2.3**, the raw data had a standard deviation of 0.3254.

Global lowess normalised data had a standard deviation of 0.1218, whereas block lowess normalised data had a standard deviation of 0.1081. Therefore, block normalisation reduced the spread of the data.

One further consideration of block LOWESS normalisation is the effect on the *f* value due to the reduced number of data points per block, compared to the whole array. It was found that increasing the value of *f* to 0.25 for block normalisation produced smoothed lines of the most accurate fit.

2.13.2.2.4 Duplicate rejection

Following normalisation, duplicate clone spots on the array are compared to ensure that each spotted clone is giving an identical hybridisation ratio. This is carried out by taking the median of the normalised *Test/Ref* ratios of the duplicates and assessing the deviation of the original ratios from this median. If duplicates lie outside the greater of 10% or 0.1 of this median, then the entire clone is rejected, if not, this median is used to calculate the final log2 ratio for the clone.

2.13.2.2.5 Identification of significant changes

2.13.2.2.5.1 Rationale

The ultimate aim of microarray CGH experiments is the identification of regions of copy number change, and where these regions begin and end. Accurate breakpoint identification can help to identify and minimise regions harbouring genes of interest and importance in a tumour type. The initial stages of analysis, from overlaying image files through to normalisation and duplicate rejection, are concerned with producing the best possible data in order that false changes are minimised, and actual changes are retained. This gives the best possible platform for identifying significant changes that may have biological relevance.

2.13.2.2.5.2 Problems faced in identifying changes

Theoretically, the output log2 ratios for each clone are representative of the number of copies of the test genome per copy of the reference genome. For example, a diploid tumour losing one copy of chromosome 15 would give a ratio of 0.5, one copy of the tumour genome per 2 copies of the reference genome, and an expected log2 ratio of -1. Therefore, identification of copy number changes should be a case of simply observing which clones are at the theoretical log2 ratio.

However, these theoretical thresholds are rarely met. In theory, only two factors should have an effect on the thresholds: contaminating normal DNA, which would dilute the change; and tumour ploidy, where copy number change in a polyploid tumour, for example loss of one chromosome in 3 in a

triploid tumour, results in a smaller log2 ratio difference. To account for both of these factors, one requires accurate information regarding the ploidy status of the tumour, and the amount of contaminating normal, to adjust thresholds, neither of which are easy to determine.

Yee-Loi Wan of our lab carried out experiments examining the effects of contaminating normal on the 16q CGH profile of the breast cancer cell line, MPE-600. This is a diploid cell line with a single copy loss of 16q. Since the DNA came from a pure population of cells, a log2 ratio of -1 would be expected with no contaminating normal present. However, the mean log2 ratio of clones in the deleted region was consistently less than the expected ratio **(Figure 2.4)**.

These differences are likely to be due to a number of factors inherent within the experimental and analytical procedure. The theoretical threshold requires absolute accuracy throughout the preparation of the arrays, the hybridisation, washing and analysis. In a procedure involving such a large number of stages, variation is very likely to occur such that theoretical values are not observed. These variations can occur at the stage of clone amplification, printing, array hybridisation, washing, and data analysis. It is important to note, however, that although the threshold values are not met, the values observed in the experiment in **Figure 2.4** are consistently the same proportion below the theoretical value. Thus, the data from the arrays is valid for identifying copy number variation.

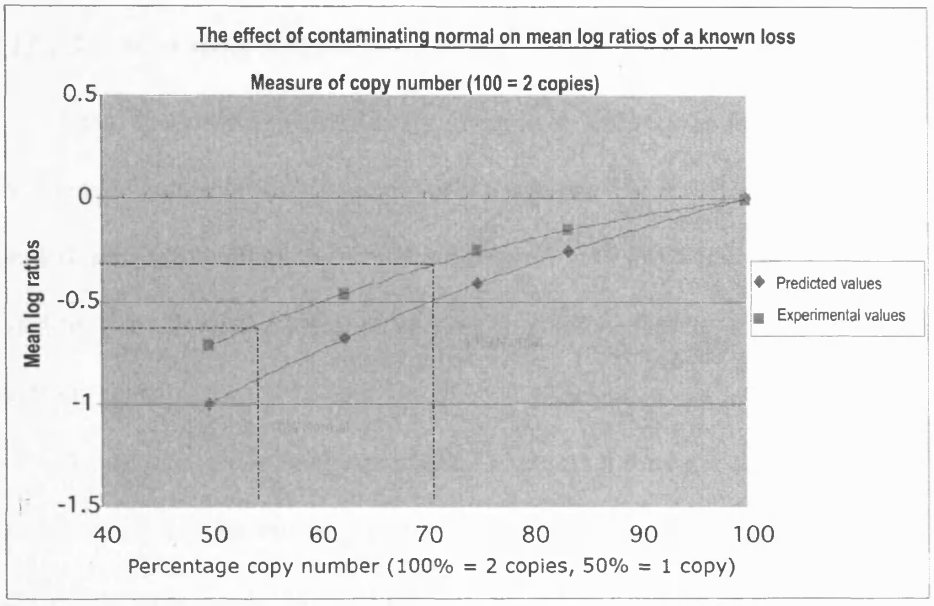

Figure 2.4 Effect of contaminating normal on known loss. Contamination of MPE-600 DNA with a known loss of 16q with normal DNA reduces the observed log2 ratio. The experimental log2 ratios always fail to reach the expected values, even where there is no contaminating normal. The difference between the expected and actual results appears proportionally the same through different levels of contaminating normal.

2.13.2.2.6 Identifying significant changes

Since theoretical thresholds are rarely met, and require presumed knowledge of tumour ploidy and normal tissue content, a different method of identifying significant changes was required. A series of 7 normal-normal hybridisations, both sex-matched and sex-mismatched, were used to derive the method.

A box plot of the final, normalised log2 ratios for each chromosome following a normal-normal hybridisation reveals differences in the spread of data within each chromosome (Figure 2.5a). These differences were conserved between control experiments. For example, chromosome 19 frequently showed a greater spread of data than other chromosomes. Thus, the distribution of data for each chromosome was different to the distribution for the overall array. Therefore, thresholds derived from the distribution of the whole array would not be as accurate for individual chromosomes, leading to false positive and negative calls of copy number change.

In order to overcome this, the data was rescaled in order to transform the data for each chromosome onto the same distribution as the whole array. Scaling factors were derived by calculating the ratio of the chromosome interquartile range (IQR) to the autosome IQR. The mean ratio for each chromosome from seven control hybridisations was used as a scaling factor. Log2 ratios were scaled on a per chromosome basis by dividing each ratio by the appropriate scaling factor (**Table 2.5**). This resulted in a more comparable spread of data between chromosomes (Figure 2.5b), reducing the potential for false positives or negatives. This scaling was not carried out on the sex chromosomes.

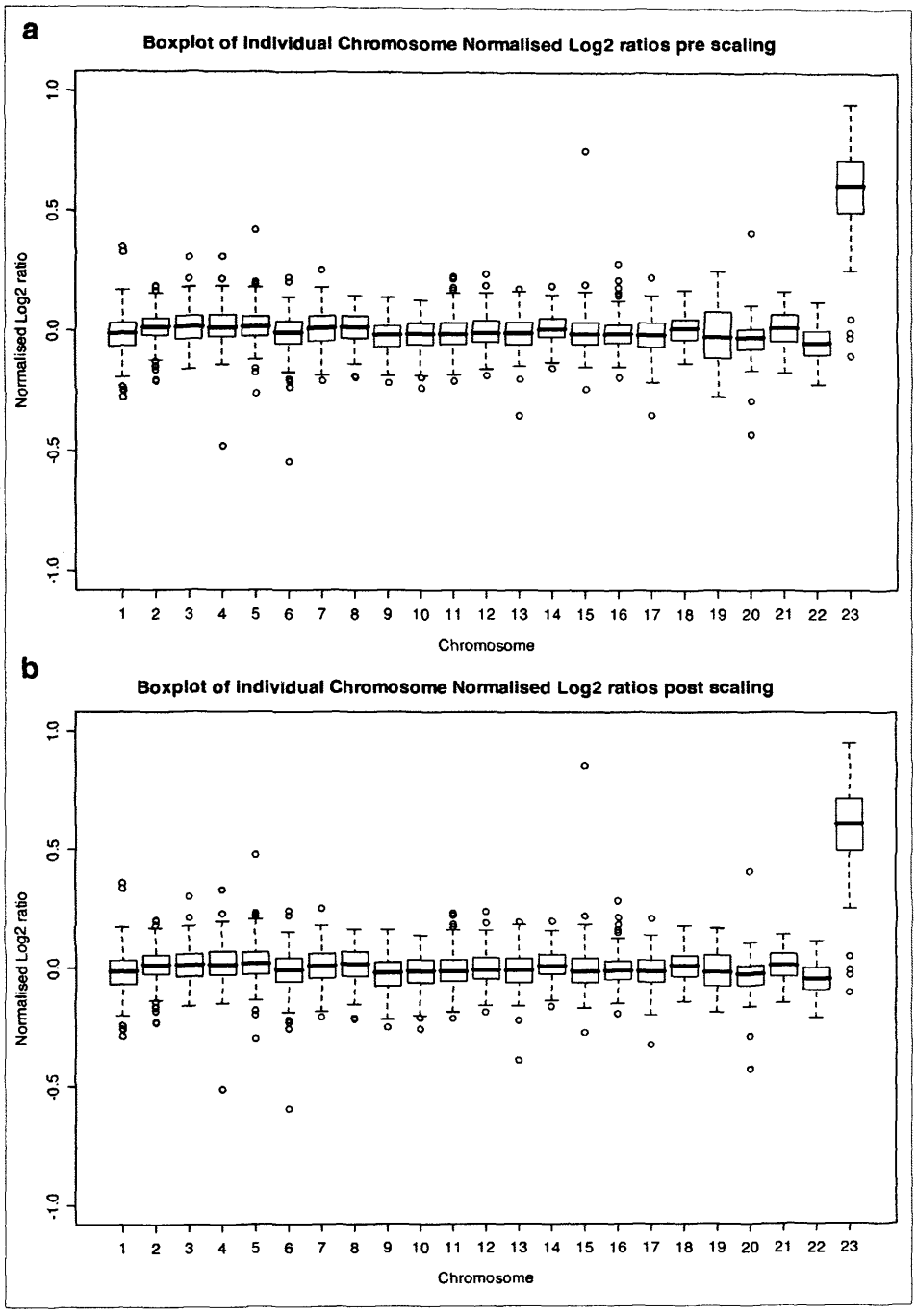

Figure 2.5 Box plots of the spread of normalised log2 ratios from a normal male vs. female hybridisation. a) Pre-scaling, there is a greater variability in the spread of data between chromosomes, particularly in chromosome 19. b) After rescaling of the data, the distribution of data between each chromosome is more even

Table 2.5 Scaling factors for individual autosomes derived from chromosome interquartile ranges from 7 normal-normal hybridisations

Chromosome	Scaling Factor	Chromosome	Scaling Factor
1	0.965973938	12	0.995602788
2	0.910571526	13	0.902563854
3	1.004879797	14	0.950534457
4	0.938298957	15	0.883567966
5	0.878673476	16	0.991388402
6	0.918211228	17	1.077342838
7	1.006211423	18	0.949672773
8	0.892522767	19	1.467918832
9	0.861630166	20	1.008651688
10	0.92227046	21	1.175069821
11	0.97822635	22	1.058064909

A histogram of the scaled, normalised data (**Figure 2.6**) demonstrates that the log2 ratios are normally distributed about a median of approximately 0. For each array, the median (Md) and standard deviation (σ) of the scaled log2 ratios of the autosomal clones were calculated. Since most regions of copy number change are greater than one clone in length, less stringent thresholds were set for consecutive clone changes. Therefore, three thresholds were initially set based on the 2-sided z-score for three probability values: For a single clone change, the threshold was $Md \pm 3.291 * \sigma$ ($p=0.001$); for 3 consecutive clones, the threshold was $Md \pm 2.576 * \sigma$ ($p=0.01$); and for 5 consecutive clones, the threshold was $Md \pm 1.960 * \sigma$.

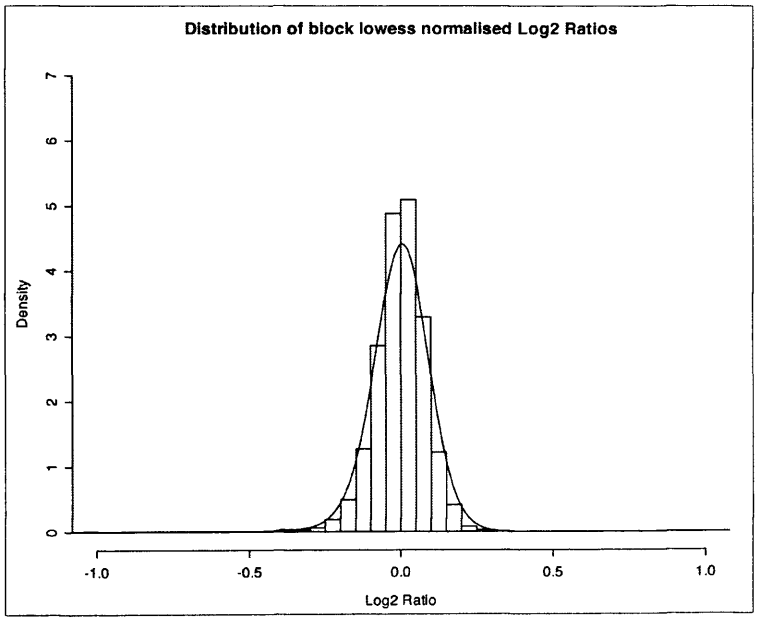

Figure 2.6 Frequency distribution of normalised log2 ratios. The normalised log2 ratios follow a normal distribution about a median of 0.

In addition to the raw log2 ratio, a 3 and 5 clone local median was calculated for each clone. These medians were compared to the 3 and 5-clone thresholds respectively. If the local median lay outside its respective threshold, the clones used to calculate that median were all considered to have a copy number change. Since a local median of clones is used, rather than a mean, a majority of clones used to calculate a local median must be above the respective threshold.

Changes were identified using the single clone threshold first, followed by the 3-clone threshold, and finally the 5-clone threshold. If a particular clone had a copy number change called at a more stringent threshold, it was not considered at a less stringent threshold. This is summarised in (**Figure 2.7**). This removes the possibility of false calls. For example, if 2 of 3 consecutive clones have a change that is detected at the 1 clone threshold, taking a 3 clone median of these clones would increase the area of copy number change by one clone either side, since the median of these clones would be skewed by the 2 consecutive changes at the 1 clone threshold and would be greater than the 3 clone gain threshold.

Finally, the assumption was made that if a clone appeared to not have any change, but was flanked by clones with identical called changes, then that clone would also be called changed. This assumption was already made when calculating local medians, since only a majority, not all, of the clones used to calculate the local median are required to exceed the respective threshold. This takes into account some clones that may be flanked by clones with copy number changes.

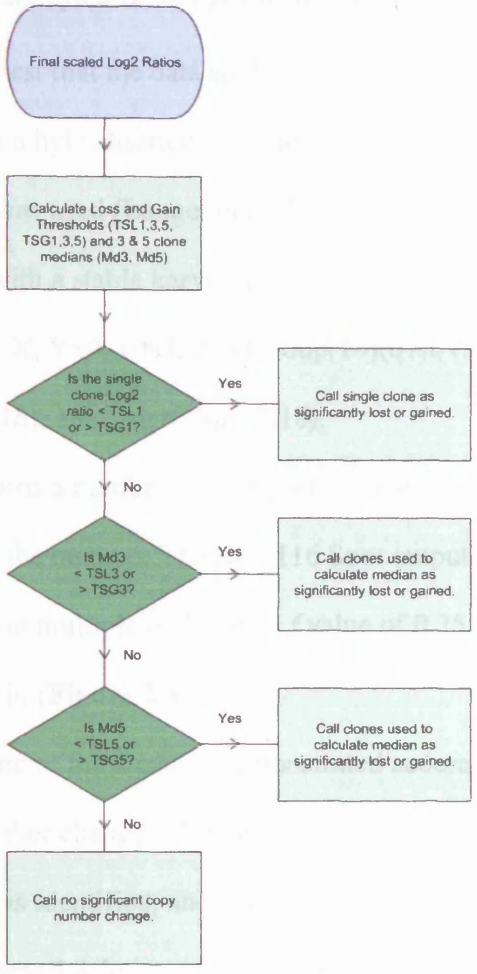

Figure 2.7 Flowchart for selecting significant copy number changes. Once a particular clone has been called lost or gained, it is not considered at lower thresholds.

The final analysis program, which carries out analysis using the file derived from UCSF Spot (Jain et al. 2002), was written in R (Team 2006). This carries out the analysis described above in one process with user-definable parameters of the *f* value for lowess normalisation, and the multiple of *Drosophila* clone intensities used for initial spot rejection.

2.13.2.2.7 Testing significant changes using the HCT116 cell line

In order to test that the data analysis was identifying significant changes, data from a hybridisation of normal female DNA to the colon cancer cell line HCT116 was used (Langer et al. 2005). This is a microsatellite unstable cell line with a stable karyotype of:

45 (43-45), X, Yx0, 10x1, der(10)dup(10)(q?)t(10:16), 16x1, der(16)t(8;16), 18x1, der(18)t(17;18).

This cell line contains a number of characterised copy number changes, which can be used to test the method. The HCT116 Spot output file was run using a *Drosophila* rejection multiple of 2 and an *f* value of 0.25. A plot of the results and calls is shown in (**Figure 2.8**).

The outcome of the analysis demonstrated accurate identification of expected copy number changes. The duplicated region in the derivative chromosome 10 was identified, and demonstrated that the duplicated region is interstitial, with a small deletion of the 10qter. The other known karyotypic changes were also identified.

Furthermore, two distinct small regions of copy number change were identified, a copy number gain of 3 clones on chromosome 5q, and a deletion of 2 clones on chromosome 16p. Although other single clone changes were also present, many of these were clones known to 'misbehave' in hybridisation and produce unexpected results, possibly due to homologous content to other chromosomes.

The analysis did not miss regions which could have been identified by eye, nor did it identify any 'false positive' regions. Thus it can be deemed an accurate and sensitive method for analysis of microarray CGH data.

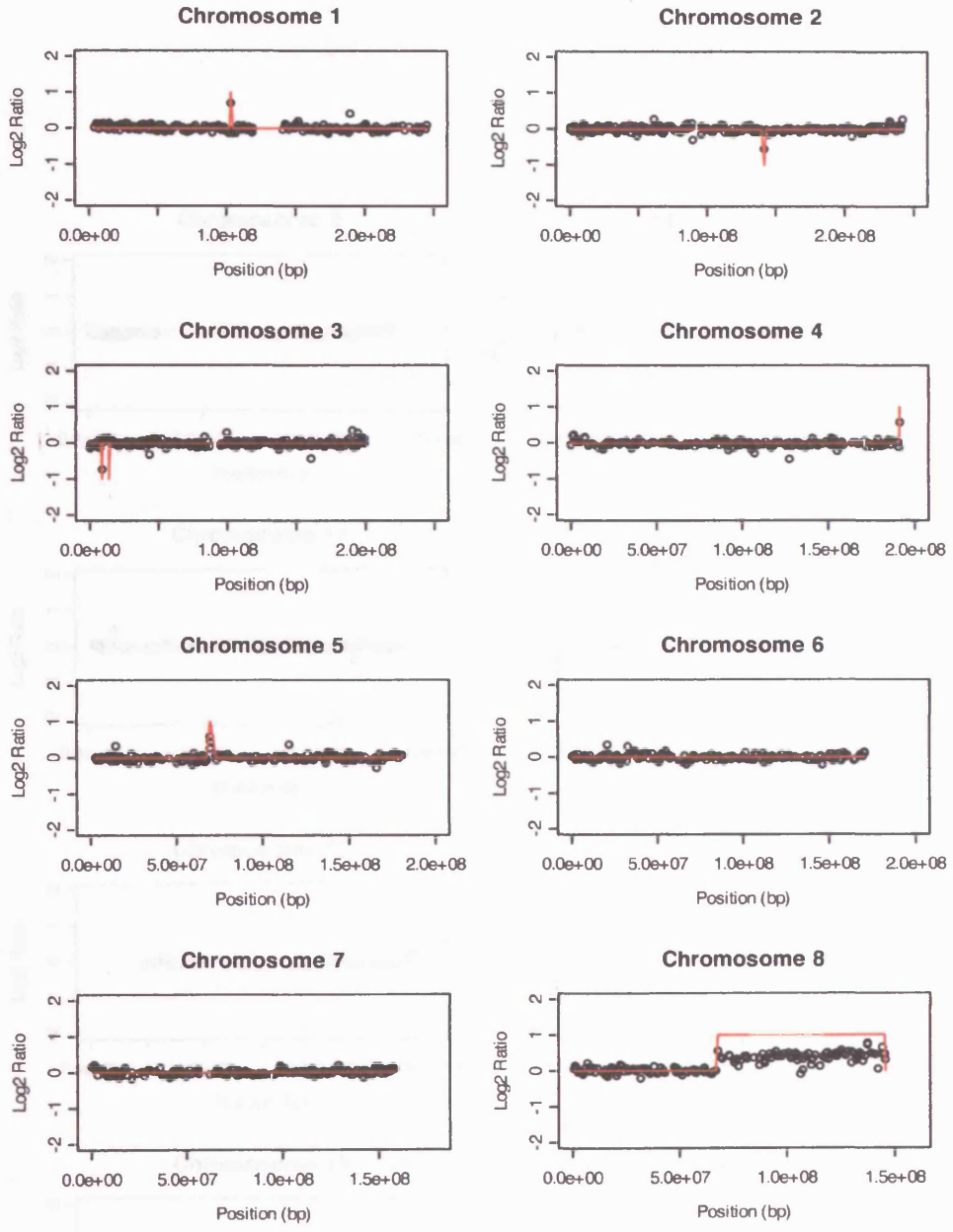

Figure 2.8 Chromosome output plots for the HCT116 colon cancer cell line. Individual chromosome plots are shown after normalisation and analysis. Scaled, normalised log2 ratios are shown as black circles on each plot. The copy number change call is shown as a red line, a change of 1 indicates a gain, a change of -1 indicates a deletion, and 0 indicates no change. (Continued on following two pages)

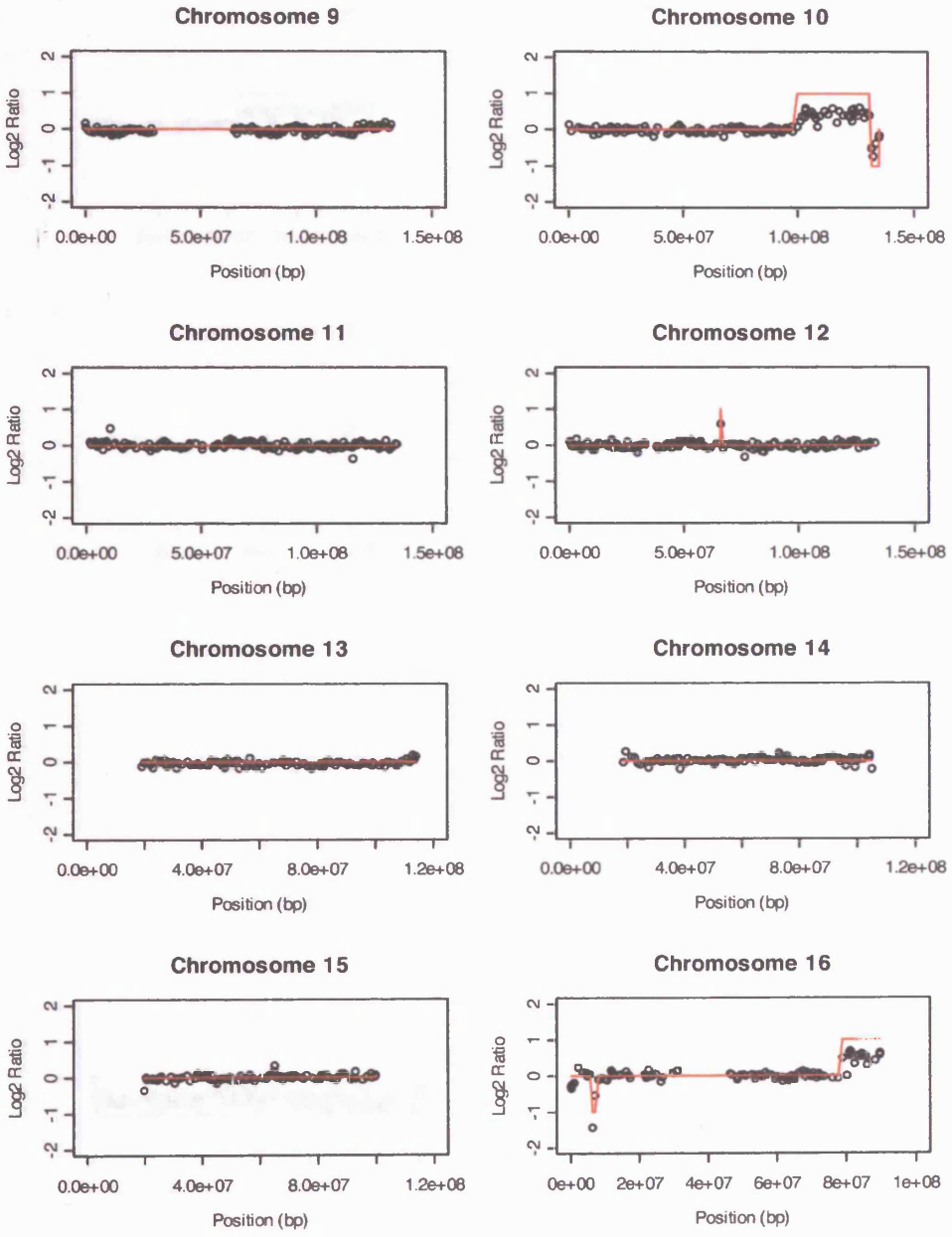
Chromosome 9
Log2 Ratio
Position (bp)
0.0e+00
5.0e+07
1.0e+08
1.5e+08
Chromosome 10
Chromosome 11
Chromosome 12
Chromosome 13
4.0e+07
8.0e+07
1.2e+08
Chromosome 14
Chromosome 15
Chromosome 16
0e+00
2e+07
4e+07
6e+07
8e+07
1e+08

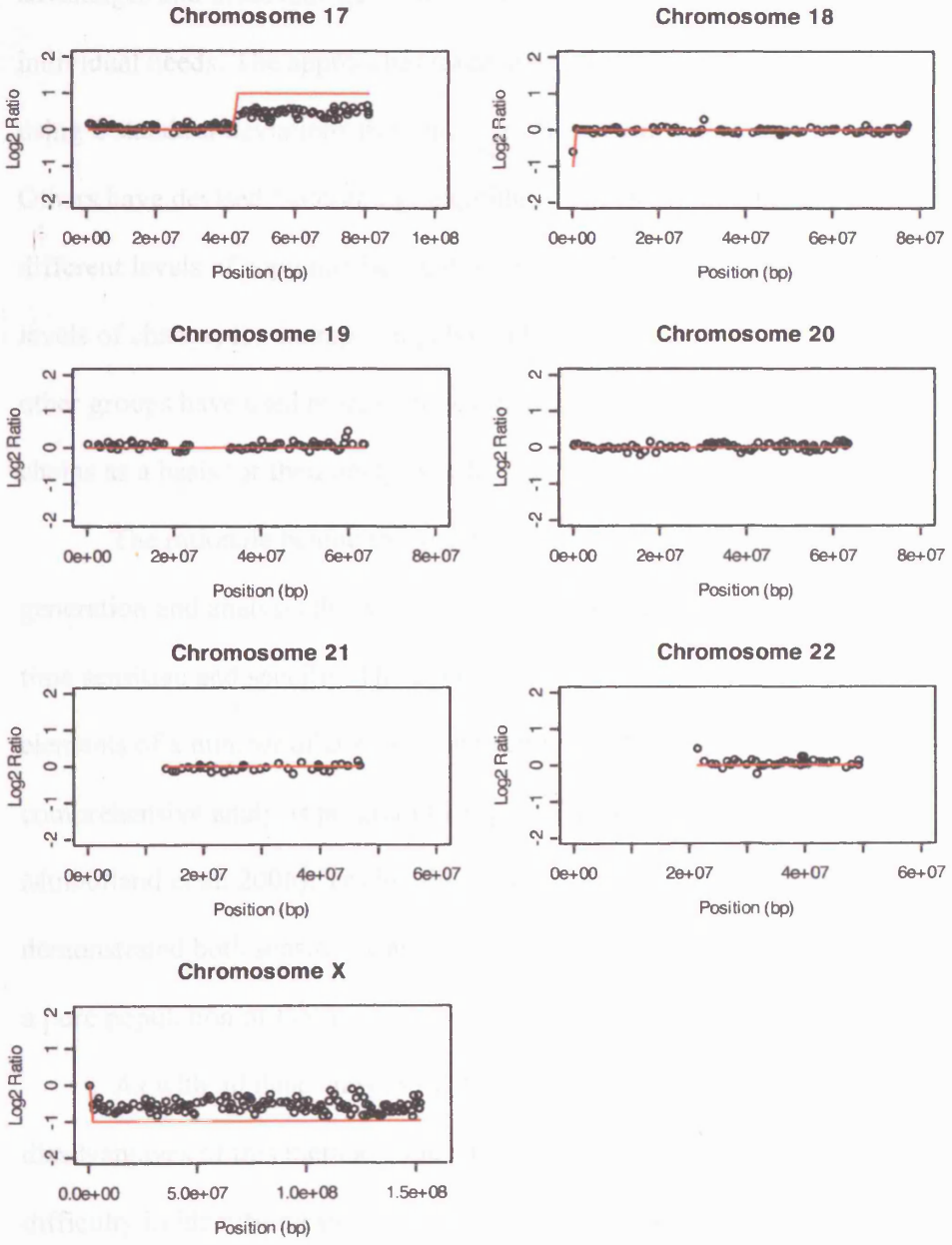
Chromosome 17
Log2 Ratio
-2 -1 0 1 2
0e+00 2e+07 4e+07 6e+07 8e+07 1e+08
Position (bp)
Chromosome 18
Log2 Ratio
-2 -1 0 1 2
0e+00 2e+07 4e+07 6e+07 8e+07
Position (bp)
Chromosome 19
Log2 Ratio
-2 -1 0 1 2
0e+00 2e+07 4e+07 6e+07 8e+07
Position (bp)
Chromosome 20
Log2 Ratio
-2 -1 0 1 2
0e+00 2e+07 4e+07 6e+07 8e+07
Position (bp)
Chromosome 21
Log2 Ratio
-2 -1 0 1 2
0e+00 2e+07 4e+07 6e+07
Position (bp)
Chromosome 22
Log2 Ratio
-2 -1 0 1 2
0e+00 2e+07 4e+07 6e+07
Position (bp)
Chromosome X
Log2 Ratio
-2 -1 0 1 2
0.0e+00 5.0e+07 1.0e+08 1.5e+08
Position (bp)

2.13.2.3 Data analysis discussion

Current literature contains many and varied methods and algorithms for the generation and analysis of genomic microarray data. Each with its own advantages and disadvantages, and often designed for a particular researcher's individual needs. The approaches taken are diverse. The simplest involve using 2 standard deviations from the median as a threshold (Sharp et al. 2005). Others have devised 'smoothing' algorithms, which present the data as different levels of copy number, and so are useful for identifying different levels of change, for example in polyploidy tumours (Jong et al. 2004). And other groups have used more complex models, including Hidden Markov chains as a basis for their analysis (Chen et al. 2005).

The rationale behind this method was to devise a method of data generation and analysis that was simple to use and understand, but at the same time sensitive and specific. The devised method is not unique, it has taken elements of a number of analyses, and combined them to produce a comprehensive analysis program (Yang et al. 2002; Fiegler et al. 2003; Mulholland et al. 2006). Testing the method using a known cell line demonstrated both sensitivity and specificity in identifying known changes in a pure population of DNA.

As with all data analysis methods there are distinct advantages and disadvantages of this method. One particular disadvantage could be a difficulty in identifying significant changes in a sample with a large amount of copy number variation, since multiple changes would increase the spread of the array data, and thus artificially increase the thresholds, and possibly miss significant changes. Furthermore, the method cannot identify which changes

are biologically genuine, rather than as a result of aberrant clone behaviour. Recent reports have identified large-scale copy number variation in the human genome between individuals, and this must be taken into account when identifying regions of change.

Chapter 3

Fumarate Hydratase (*FH*) mutations in Hereditary Leiomyomatosis and Renal Cell Cancer (HLRCC)

3.1 Introduction

The inherited multiple tumour syndrome hereditary leiomyomatosis and renal cell cancer (HLRCC) is caused by germline mutations in the *FH* gene encoding the Krebs' cycle enzyme fumarate hydratase (FH). A wide variety of pathogenic variants were identified in the initial set of families in which the mutations were discovered, including whole gene deletions, missense and nonsense changes (Tomlinson et al. 2002). All the mutations have been shown to serve the same purpose, reducing the activity of the FH protein, by activity assays of patient lymphoblastoid cell lines (Alam et al. 2003).

While heterozygous germline mutations in *FH* result in HLRCC, bi-allelic mutations cause the fumarase deficiency syndrome, characterised by gross developmental delay and death within the first decade (Rustin et al. 1997).

The aim of the work in this Chapter was to examine the frequency of germline *FH* mutations in a cohort of sporadic uterine leiomyoma patients to examine the contribution they make to leiomyoma prevalence. Within this, the association of *FH* mutations with ethnicity was also examined in order to assess the contribution of *FH* mutations in the earlier-onset and more prevalent uterine leiomyomas in African and Afro-Caribbean patients than Caucasian patients. In addition, patients with HLRCC and related syndromes were also screened to identify novel mutations. A series of cancer cell lines was also screened to assess the role of *FH* mutations in the common cancers.

In silico functional analysis of all known HLRCC and FH deficiency mutations was carried out in order to assist with the identification of the potential pathogenic effects of novel identified germline mutations. This

analysis involved examining the structural distribution and interactions of *FH* missense mutations, given prior knowledge of effects on activity. As a part of this, the distribution of HLRCC and FH deficiency mutations was studied to examine the significance of differences in the mutation spectra of these two conditions. Other novel mutations, including missense changes to the mitochondrial targeting sequence, splice site mutations and non-coding variants were also examined in order to assess their pathogenicity.

3.2 Materials and Methods

3.2.1 Sample Collection

All fresh tumour and blood/normal DNA samples from patients with diagnosed uterine leiomyomas were screened for mutations. In total 334 unselected samples from sporadic leiomyoma patients were screened. Within this sample cohort, 232 patients provided ethnicity data: 75 patients were of African or Afro-Caribbean ethnicity, 55 patients were Caucasian, and 102 patients were of other ethnicities. In addition, 26 selected samples with features of HLRCC were provided by clinical collaborators and screened for mutations.

3.2.2 Cancer cell line screening

In order to assess the role of *FH* mutations in a variety of cancers, an array of 70 cancer cell lines was screened. These cell lines (**Table 3.1**) represented a variety of tissue types, including colon, breast, lung and pancreas.

3.2.3 Mutation screening and DNA sequencing

Initial mutation screening was carried out by fluorescent SSCP analysis, as described in Chapter 2 (2.5.1). Screening was carried out on PCR products amplified using FAM-labelled primers using the described conditions (**Table 3.2**). Samples with a change from the majority (assumed to be homozygous normal), such as those shown in **Figure 3.1**, were selected for sequencing. In addition, one apparently normal sample was also sequenced to ensure that it was representative of a normal sample. Sequencing was carried

out by re-amplification of the fragment with unlabelled primers by the same PCR conditions, followed by sequencing (2.6). Observed changes were analysed using DNA strider software to identify amino acid change.

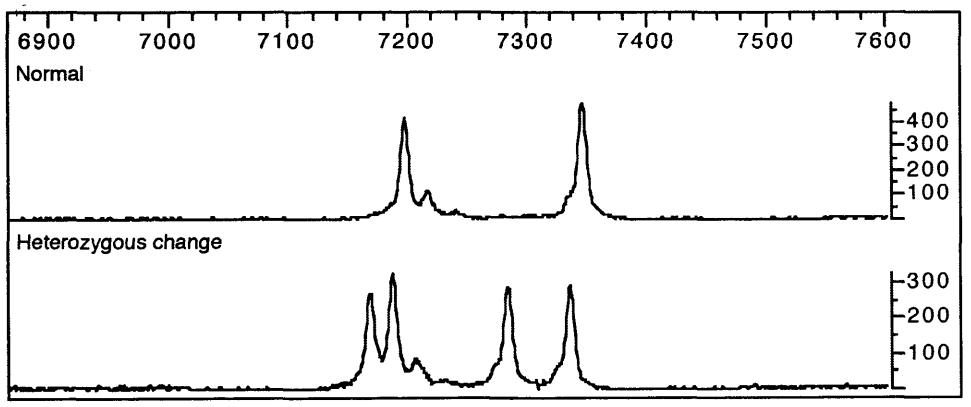

Figure 3.1 Example of a change observed by SSCP. There is an obvious difference between the normal sample, which has only two peaks, indicative of homozygosity, and the apparent heterozygous change, which has 4 peaks.

Table 3.1 Cell lines screened for *FH* mutations

Cell Line	Tissue	Cell Line	Tissue
U87	Astrocytoma	A459	Lung
K562	B-cell lymphocyte	CaLu-1	Lung
HT1376	Bladder	A549	Lung
L88	Bone marrow	SKMES	Lung
MDA-MB488	Breast	LUDLU-1	Lung
BT-20	Breast	NCI-H2170	Lung
MDA-MB231	Breast	T84	Lung
MCF-7	Breast	NCIH69	Lung
MDA-MB415	Breast	NCI-H520	Lung
SKBR3	Breast	MOLT4	Lymphocyte
T47D	Breast	IM9	Lymphocyte
MDA-MB361	Breast	U937	Lymphoma
MDAMB435	Breast	P3HR1	Lymphoma
ZR-75	Breast	SK23	Melanoma
MDA-MB157	Breast	DX3	Myeloma
JAMA-2	Breast	NB100	Neuroblastoma
Hela S3	Cervical Carcinoma	NFS-10-B7	Neurofibrosarcoma
HT29	Colon	SCC15	Oral carcinoma
Colo741	Colon	SKOV 3	Ovarian
SW620	Colon	TR175	Ovarian
Colo320	Colon	Paca-3	Pancreas
LoVo	Colon	Hs766T	Pancreas
Caco2	Colon	HPAF	Pancreas
HCT116	Colon	PANC-1	Pancreas
HCA-7	Colon	CF Pac-1	Pancreas
A431	Epithelial Carcinoma	Detroit 562	Pharynx
U118	Glioblastoma	DU145	Prostate
SCC25	Head and neck	PC3	Prostate
TRI26	Head and neck	786PRC9	Renal
TRI46	Human Buccal	RCC-VHL	Renal
KG1	Leukemia	NCI-H1385	Squamous cell carcinoma
HL60	Leukemia	SCC-4	Squamous cell carcinoma
ML-1	Leukemia	Jurkat	T-cell
PLC/PRF/S	Liver	NTERA.scl.dl	Testicular
HepG2	Liver	JAR	Trophoblast

Table 3.2 Primer sequences for amplification of *FH* exons. Exon 5 was split into two fragments due to its length. Primers were labelled with FAM. Primers from (Tomlinson et al. 2002) were used for screening.

Primer Name	Primer Sequence	Product Length	PCR program[1,2]
Exon 0 F	GTGTGAGGCTGTTGATTGGA	258	EJ55
Exon 0 R	CTGCGCTCACCATTCGAG		
Exon 1 F	GATGCGATTACTTTTGATCCTG	261	EJ55
Exon 1 R	TGACTCATGAATACAGCCTACTTC		
Exon 2 F	CTTTTGCATCTGCCAAAATAA	264	AR55
Exon 2 R	TGCCAGAGCATATCGTCATC		
Exon 3 F	CTCTGTGGCATAATCAGCATT	300	AR55
Exon 3 R	CAATCTCAGGTATGCTTTTCAA		
Exon 4 F	TTTGTTTTTGTTGCCTCTGATTT	295	EJ55
Exon 4 R	ATTGGCCATTTGTACCAAGC		
Exon 5a F	TTTGCTCATCATAAGATTTGAAGT	300	AR55
Exon 5a R	CCTTTTCTGCAAAGCCAATTC		
Exon 5b F	TGCAATGACAAGAATAAAAGCTG	215	AR55
Exon 5b R	TCAAGACAGGAACACTCAGAAAA		
Exon 6 F	TTTAACTTGTTCACCCATCTAGGA	293	AR55
Exon 6 R	GGACCTAGTCAAGTTTTAGCTCCA		
Exon 7 F	ATGGTTGGGCCTTGCTTTAT	300	EJ55
Exon 7 R	CCAAGATAATAAGCCTTTGGTCA		
Exon 8 F	AAAGATTAAAAATGTGTTACACTCAGC	234	EJ55
Exon 8 R	TCCACTTGTCTCTTAAAAATGGTTT		
Exon 9 F	GCTAACCCATATGTCGTCTTTTT	250	EJ55
Exon 9 R	CGTTTTTAAGAAATGGGAGTCTG		

[1] Details of programs can be found in Chapter 2 (2.3.2.1)

[2] All PCR reactions contained 1.5mM $MgCl_2$ and 5% v/v DMSO in a 25µl reaction with 25ng template genomic DNA

3.2.4 Mutation functional and structural analysis

In order to assess the potential pathogenic effects of novel mutations, a number of strategies were undertaken. Initially, the functional effects of observed missense mutations were initially predicted using the PolyPhen program, which predicts the functional effects of coding SNPs on a protein (Ramensky et al. 2002) . Analysis of other mutations was carried out on an individual basis, dependent on the type of mutation..

In addition, several *FH* sequences were aligned using the ClustalW multiple alignment tool (Thompson et al. 1994) visualised with JalView (Clamp et al. 2004), in order to visualise conservation of residues across species. FH protein sequences for this alignment were obtained from the Entrez protein database (http://www.ncbi.nlm.nih.gov/entrez) for 8 species **(Table 3.3)**

Table 3.3 Species and ID numbers for FH protein sequences used for multiple alignment in ClustalX

Species	**FH protein Entrez ID**
Homo sapiens	NP_000134.2
Mus musculus	NP_034339.1
Danio rerio	NP_957257.1
Caenorhabditis elegans	O17214
Drosophila melanogaster	AAS14209.1
Arabidopsis thaliana	BAB08741.1
Saccharomyces cerevisiae	P08417
Escherichia coli	AP_002232.1

The locations of missense mutations on the structure of the FH protein were studied to examine the relationship between the physical location of a mutated residue, particularly to identify any physical clustering of mutations resulting in renal cell carcinoma and to examine any differences in the distribution of mutations resulting in HLRCC and FH deficiency.

The locations of mutations were modelled onto the structure of *E. coli* fumarase C (Protein data bank ID 1FUO) (Weaver et al. 1995) using UCSF Chimera (Pettersen et al. 2004). The protein is a homotetramer with 2 2 2 symmetry (Weaver et al. 1995). However, the deposited database structure is a homodimer. In order to model the tetrameric structure, the unit cell function of Chimera was utilised to produce an accurate interaction of two homodimers (Figure 3.6). The role of individual residues mutated in HLRCC patients, and

the possible effects of the mutations, were determined by several criteria by examination of the equivalent *E. coli* residue:

i) Examination of interactions with other residues. This includes examining the hydrophobic, electrostatic and hydrogen bonding interactions with other residues. Mutations removing such interactions can potentially destabilise protein folding and enzyme function.

ii) Steric effects. This examines changes in both the size and the torsion angles imposed by the mutated residue compared to the original residue.

iii) Active site residues. The catalytic mechanism of FH is now well understood, and the active site residues have been identified. Mutations to these residues, or in the proximity of them, would have an adverse effect on protein function.

3.3 Results

3.3.1 *FH* mutation screening

In total, 360 patients with uterine leiomyomas, including 26 patients provided on the basis of an HLRCC or apparently related phenotype, and 70 cancer cell lines were screened for *FH* mutations. Screening of patient and tumour samples identified 24 DNA sequence variants in 97 patients, and 9 cell line samples (**Table 3.4**). 7 of these variants, occurring in 55 patients and 8 cell lines, were synonymous coding SNPs. 11 variants, observed in 25 patients and 1 cell line, were missense changes. 4 variants, observed in 17 patients, were insertion/deletion mutations, 2 of which occurred in coding regions, and the remaining 2 were intronic. One variant in one patient altered the splice acceptor site of exon 3, and finally, one variant in one patient occurred 25 bases upstream of the transcriptional start (**Table 3.4**, **Figure 3.2**, **Figure 3.3**).

16 of these variants have not been previously reported in the literature or SNP databases (Shown in **Figure 3.2**, **Figure 3.3**). 4 of the remaining changes (Q142R, K187R, R190H and G354R) are known HLRCC mutations (Alam et al. 2003). One mutation (ins434K) has been previously associated with FH deficiency (Coughlin et al. 1998), and more recently with ovarian mucinous cystadenoma (Ylisaukko-oja et al. 2006). The final 3 polymorphisms are reported synonymous SNPs in the dbSNP database (Sherry et al. 2001)(A60A = rs10926501, P266P = rs1049719, and C391C = rs12087951).

Table 3.4 All identified *FH* sequence changes

Exon[1]	Mutation type	Nucleotide Position[2]	Wild type codon/sequence[3]	Mutated codon/sequence[3]	Amino Acid Change[4]	No. samples
0	Non-coding*	-25	aaccggc	aacgggc	N/A	1
0	Missense*	36	TAC	CAC	Y2H	7
0	Missense*	69	CCC	GCC	P13A	1
0	Missense*	85	CCA	CTA	P18L	5
0	Missense*	126	GCC	ACC	A32T	1
0	Synonymous*	137	TCG	TCA	S35S	3
0	Synonymous*	149	CCG	CCA	P39P	5
1	Synonymous*	260	ACG	ACA	T33T	1
2	Synonymous SNP	341	GCC	GCT	A60A	16
3	Splice acceptor*	441-2	cagGTA	cggGTA	N/A	1
3	Missense*	558	CAT	CCT	H133P	1
3	Missense	586	CAG	CGG	Q142R	2
3	1bp insertion*	588+27	TTTGGT	TTTTGGT	N/A	9
4	Missense	721	AAG	AGG	K187R	1
4	1bp deletion*	727	GGACGT	GACGT	G189fsX211	1
4	Missense	730	CGT	CAT	R190H	2
6	Synonymous	959	CCG	CCA	P266P	24
6	Missense*	1045	ATA	ACA	I295T	1
7	2bp deletion*	1141-35	TTTAGTC	TTGTC	N/A	4
7	Missense	1221	GGA	AGA	G354R	1
8	Synonymous	1334	TGC	TGT	C391C	7
8	Synonymous*	1370	AAT	AAC	N403N	8
9	3bp insertion	1461	CAAAAAT	CAAAAAAAAT	ins434K	3
9	Missense SNP*	1504	TAT	TGT	Y448C	1

[1]Indicates the primer set in which the change was identified

[2]Numbered from *FH* mRNA (Genbank accession NM_000143)

[3]Capital letters indicate coding bases, lowercase letters indicate intronic/other regions

[4]Amino acids in exon 0, encoding the mitochondrial signal sequence, are labelled separately from those in the cytosolic protein, due to historical mis-assignment of the first codon.

*Represents novel changes identified in this study

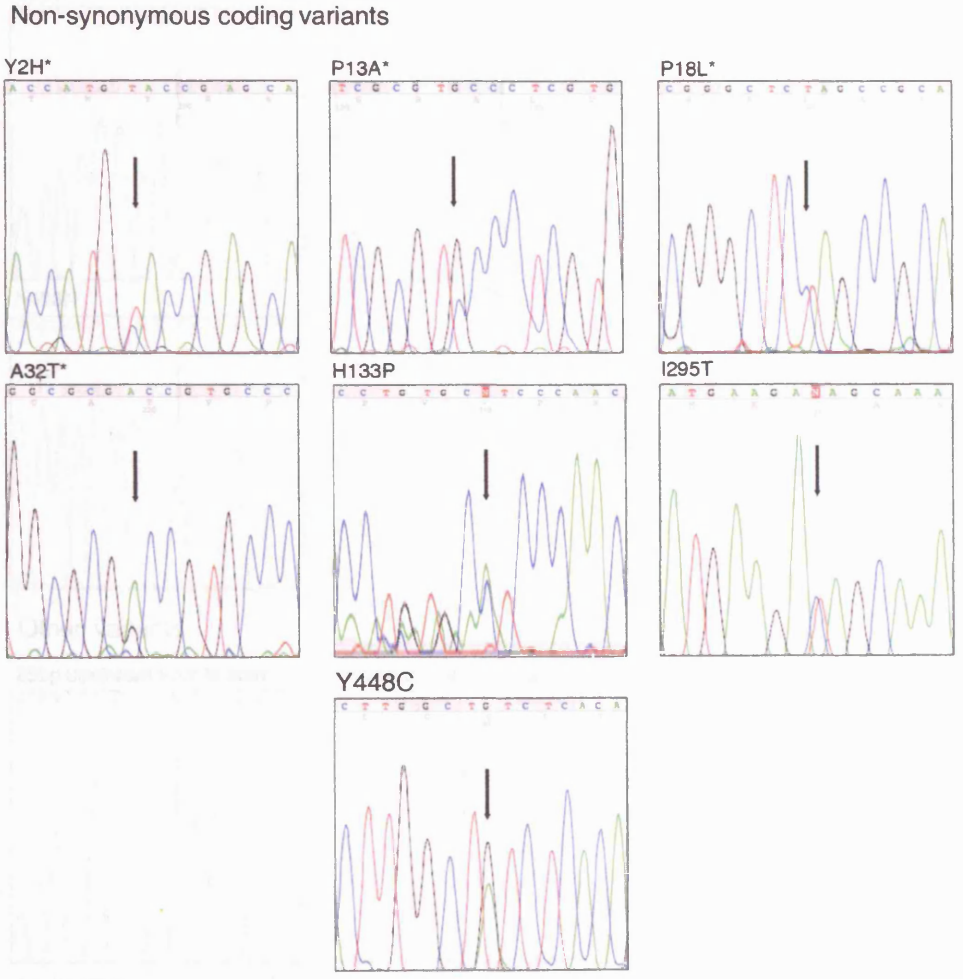

Figure 3.2 Novel non-synonymous coding changes identified in this study. The location each polymorphism is indicated by an arrow. Mutations highlighted with * are variants in the mitochondrial targeting sequence.

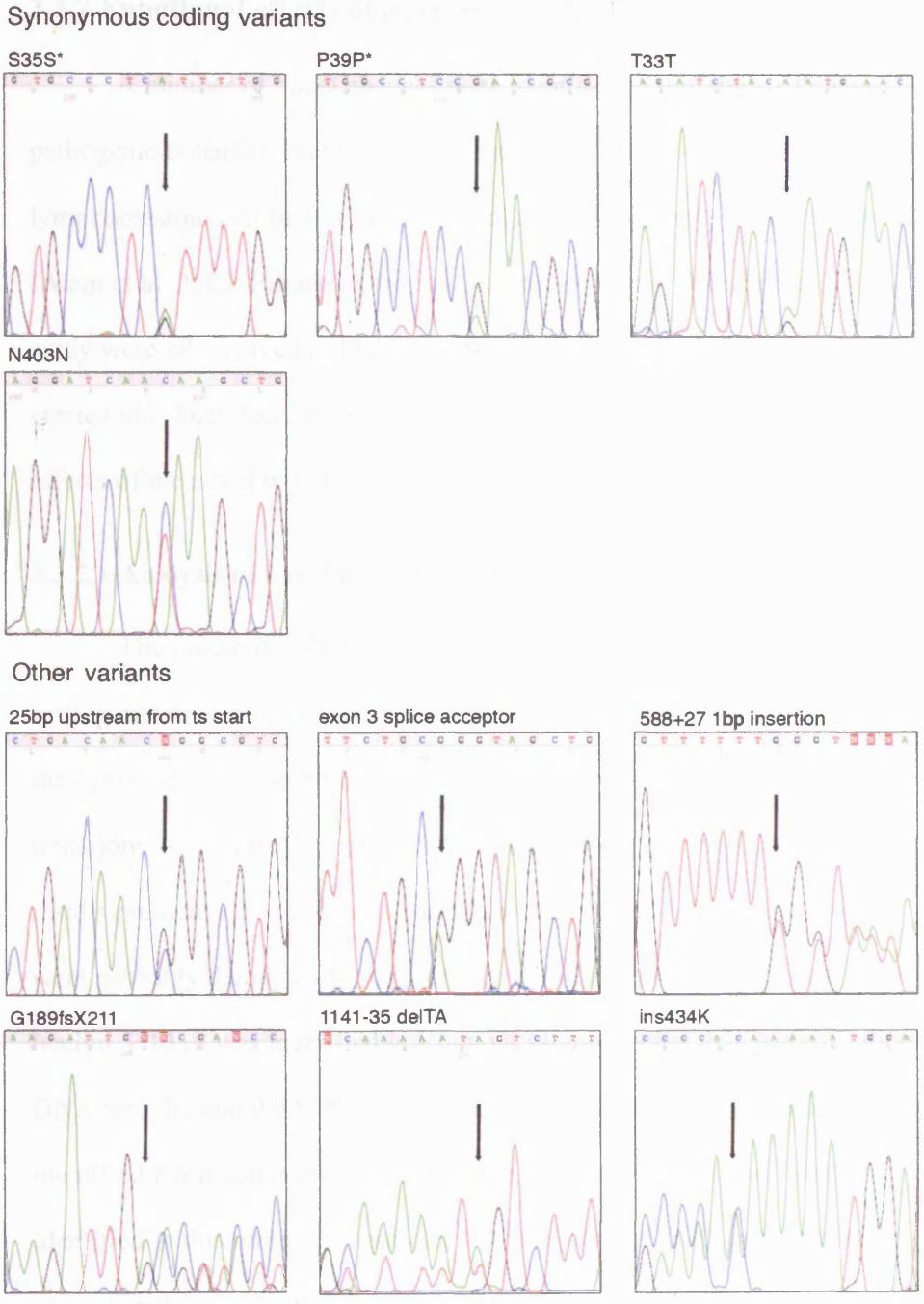

Figure 3.3 Novel synonymous coding variants and other novel variants observed in this study. Variants marked with * occur in the mitochondrial targeting sequence. Positions of intronic variants are relative to the nearest mRNA position.

3.3.2 Functional effects of novel polymorphisms

A number of novel changes were identified in this study of uncertain pathogenic potential. Previous studies have used FH activity in lymphoblastoid cell lines as a measure of the pathogencity of a mutation (Alam et al. 2003; Pithukpakorn et al. 2006). However, the samples in this study were all received as DNA samples, and so activity assays could not be carried out. Therefore, an *in silico* approach was used to identify the possible effects of the novel mutations on FH function.

3.3.2.1 Analysis of novel missense mutations

The online PolyPhen tool was initially used to predict the effects of the coding missense mutations. The results (**Table 3.5**) predicted the effects for the cytosolic missense mutations, but failed to predict the effects of the exon 0 mutations due to insufficient similar protein sequences in the database. The results predicted that 2 of the novel missense changes, H133P and Y448C, were probably damaging to the protein, while the third, I295T, was probably benign. H133P was identified in a tumour sample, rather than a constitutional DNA sample, and the K187R mutation, which was among the original identified *FH* mutations in HLRCC (Tomlinson et al. 2002), was also identified in this tumour. Therefore, it is likely that H133P represents the second 'hit' in an HLRCC leiomyoma. Furthermore, H133 has been identified as an active site residue in the FH protein (Weaver and Banaszak 1996), and so mutation of this residue should have a deleterious effect on the protein activity.

The prediction of Y448C as potentially damaging is a surprising result for a number of reasons. As is shown in the next section, Y448 is not very well conserved between species, although the shape of the residue is conserved. Secondly, the patient with the mutation was 62 years old when she was diagnosed with uterine leiomyomas. Generally, HLRCC patients present in their 20's and 30's (Alam et al. 2005a), although there is one recent report of a patient with an R58X mutation presenting at 55 years of age (Varol et al. 2006). Therefore, in order to further examine the potential pathogenic effect of this mutation, analysis in the context of sequence conservation and structure was carried out (See 3.3.4). A similar analysis was carried out on the I295T mutation.

Table 3.5 Predicted effects of novel missense mutation by PolyPhen

Mutation	Predicted Effect	Comments
Y2H	Unknown	No data for prediction
P13A	Unknown	No data for prediction
P18L	Unknown	No data for prediction
A32T	Unknown	No data for prediction
H133P	Probably Damaging	Mutation disrupts ligand binding site
I295T	Benign	No predicted effect of substitution
Y448C	Probably Damaging	Predicted on basis of alignment

3.3.2.2 Further analysis of exon 0 missense mutations

The region encoded by exon 0 contains a 43-residue region that targets FH to the mitochondrial matrix. Once the protein has been transported into the matrix, this region is cleaved by specific proteases, leaving the final functional protein. These sequences are sufficient to target a protein to the mitochondria by fusing them to non-mitochondrial proteins (Roise and Schatz 1988). While little homology exists between signalling sequences of different mitochondrial proteins, the signal sequences share common features. Firstly, the sequence contains a mixture of positively charged and hydrophobic residues along its length, with a strong bias against negatively charged residues. Secondly, the sequences are amphiphilic, and projection of the sequence onto a helical wheel results in a pronounced segregation of charged and hydrophobic residues to either face of the wheel, forming an amphipathic helix (Roise and Schatz 1988).

This positively charged amphipathic helix is sufficient in itself to target a protein to the mitochondrial matrix, since artificially constructed amphiphilic signal sequences, with no homology to known mitochondrial signal sequences, are able to target a protein to the mitochondria (Roise and Schatz 1988). The first 18 residues of the FH signal sequence follow this pattern (**Figure 3.4**a). However, subsequent residues form a hydrophobic helix prior to the start of the cleaved final protein (**Figure 3.4**b). The effects of each missense mutation on the amphiphilicty of the predicted helix were assessed. None of the mutations affected the amphipathic nature of the helix, and so are assumed not to affect the mitochondrial targeting ability of the sequence. To confirm this, the mitochondrial leader sequence was used as the basis for a BLAST search against other eukaryotic FH signal sequences. None of the sites of mutation were conserved between species. Therefore, it can be concluded that the four exon 0 missense mutations, Y2H, P13A, P18L, and A32T, are probably benign.

3.3.2.3 Functional effects of other novel coding mutations

In addition to the 7 novel missense changes, two novel nonsense mutations were identified, G189fsX211 and ins434K. The latter mutation has previously been described in FH deficiency patients (Coughlin et al. 1998), and more recently in ovarian mucinous cystadenoma (Ylisaukko-oja et al. 2006), and so is known to affect FH activity. Therefore, it can be added to the spectrum of HLRCC mutations. G189fsX211 joins a list of 21 nonsense mutations reported to date in HLRCC and FH deficiency patients (Coughlin et

al. 1998; Kiuru et al. 2002; Tomlinson et al. 2002; Alam et al. 2003; Martinez-Mir et al. 2003; Toro et al. 2003; Chuang et al. 2005; Badeloe et al. 2006; Chuang et al. 2006a; Wei et al. 2006b). It has previously been shown that truncated FH proteins are unstable, affecting FH activity by reducing the available enzyme (Alam et al. 2003). Since truncating mutations have been observed throughout the protein, it can be assumed that the protein resulting from this mutation is also unstable, and so the mutation is pathogenic.

3.3.2.4 Functional effects of novel non-coding mutations

The final 4 novel mutations comprised variants in non-coding regions of the gene that have not been reported in publicly available databases. Three of these mutations occured within the introns close to the exon boundary, and the fourth occured 25bp upstream of the transcription start. Of the intronic mutations, one mutated the fully conserved AG motif of the splice acceptor site in exon 3 to GG. This mutation would abolish splicing of this exon, resulting in deletion of exon 3 from the final mRNA. Including this variant, 5 splice donor and acceptor mutations have been reported in HLRCC and FH deficiency patients, all of which affect the conserved GT and AG motifs defining the splice donor and acceptor sites (Chuang et al. 2005; Badeloe et al. 2006; Wei et al. 2006b).

In order to assess the effects of the other non-coding mutations, the comparative genomics track of the UCSC genome browser was used to examine the conservation of these regions between species. Regions of high sequence conservation have been shown to represent potentially important

regulatory regions, including transcription factor and enhancer binding sites and the splice branch sites, which occur approximately 30bp upstream from the splice acceptor site.

The intronic insertion downstream from the exon 3 splice donor site (588+27) occurs in a region of little conservation between species, and is at the wrong end of the intron to affect the branch site. Therefore, it is likely that this polymorphism is a novel insertion-deletion SNP and pathogenically benign. The second intronic polymorphism, a 2bp deletion 35bp upstream of the exon 7 splice acceptor site, is highly conserved and adjacent to the branch site, but the deletion does not appear to affect this site. Again, this mutation appears to be benign.

The final non-coding mutation, 25bp upstream from the transcription start, occurs in the middle of a CpG island that encompasses all of exon 0. The mutation is a transversion of a C to a G, which removes one CpG group, but creates a new one 1bp downstream. Analysis of this sequence showed that the nucleotide is not well conserved between species. The program FPROM (Solovyev et al. 2006) was used to identify promoter sequences in the locality of this base, and found no promoter sequences. Therefore, it is most likely that this mutation is benign.

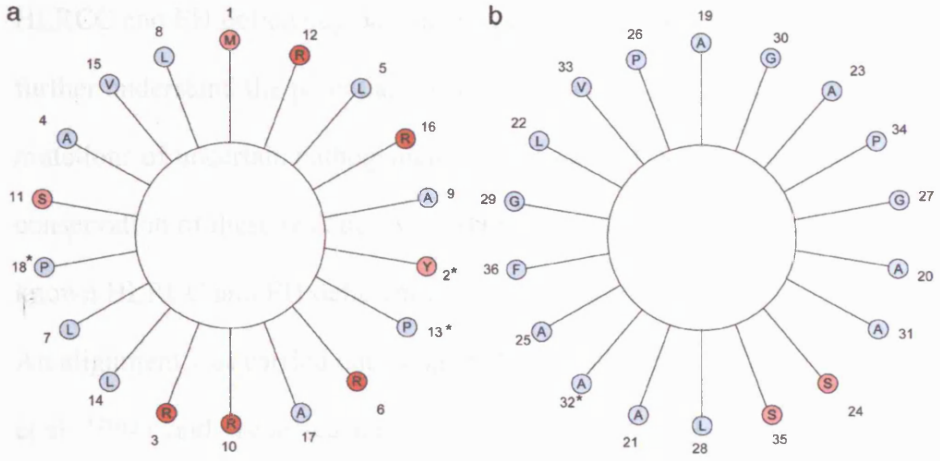

Figure 3.4 Helical wheel projection of the first 36 residues of the FH mitochondrial signal sequence. The first 18 residues (a) form a positively charged amphipathic α-helix, whereas the second 18 residues (b) form a hydrophobic helix, with the exception of two serine residues. The residues affected by the observed mutations are highlighted with *. None of the observed mutations affect the amphipathic nature of either helix, and so the mutations are likely to be benign.

3.3.3 Multiple sequence alignment

A wide variety of missense mutations have now been described in HLRCC and FH deficiency patients in the literature (**Table 3.7**). In order to further understand the potential role of the two remaining novel missense mutations of uncertain pathogenicity, I295T and Y448C, the sequence conservation of these residues was examined alongside the conservation of known HLRCC and FH deficiency missense mutations.

An alignment was carried out using the ClustalW alignment tool (Thompson et al. 1994), and visualised and coloured using Jalview (Clamp et al. 2004)(**Figure 3.5**). Despite the selection of species being evolutionarily diverse, a very high level of homology exists, particularly when the mitochondrial signal sequence is not taken into account (**Table 3.6**).

Mapping the locations of known missense mutations onto this alignment demonstrated that every reported missense mutation (**Table 3.7**) altered a residue that was conserved throughout species, either exactly, or by shape and type. I295 was found to be conserved exactly across species, and to reside in a block of very highly conserved residues. Y448 was less well conserved, and it appeared that the hydrophobicity of the phenyl group was more necessary than any interactions due to the hydroxyl group since this residue was replaced with hydrophobic residues of a similar bulk in other species, such as phenylalanine and valine. Therefore, based on sequence conservation, I295T appears to be a more likely pathogenic mutation than Y448C.

Table 3.6 Homology of FH polypeptide sequences from different species to human cytosolic FH. Alignment and assessment of homology was carried out using BLAST (Tatusova and Madden 1999).

Species	**% Identical residues to human FH**	**% homologous residues to human FH**
Mus musculus	96% (451/467)	98% (460/467)
Danio rerio	87% (410/467)	94% (443/467)
Caenorhabditis elegans	76% (352/460)	86% (399/460)
Drosophila melanogaster	68% (316/458)	81% (372/458)
Arabidopsis thaliana	71% (327/460)	82% (380/460)
Saccharomyces cerevisiae	67% (313/464)	81% (376/464)
Escherichia coli	60% (280/462)	76% (354/462)

Table 3.7 All reported HLRCC and FH deficiency missense mutations

HLRCC Missense Mutations							
Exon	WT codon	Mutant codon	Nucleotide Position on mRNA (NM_000143)	WT residue	Amino Acid Position	Mutant Residue	Reference
2	AAC	ACC	352	N	64	T	(Tomlinson et al. 2002)
2	GCT	CCT	381	A	74	P	(Tomlinson et al. 2002)
3	TTA	TCA	427	L	89	S	(Wei et al. 2006b)
3	CAT	CGT	436	H	92	R	(Chuang et al. 2005)
3	CAG	AAG	456	Q	99	K	(Badeloe et al. 2006)
3	AGC	ATC	505	S	115	I	(Martinez-Mir et al. 2003)
3	AGA	GGA	510	R	117	G	(Wei et al. 2006b)
3	CAT	CGT	571	H	137	R	(Tomlinson et al. 2002)
3	CAG	CGG	586	Q	142	R	(Tomlinson et al. 2002)
4	TCA	TTA	592	S	144	L	(Toro et al. 2003)
4	AAT	AGT	595	N	145	S	(Toro et al. 2003)
4	CCC	CTC	607	P	149	L	(Chuang et al. 2005)
4	ATG	ACG	616	M	152	T	(Toro et al. 2003)
4	CAC	CGC	619	H	153	R	(Kiuru et al. 2002)
4	ATC	ACC	718	I	186	T	(Alam et al. 2003)
4	AAG	AGG	721	K	187	R	(Tomlinson et al. 2002)
4	CGT	CAT	730	R	190	H	(Tomlinson et al. 2002)
4	CGT	TGT	729	R	190	C	(Wei et al. 2006b)
4	CGT	CTT	730	R	190	L	(Toro et al. 2003)
5	GCT	ACT	852	A	231	T	(Ylisaukko-oja et al. 2006)
5	GGT	GTT	877	G	239	V	(Tomlinson et al. 2002)
6	AAT	TAT	960	N	267	Y	(Alam et al. 2005b)
6	CAT	TAT	984	H	275	Y	(Toro et al. 2003)
6	GTT	GAT	997	V	279	D	(Toro et al. 2003)
6	ACT	CCT	1023	T	287	P	(Chuang et al. 2006a)
6	CTG	CCG	1036	L	292	P	(Toro et al. 2003)
6	AAT	GAT	1050	N	297	D	(Toro et al. 2003)
6	AAT	AAA	1052	N	297	K	(Wei et al. 2006b)
6	GAA	AAA	1095	E	312	K	(Alam et al. 2003)
6	AAT	AAA	1115	N	318	K	(Alam et al. 2003)
6	AGC	GGC	1125	S	322	G	(Wei et al.

							2006b)
6	AGT	AAT	1129	S	323	N	(Alam et al. 2003)
7	GCC	GAC	1186	A	342	D	(Wei et al. 2006b)
7	GTC	CTC	1212	V	351	L	(Martinez-Mir et al. 2003)
7	GGA	AGA	1221	G	354	R	(Alam et al. 2003)
8	TCA	CCA	1287	S	376	P	(Wei et al. 2006b)
8	CAG	CCG	1348	Q	396	P	(Wei et al. 2006b)
9	ATG	ATA	1394	M	411	I	(Carvajal-Carmona et al. 2006)
9	TAT	TGT	1426	Y	422	C	(Toro et al. 2003)
9	CTG	CCG	1552	L	464	P	(Alam et al. 2003)
FH Deficiency Missense Mutations							
3	CCT	CGT	553	P	131	R	(Alam et al. 2003)
5	GCT	ACT	954	A	265	T	(Coughlin et al. 1998)
6	CAT	CTT	985	H	275	L	(Deschauer et al. 2006)
6	GAA	CAA	1116	E	319	Q	(Bourgeron et al. 1994)
7	CAG	CCG	1159	Q	333	P	(Phillips et al. 2006)
8	GAT	GTT	1306	D	382	V	(Coughlin et al. 1998)

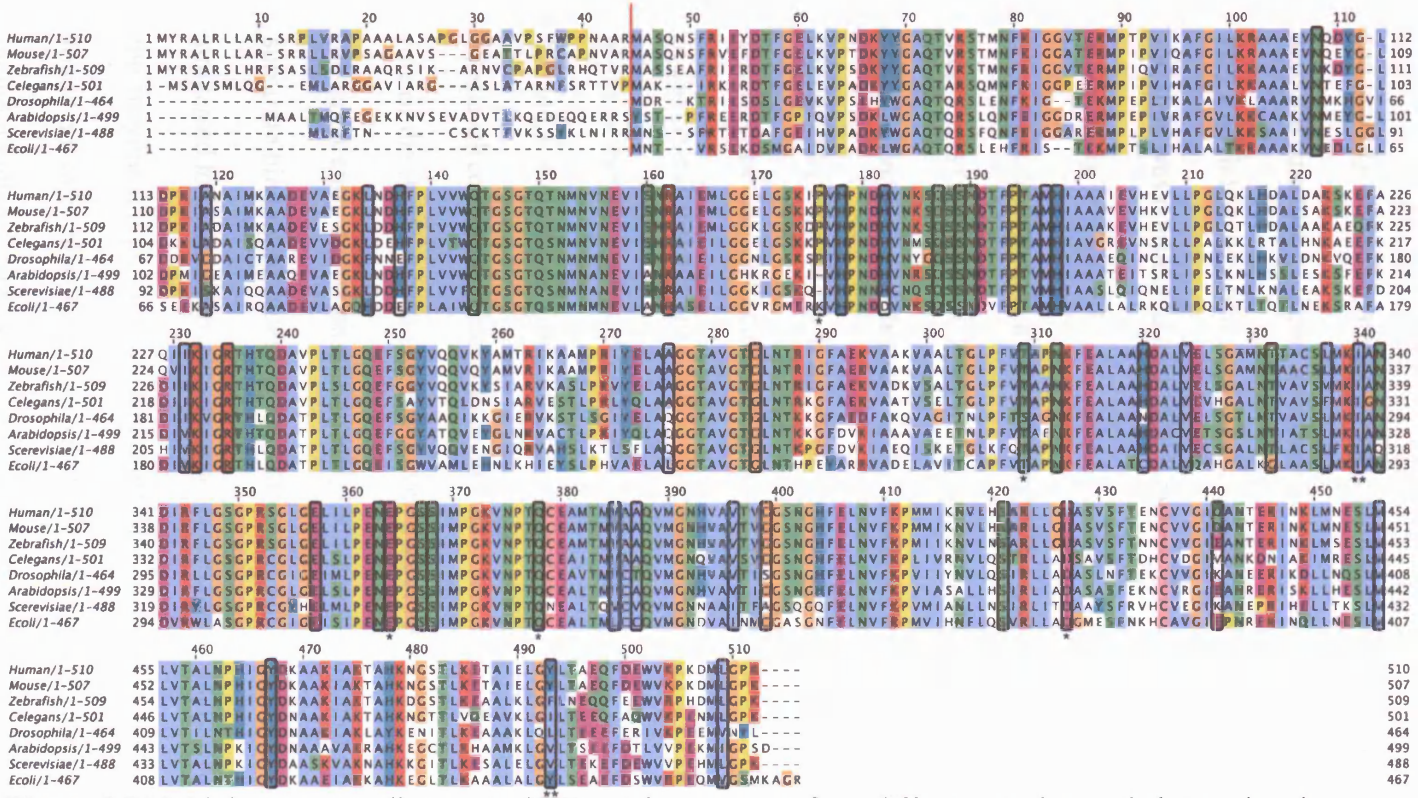

Figure 3.5 Multiple sequence alignment of FH protein sequences from different species carried out using the CLustalW multiple alignment tool. Locations of HLRCC and FH deficiency (highlighted by *) missense mutations are highlighted by black boxes. The location of the I295T and Y448C mutations are highlighted by **. The red bar marks the end of the mitochondrial signal sequence

3.3.4 Structural effects of *FH* mutations

In order to assess the effects of germline *FH* mutations on the structure and activity of the fumarate hydratase protein, known mutations were mapped onto the structure of *E.coli* fumarase C (Weaver et al. 1995). This protein has very high homology and similar reaction kinetics to the human FH protein, and thus was considered a suitable structure for modelling mutations (Weaver et al. 1995).

E.coli Fum C is a tetrameric protein comprised of 4 identical 50kDa monomers (**Figure 3.6**). Each monomer contains three distinct domains: two globular domains at either end of the molecule, separated by a 5 α-helical bundle. The association of this helical domain results in tetramer formation. The enzyme has four active sites (**Figure 3.6** – yellow arrows). The solution of the crystal structure of *E.coli* FumC, demonstrated two ligand binding sites in the active site region, deemed A and B (Weaver et al. 1995). The A site is formed from residues from 3 monomers and was shown to be the catalytic site by site-directed mutagenesis experiments (Weaver and Banaszak 1996). The role of the B site, which is formed from a single monomer, is less clear, since it is apparently not required for catalysis, since mutation of one of the substrate binding residues does not affect FH activity. It was initially suggested to be an allosteric site, responsible for the increased activation of the enzyme at high substrate concentrations (Rose 1997), although this was found not to be physiologically viable since activation by common anions, including other Krebs cycle intermediates such as citrate, would obscure this effect *in vivo (Rose and Weaver 2004).*

Rose and Weaver suggested that the B-site is an integral part of the active site, involved in the transfer of substrate to the catalytic A-site. They showed that while mutation of substrate binding residues in the B-site does not affect enzyme activity, it does alter the rate limiting step of the reaction. Instead of being rate-limited in the enzyme recycling to a basic form ready to bind the next molecule of fumarate, the rate-limiting step becomes the release of substrate from the enzyme (Rose and Weaver 2004).

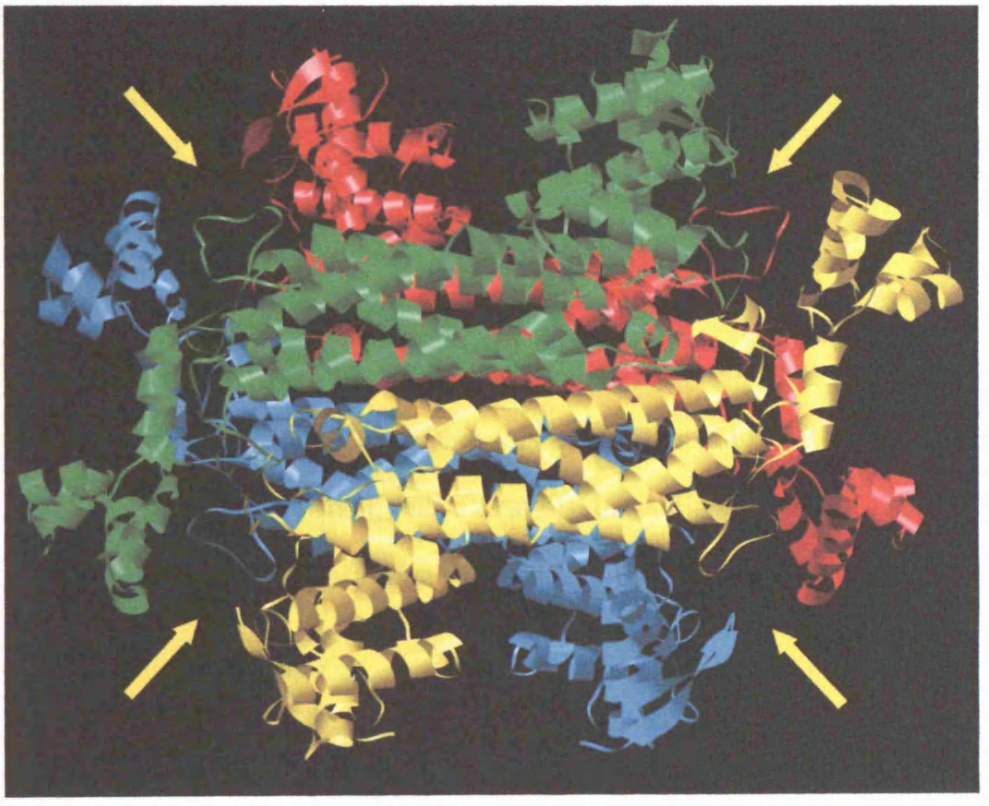

Figure 3.6 Homotetrameric structure of *E. coli* Fum C. Each subunit is coloured separately. The yellow arrows indicate the approximate locations of the 4 pairs of A and B-sites of the enzyme. The model was made using UCSF Chimera.

3.3.4.1 Distribution and effects of known HLRCC mutations

To date, 43 separate missense mutations have been identified in patients with HLRCC, and a further 7 missense mutations have been found in FH deficiency patients (**Table 3.7**). In order to further understand the effects of these mutations on the FH protein, and how they may affect the activity of the protein, the location of each mutation was mapped onto the structure of *E.coli* FumC. Initially, the mutations were mapped onto a single monomer to identify clustering to any particular domain (**Figure 3.7**). It was observed that mutations clustered more to the globular domains, particularly the larger N-terminal globular domain.

Since the globular domains of the FH monomer are responsible for active site formation, it was decided to examine the location of the mutations in the context of an active site. The results (Figure 3.8) showed that the majority of missense mutations in the globular domains were physically close to the active site, and many were within close proximity to the two ligand binding sites. Thus, mutations in the globular domains of FH are likely to disrupt active site formation, and so catalysis. In addition, the locations of FH deficiency missense mutations did not cluster differently to HLRCC mutations.

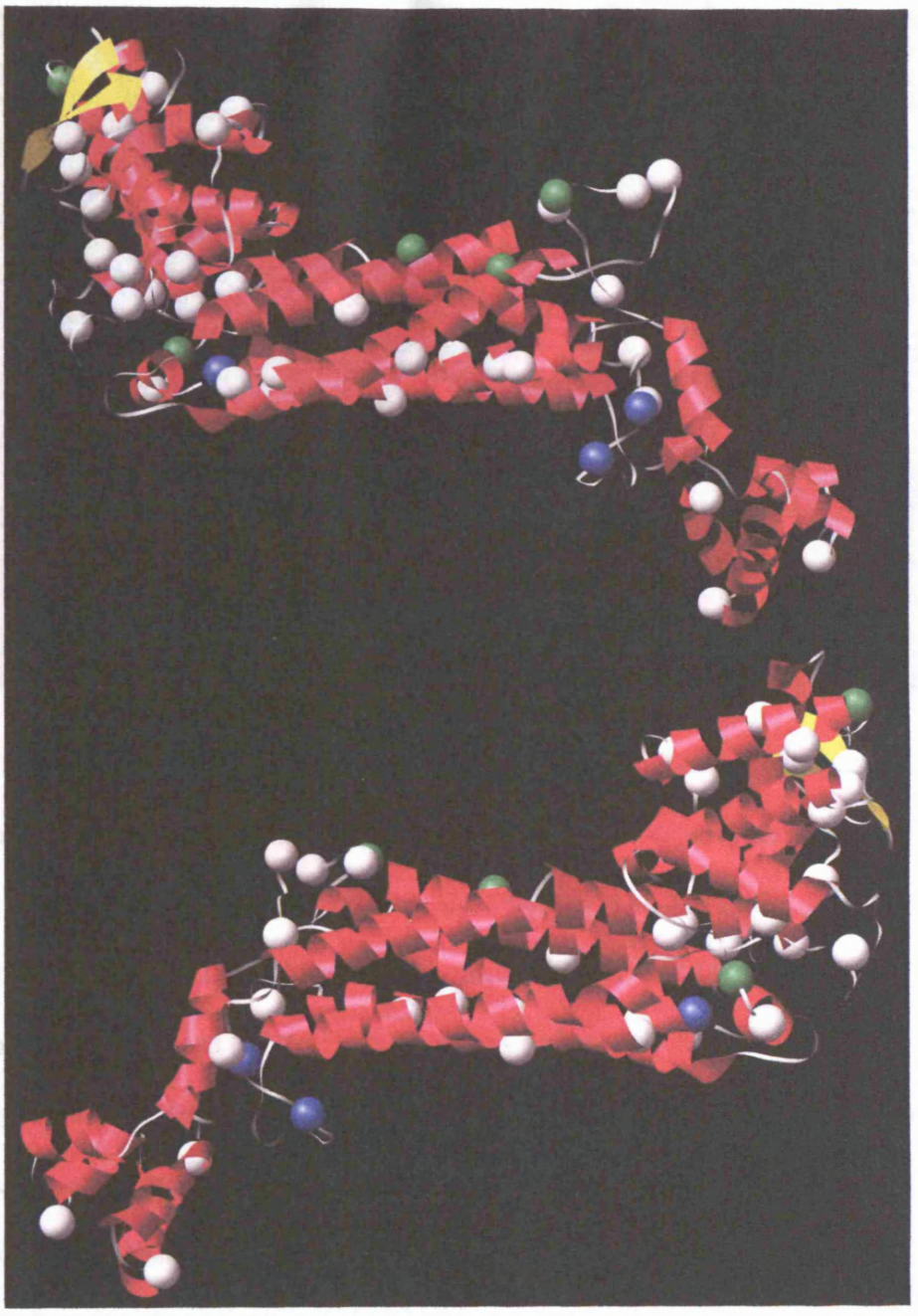

Figure 3.7 Location of HLRCC and FH deficiency missense mutations on a monomer of *E.coli* FumC. HLRCC missense mutations (white) and FH deficiency mutations (green, blue = both HLRCC and FH deficiency) cluster to either end of the monomer with fewer mutations occurring in the helical bundle. The monomer is viewed from both sides to show the location of all mutations.

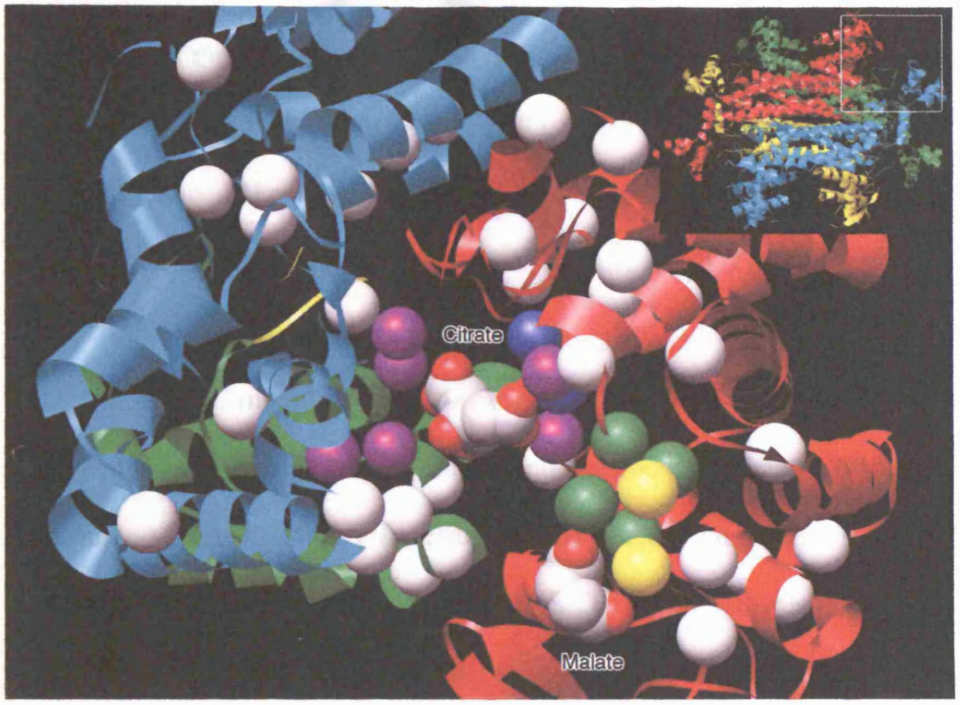

Figure 3.8 Clustering of HLRCC and FH deficiency missense mutations to the active site region of FH. In this model, FH was co-crystallised with citrate and malate, which occupy the active site (Weaver et al. 1995). Focusing on a single active site, formed from 3 monomers, HLRCC and FH deficiency missense mutations (white) were found to be physically close to the two ligand binding sites in each FH active site. Purple residues represent catalytic A-site residues, with blue residues being mutated in HLRCC and/or FH deficiency. Green residues form the ligand binding B-site, with yellow residues found mutated in HLRCC and/or FH deficiency. The tetramer is shown for reference with the region of interest boxed.

In order to more closely observe how particular mutations can affect the activity of the protein, the 4 known HLRCC mutations observed in this study (Q142R, K187R, R190H and G354R), which have previously been shown to reduce FH activity in lymphoblastoid cell lines from HLRCC patients (Alam et al. 2003), were examined in more detail. These 4 mutations cover the 3 domains of the FH monomer.

2 HLRCC mutations of Q142 have been reported to date, one missense change, Q142R (Tomlinson et al. 2002), and one nonsense change, Q142X (Martinez-Mir et al. 2003). This residue occurs in the large N-terminal globular domain, very close to the active site. The *E.coli* equivalent, Q138, forms a number of H-bond interactions with both main chain carboxyl groups and side chains of nearby residues (**Figure 3.9**a). Also involved in these interactions is N59, the human equivalent of which, N64, is mutated in HLRCC patients. The residues within the N-terminal globular domain form a mesh of H-bond and salt bridge interactions which align the residues of the nearby catalytic and ligand binding sites. Therefore, mutations that disrupt these interactions, such as Q142R and N64T, would lead to alterations in the structure of the active site, and so would, at the very least, disrupt, if not completely remove, enzyme activity.

R190 and K187 (R186 and K183 in *E.coli* respectively) are both highly conserved in FH proteins across species. They are also physically close within the protein, occurring in the smaller C-terminal globular domain. To date, 3 separate missense mutations have been reported at R190 (R190H, R190L, R190C) in both HLRCC and FH deficiency patients (Gellera et al. 1990; Tomlinson et al. 2002; Toro et al. 2003; Wei et al. 2006b). K187R has

also been observed in both patient groups (Coughlin et al. 1998; Tomlinson et al. 2002). Examining the interactions of the *E.coli* equivalent residues (**Figure 3.9b**) demonstrated salt bridge and H-bond interactions between these residues, and E308, the *E.coli* equivalent of E312, which has also been reported as mutated in HLRCC patients (Alam et al. 2003). Overall the pattern of salt bridge and H-bonding interactions draws together residues from 3 monomers, and is likely to be important in both forming and stabilising the catalytic site, since 2 active site residues are adjacent to this interaction. Furthermore, mutation of either of these residues would disrupt interactions between monomers, and so affect tetramer formation.

G354 (G350 in *E.coli*) occurs in the central α-helical bundle, away from the active site of the enzyme. The residue faces into the centre of the monomer bundle, in a very hydrophobic region with close packing of residues (**Figure 3.10**). Mutation of this residue to arginine would have a massive effect on helix packing due to this residue being firstly very large, which would disrupt the close packing of the residues, and secondly very hydrophilic. Therefore, this mutation is likely to destabilise the entire monomer, reducing the available monomers for tetramer formation, and thus the overall activity of the enzyme.

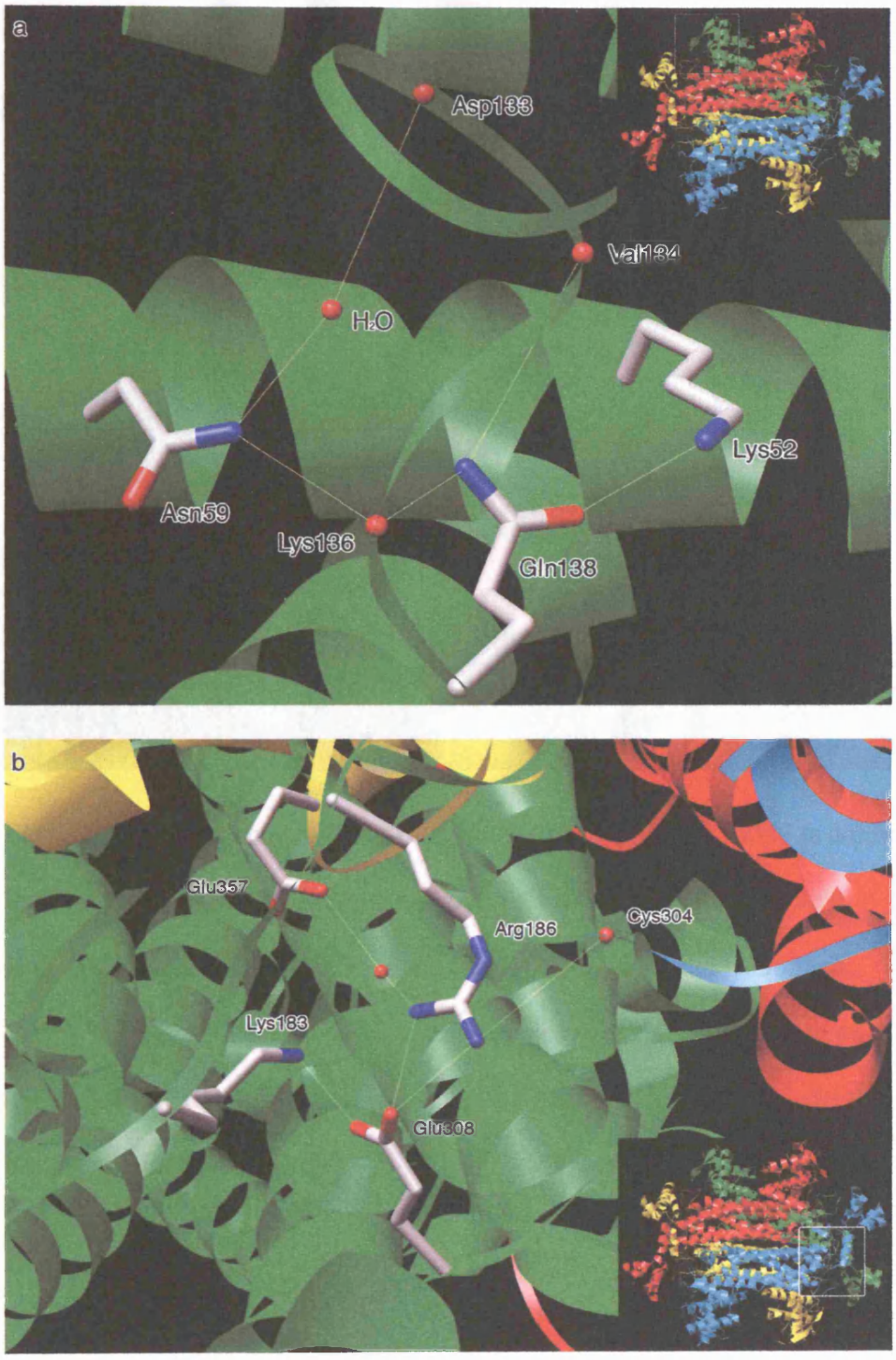

Figure 3.9 Interactions of *E.coli* equivalents of Q142 (a - Q138) and R190 (b - R186). Fine lines between residues indicate predicted H-bond and salt bridge interactions. The full protein is shown for reference with the region of interest highlighted. For a detailed description, see the main text.

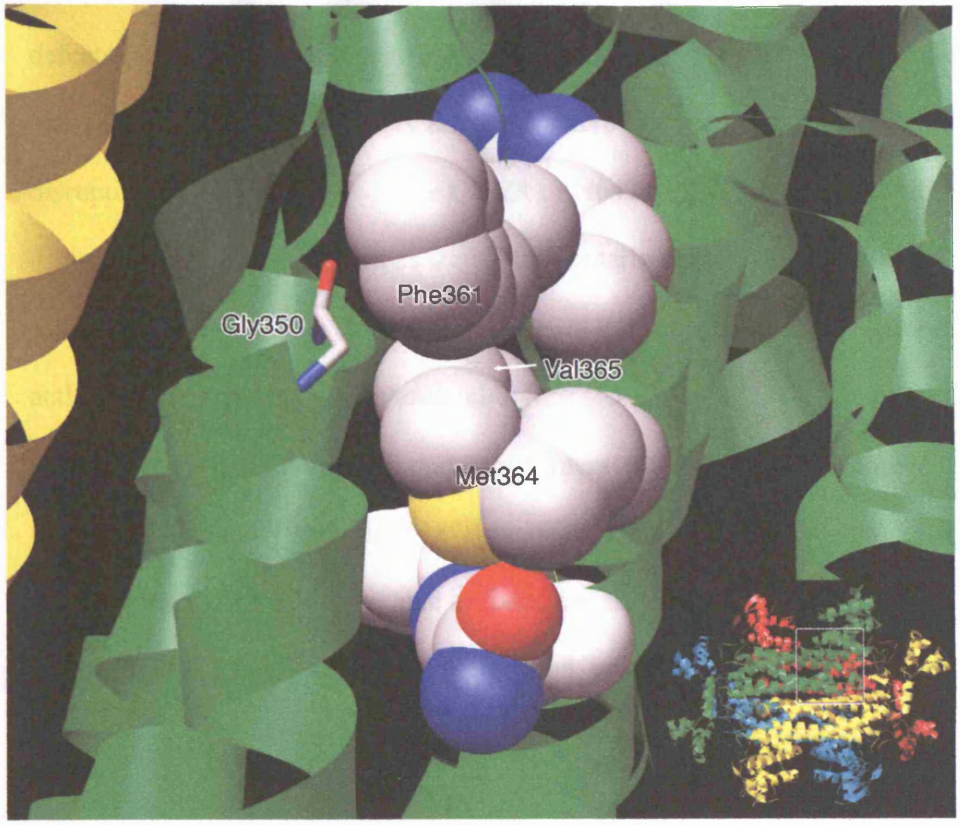

Figure 3.10 Interactions of G350 (*E.coli* equivalent of G354). G350 is on the inside of an α-helix within the central 5-helix bundle in a closely packed hydrophobic region. Nearby residues, such as F361, M364 and V365 are shown as spacefill models to emphasise this close packing. Mutation to an arginine would disrupt this close packing, and so would disrupt the helical bundle within the monomer.

Each of these mutations demonstrates the three possible effects of FH defects on the protein, each contributing to a reduction in activity in a different manner. Firstly, a mutation may affect the active site, either by local disruption, for example due to the Q142R or N64T mutations, or by mutation of an active site residue, such as the N145S mutation. Monomers with such mutations would be able to form into full tetramers, but would lack function at active sites formed by the mutated subunit.

Secondly, the mutation may affect interactions with other subunits, as is the case for the R190H and K187R mutations. Monomers with such mutations may or may not be able to form tetramers, but the interactions between the subunits would be compromised, which could possibly lead to a dominant negative effect. Such an effect has previously been reported for the R190H and K187R mutations, which showed an approximately 80% reduction of FH activity, instead of the expected 50% (Alam et al. 2003).

The final group of mutations appear to disrupt the structure of the monomer before tetramer formation occurs, such as G354R. Therefore, it is predicted that these subunits will not form into tetramers. Therefore, all the FH homotetramers would contain wild type monomers, but the reduced overall amount of FH would lead to a reduction in enzyme activity.

In each of these scenarios, a second hit affecting the enzyme would result in a complete loss of FH activity within a cell. And it is this loss of activity that appears to be the trigger for tumorigenesis in HLRCC.

3.3.4.2 Structural effects of novel mutations

The three novel missense mutations, H133P, I295T and Y448C were mapped onto the structure in an attempt to better understand their potential effect on the protein. The equivalent *E. coli* residues for each of these residues are H129 (for H133), Y444 (for Y448) and I291 (for I295).

PolyPhen had already predicted a disruptive effect of the H133P mutation on the protein due to ligand binding. These interactions, shown in **Figure 3.11**, bind the malate ligand to the non-catalytic B-site of the enzyme. Mutation of this residue to a proline would completely remove this interaction. This is not the end of the story with this residue, however, since Weaver *et al* have carried out studies using an H129N *E.coli* FumC mutant. They demonstrated that this mutation does not have an effect on FH activity, although it does alter the rate-limiting step of the enzyme (Weaver et al. 1997). However, one of the important characteristics of the B-site is the π-helical structure, which involves residues H129 to N135 (Weaver 2000). While the H129N mutation removes the interaction with malate, it may not destabilise the π helix. The restricted structure of proline would have a destabilising effect on this helix, and so may yet have a derogatory effect on enzyme activity, and if so this effect probably occurs through reducing access of the substrate to the active A-site.

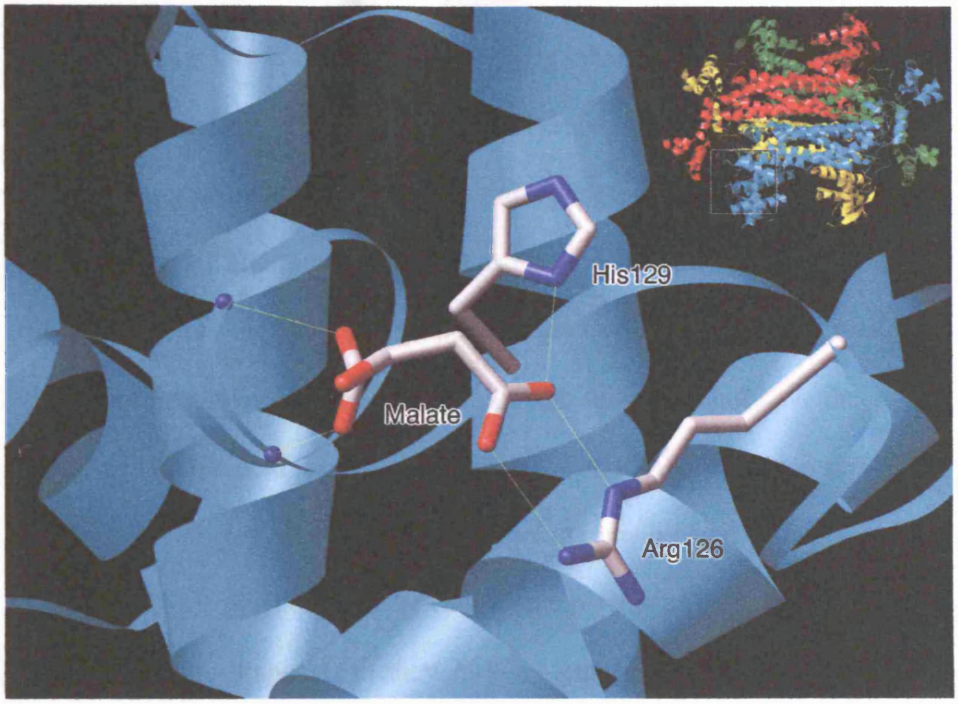

Figure 3.11 Ligand binding interaction of H129 in *E.coli* FH. This residue forms salt bridge interactions with co-crystallised malate in the B-site of the enzyme. The malate also interacts with R126 (not conserved in humans) and the main chain amide groups of residues 131 and 132. Shown residues are coloured in standard atomic colours.

I291 sits in a hydrophobic pocket at the core of the 5 helix bundle (**Figure 3.12**a) and is closely surrounded by other hydrophobic residues. The effects of mutation of this residue to a threonine are not clear cut. The mutation would not disrupt helix packing by increasing the bulk of the residue, since isoleucine and threonine are of a similar size. However, the addition of a polar group into the hydrophobic pocket may destabilise the helix packing, and so compromise enzyme activity although this might not have the effect of a charged amino acid such as the effect of the G354R mutation described above. Therefore, the effects of this mutation remain elusive.

Y444 is positioned at the edge of the protein away from the active site (**Figure 3.12**b). It appears to show H-bond and salt bridge interactions with two nearby residues, K420 (K424 in humans) and E423 (K427 in humans, which would retain this interaction). K420 and E423 are part of an α-helix which appears to interact with a looped region from another subunit. Thus Y444 may stabilise inter-subunit packing. Mutation of this residue to a cysteine would remove these interactions, since although the thiol group is polar, the smaller size of the residue would increase the distance between the potentially interacting atoms. This disruption could affect inter-subunit interactions by the α-helix.

The results of this fail to conclusively suggest a pathogenic role for either the I295T or Y448C mutations, while the role of the H133P mutation also remains controversial based on the work of Weaver *et al (Weaver et al. 1997).* Both I295T and Y448C elude to a possible effect on enzyme activity. However, to confirm this, more studies would need to be carried out. These will be discussed later on.

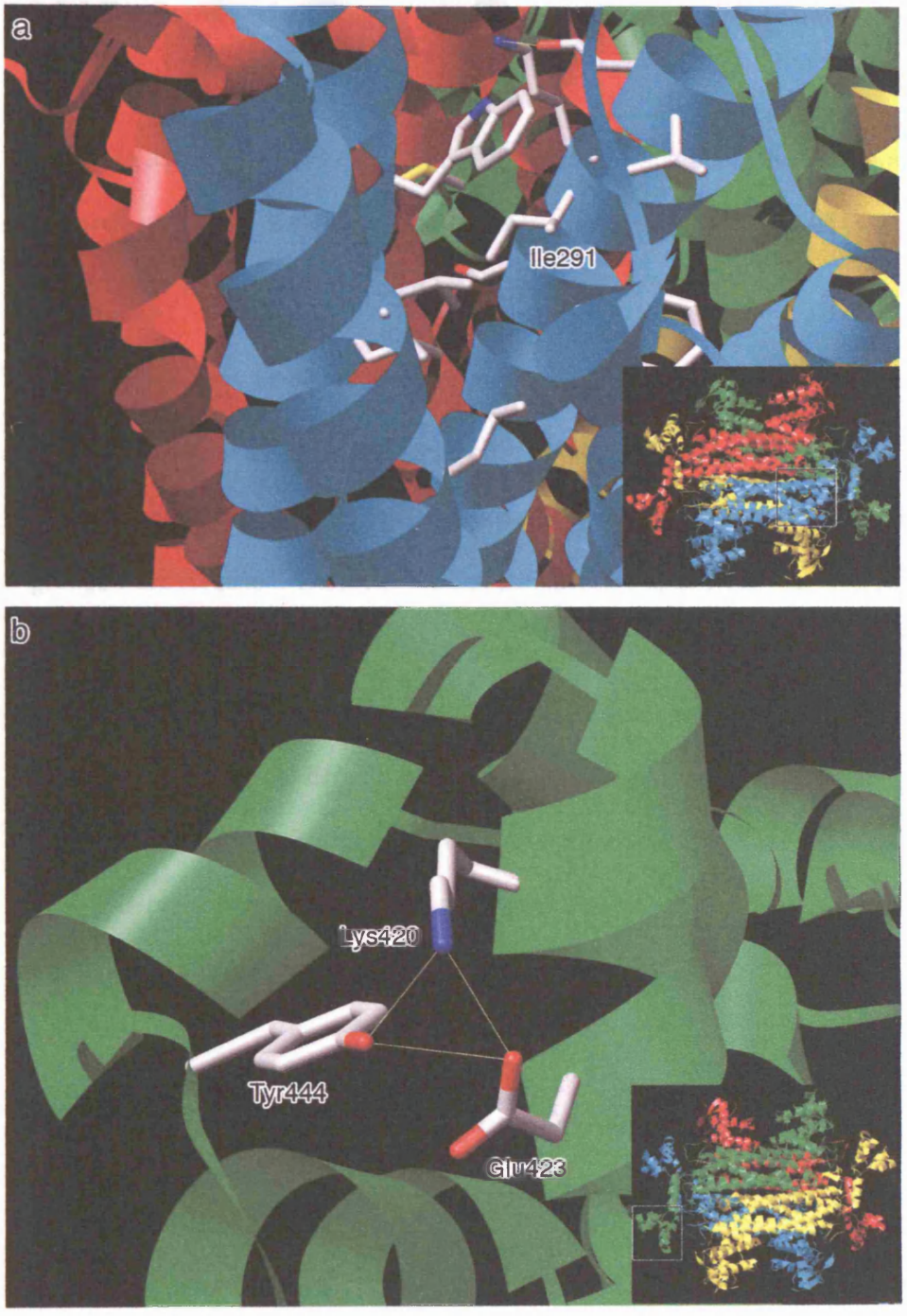

Figure 3.12 Location and interactions of the two novel missense mutations I295T (a) and Y448C (b). For a description of the interactions, see main text.

3.3.5 Frequency of pathogenic *FH* mutations in uterine leiomyoma patients

In assessing the frequency of pathogenic *FH* mutations, the three novel missense mutations, the pathogenic effects of which were uncertain, H133P, I295T and Y448C, were considered to be pathogenic.

3.3.5.1 Frequency of *FH* mutations in uterine leiomyoma patients

In order to assess the frequency of *FH* mutations in patients with uterine leiomyomas, 334 uterine leiomyoma patients from a variety of sample groups were screened. This set excluded patients sent specifically to the laboratory for HLRCC mutation testing. The screen identified pathogenic *FH* mutations in 7/335 (2.1%) of unselected leiomyoma cases. Therefore, the occurrence of germline *FH* mutations in uterine leiomyoma cases is very rare, and is not a significant cause of uterine leiomyoma onset.

In patients with HLRCC related symptoms sent to the laboratory for *FH* screening, 6/26 (23%) patients showed sequence mutations in the *FH* gene.

3.3.5.2 Frequency of FH mutations in Afro-Caribbean patients

Within the group of unselected uterine leiomyoma cases, ethnicity was reported for 232 samples (**Table 3.8**). The patients were grouped into three categories of ethnicity: African and Afro-Caribbean; Caucasian; and other (patients with reported ethnicities who were neither Caucasian nor African/Afro-Caribbean). Patients of African and Afro-Caribbean ethnicity were found to be significantly younger ($p<0.001$, Wilcoxon-signed rank test)

than Caucasian patients and those of other ethnicities at the time of sample collection. Six of the *FH* mutations identified in this study were from patients with reported ethnicities. Three of these, R190H, ins434K and K187R/H133P were observed in Caucasian patients, and 3, I295T, and 2 occurrences of ins434K, were observed in patients of other ethnicities. Therefore, despite the younger age of leiomyomas in African and Afro-Caribbean patients, which mimics the younger age of onset in HLRCC patients, mutations in *FH* do not appear to play an important role in the earlier onset of leiomyomas in these patients.

Table 3.8 Distribution of patients by ethnicity and number of *FH* mutations.

Ethnic Group	**Number of samples**	**Age of onset (yrs)**		**No. *FH* mutations**
		Mean	**SD**	
African/Afro-Caribbean	75	40.83[1]	7.01	0[2]
Caucasian	55	46.15[1]	7.38	3[2]
Other	102	45.57[1]	6.63	3[2]

[1]African/Afro-Caribbean patients are significantly younger than Caucasian and other patients ($p<0.001$ Wilcoxon signed-rank test).

[2]No significant difference in the frequency of *FH* mutations in African/Afro-Caribbean patients, and Caucasian/other patients ($p=0.18$, Fisher's exact test).

3.3.5.3 *FH* mutations in cancer cell lines

In order to assess the effects of *FH* mutations on a variety of cancers, a panel of 70 cancer cell lines was screened. Only one missense change was

identified in all the samples, an exon 0 A32T mutation in cell line DU145. However, no definitively pathogenic mutations in *FH* were identified.

3.4 Discussion

The work in this Chapter aimed to examine the frequency of pathogenic and potentially pathogenic *FH* mutations in sporadic uterine leiomyoma patients and in cancer cell lines. In addition, further possible HLRCC patients were screened in order to identify novel mutations to expand the mutation spectrum. The frequency of *FH* mutations in different ethnic groups was also studied. In addition to this, the function of *FH* mutations, particularly in relation to common patterns of mutation and the effects of these mutations on protein structure, was studied *in silico*.

Overall it was found that the prevalence of *FH* mutations in uterine leiomyoma patients was very low, in this study occurring with a frequency of 2.1%. Therefore, HLRCC plays only a very small part in the overall prevalence of uterine leiomyomas in the general population. Previous work by Barker *et al* demonstrated a low frequency of allelic imbalance of *FH* sporadic uterine leiomyomas, but no somatic mutations, in 129 leiomyomas from 21 patients (Barker et al. 2002).

Interestingly, only 6/26 (23% of) patients with HLRCC-like features were identified to have germline *FH* mutations. In several cases, *FH* screening was requested for patients with early onset renal cancer of different pathology to the papilliary carcinomas associated with HLRCC (Alam et al. 2003), but no other HLRCC-like symptoms, where screening for other predisposition genes, such as *VHL*, had not shown any mutation. However, this still does not account for a number of patients with almost certain HLRCC, including uterine and skin leiomyomas and renal cancer, that did not demonstrate a

mutation. When *FH* was initially identified as the gene responsible for HLRCC, 12/50 (24%) of families had no detectable mutations in *FH (Tomlinson et al. 2002; Alam et al. 2003)*. Yet, for 3 of these families, FH activity was reduced by approximately 50% (Alam et al. 2003). Therefore, screening techniques were missing some pathogenic alterations.

This would also suggest that pathogenic alterations have been missed in this study, and that the actual frequency of germline *FH* mutations in uterine leiomyoma patients may be higher than is reported here. It is likely that novel sequence variants exist which result in the observed reduction of FH activity in patients without apparent *FH* mutations. In order to identify these mutations, a number of different screening techniques could be used which have not been used to date. Screening for deletions of individual exons has not been carried out. Deletion of one or more exons would render the translated protein enzymatically useless. In order to test for this, techniques such as multiplex amplifiable probe hybridisation (MAPH) and multiplex ligation dependent probe amplification (MLPA) could be used (Sellner and Taylor 2004).

A number of splice site mutations have been reported in HLRCC patients, including a novel mutation in this study. Thus defects in splicing of the precursor RNA appear to have a detrimental effect on the protein. In order to test for variants affecting splicing, an mRNA-based approach could be used to detect different length transcripts. Furthermore, changes in mRNA expression could also have an effect on enzyme activity, therefore, testing expression by quantitative PCR could also identify novel changes.

Unfortunately, RNA was unavailable for a number of these studies and so this could not be carried out.

Assuming from the initial study that 24% of *FH* mutations were novel variants not able to be detected by the techniques used in this study, this would only increase the number of identified mutations by 2 or 3 in total, leading to an increase in prevalence of *FH* mutations in uterine leiomyoma patients to 2.8%. Therefore, *FH* mutations can still be considered to play only a small part in uterine leiomyoma prevalence in the general population.

The prevalence of *FH* mutations in African and Afro-Caribbean patients was also studied to examine the possible role that these mutations may play in the multiple uterine leiomyoma phenotype observed in these patients. Despite these patients having a lower age of onset than Caucasian patients or patients of other ethnicities, as is observed in HLRCC patients, no *FH* mutations were identified, fewer than in Caucasian and other patients. Therefore, it can be concluded that *FH* mutations are not responsible for the earlier onset and greater multiplicity of uterine leiomyomas in African and Afro-Caribbean patients.

The 70 cell lines screened appeared to contain no *FH* mutations. This could be a result of either of two things. Firstly, *FH* mutations may not contribute to the pathogenesis of the variety of cancers represented by the cell lines. Secondly, since a cell line contains a pure population of cells, homozygous *FH* mutations may have been missed by SSCP. Therefore, a screen carried out by sequencing the *FH* gene directly could have provide a better idea of the prevalence of *FH* mutations in these cell lines.

A number of novel mutations were identified in this study. The gold standard for assessing *FH* mutations pathogenicity is to study *FH* activity in patients' cells (Alam et al. 2003; Pithukpakorn et al. 2006). This option was not available due to the methods of sample collection for this study and so alternative *in silico* approaches were taken. These studies resulted in the probable exclusion of all the exon 0 missense mutations as pathogenic, based on their minimal effect on the amphiphilic nature of the mitochondrial leader sequence. In addition, the intronic sequences, excluding the splice acceptor sequence of exon 3, were also provisionally excluded as pathogenic mutations. The results for the novel coding missense mutations, H133P, I295T and Y448C, and the pre-transcription start mutation were not as conclusive.

In order to obtain a definitive answer for the effects of these variants on FH activity, and so to assess their pathogenicity, further studies would need to be carried out. Fusing the mutant leader sequence to a fluorescent reporter protein such as GFP and examining the subcellular localisation of the resultant molecule could assess the effects of the exon 0 mutations. The effects of novel missense mutations could be assessed by site-directed mutagenesis to obtain mutant *FH* cDNA at each of those locations and measuring the enzyme activity of *in vitro* transcribed mutant protein compared to wild-type protein. The effects of intronic mutations could be assessed by examining splice variants in mRNA. Finally, the effect of the pre-transcription start mutation could be assessed by expression analyses of FH in tissues with and without the novel mutation.

In conclusion, *FH* mutations appear to be a rare, but important, hereditary cause of uterine leiomyomas, and are not responsible for the

multiple leiomyoma phenotype observed in African and Afro-Caribbean patients. The spectrum of mutations demonstrated that highly conserved residues were more likely to be mutated in HLRCC and FH deficiency patients, which are more likely to result in loss of function of the enzyme resulting in disease.

Chapter 4

Apoptosis and Ultrastructure of HLRCC and sporadic uterine leiomyoma

4.1 Introduction

In HLRCC, *FH* acts as a classical tumour suppressor gene, requiring complete loss of activity for tumorigenesis to occur (Alam et al. 2003). This results in subsequent disruption of the Krebs cycle, since no other energetically viable pathway exists to convert fumarate to malate in human cells. The emergence of pseudo-hypoxia as an important mechanism in HLRCC tumour pathogenesis still leaves several questions related to tumour pathogenesis (Pollard et al. 2005a; Pollard et al. 2005b; Selak et al. 2005). One such question regards the resistance to apoptosis of HLRCC tumour cells.

One of the roles of the hypoxic response, involving HIF1-α, is to protect a cell undergoing short-term hypoxia, with the expectation of eventual reoxygenation. However, normal cells exposed to chronic hypoxia eventually die (Jung et al. 2001). Tumour formation in HLRCC suggests that this cell death does not occur in cells with complete loss of wild-type *FH*, despite constitutive activation of HIF1α (Isaacs et al. 2005; Pollard et al. 2005b). The question, therefore, regards the mechanisms utilised by HLRCC cells to stay alive.

Ultrastructural studies of sporadic uterine leiomyomas have demonstrated a number of distinguishing features distinguishing them from the myometrium, including alterations of intermediate filaments (Richards et al. 1998) and extracellular matrix (Leppert et al. 2004). This is discussed in greater depth in chapter 1 (1.1.2). Tumours from the HLRCC-related tumour syndrome hereditary paragangliomatosis and phaeochromocytoma (HPGL), resulting from mutations in three of the genes encoding subunits of the succinate dehydrogenase (SDH) complex, have also been examined

ultrastructurally and have demonstrated an increased number of mitochondria in the cytoplasm of tumour cells from these patients (Douwes Dekker et al. 2003).

The work in this chapter examines the expression and distribution of several markers related to apoptosis and cell proliferation in order to examine the involvement of these mechanisms in HLRCC and sporadic leiomyoma pathogenesis. Particular focus is paid to markers previously shown to be related to uterine leiomyoma pathology or the resistance of hypoxic cells to apoptosis. Furthermore, ultrastructural studies of HLRCC and sporadic leiomyomas were carried out in order to identify potential novel differences between the two species of leiomyomas, which may provide clues to mechanisms of pathogenesis.

4.2 Materials and Methods

4.2.1 Immunohistochemistry

Immunohistochemistry was carried out as described in Chapter 2 (2.8.2) on 9 uterine leiomyomas and 4 myometrium samples from 8 HLRCC individuals with known germline FH mutations, 13 uterine leiomyomas and matched myometrium from 13 sporadic cases (women without germline FH mutations and no evidence of cutaneous leiomyomatosis), and a further 4 sporadic uterine leiomyomas. Seven antibodies against markers of apoptosis and proliferation, and one against a cytoskeletal protein were used (Table 4.1). Bcl-2, Bax and PCNA were all chosen due to previous reports of altered expression in sporadic uterine leiomyomas (Dixon et al. 2002; Wu et al. 2002; Kovacs et al. 2003). The Bcl-2 family members Bcl-x and Bak, and the Inhibitor of apoptosis (IAP) family members Survivin and c-IAP-2 have all been associated with resistance of hypoxic cells to apoptosis (Dong et al. 2002; Dong et al. 2003; Dong and Wang 2004; Yang et al. 2004; Sasabe et al. 2005). Desmin expression was studied as a result of ultrastructural observations. All samples were confirmed as either myometrium or leiomyoma based on serial haematoxylin and eosin stained sections (Figure 4.1A). Intensity of staining was calculated by semi-quantitative observation as described in chapter 2 (2.8.2).

Table 4.1 Details of antibodies used for immunohistochemistry

Antigen	Source	Dilution	Positive Control	Supplier
Bcl-2	Mouse	1:25	Tonsil	Dako
Bak	Rabbit	1:40	Tonsil	Abcam
Bcl-$x_{L/S}$	Rabbit	1:100	Normal Colon	Dako
cIAP-2	Rabbit	1:50	Tonsil	Santa Cruz
Bax	Rabbit	1:200	Breast Carcinoma	Santa Cruz
Proliferating Cell Nuclear Antigen (PCNA)	Mouse	1:1000	Tonsil	Dako
Survivin	Rabbit	1:2000	Melanoma	Abcam
Desmin	Mouse	1:50	Myometrium	Dako

4.2.2 Electron Microscopy

Four uterine leiomyomas from one HLRCC individual with a known germline *FH* mutation, and 2 uterine leiomyomas and matched myometrium from 2 sporadic cases were collected fresh from surgery and fixed in glutaraldehyde phosphate buffer. Electron microscopy was carried out as described in Chapter 2 (2.9).

4.2.3 Tissue cell density

Tissue cellularity was assessed on haematoxylin and eosin stained paraffin sections by nuclear density. Nuclei were counted in 10 random 625μm^2 sections of a 10 x 10 graticule in 10 random, high power, fields.

4.2.4 Data Analysis

Results for immunohistochemistry were collated and analysed using the Mann-Whitney U test using R. A p-value of less than 0.05 was considered significant.

4.3 Expression of apoptotic proteins in HLRCC and sporadic uterine leiomyomas

Immunohistochemistry was carried out on myometrium and uterine leiomyomas from HLRCC and sporadic cases to examine the expression of proteins involved in apoptosis, and of the proliferative marker PCNA. A summary of results is shown in Table 4.2, and examples of staining are shown in Figure 4.1. Increased expression of Bcl-2 and PCNA was observed in both HLRCC ($p=0.049$ and $p=0.033$ respectively, Mann-Whitney) and sporadic ($p=0.015$ and $p=0.048$ respectively, Mann-Whitney) leiomyomas (Figure 4.1B and C) compared to normal myometrium from HLRCC or sporadic leiomyoma patients as appropriate.

Furthermore, HLRCC leiomyomas showed an increase in expression of Bcl-x ($p=0.015$, Mann-Whitney, Figure 4.1D) and a concurrent decrease in the expression of Bak ($p=0.048$, Mann-Whitney, Figure 4.2), changes not observed in sporadic cases. For Bak, HLRCC myometrium also demonstrated decreased expression compared to non-HLRCC myometrium ($p=0.0072$, Mann-Whitney, Figure 4.2). Expression levels of Bax, Survivin and c-IAP2 were not significantly altered.

Table 4.2 Summary of immunohistochemistry results for apoptotic and proliferative markers in HLRCC and non-HLRCC myometrium and uterine leiomyomas. Data are shown as the median score followed by the range of values and the number of samples. Where all data had the same score, no range is shown.

	Antibody						
Tissue	**Bcl-2**[1]	**Survivin**[1]	**c-IAP2**[1]	**Bak**[1]	**Bax**[1]	**Bcl-x**[1]	**PCNA**[2]
HLRCC Myometrium	0 (0-1) (n=3)	0 (0-1) (n=2)	1 (n=2)	1 (1-2) (n=4)[5]	2 (2-3) (n=4)	1 (n=3)	1 (1-2) (n=2)
Non-HLRCC Myometrium	1 (0-2) (n=13)	2 (1-4) (n=9)	2 (1-3) (n=13)	3 (2-4) (n=10)	2 (1-3) (n=12)	2 (1-3) (n=11)	2 (0-3) (n=10)
HLRCC Uterine Leiomyoma	2 (0-2) (n=9)[3]	2 (0-3) (n=9)	1 (1-3) (n=9)	1 (0-1) (n=7)[4]	2 (1-4) (n=9)	3 (1-3) (n=9)[3]	4 (2-4) (n=9)[3]
Sporadic Uterine Leiomyoma	1 (0-2) (n=13)[3]	3 (1-4) (n=13)	2 (1-2) (n=14)	3 (2-4) (n=14)	2 (1-3) (n=14)	3 (1-4) (n=13)	2 (2-4)

[1]Scored by semi-quantitative observation: Absent (0), weak (1), moderate (2), strong (3), and very strong (4).

[2]Scored by frequency of nuclear staining: <10% (0), 10-25% (1), 25-50% (2), 50-75% (3), >75% (4).

[3]Significantly greater in leiomyomas than myometrium ($P<0.05$).

[4]Significantly less in leiomyomas than myometrium ($P<0.05$).

[5]Significantly less in HLRCC myometrium than non-HLRCC myometium ($P<0.05$).

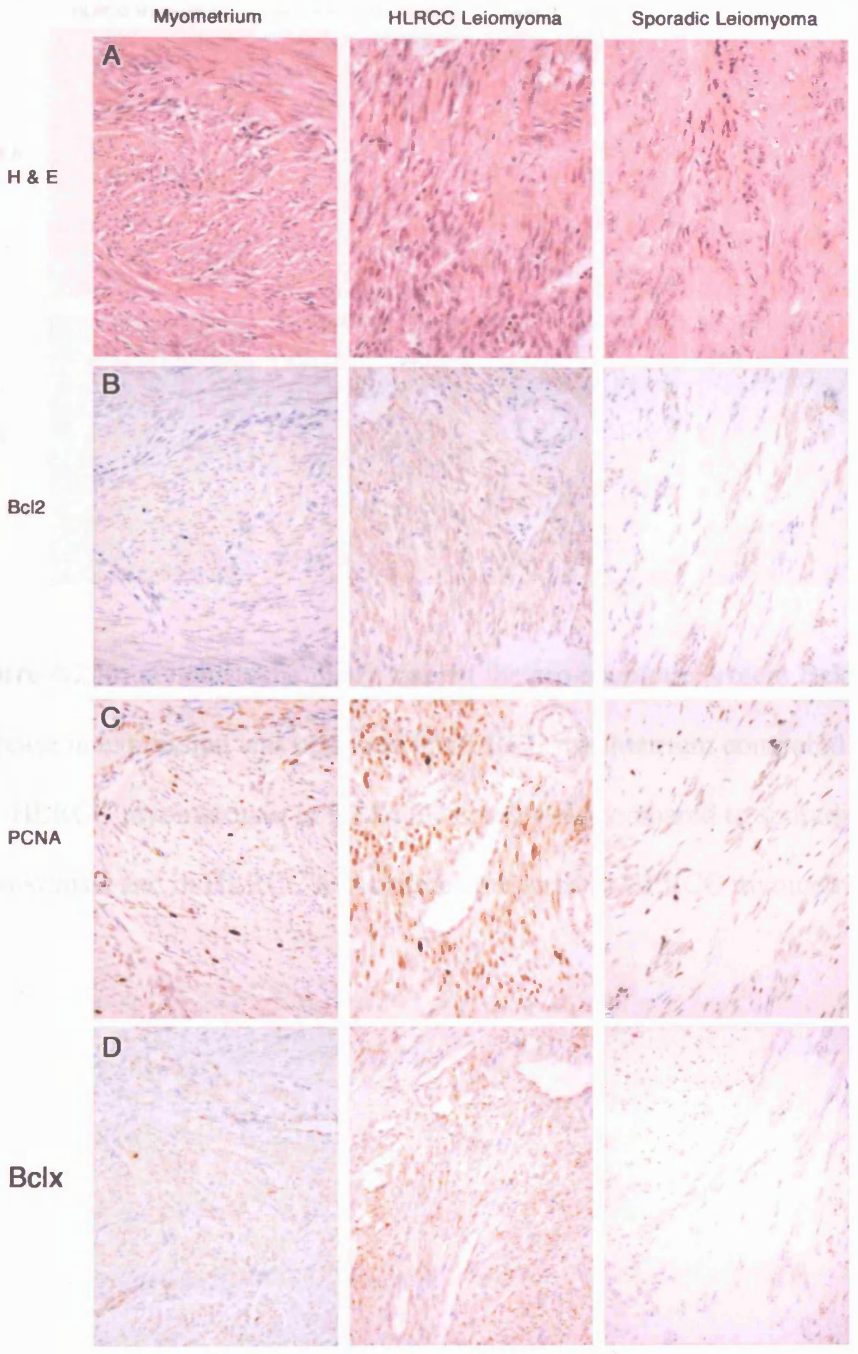

Figure 4.1 Representative heamatoxylin and eosin-stained sections (A) and examples of immunohistochemistry for Bcl-2 (B), PCNA (C), and Bcl-x (D). An increase in Bcl-2 staining and PCNA is observed in HLRCC and sporadic leiomyomas compared to myometrium (B,C). Increased Bcl-x is also observed in HLRCC leiomyomas compared to myometrium (D)

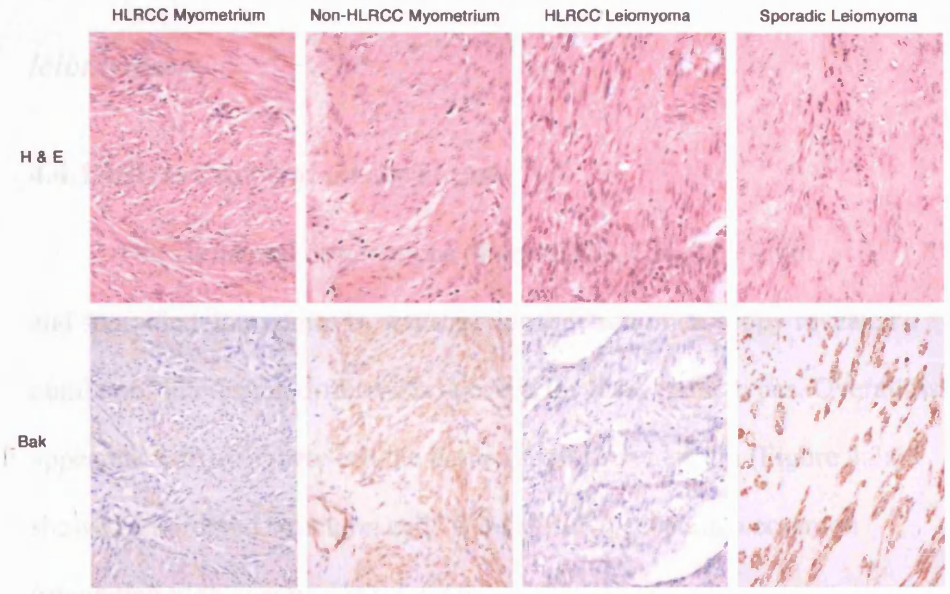

Figure 4.2 Immunohistochemistry against the pro-apoptotic protein Bak. A decrease in expression was observed in HLRCC myometrium compared to non-HLRCC myometrium, in HLRCC leiomyomas compared to sporadic leiomyomas, and in HLRCC leiomyoma compared to HLRCC myometrium.

4.4 Ultrastructural Aberrations in HLRCC and sporadic uterine leiomyomas

4.4.1 Ultrastructural observations

Ultrastructural observations of non-HLRCC myometrium, and HLRCC and sporadic leiomyomas by transmission electron microscopy revealed a number of interesting differences between the three tissue types. Overall tissue appearance differed between the tissue types. Myometrium (Figure 4.3a) showed an ordered structure; cells were closely packed in a common orientation with evenly sized, light nuclei. The HLRCC leiomyomas demonstrated some breakdown of this order (Figure 4.3b); cells appeared to be more compact and failed to align along a common axis, nuclei were electron dense and of uneven shape and size. Ultrastructure of sporadic leiomyomas showed an even greater breakdown in order (Figure 4.3c); cells were clustered in islands within an extensive collagen matrix. Nuclei again appeared more electron dense than in the myometrium, and demonstrated irregular architecture.

The electron micrographs also appeared to reveal a difference between the cellularity of the HLRCC and sporadic leiomyomas, due to the increased collagen matrix in the latter. This was confirmed by counting cell density in haematoxylin and eosin stained paraffin sections. The patchy nature of sporadic uterine leiomyoma tissue increased the range of cell densities observed compared to myometrium and sporadic leiomyomas, which were more homogeneous. To overcome this effect, minimum observed cell density was used for statistical analysis. HLRCC leiomyomas (median density=26

nuclei/field, IQR=31.6) had a greater cell density than sporadic leiomyomas (median minimum density=14, IQR=4.25, p=0.031, Mann-Whitney) and myometrium (median minimum density=13, IQR=8.25, p=0.01, Mann-Whitney).

Ultrastructural differences were also observed in the ultrastructure of the collagen matrix. In myometrium, collagen fibrils were organised into tight bundles (Figure 4.3d). Collagen fibrils in HLRCC leiomyomas showed some disorganisation; bundling of the fibrils appeared less tight than in the myometrium (Figure 4.3e). Collagen in sporadic leiomyomas appeared very disorganised; fibrils failed to bundle and appeared randomly scattered throughout the matrix (Figure 4.3f).

The most striking intracellular difference observed was the variation of order and distribution of intermediate filament structure. In both sporadic and HLRCC leiomyomas, intermediate filaments formed disordered structures in the cytoplasm (Figure 4.3h-k), losing the common polarity observed in the myometrium (Figure 4.3g), and forcing myofilament structures and other organelles to the cell periphery. These variations also differed between species of leiomyoma: in sporadic tumours the intermediate filaments were spread diffusely throughout the cytoplasm (Figure 4.3j,k); whereas in HLRCC leiomyomas, they formed large, 'thumbprint'-like aggregates (Figure 4.3h,i).

HLRCC leiomyomas also demonstrated other interesting changes. These included the presence of autophagosomes in several cells (Figure 4.3l), and some differences in mitochondrial morphology, including swelling, loss of membranes, and the presence of matrical densities (Figure 4.3m). However, equivalent mitochondrial changes were also observed in normal myometrium

fixed and processed at the same time, so the relevance of these changes could not be confirmed.

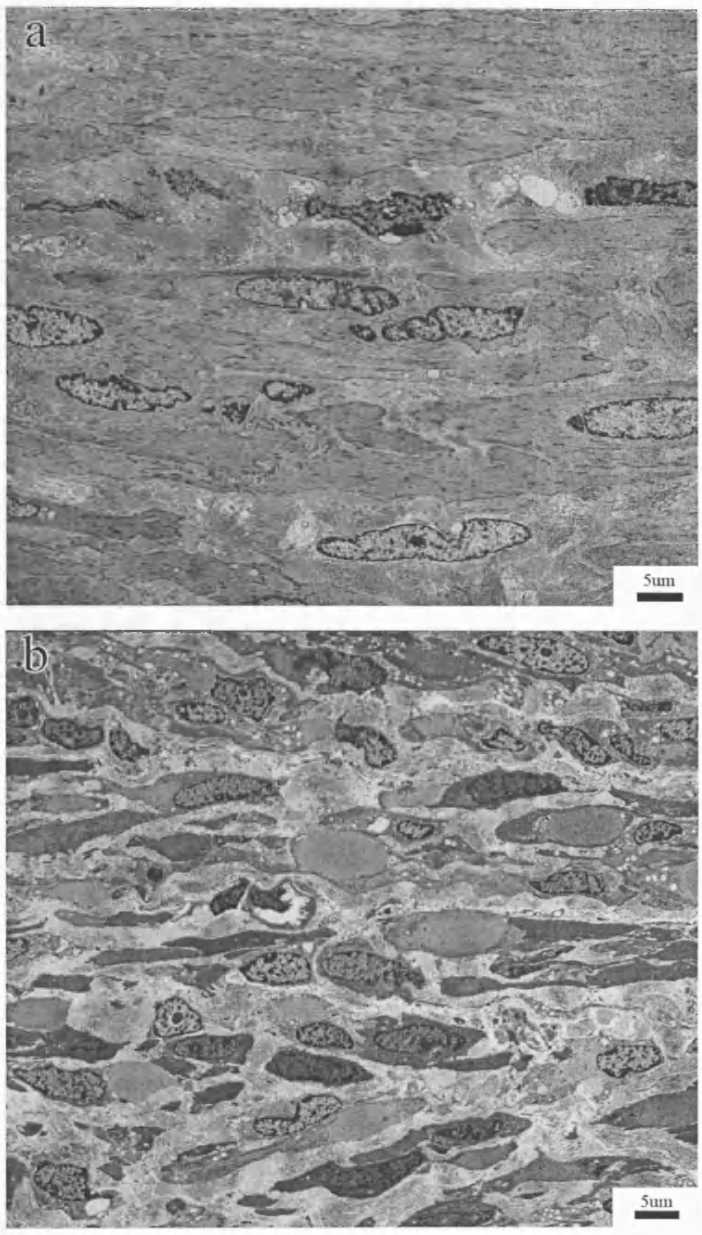

Figure 4.3 Ultrastructural observations of myometrium and HLRCC and sporadic leiomyomas. A scale bar is shown in all micrographs for size comparison. a) Myometrium – The tissue is well structured with a common alignment of cells, light, even structured nuclei, and an ordered extracellular matrix. (ECM). b) HLRCC leiomyoma – A breakdown of order is apparent, there is an increased cell density and a less ordered ECM and nuclear structure. Large filamentous deposits are evident in the cytoplasm.

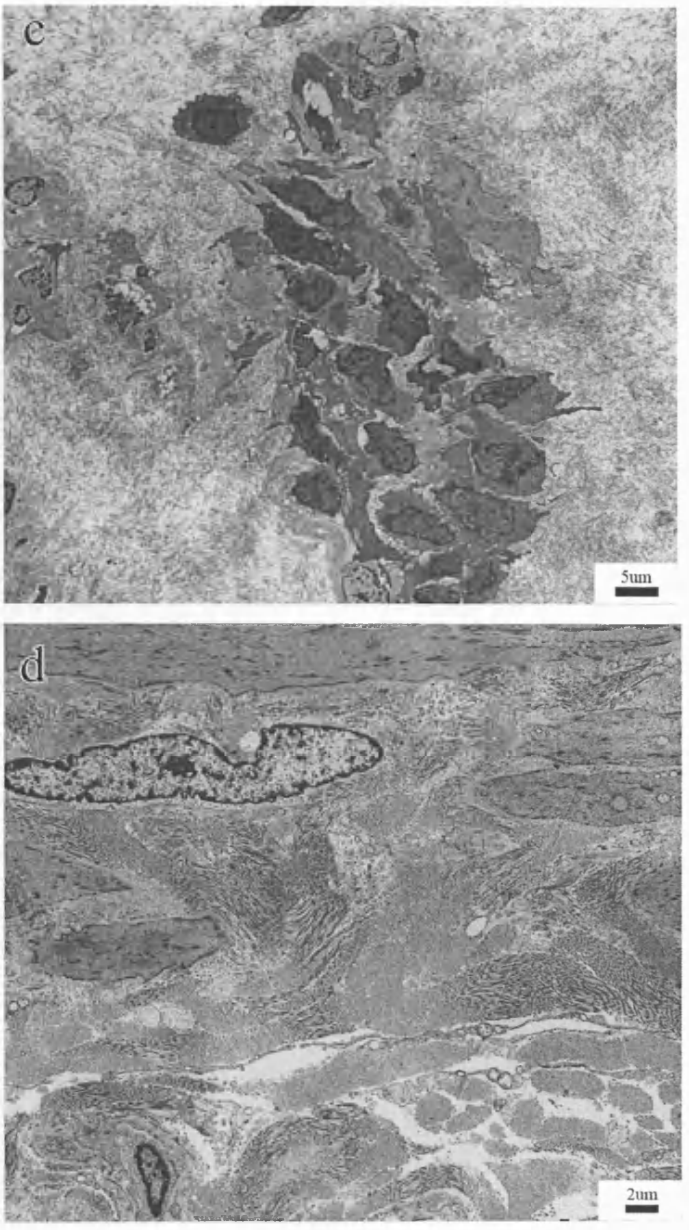

Figure 4.3 (Cont'd) c) Sporadic leiomyoma – The tissue shows extensive breakdown of order, with small islands of cells within an extensive collagen matrix. The ECM appears highly disordered, and the cell cytoplasm appears packed with filamentous deposits, and the nuclei are dark and lacking even structure. d) Collagen ECM of myometium – The ECM in myometrium is highly ordered, the collagen fibrils form neat bundles of defined orientation.

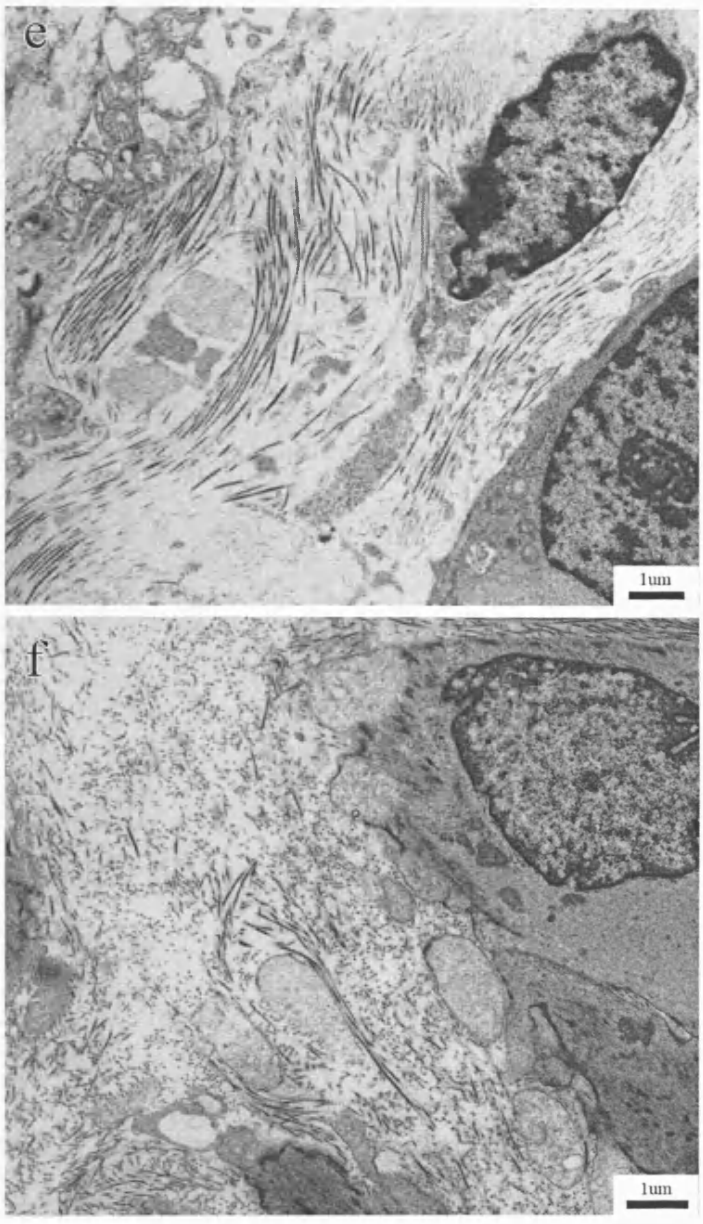

Figure 4.3 (Cont'd) e) ECM in HLRCC leiomyoma – While some orientation is evident, the structure is disjointed. The collagen fibrils appear to form less tight bundles, compared to the neat bundles observed in the myometrium. f) ECM in sporadic leiomyoma – Evidence of collagen fibril orientation and structure appears completely lost. The fibrils fail to form bundles and appear randomly scattered between cells.

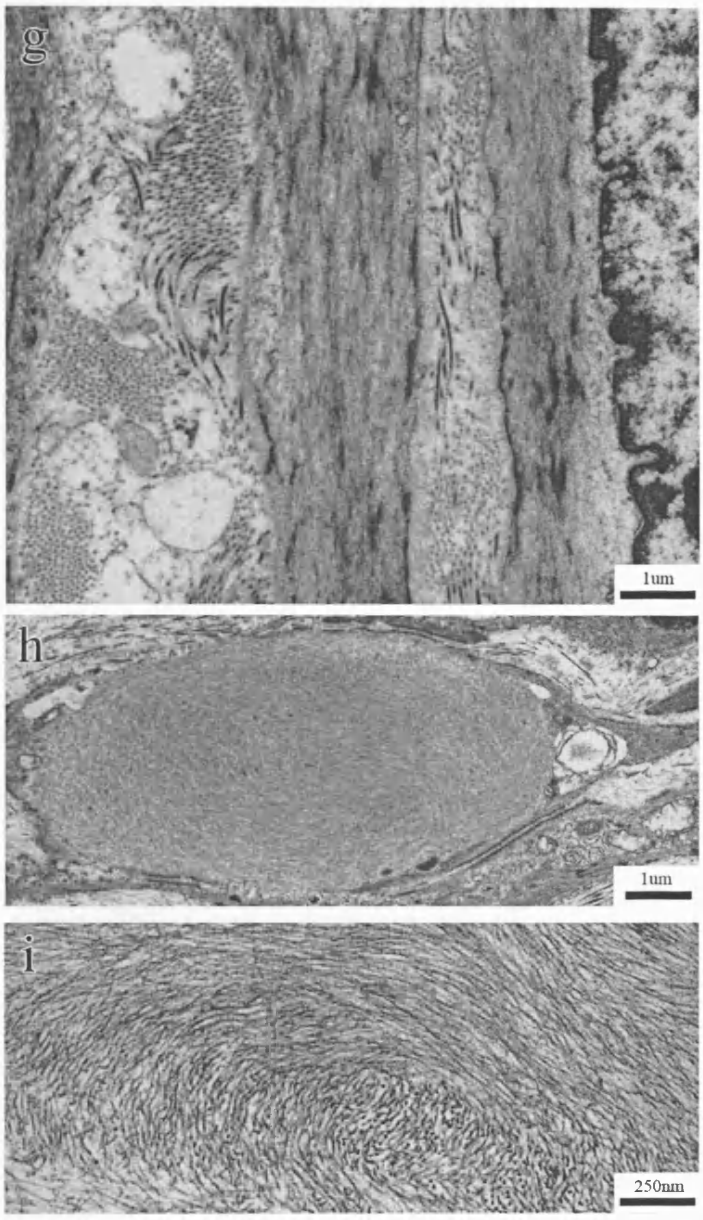

Figure 4.3 (Cont'd) g) Filament structures in myometrium – Filaments in the myometrium are well ordered, running parallel to the cell's long axis, with frequently and regularly interspersed dense bodies along the filaments. h & i) Aggregation of filaments in HLRCC leiomyomas – A majority of cells in HLRCC leiomyomas contained 'thumbprint'-like accumulations of intermediate filaments, spiralling within the cell. These aggregates forced myofilament dense bodies and other organelles to the cell periphery.

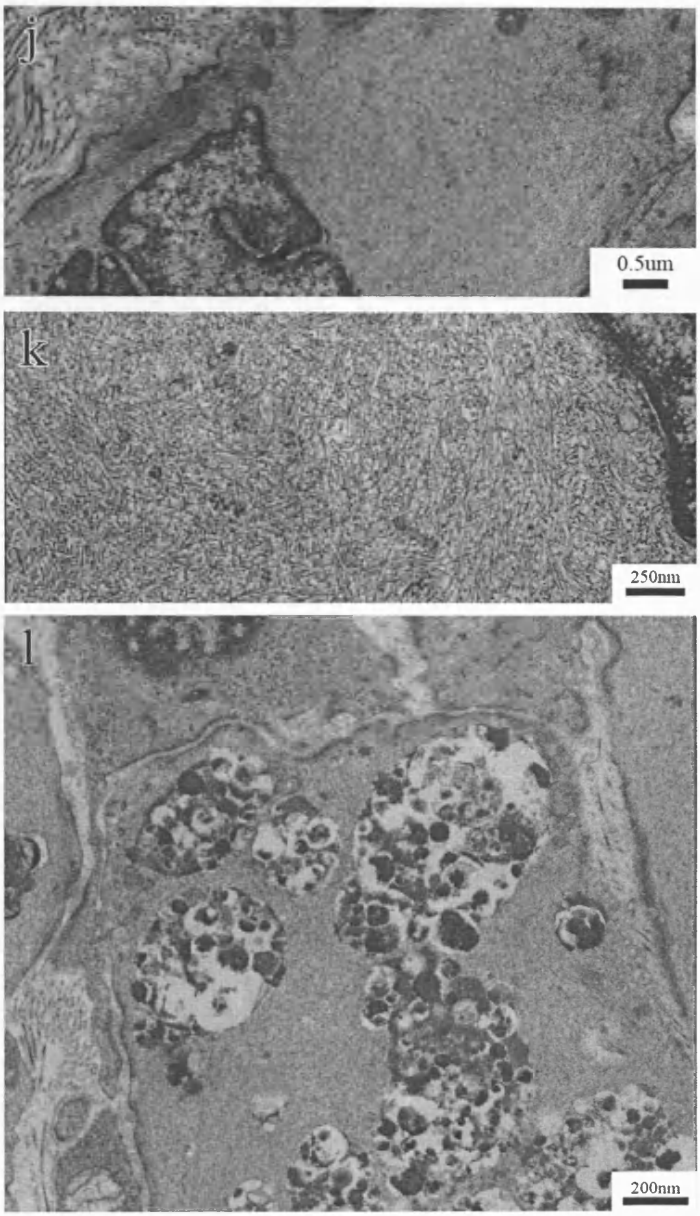

Figure 4.3 (Cont'd) j & k) Filament structures in sporadic leiomyomas – As in HLRCC leiomyomas, filament structures are broken down. The cytosplasm is packed with a jumble of intermediate filaments, without the spiralling pattern observed in HLRCC tumours, which again force organelles and contractile elements to the cell periphery. l) Autophagosomes in HLRCC leiomyomas – Autophagosomes were observed in a few cells inboth HLRCC and sporadic leiomyomas.

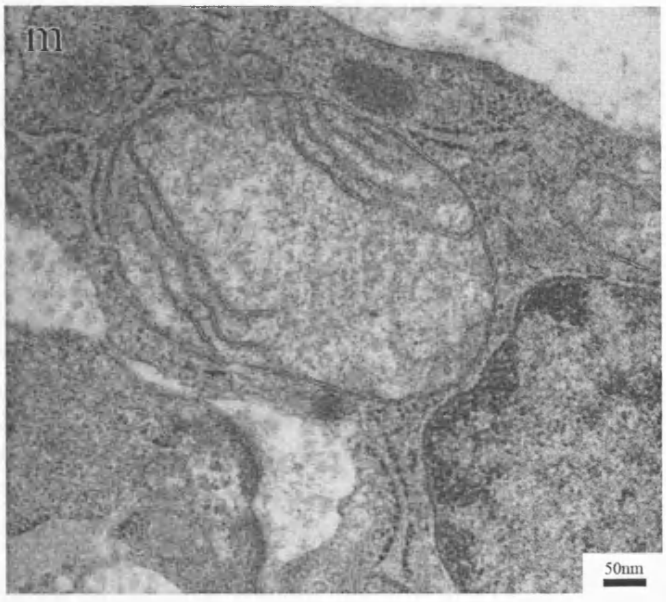

Figure 4.3 (Cont'd) m) Mitochondrial swelling observed in HLRCC leiomyoma – A number of mitochondria in HLRCC tumour cells were observed to have swollen mitochondria. In this case, the swollen mitochondria is surrounded by several apparently normal mitochondria. In some cases the cristae appeared lost. Swollen mitochondria were also observed in the myometrium and sporadic leiomyoma samples. Consequently, this swelling may be a result of fixation rather than tumorigenesis.

4.4.2 Desmin Immunohistochemistry

In order to identify proteins implicated in the 'thumbprint' aggregates of intermediate filaments observed in HLRCC leiomyoma ultrastructure, immunohistochemistry was carried out for the muscle intermediate filament protein Desmin (Figure 4.4). Immunostaining for Desmin mimicked the patterns observed by electron microscopy. In the myometrium, staining was diffuse, with no evidence of filament aggregation, and appeared ordered. Staining in sporadic leiomyomas was also diffuse, but lacked order and had evidence of some aggregation. Finally, staining in HLRCC leiomyomas was limited to large aggregates of about the same size as those observed ultrastructurally, with little staining elsewhere in the cell.

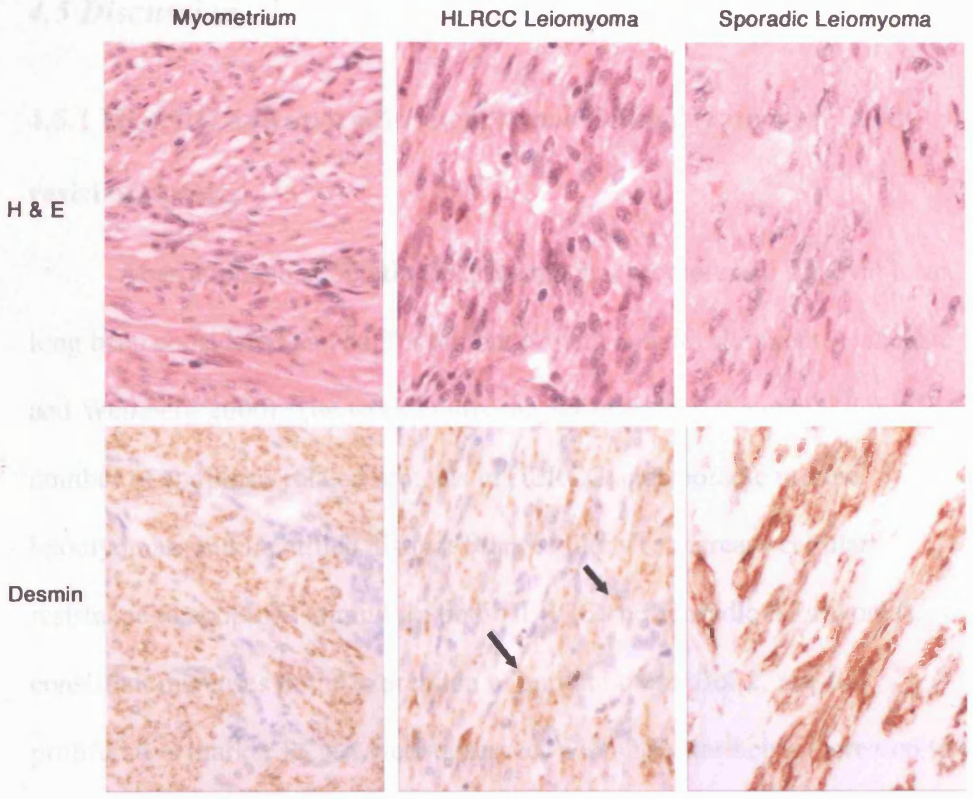

Figure 4.4 Immunohistochemical staining for the intermediate filament protein Desmin. Staining in myometrium shows ordered staining in line with the observed ordered smooth muscle structure. Staining in HLRCC leiomyomas reveals aggregates (arrowed) of a similar scale to those observed by electron microscopy. Staining in sporadic leiomyomas appears disordered with less evidence of aggregation than the HLRCC leiomyomas.

4.5 Discussion

4.5.1 HLRCC and sporadic leiomyomas demonstrate a tendency to resist apoptosis

Aberrations in apoptotic mechanisms that promote cell survival have long been considered as vital for tumour growth and development (Hanahan and Weinberg 2000). The work in this chapter examined the expression of a number of apoptosis related proteins in HLRCC and sporadic uterine leiomyomas, and identified distinct changes likely to increase cellular resistance to apoptotic stimuli. In both HLRCC and sporadic leiomyomas, consistent increases in the expression of anti-apoptotic Bcl-2, and the proliferative marker PCNA were observed, with the latter being increased to a greater extent in HLRCC leiomyomas. The results for sporadic tumours are in agreement with previous studies, which have observed an increase in Bcl-2 and PCNA in sporadic leiomyomas (Dixon et al. 2002; Kovacs et al. 2003).

Furthermore, changes in two other markers were identified solely in HLRCC leiomyomas: an increase in expression of anti-apoptotic Bcl-x; and a concurrent decrease in expression of pro-apoptotic Bak. The observed changes imply that both HLRCC and sporadic leiomyoma cells have acquired an increased resistance to apoptosis compared to the host myometrium. However, the difference in the pattern of marker expression implies that perhaps separate mechanisms are followed to come to the same outcome. The alterations in Bcl-x and Bak may also imply a greater resistance to apoptosis, and the increased expression of PCNA implies a greater rate of proliferation in HLRCC compared to sporadic leiomyomas. In addition, alterations in the level

of Bak between myometrium from HLRCC and non-HLRCC patients is intriguing, and may point to a reduced basal level of apoptosis in these cells.

Expression of the other studied apoptotic factors, Survivin and cIAP2, did not significantly differ in either HLRCC or sporadic uterine leiomyomas, despite previous associations with hypoxia. This could imply that they require further regulation in addition to hypoxia, or that the hypoxic response observed in other cell types does not apply to leiomyoma cells. The lack of altered expression of Bax was not as surprising given previous differing results of expression analyses in leiomyomas (Dixon et al. 2002; Wu et al. 2002; Kovacs et al. 2003).

As previously described, current evidence suggests that pseudo-hypoxic drive is the key mechanism of pathogenesis in both HLRCC and HPGL tumours (Isaacs et al. 2005; Pollard et al. 2005a; Pollard et al. 2005b; Selak et al. 2005). However, cells exposed to chronic hypoxia eventually undergo apoptosis, should other mechanisms to increase the cell's oxygen supply fail, such as the release of angiogenic factors (Jung et al. 2001).

Interplay between hypoxia and apoptosis exists as a result of VEGF signalling. Several studies have demonstrated that VEGF acts as a survival factor in endothelial cells by increasing expression of Bcl-2 (Nor et al. 1999; Cai et al. 2003). This activation occurs via the PI-3-K and MAPK pathways, and has been shown to occur in response to HIF1-α activation (Trisciuoglio et al. 2005).

Although cells from HLRCC and HPGL tumours both appear to undergo chronic hypoxia, the work in this chapter demonstrates an apparent increase in resistance to apoptosis by increased expression of anti-apoptotic

markers. The highly vascular nature of HLRCC leiomyomas suggests that a ready supply of oxygen is available to the cell. Therefore, it is likely that alternative mechanisms of oxygen sensing override the pro-apoptotic effects of the chronic hypoxia signal from HIF1-α, and increase the expression of anti-apoptotic proteins to compensate.

In vitro evidence already exists for this theory, in a study carried out by Sasabe and colleagues, who examined the role of artificially activated HIF1-α in oral squamous cell carcinoma cells. They cultured cells expressing the activated HIF1-α in both normoxic and hypoxic environments for 24hrs and examined the expression of apoptosis-related proteins. They discovered increased expression of Bcl-2 and Bcl-x_L, in cells cultured in both conditions, but with a greater increase in cells cultured under normoxic conditions. Control cells under hypoxic conditions showed a decrease in Bcl-2 and Bcl-x_L expression, and an increase in expression of pro-apoptotic Bax and Bak (Sasabe et al. 2005).

In addition to this work, Dong and Wang discovered that cells surviving repeated rounds of hypoxia and reoxygenation demonstrated an increase in Bcl-x_L, suggesting a role for this protein in the protection of cells from hypoxic injury (Dong and Wang 2004). In both of these studies, increases in expression of identical proteins to those in this chapter were observed.

4.5.2 Ultrastructural features of HLRCC and sporadic leiomyomas

Previous ultrastructural observations of sporadic leiomyomas have demonstrated a number of aberrations. HLRCC and sporadic leiomyomas appear ultrastructurally distinct, but still with certain similarities beteen cells.

One such difference is the increased cell density in HLRCC leiomyomas, which lack the more expansive collagen matrix observed in the sporadic leiomyomas. This increased density may be due to increased cell proliferation, which appears evident due to the greater increase in the expression of PCNA in HLRCC leiomyomas than their sporadic counterparts, thus the cells are proliferating too quickly to lay down the more expansive extracellular matrix observed in sporadic leiomyomas. Another hypothesis is an alternative role of TGFβ in the pathogenesis of HLRCC and sporadic leiomyomas. It has previously been demonstrated that TGFβ-3 signalling in uterine leiomyomas results in accumulation of extracellular matrix through increased expression of proteins such as collagen . The reduced amount of matrix in HLRCC leiomyomas may be due to a reduction in TGFβ-3 signalling. However, TGFβ-3 expression has been shown to be activated by HIF1α in trophoblast cells (Nishi et al. 2004).

The disrupted collagen structure in HLRCC leiomyomas is of particular interest due to similar post-translational modifications of the collagen precursors (pro-collagen) and HIF1-α. Both proteins are modified by prolyl-4-hydroxlyases (P4H): for HIF1-α, to target it for destruction; and for collagen, to stabilise the formation of the distinctive collagen triple-helix (Myllyharju 2003). The reaction for both targets, despite being carried out by different enzymes, is identical. It is possible that succinate inhibits collagen P4H in the same way as HIF1-α P4H, which could result in disrupted collagen structure. However, without proline hydroxylation, the collagen triple helix has a melting temperature of approximately 21°C, and so is not physiologically viable (Mizuno et al. 2004).

One study of HT1080 fibroblasts under hypoxia has shown an increase in the expression of the collagen P4D-α subunit possibly to overcome the inhibition of the enzyme by reduced oxygen levels (Fahling et al. 2004). Since collagen fibrils are observed in HLRCC leiomyomas, this is likely to be true. The same study also showed a decrease in matrix metalloproteinase expression under hypoxia.

Fibrosis by increased deposition of extracellular matrix is a defining characteristic of uterine leiomyomas (Maruo et al. 2004). Studies on sporadic leiomyomas, the results of which are repeated here, demonstrate breakdown of order in the formation of collagen fibres (Leppert et al. 2004). There is also ultrastructural evidence for differing compositions of collagen isoforms in fibrils from myometrium and sporadic leiomyomas (Leppert et al. 2004). Furthermore, patients with Alport syndrome, which occurs due to germline deletions in the COL4A5 and COL4A6 genes, which encode collagen IV, a basement membrane collagen, exhibit diffuse leiomyomatosis, particularly of the oesophagus and vulva (Cochat et al. 1988). The true importance of the role of collagen in leiomyoma pathogenesis has yet to be determined, but certainly changes in collagen ultrastructure are among the more distinct observations in both sporadic and HLRCC tumours.

Disorganised cytoskeletal structures are also well characterised in sporadic leiomyomas. In both sporadic and HLRCC leiomyomas, disorganised intermediate filament structures, staining positive for desmin, are observed. In HLRCC leiomyomas, these disorganised filaments form distinct 'thumbprint' aggregates within the cytoplasm, whereas in sporadic leiomyomas these aggregates are more diffusely spread throughout the cytoplasm. Previous

studies have demonstrated a wide variety of cytoskeletal aberrations in sporadic leiomyomas, from small numbers of loosely distributed filaments, to large aggregates. Such a variety was observed in this study. In HLRCC leiomyomas, the desmin aggregates were larger and occurred more frequently. Furthermore, they had a more defined structure than the diffuse aggregates in sporadic leiomyomas.

The significance of this breakdown in intermediate filament structure is not understood. It may represent an imbalance in the control of the equilibrium of synthesis and turnover of cytoskeletal proteins, particularly desmin, which plays an important role in global intermediate filament organisation in the cell (Paramio and Jorcano 2002). It would also suggest that the leiomyoma cells have lost their contractile ability, since no defined polarity is observed in the filaments. This loss of contracile ability has been previously described in uterine leiomyomas (Tsibris et al. 2002). Where these accumulations have been observed before, it has been hypothesised that they are a secondary effect of tumour growth, rather than a mechanism of pathogenesis (Eyden et al. 1992).

The presence of autophagosomes in some cells in HLRCC leiomyomas may be a cellular response to a shortage of energy, due to the cessation of the Krebs cycle (Lum et al. 2005). However, the levels of autophagy, the process whereby a cell consumes itself by the formation of lysosomes during periods of extreme energy and nutrient shortage (Lum et al. 2005), has been described as being naturally increased in muscle cells, and the observation of autophagosomes in only a small number of cells may be representative of normal tissue turnover (Gevers 1984).

Previous ultrastructural studies of HPGL tumours demonstrated an apparent increase in the numbers of mitochondria and aberrations in mitochondrial morphology. In these tumours, the cytoplasm appears packed with mitochondria (Douwes Dekker et al. 2003). In HLRCC tumours, morphological aberrations were observed in the mitochondria, including mitochondrial swelling, and reductions in the numbers of cristae. However, these aberrations were also observed in samples of mitochondria fixed simultaneously. Since mitochondria are notoriously difficult to fix for electron microscopy, it is not possible to confirm whether the changes observed in HLRCC leiomyomas are a result of pathogenesis, or an artefact of tissue fixation. Furthermore, the numbers of mitochondria did not appear to be increased in the HLRCC or sporadic leiomyomas compared to the myometrium.

4.5.3 Conclusions

The results described in this chapter suggest important differences in the pathways, and ultrastructure of HLRCC and sporadic uterine leiomyomas. These differences imply distinct mechanisms of pathogenesis resulting in a similar outcome. Apoptosis plays an important role in the development of both HLRCC and sporadic tumours, with increased expression of pro-survival factors occurring in both. However, different patterns of expression suggest that different pathways are followed to arrive at a similar outcome. A similar situation is observed ultrastructurally, whereby similar cell and tissue features, such as collagen and intermediate filament structure, are both affected by the process of tumorigenesis, but with slightly differing outcomes. Therefore, the

data show that the pathogenesis of HLRCC and sporadic leiomyomas only partially overlaps.

Resistance to apoptosis appears to be important in HLRCC leiomyomas, as it is in many other tumour types (Hanahan and Weinberg 2000). The pattern of expression of different factors involved in apoptosis mimics those observed in other studies examining resistance of apoptosis in cells exposed to hypoxia (Dong and Wang 2004; Sasabe et al. 2005). Therefore, alternative mechanisms of oxygen sensing, which detect the continued presence of molecular oxygen in the cell, despite the chronic hypoxia signal from the continued stabilisation of HIF1-α, are likely to play a vital role in the pathogenesis of HLRCC tumours. This may also have implications for related tumour conditions such as HPGL and VHL. The identification of these pathways may provide suitable targets for pharmacological intervention, which could lead to reduction in the tumour cells resistance to apoptosis.

Chapter 5

Analysis of the mitochondrial genome in HLRCC and sporadic uterine leiomyomata

5.1 Introduction

5.1.1 Anatomy of the mitochondrial genome

In addition to the nuclear genome, eukaryotic cells contain specific organelle genomes, perhaps the best known examples of which are the mitochondrial and chloroplast genomes. The human mitochondrial genome (mtDNA) is a circular molecule of approximately 16.6kbp (Figure 5.1) (Anderson et al. 1981; Andrews et al. 1999). It contains 37 genes encoding 13 polypeptides, 2 rRNAs and 22 tRNAs. The 13 polypeptide genes (**Table 5.1**) encode components of the oxidative phosphorylation pathway. The rRNAs and tRNAs are used for translation of the mtDNA polypeptide genes, which utilise a slightly different genetic code to the nuclear genome (Anderson et al. 1981).

A single mtDNA molecule can be divided into two distinct regions: the coding region, containing the polypeptide and RNA genes; and the D-loop region, which contains all the control elements of the molecule, including replication and transcription origins. The D-loop is the most variable region of the mtDNA molecule, particularly within the two hypervariable segments (HVS) (Clayton 1992; Brandon et al. 2005).

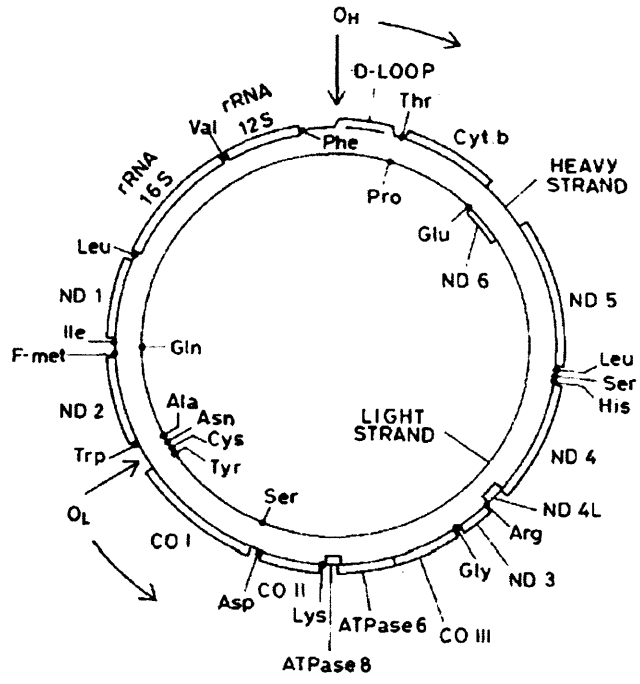

Figure 5.1 The mitochondrial genome, including the location of polypeptide, rRNA and tRNA genes (Taken from www.mitomap.org (Brandon et al. 2005)).

Table 5.1 Polypeptide genes encoded by the mitochondrial genome

Gene Name	OXPHOS complex	Encoding strand
ND1	NADH Dehydrogenase (Complex I)	H-strand
ND2	NADH Dehydrogenase (Complex I)	H-strand
CO1	Cytochrome c Oxidase (Complex IV)	H-strand
CO2	Cytochrome c Oxidase (Complex IV)	H-strand
ATP8	ATP synthase F0 (Complex V)	H-strand
ATP6	ATP synthase F0 (Complex V)	H-strand
CO3	Cytochrome c Oxidase (Complex IV)	H-strand
ND3	NADH Dehydrogenase (Complex I)	H-strand
ND4L	NADH Dehydrogenase (Complex I)	H-strand
ND4	NADH Dehydrogenase (Complex I)	H-strand
ND5	NADH Dehydrogenase (Complex I)	H-strand
ND6	NADH Dehydrogenase (Complex I)	L-strand
CYTB	Cytochrome b-c_1 complex (Complex III)	H-strand

Replication and transcription within the mitochondrial genome also differ from their nDNA equivalents. Replication occurs independently of S-phase in the rest of the cell (Lightowlers et al. 1997). There are two theories of mtDNA replication: the first is a more conventional leading and lagging strand replication, as observed in plasmid replication in bacteria (Holt et al. 2000). The second involves separate replication origins for each strand of the molecule. Firstly, the purine-rich H (heavy) strand is synthesised, using the pyrimidine-rich L (light) strand as a template, with an origin within the D-loop

region. Once approximately 2/3 of the H-strand has been synthesised, displacement of a particular site forms a stem-loop structure which acts as a primase recognition site for L-strand synthesis (Brown et al. 2005).

Mitochondrial transcription occurs as a polygenic synthesis from core promoters for H and L-strand transcription. H-strand transcription, which occurs in the opposite direction to traditional mtDNA base numbering and encodes a majority of the encoded genes, is terminated after transcription of the complete genome. The resulting RNA molecule is then processed to produce either mRNAs, rRNAs or tRNAs. Since a number of genes overlap, the processing of the transcript determines the level of each RNA species. Processing of the RNA results in the completion of the coding sequence of some genes. For example, the stop codon of the ND2 gene is completed by poly-adenylation of the processed mRNA (Clayton 1992).

5.1.2 Mitochondrial Genetics

Mitochondrial genetics is different from the Mendelian genetics of the nuclear genome in a number of aspects. Firstly, while the nuclear genome is diploid in a cell, with only two copies of each chromosome, the mitochondrial genome exists in multiple copies, often several thousand, in a single cell (Penta et al. 2001). This gives rise to an important concept of mitochondrial genetics – homoplasmy and heteroplasmy. Homoplasmy occurs when all the copies of the mitochondrial genome are identical. Heteroplasmy occurs when there is a mixture of two or more mitochondrial genotypes (Lightowlers et al. 1997). This has implications for the effects of mtDNA mutations in disease, as will be discussed later on.

A further difference occurs in the mode of inheritance; mtDNA inheritance is uniparental, coming only from the mother (Case and Wallace 1981). While a few reports exist detailing paternal inheritance, paternal mtDNA has been found not to transmit to subsequent generations (Gustafson 2002), even with assisted reproduction techniques such as intracytoplasmic sperm injection (Sutovsky et al. 2004). This uniparental inheritance has been a useful characteristic for evolutionary geneticists, who have used ethnic variations in mtDNA to trace human evolution and geographical divergence, and have identified a number of separate mitochondrial haplogroups (Wallace et al. 1999). For example, most Western Europeans belong to haplogroup H (Helena), while Native American and East Eurasian peoples are strongly representative of haplogroup A (Malhi et al. 2004).

The reference sequence for mtDNA is the revised Cambridge Reference sequence (Anderson et al. 1981; Andrews et al. 1999). Originally sequenced by Fred Sanger and colleagues (Anderson et al. 1981), it was updated following improvements in sequencing technology (Andrews et al. 1999). This sequence belongs to haplogroup H2b, and other haplogroups are defined by their deviations from this sequence (Carelli et al. 2006).

5.1.3 Mitochondrial mutations and disease

As with the nuclear genome, mutations in mtDNA have been associated with a number of disorders (Taylor and Turnbull 2005). Many of these disorders are inherited, such as Lebers's hereditary optic neuropathy (characterised by optic nerve dysfunction leading to blindness in young adults), which results from hetero- or homoplasmic mutations in three of the

genes encoding Complex I subunits (*ND1, ND4,* and *ND6*) (Man et al. 2002), and MERRF (Myoclonic Epilepsy with Ragged Red Fibres), which is a result of heteroplasmic mutations in the Leucine tRNA gene (Enriquez et al. 1995). There is also thought to be an involvement of mtDNA in age-related disorders such as diabetes (Martin Negrier et al. 1998).

The nature of mitochondrial genome inheritance, and its multiple copies within the cell, complicate the inheritance of a disease gene, particularly in disorders requiring heteroplasmic mutations. In a number of these conditions, an affected patient's mother may be a carrier of an mtDNA-encoded disease without herself demonstrating any symptoms. Similarly, affected patients' siblings may be unaffected or have less severe disease, despite inheriting the same mtDNA as the affected sibling. This discrepancy leads to the suggestion that a threshold of mutant mtDNAs must be inherited in order for a disorder to present. Theoretically, a child should be heteroplasmic for a mutation at the same level as the mother. However, a genetic bottleneck occurs at the point of oocyte maturation, where a selected proportion of mtDNA molecules are transmitted into each primary oocyte. Oocyte maturation is associated with a rapid replication of this mtDNA population. This bottleneck can lead to a random shift in mutational load between individuals resulting in the observed familial discrepancies (Taylor and Turnbull 2005).

The proximity of the mitochondrial genome to the functioning electron transport chain increases its susceptibility to oxidative damage (Beckman and Ames 1999). Furthermore, the lack of the protective nucleosome structure observed in nDNA increases its susceptibility even further (Beckman and

Ames 1999). As a consequence, it has become the focus of study for somatic mutations, in particular in tumour and cancer syndromes.

Mutations in the mitochondrial genome have also been observed in a variety of cancers (**Table 5.2**). The first of these reports, by Polyak *et al,* identified homoplasmic changes in 7 out of 10 studied colorectal cancer cell lines. These changes were somatic and absent in matched patient tissue, yet their selection to homoplasmy (Polyak et al. 1998). The significance of this homoplasmy is not known, it may confer a growth advantage on the cell, however, mathematical modelling has demonstrated that genetic drift can lead to homoplasmy without phenotypic selection (Elson et al. 2001).

Since Polyak *et al*'s landmark study, somatic mutations have been identified in a variety of tumour types, including breast (Bianchi et al. 1995), prostate (Petros et al. 2005), kidney (Horton et al. 1996), and gastric cancers (Alonso et al. 1997). Somatic mutations have been described in the D-loop region, in all 22 tRNAs, both rRNAs and all 13 polypeptide encoding genes (Chatterjee et al. 2006). Associations have also been made with hereditary tumour types, in particular multiple lipomas associated with MERFF (Holme et al. 1993), and an increased incidence of breast cancer in African-American women carrying the G10398A polymorphism (Canter et al. 2005).

In addition to point mutations, mitochondrial genomic instability has been observed in tumours (Bianchi et al. 2001). A number of poly-C tracts occur within the D-loop and coding regions and these can be polymorphic through slippage (Bianchi et al. 2001). Larger deletions have also been described in the literature, including a 4977bp deletion, shown to be

heteroplasmic in breast cancers, and shorter deletions that have been described in colorectal cancers among others (Bianchi et al. 1995).

A study by Aikhionbare *et al* examined the potential of mtDNA mutations as prognostic markers in colorectal cancer patients by studying the accumulation of mtDNA mutations in normal, pre-cancerous (adenomatous polyps) and cancer specimens by RFLP analysis. The study identified 38 sequence variants, none of which were tumour specific. However, the accumulation of mtDNA mutations correlated with tumour progression, suggesting mtDNA mutation accumulation as a potential prognostic marker (Aikhionbare et al. 2004).

Table 5.2 A selection of cancer sites and associated somatic mDNA mutations (Data from (Chatterjee et al. 2006)).

Cancer Site	**Mutated Genes**	**Mutation types**
Bladder	CYTB, ND3	Deletion (CYTB), Missense (ND3)
Colon	CYTB, ND5, ND4L, CO3, CO2, CO1, ND1	Missense (CYTB, ND5, ND4L, CO3, CO2, ND1) Truncation (CO1) Frameshift (ND1, ND5) Deletion (ND1)
Pancreas	CYTB, ND6, ND4, ND3, CO3, ATP6, CO2, CO1, ND2, ND1	Missense (CYTB, ND6, ND4, CO3, ATP6, CO2, CO1, ND2, ND1)
Ovary	CYTB	Nonsense
Thyroid	CYTB, ND6, ND5, ND4, ND4L, ND3, CO3, ATP6, CO2, ND2, ND1	Missense (CYTB, ND6, ND5, ND4, ND3, CO2, ND2, ND1) Deletion (CYTB, CO2)
Breast	ND5, ND4	Missense (ND5, ND4) 4977bp deletion (Various)
Prostate	ND5, CO1, ND1	Missense (ND5, CO1, ND1)
Head and Neck	ND4	Missense
Medulloblastoma	ND4L	Missense

5.1.4 Difficulties and controversies of mtDNA screening

The association of particular mtDNA mutations with diseases, particularly cancer, has been the subject of much controversy. Salas *et al* recently published a scathing paper on the role of mtDNA mutations in cancer (Salas et al. 2005). They attacked a number of studies of inherited and somatic mtDNA mutations in cancer. A number of their points are valid, particularly regarding association studies of cancers with mtDNA mutations. The huge number of phylogenetic differences between the different haplogroups makes a traditional case-control study very difficult, since cases and controls with matching ethnicities may not have identical mtDNA haplogroups. For example, in Western Europe, although haplogroup H is predominant, representing approximately 50% of the population, the remaining 50% are represented by at least 7 other haplogroups. This study was designed to represent the situation in approximately 1500AD, before the European expansion, and so all these other haplogroups are likely to be from Caucasians (Torroni et al. 1996). Therefore, ethnicity does not necessarily denote mtDNA haplogroup.

Salas *et al* also attacked the concept of haplotype shifting, where the mtDNA of a patient of one haplogroup acquires homoplasmic mutations that result in a shift to a SNP defining a different haplogroup (Salas et al. 2005). This haplotype shift can occur at a single nucleotide position, or several nucleotides in a mtDNA molecule can mutate to SNPs indicative of the same haplogroup. It is this latter effect, where a whole mtDNA molecule appears to shift from one haplotype to another unrelated haplotype that draws the most

criticism (Salas et al. 2005). For example, a report by Jeronimo *et al* where one case accumulated 18 somatic mutations, each indicative of haplogroup W (a Western European haplogroup (Torroni et al. 1996)), was highly suggestive of sample contamination (Jeronimo et al. 2001). However, this phenomenon of haplotype shifting has been demonstrated for single nucleotides. Linnartz *et al* described a patient with myelodysplasic syndrome (MDS) with mtDNA haplotype U. They tracked the slow progression of MDS to acute leukaemia demonstrating a low-level early heteroplasmy, which reached 50% when the cells were in transformation, and became a homoplasmic haplotype shift when the leukaemia arose (Linnartz et al. 2004). The significance of this haplotype shifting is unknown, since many mutations that occur as a part of this shift occur in the germline of many people of other haplogroups, with no apparent increase in cancer prevalence within those groups. It may represent an example of genetic drift (Elson et al. 2001).

The controversies described above have arisen partly due to the great care required in designing a screening strategy. Many studies have been carried out on the basis that mtDNA copy number is far in excess of nDNA copy number. However, highly homologous (>99%) mitochondrial pseudogene regions are present within the nuclear genome, which may present false heteroplasmy (Parr et al. 2006). The regions of greatest homology are observed on chromosomes 1, 5 and 17. Therefore, great care must be taken in designing PCR primers for mitochondrial genome screening in order to only amplify true mtDNA. The best approach for primer design is a long-range PCR taking advantage of the fact that none of the pseudogene regions

encompasses the entire mtDNA molecule. Therefore, it is possible to design primers that completely exclude the possibility of pseudogene amplification.

In addition to their role in disease, mtDNA mutations have been shown to accumulate as a result of natural aging (Chomyn and Attardi 2003), and are thought to play a role in muscle degradation and other effects of aging (Chomyn and Attardi 2003).

5.1.5 The Affymetrix Mitochip for the analysis of mtDNA sequences

The Affymetrix human mitochondrial resequencing array is a tool allowing the sequencing of the entire mitochondrial genome in one experiment. The array was originally conceived by Maitra *et al* and consists of a series of 8 25-mer oligonucleotide probes for each base position within the mitochondrial genome, 4 probes for each strand. Each probe is varied at the central position to incorporate each possible nucleotide, A,G,C or T. Labelled amplified mtDNA is hybridised to the array and stringently washed to allow discrimination between alleles (Maitra et al. 2004; Zhou et al. 2006).

In order to account for common variation, the D-loop region is overtiled with 245 common variants observed in the FBI database of mitochondrial mutations (Fox 1996). This overtiling particularly takes into account polymorphisms within 25 base pairs of each other, which would occur on the same arrayed oligonucleotide (Zhou et al. 2006).

5.1.6 Aims of this chapter

Given that mutations in *FH* result in uterine leiomyoma formation due to a blockage in oxidative metabolism at the level of the Krebs cycle, and the absence of *FH* mutations in sporadic leiomyomas, it was decided to

investigate the potential role of the mitochondrial genome (mtDNA) in sporadic leiomyoma pathogenesis. As mentioned above, the mitochondrial genome is highly susceptible to damage and mutation. This high mutation frequency, coupled with the high prevalence of uterine leiomyomas, makes it an important screening target. It was also decided to use mtDNA mutations as an indirect measure of reactive oxygen species (ROS) in the mitochondria, and to use this to examine the difference in ROS production in HLRCC uterine leiomyomas, which have a known mitochondrial defect, and sporadic uterine leiomyomas.

The aims of the work in this chapter were:

i) To investigate the presence of mtDNA mutations in sporadic uterine leiomyomas, and to assess the potential pathogenic role of any observed changes.

ii) To compare the frequency and spectrum of mtDNA changes in sporadic uterine leiomyomas with HLRCC leiomyomas to assess the presence of high-energy species in HLRCC mitochondria.

5.2 Materials and Methods

5.2.1 Sample Collection

Thirteen pairs of matched normal (blood or myometrium) and leiomyoma DNA samples were selected at random from the pool of sporadic uterine leiomyoma samples without germline *FH* mutations. In addition, 3 HLRCC leiomyomas from a patient with a K187R germline mutation, and known LOH, plus the patient's germline DNA, derived from a blood sample were also chosen for analysis.

5.2.2 Affymetrix mtDNA resequencing array protocol

Samples were analysed using the Affymetrix mtDNA resequencing array v2.0. Since this protocol requires a single long-PCR amplification, rather than nested PCR, sequence artefacts as a result of multiple PCR steps are minimised.

The procedure is described in Chapter 2 (2.11.2). Data from these arrays were analysed as a single batch using a quality score threshold of 3 and a diploid genome model in order to identify regions of heteroplasmy. Tumour and normal samples were compared alongside each other as described in the Affymetrix recommendations for analysis (http://www.affymetrix.com/Auth/support/technical/other/mito_support_docs.pdf). In order to identify changes in the tumour with respect to the normal, a number of criteria were applied:

i) Changes were discarded if they occurred within or flanking a stretch of no-calls in both tumour and normal DNA.

ii) Where a region was over-tiled, changes were accepted or discarded on the basis of occurring in all the over-tiled fragments for the same position.

5.2.3 Analysis of detected mutations

Observed mutations were compared to known polymorphisms reported in the Mitomap database (Brandon et al. 2005) and within the literature. Phylogenetic analysis of mutations to identify instances of haplotype switching were carried out with reference to the Mitomap phylogenetic tree (Brandon et al. 2005). Protein missense mutations were analysed using the PolyPhen tool to identify the effects of amino acid polymorphisms on the overall function of the protein (Ramensky et al. 2002).

5.3 Results

5.3.1 Resequencing analysis of mtDNA from uterine leiomyoma and matched normal samples

In total, 30 hybridisation experiments were carried on 16 tumour samples from 14 patients. Hybridisations were successful for 28/30 arrays analysed. Two arrays, 200103 leiomyoma, and 200144 myometrium, had very low call rates Table 5.3. While the overall call rates for each array appeared low (median = 68.75%), the call rates for the coding regions, containing all the polypeptide and RNA genes, but not the D-loop, was far higher (Median = 91.98%). This discrepancy is due to the overtiling of the D-loop region for common polymorphisms, since many of these overtiled regions will not hybridise DNA in a particular sample, thus increasing the number of 'no-calls'.

Mutations relative to the normal mitochondrial genome were observed in 6 sample pairs, AHF2, 000357, TB02 0341, 200061, TB03 0152, and TB04 0107 (**Table 5.4**). The remaining 8 analysed sample pairs contained no mutations following analysis by the criteria described above. In total, 26 mutations were observed. A majority (81%) of the observed mutations were transversions, with only 19% transitions. The maximum number of mutations observed in a single sample was 6 (**Table 5.4**), which occurred in 2 samples (000357 and TB02 0341). The remaining samples contained 5 (AHF2), 4 (200061 and TB04 0107) and 1 mutation (TB03 0152). Of all 26 mutations, only one, in sample TB03 0152, was homoplasmic. 18 of the mutations occurred in protein coding genes, but only 12 of these were missense changes

(**Table 5.5**). 3 mutations occurred in genes encoding tRNAs (1 in each of tRNA-Ile, tRNA-Val and tRNA-Gly) although none of these mutations occurred in the anticodon region of the molecule. One mutation occurred in the 16S rRNA, and 4 mutations occurred in the D-loop region. No consistent sites of mutation were observed.

Table 5.3 Individual array call rates and number of mutations observed.

Sample Name[1]	Normal Call Rate		Leiomyoma Call Rate		Number of mutations
	Total	Coding[2]	Total	Coding[2]	
000357	72.79%	94.73%	70.94%	93.40%	6
100179	63.60%	84.84%	68.41%	92.17%	0
200061	53.71%	74.30%	58.36%	80.01%	4
200103	59.71%	80.18%	26.61%[3]	35.58%	N/A
200144	39.60%[3]	53.56%	66.02%	85.36%	N/A
AH	60.14%	78.30%	63.93% (AHF2)	82.32%	5
			69.09% (AHF4)	91.79%	0
			72.95% (AHF5)	94.65%	0
FG4	70.28%	93.79%	71.91%	94.41%	0
TB02 0341	62.82%	87.27%	62.01%	84.86%	6
TB02 0431	74.60%	95.15%	74.90%	95.09%	0
TB03 0152	70.20%	94.04%	70.77%	94.10%	1
TB03 0413	74.63%	95.31%	73.15%	94.52%	0
TB03 0438	74.56%	95.29%	74.90%	95.42%	0
TB03 0566	65.54%	89.42%	70.58%	92.50%	0
TB04 0107	67.74%	89.51%	64.72%	86.40%	4

[1]Sample name refers to the patient

[2]Coding region call rates were calculated from position 577 (tRNA-Phe) to 16023 (tRNA-Pro) containing all the coded polypeptides and RNAs

[3]Call rates were considered too low and samples were not analysed

Table 5.4 Observed differences between normal and tumour mtDNA in uterine leiomyomas. The reference is the revised Cambridge Reference Sequence (Andrews et al. 1999).

Tumour Sample	Mitomap Pos	Reference	Normal	Tumour	Change	Mutation Type	Gene	AA Change
AHF2	383	t	t	w	t - a	Heteroplasmic	D-loop	
AHF2	7358	a	a	m	a - c	Heteroplasmic	COX1	V485V
AHF2	8207	c	c	y	c - t	Heteroplasmic	COX2	P208S
AHF2	8668	t	t	y	t - c	Heteroplasmic	ATP6	W48R
AHF2	12357	a	a	m	a - c	Heteroplasmic	ND5	M7I
000357	1656	a	a	m	a - c	Heteroplasmic	tRNA-Val	
000357	2217	c	c	m	c - a	Heteroplasmic	16S rRNA	
000357	3798	c	c	m	c - a	Heteroplasmic	ND1	T164T
000357	13249	t	t	w	t - a	Heteroplasmic	ND5	S305T
000357	15742	c	c	m	c - a	Heteroplasmic	CYTB	L332L
000357	4770	g	g	k	g - t	Heteroplasmic	ND2	A101S
TB02 0341	8192	a	a	m	a - c	Heteroplasmic	COX2	N203H
TB02 0341	11691	g	g	k	g - t	Heteroplasmic	ND4	G311V
TB02 0341	13560	c	c	m	c - a	Heteroplasmic	ND5	A408A
TB02 0341	15051	t	t	w	t - a	Heteroplasmic	CYTB	L102Q
TB02 0341	16126	t	t	k	t - g	Heteroplasmic	D-loop	
TB02 0341	16445	t	t	w	t - a	Heteroplasmic	D-loop	
200061	3511	a	a	r	a - g	Heteroplasmic	ND1	T69A
200061	9813	t	t	w	t - a	Heteroplasmic	COX3	F203I
200061	10054	g	g	s	g - c	Heteroplasmic	tRNA-Gly	
200061	15814	a	a	m	a - c	Heteroplasmic	CYTB	V356V
TB04 0107	4272	t	t	k	t - g	Heteroplasmic	tRNA-Ile	
TB04 0107	10735	a	a	m	a - c	Heteroplasmic	ND4L	Y89C
TB04 0107	11058	t	t	w	t - a	Heteroplasmic	ND4	I100N
TB04 0107	11062	c	c	y	c - t	Heteroplasmic	ND4	S101S
TB03 0152	152	t	t	c	t - c	Homoplasmic	D-loop	

Table 5.5 Number and type of mutations observed in mtDNA protein-coding regions. Genes are ordered as they appear on the mtDNA

Gene	Missense Mutations	Silent Mutations
ND1	1	1
ND2	1	0
COX1	0	1
COX2	2	0
ATP6	1	0
COX3	1	0
ND4L	1	0
ND4	2	1
ND5	2	1
CYTB	1	2

5.3.2 Haplotype shifting

In order to assess whether any mutations were present as polymorphisms in a different mtDNA haplogroup, the mutations were compared against known polymorphisms for different haplogroups (Brandon et al. 2005) (Table 5.6). Of the 26 observed mutations, 9 occurred at sites of known haplogroup polymorphisms, although only 5 of these matched the reported polymorphisms.

Table 5.6 Observed mutations in positions of known mtDNA haplogroup polymorphisms.

Site of mutation	**Observed Mutation**	**Reported Polymorphism**	**Haplogroups with reported polymorphism**
152	T - C	T - C	T2, K1, H2
1656	A - C	A - G	H4, H6
2217	C - A	C - T	K2
3511*	A - G	A - G	H2, H16
3798	C - A	C - T	M27
8668	T - C	T - C	H10, L1c
9813*	T - A	T - A	K1
11062	C – T	C - T	D2
16126	T – G	T - C	T3, T2, T1, J4, J3, J2, J1

*Polymorphisms result in protein missense mutation

5.3.3 Functional effects of observed mtDNA mutations

In order to assess the functional effects of the observed coding mutations on the proteins, analysis of each mutation was carried out using the PolyPhen tool (Ramensky et al. 2002). Results of this analysis (**Table 5.7**) suggested that 9 of the 12 missense mutations had a potentially damaging effect on the encoded protein, two mutations were likely to be benign, and the effect of one mutation was unknown due to a lack of homologous sequences.

Table 5.7 PolyPhen predictions of effects of observed mtDNA mutations

Sample	Gene	Mutation	Polyphen Prediction	Remarks
AHF2	COX2	P208S	Probably Damaging	Close to functional site
AHF2	ATP6	W48R	Probably Damaging	Original Trp highly conserved
AHF2	ND5	M7I	Unknown	No alignment with other sequences
000357	ND5	S305T	Probably Damaging	Original Ser highly conserved
000357	ND2	A101S	Benign	Original Ala not well conserved, mutation conserves shape
TB02 0341	COX2	N203H	Probably Damaging	Close to functional site and other chains
TB02 0341	ND4	G311V	Probably Damaging	Original Gly highly conserved
TB02 0341	CYTB	L102Q	Possibly Damaging	Highly conserved Leu, mutation close to ligand
200061	ND1	T69A	Benign	Original Thr not well conserved, mutation conserves shape
200061	COX3	F203I	Probably Damaging	Close to ligand, close to other chains
TB04 0107	ND4L	Y89C	Probably Damaging	Residues of similar type highly conserved
TB04 0107	ND4	I100N	Probably Damaging	Conserved size and hydrophobicity

In order to assess the potential pathogenic effects of mutations in the rRNA and tRNA genes, the structures of these molecules were studied to identify altered interactions within the molecule (**Figure 5.2**). These results showed that the mutations in nucleotides 10054, affecting tRNA-Gly (**Figure 5.2**a) , and 4272, affecting tRNA-Ile (**Figure 5.2**b), both disrupt secondary structural interactions within the tRNA molecule, and may, therefore, have a detrimental affect on translation. The mutation of nucleotide 1656, affecting tRNA-Val (**Figure 5.2**c) does not affect secondary structural interactions. However, mutations in the looped regions of mitochondrial tRNA molecules have been described in a number of mitochondrial diseases, such as MELAS (mitochondrial myopathy, encephalopathy, lactic acidosis and stroke-like episodes) (Goto et al. 1994).

The observed 16S rRNA mutation has not been previously reported, nor have any confirmed pathogenic mutations been reported within the 16S rRNA. Analysis of the secondary structural interactions (**Figure 5.2**d) showed that this base does not pair with any other base within the rRNA molecule. Any further pathogenic effect cannot be confirmed.

The function of mutations in the D-loop region are more difficult to ascertain. Only one of these mutations, T152C has been previously described and is associated with haplogroups T2, K1 and H2 (Brandon et al. 2005). There has also been a report of this mutation occurring in a patient with ovarian carcinoma (Liu et al. 2001). The other observed mutations have not been previously described, and do not occur in any described functional elements of the D-loop. Therefore, their function remains unknown.

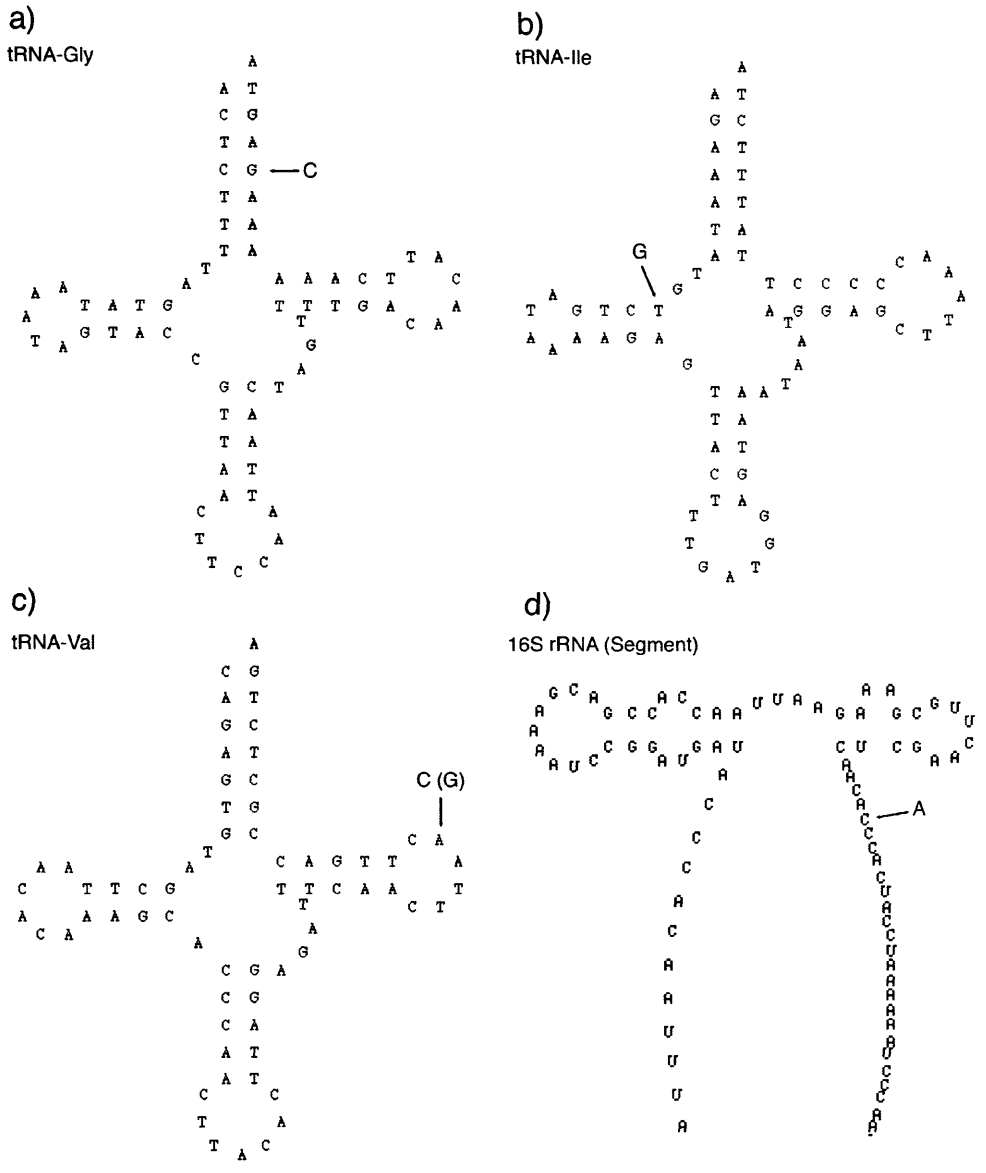

Figure 5.2 Analysis of the secondary structure of tRNA and rRNA molecules affected by observed mtDNA mutations in uterine leiomyomas. a & b) Mutations in the tRNA-Gly and tRNA-Ile molecules disrupt base-pairing interactions within the molecule. Mutations affecting tRNA-Val (c) and the 16S rRNA (d) do not affect these interactions. RNA structures were obtained from the mtSNP database (Chuang et al. 2006b).

5.3.4 mtDNA mutations in HLRCC uterine leiomyomas

The total number of observed mutations in the 3 HLRCC leiomyomas was compared to the numbers observed in sporadic leiomyomas by a Wilcoxon signed-rank test in R. The number of mutations observed in HLRCC leiomyomas was not greater than those observed in sporadic uterine leiomyomas ($p=0.8627$).

5.4 Discussion

Reports of mtDNA mutations in a number of different tumour types occur frequently in the literature (Chatterjee et al. 2006). Here, mtDNA mutations have been identified in 6/14 (43%) uterine leiomyoma samples from both sporadic and familial cases. The true pathogenic effects of these mutations have not been established. There is no common theme linking the mutations, be it a shift to a common haplogroup, or mutations in similar genes or of similar types. Therefore, it is unclear whether the mutations are causative, or an effect of tumour growth leading to increased mutagenesis.

The consequences of mtDNA mutations have been hotly debated. In tumour cells, the mitochondria appear to be under persistent oxidative stress, signified by the presence of high levels of ROS (Brown and Bicknell 2001). This stress arises due to hypoxic conditions at the centre of the tumour (Knowles and Harris 2001). This stress could be the cause of frequently observed mtDNA mutations in tumours. The question of whether these mutations then provide a growth advantage to the tumour cell is as yet undetermined. The accumulation of mutations may be a result of a vicious cycle. Initially, tumour hypoxia leads to an increase of ROS in the cell, which damage mtDNA. This leads to changes in the electron transport chain, which could further increase the ROS in the mitochondria, which further damages mtDNA, and so on. ROS are known to function as secondary messenger molecules within the cell, influencing metabolism, gene expression, and cell proliferation, among others (Gamaley and Klyubin 1999).

This has implications for leiomyoma pathogenesis. It was interesting to note that 5/6 samples with mutations had accumulated several changes (**Table 5.4**). It is possible that the vicious cycle of mutation described above is occurring in these tumours. The predicted increasing levels of ROS in the cell could act as secondary messengers increasing cell proliferation and tumour growth (Gamaley and Klyubin 1999), and also increase the likelihood of further genetic aberration, possibly cytogenetic changes to the nuclear genome.

It is also possible that mtDNA mutations arose as a consequence of cell aging due to proliferative growth, in a similar manner to the accumulation of mtDNA mutations as a consequence of aging (Chomyn and Attardi 2003). Unfortunately, data regarding the size of the samples used in this study was not taken, which could have been used to examine the correlation between tumour size, as a measure of tumour age, and mtDNA mutation frequency.

5.4.1 mtDNA mutations in HLRCC uterine leiomyomas

It was predicted that the deleterious effects on Krebs cycle metabolism of the *FH* mutations observed in HLRCC patients would transfer to the electron transport chain, resulting in an increase in ROS production, and so an increase in mtDNA mutations. However, the results of this study showed mutations in only one familial sample, AHF2, and no significant difference in mtDNA mutation prevalence between sporadic and familial samples.

It appears, therefore, that the initial assumption was wrong, and that blocking of the Krebs cycle may not have a significant effect on ROS production through aberrant effects on the electron transport chain. This could

imply that it is still functioning in some capacity, perhaps using NADH produced from other cellular processes such as the pentose phosphate pathway (Wood 1986).

The mutations observed in the one HLRCC leiomyoma may have arisen in a similar manner to those observed in the other leiomyoma samples. Again, it would be interesting to see if there was a correlation between tumour size and mtDNA mutation frequency.

5.4.2 The Mitochip – conceptually flawed?

The conclusions drawn from this study are entirely dependent on the sensitivity and specificity of the screening method. While the Mitochip allows the sequencing of an entire mtDNA molecule in one experiment, some difficulties with the array perhaps point to conceptual flaws, both within the array design, and within resequencing technology as a whole. One of the major problems encountered with using the Mitochip was the high number of no-calling bases. In the two samples with such a low call rate that the sample pairs were excluded from analysis (200103 leiomyoma and 200144 normal), the low call rate was due to a weak signal. However, in a number of other arrays, weak signal accounted for only a small amount of reduction in call rate. During analysis of the different sets of data, regions of no call were observed to occur in blocks, rather than randomly spread throughout the data set. More importantly, these blocks occurred at the same point in both tumour and matched normal samples.

Resequencing arrays are designed on the principles of allelic discrimination – being able to discriminate between a single base at a

particular point (Maitra et al. 2004). Each arrayed 25 base oligonucleotide consists of the base of interest flanked by 12 bases either side. This central base varies for each of the 4 DNA bases, and is also present as a reversed sequence. In a hybridisation experiment, sample DNA is hybridised to the array (**Figure 5.3**a). The flanking sequences either side of the base of interest will hybridise as well, despite the mismatch at the central base. In order to identify the appropriate base(s), a stringent enough washing procedure to allow allelic discrimination at a single base mismatch must be used. This removes the mismatched DNA, resulting in the correct base(s) being called.

However, this procedure falls down when a homoplasmic mutation occurs. For the oligo defining the base where the mutation occurs, the situation in **Figure 5.3**a occurs, and the mutation is called. However, for the 12 bases tiled either side of the mutation, the situation in **Figure 5.3**b occurs, and a mismatch occurs in the flanking bases to the base of interest. The washing procedure removes the mismatched bases, and hence no base is called at positions flanking a mutation.

This difficulty is compounded by the massive variability in the mitochondrial genomes of different ethnic groups, which would lead to a succession of no-calls in bases varying from the reference sequence. This has been approached in the D-loop region by overtiling 245 of the most common haplotype variants observed in the FBI database (Fox 1996). However, a number of common, haplotype-defining SNPs occur within the coding region, from bases 577 to 16023. This region has not been overtiled on the Mitochip, which was created from the rCRS, representing haplogroup H2 (Andrews et al. 1999). Thus, mtDNAs from different haplogroups will contain a number of

coding region SNPs not tiled for on the array, and long runs of 'no-call' bases will frequently occur, as was observed in the results from this chapter.

In theory, these affected bases should be called in the middle of a run of no-calls. However, in practice this did not occur and made calling mutations in the coding region very difficult. In most cases, the runs of no-called bases were observed in both the constitutional and tumour DNA, indicating the patient was not from haplogroup H2. Only heteroplasmic mutations not flanked by no-calls could be reliably called.

A further limitation of the Mitochip is its inability to identify deletion mutations. A number of common deletion polymorphisms, particularly within poly-C tracts, have been reported (Bianchi et al. 2001). Furthermore, there is no means of detecting well characterised large deletions, such as the 4977 deletion (Bianchi et al. 2001). Therefore, further screening procedures should be carried out to complement the Mitochip in order to obtain the fullest mtDNA profile.

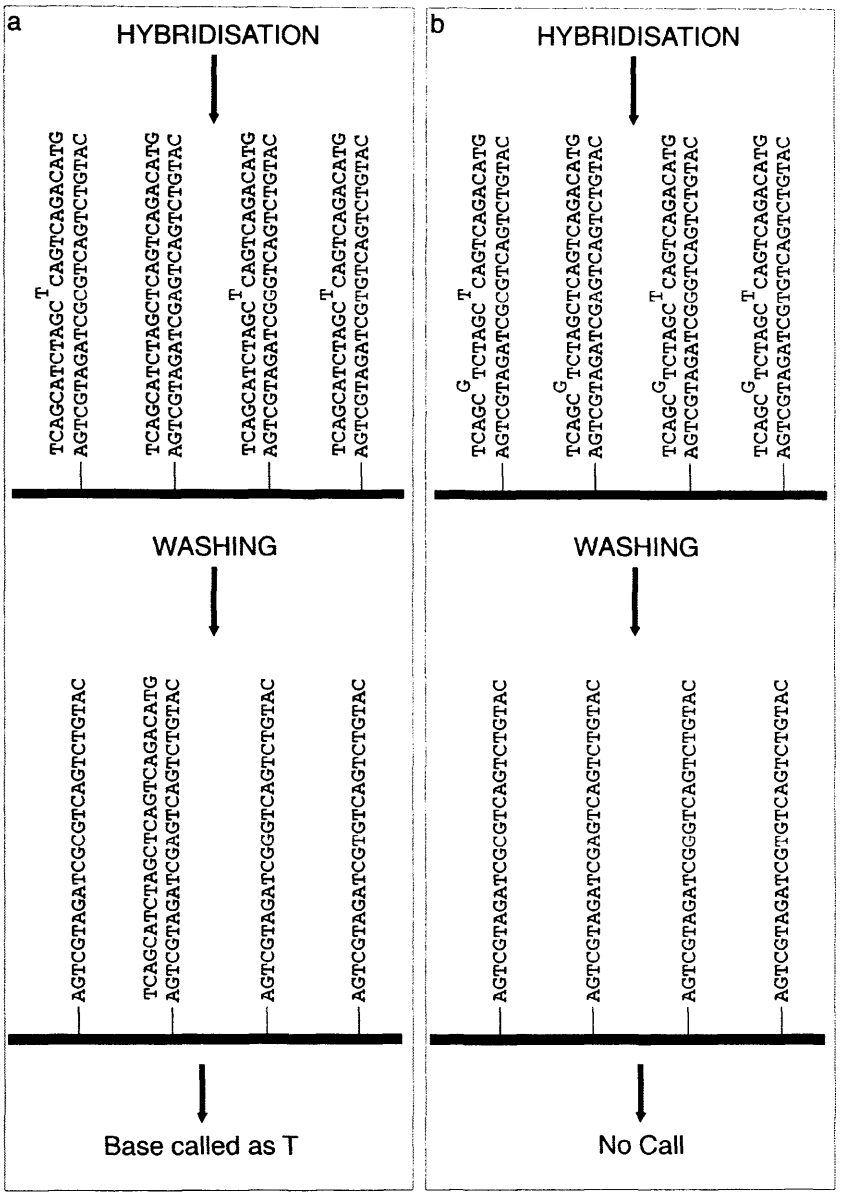

Figure 5.3 Problems with mutation detection using the resequencing arrays. a) Where the flanking sequence of the labelled DNA matches the sequence tiled onto the array, a perfect match occurs for one variant, which remains hybridised following washing, leading to a base call. b) A polymorphism at a single base would lead to imperfect hybridisation to probes representing bases either side of the polymorphism. These would be removed by washing, leading to no base being called.

5.4.3 Conclusions

Mutations of mtDNA in tumours have proven to be a controversial issue, with many arguments and opinions on the role of these mutations, and even their existence, in tumour progression (Bianchi et al. 2001; Penta et al. 2001; Salas et al. 2005). In this chapter, the potential effects of mtDNA mutations in leiomyoma pathogenesis have been examined using the Mitochip resequencing array. While mutations were detected in 6/14 samples, the role of these changes is unclear and it is possible that they are background changes.

Conversely, they may represent an important new mechanism of leiomyoma pathogenesis, particularly regarding the involvement of ROS signalling. The lack of difference in mtDNA mutation frequency between HLRCC and sporadic uterine leiomyomas suggests that they may not arise due to Krebs cycle dysfunction in HLRCC leiomyomas.

The role of these mutations is still undefined, and further molecular studies on the potential effects of these mutations and their role in tumorigenesis would need to be carried out to ascertain whether they are a cause of pathogenesis, or an effect of tumour growth.

Chapter 6

Whole Genome Microarray comparative genomic hybridisation (CGH) of uterine leiomyomata

6.1 Introduction

6.1.1 Copy number changes and tumorigenesis

Mutations at the gene level are one means of altering gene function in order to promote tumorigenesis. Examples include activating mutations proto-oncogenes, such as *KRAS2*, leading to their constitutive activation (Feig et al. 1984) and mutations in tumour suppressor genes, such as *FH*, as observed in Chapter 3, which lead to their inactivation (Tomlinson et al. 2002). However, such changes can also occur as a result of copy number variation, where specific regions of the genome are amplified or deleted, usually on a scale of tens of kb or more.

Traditionally, amplified regions tend to indicate the presence of oncogenes (Kashiwagi and Uchida 2000), where the presence of increased copies of the gene increases the expression, and effect of a gene. For example, the ERBB2 oncogene is frequently found amplified in breast cancer (Kallioniemi et al. 1992). In contrast, deleted regions are often taken to be indicative of tumour suppressor genes (Kashiwagi and Uchida 2000). In this case, one copy of the gene may be inactivated by mutation, and the second copy deleted from the genome, or both copies may be deleted as a homozygous deletion. For example, Grafstrom *et al* identified frequent homozygous deletions of the *INK4* locus on chromosome 9p21 in cutaneous melanoma (Grafstrom et al. 2005).

The locations of copy number changes in tumours are frequently studied as potential markers of novel genes involved in the development of a particular tumour. Additionally, such changes may be associated with a

patient's prognosis - the deletion of *INK4* described above is associated with decreased survival (Grafstrom et al. 2005) – and the identification of novel involved genes in these regions can help with both an understanding of the pathobiology of a particular tumour, and with the development of therapeutic strategies for patients with tumours containing such changes (Grafstrom et al. 2005).

A number of regions of frequent copy number change, with as yet unidentified target genes, have been identified. For example, deletions of chromosome 16q are common in ductal and lobular breast cancers (Rakha et al. 2006). To date one associated tumour suppressor, E-cadherin, has been identified in lobular tumours, yet no associated gene has been identified for ductal tumours (Rakha et al. 2006). In colorectal cancer, loss of 4q is a frequently recurring event associated with poor prognosis (De Angelis et al. 2001), and so identification of the involved gene or genes in this region could help to improve patient therapies.

6.1.2 Copy number variation in the human genome

In addition to the copy number changes observed in tumours, much recent focus has been given to natural copy number variation between individuals (Sebat et al. 2004; Sharp et al. 2005). Several studies have identified a number of sites throughout the genome where polymorphic deletions, insertions or inversions of genetic material are observed in constitutional DNA (Sebat et al. 2004; Sharp et al. 2005). These copy number polymorphisms (CNPs) can be associated with genes that define specific traits. For example, Sebat *et al* identified a triplication of the neuropeptide-Y

receptor (*PPYR1*), which is directly involved in the regulation of food intake and body weight (Sebat et al. 2004). Differences in CNPs have also been observed in different ethnic backgrounds (Sharp et al. 2005).

The presence of these CNPs has been found to be associated with the presence of segmental duplications, particularly intrachromosomal duplications (Sharp et al. 2005). These are regions of repeated sequence >1kb in length and of >90% identity, thought to be recently duplicated in evolutionary history (Samonte and Eichler 2002). Their high homology could be an important means of genetic recombination, leading to the observed variation in copy number (Sharp et al. 2005), although it is possible that they arise as a result of genetic recombination.

6.1.3 Microarray comparative genomic hybridisation (array-CGH)

The identification of copy number changes was originally carried out by karyotyping of metaphase chromosomes stained with Giemsa, Quinacrine or Chromomycin among others (Strachan and Read 2004). This method is time-consuming and requires a highly skilled eye, and the resolution was limited to very large copy number changes over several cytogenetic bands. Furthermore, chromosomes can only be obtained from growing cell lines, which places a limit on samples that can be analysed. However, it does allow the detection of other cytogenetic abnormalities, such as translocations, inversions and the presence of marker chromosomes. Furthermore, fluorescent *in-situ* hybridisation (FISH) can be used to examine the copy number of individual BAC clones to identify breakpoints once a region is identified (Gorman and Roylance 2006).

A later development was comparative genomic hybridisation (CGH), where normal and tumour DNA samples were labelled with different fluorescent dyes and competitively hybridised to normal metaphase chromosomes. The ratio of normal to tumour DNA was used as a measure of comparative copy number (Gorman and Roylance 2006). This technique increases the number of samples available for study, since there is no need to grow cell lines to obtain metaphase spreads. However, it is unable to detect abnormalities other than copy number change and the resolution, while more precise than karyotyping of metaphase spreads, is still limited to approximately 10Mb (Gorman and Roylance 2006).

A number of other techniques are available to measure copy number change at a very high resolution. Multiplex amplifiable probe hybridisation (MAPH) can compare gene dosage at the exon level. Patient DNA is spotted onto a nylon membrane and hybridised to a mixture of DNA probes, each specific for one exon or region with identical DNA ends for priming. After washing, the hybridised probes are amplified using a single primer pair, producing a series of different size products, which are then analysed by capillary gel electrophoresis (Sellner and Taylor 2004). Multiplex ligation dependent probe amplification (MLPA) is a similar technique, this time using a mixture of PCR primers in a single multiplex reaction to detect copy number differences between regions such as exons (Sellner and Taylor 2004). Quantitative real-time PCR using probes specific for the region of interest can also be used (Lehmann and Kreipe 2001). While these methods offer very high resolution detection of copy number change, they require presumed

knowledge of specific regions or genes involved and cannot be used as a general screening technique for whole genome copy number change.

In recent years, CGH has been superseded by microarray-based CGH, where DNA is hybridised to individual arrayed DNA probes, such as oligonucleotide probes (Pollack et al. 1999) and bacterial artificial chromosomes (BACs) (Cai et al. 2002), immobilised onto a glass slide. This has dramatically improved the resolution of the technique to allow detection of sub-megabase copy number changes that would previously have been missed by conventional CGH, while still retaining the ability to screen the entire genome in one experiment (Albertson and Pinkel 2003). Currently, this is the technique of choice for detecting copy number changes.

6.1.4 Copy number variation in uterine leiomyomas

Cytogenetic abnormalities are the most frequently observed changes within sporadic uterine leiomyomas, occurring in approximately 40% of observed cases (Ligon and Morton 2001). A large number of these abnormalities have been described in the literature, and affect many different chromosomes, although a number of non-random aberrations have been frequently reported (For a more detailed overview, see section 1.2.1.4.1) (Ligon and Morton 2001).

The work in this Chapter aimed to examine genome-wide copy number changes in uterine leiomyomas using 1Mb resolution microarray CGH. The overall aim of this project was to attempt to refine previously reported regions and to identify new regions of copy number change. In addition to this, genes within these regions were identified and compared to known protagonists of

leiomyoma pathogenesis to examine the relevance of particular genetic pathways, particularly given that some cytogenetic alterations appear to impart resistance to GnRH analogue therapy, implying that the tumours are able to grow independently from the sex hormones oestrogen and progesterone (Brosens et al. 1998).

Uterine leiomyomas from three different patient cohorts were studied: HLRCC cutaneous and uterine leiomyomas were studied in an attempt to identify novel copy number changes separate from the *FH* locus at 1q42 that could give clues as to other regions and pathways involved in the pathogenesis of these tumours; uterine leiomyomas from African and Afro-Caribbean patients were studied to see if copy number changes could give potential clues to the location of specific genetic loci predisposing to leiomyoma formation; and finally sporadic leiomyomas were studied to identify novel regions of copy number change, and to refine the locations of previously known copy number change.

6.2 Materials and Methods

6.2.1 Samples

Microarray CGH was carried out on 40 samples in total. Of these, 3 were HLRCC leiomyomas (2 uterine and 1 skin), 14 were sporadic uterine leiomyomas from Caucasian patients, 10 were similar sporadic samples but with known LOH on chromosome 7, 3 were from leiomyoma cell lines and 13 were from patients of African or Afro-Caribbean origin.

Where matched germline DNA was available for a sample, this was used as a normal control. Where this was not available, a sample of 5 pooled normal female DNAs was used as a control.

6.2.2 1Mb resolution microarray CGH

Microarray CGH, carried out using 1Mb resolution BAC microarrays, and subsequent data analysis and calling of copy number changes was carried out as described in Chapter 2 (2.11.1, 2.13.2)..

6.3 Results

6.3.1 Microarray CGH results

1Mb resolution microarray CGH was carried out on 42 samples. Of these, 37 produced useful results and 5 samples failed. Overall, 34 changes were observed throughout all the samples. In 23 samples, no copy number changes were observed. The maximum number of changes in one sample was 6.

6.3.2 Analysis of HLRCC leiomyomas

3 HLRCC leiomyoma samples (2 uterine and 1 skin) were analysed by microarray CGH to examine potential copy number changes specific to this tumour syndrome. Only 1 change was observed, a deletion of 1q41-q43 (**Figure 6.1**). This deletion contains the *FH* gene, and the deletion in this tumour was highly likely to be the 'second-hit' leading to tumorigenesis. This was confirmed by sequence analysis of the patient, who had a germline K187R mutation (Alam et al. 2003), which showed no wild-type allele in the *FH* DNA sequence. In the 2 other tumours analysed, no copy number changes were observed although LOH had previously been confirmed by sequencing.

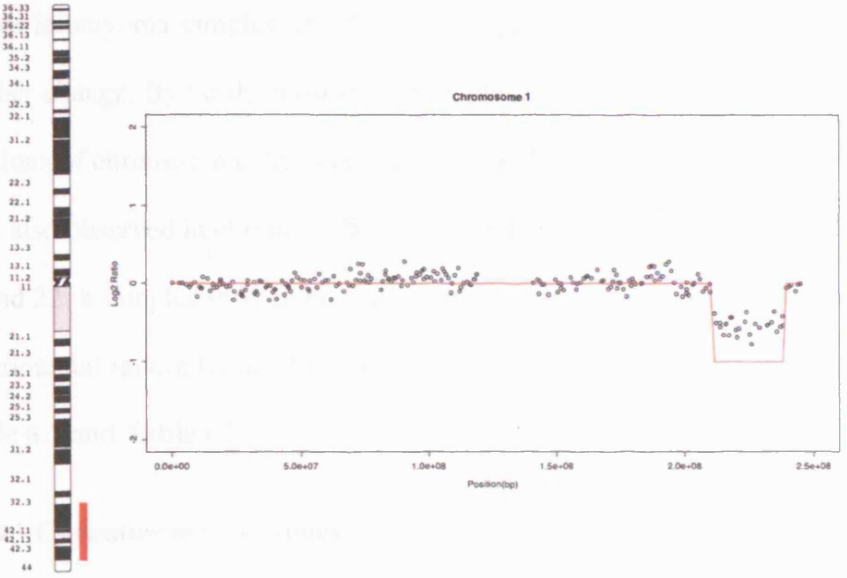

Figure 6.1 del(1)(q41-q43) in HLRCC uterine leiomyoma AHF2. The ideogram shows the location of the deletion, which encompasses the *FH* gene. The output plot shows the CGH profile for the entire chromosome plus results of the copy number change calling analysis.

6.3.3 Analysis of sporadic uterine leiomyomas

A majority of the observed copy number changes occurred in sporadic uterine leiomyoma samples. 16/24 (67%) samples contained at least one copy number change. By far the most frequently observed change involved deletions of chromosome 7q, occurring in 9/24 (38%) of samples. Changes were also observed in chromosomes 1, 3, 5, 6, 8, 9, 11, 12, 13, 14, 15, 19, 20, 21 and 22. 8 samples showed no copy number changes, with 4 of these due to experimental failure Detailed lists of the copy number changes are shown in **Table 6.1** and **Table 6.2**.

6.3.3.1 Chromosome 7 changes

9 samples demonstrated copy number changes on chromosome 7q (**Table 6.1**). 7 of these were samples selected for further study following LOH analysis of microsatellite markers by collaborators in Finland, where 165 samples from 91 patients were screened. One sample with 7q LOH (51M1) did not show any copy number change of chromosome 7, but did have a number of other copy number changes (discussed in 6.3.3.2). For the final 2 samples with 7q LOH, the experiment failed. 2 further samples from cell lines also showed deletions of 7q.

A minimum overlapping area of deletion of 3.92Mb was observed in all samples bar one (**Figure 6.2**a). The edges of this region were defined by two samples, 38M5 and 9M5 (**Figure 6.2**b), and was delimited proximally by clone RP11-148A10 (position – 104,084,406bp (UCSC)), and distally by clone RP11-5N18 (position – 108,002,467bp (UCSC)). This region contains approximately 28 known genes, and a number of transcripts (**Figure 6.2**c).

The minimum region of deletion excluded a number of previously proposed genes such as CUTL1 (Zeng et al. 1997), PCOLCE (Ligon et al. 2002), and ORC5L (Ligon and Morton 2001); all of which are proximal to this minimum region. This region does contain a number of interesting candidates. *LHFPL3* (Lipoma HMGIC fusion partner-like 3) is a gene with high identity to the *LHFP* gene family, which are fusion partners of HMGIC in translocations observed in lipomas (Petit et al. 1999). The frequency of HMGIC translocations in sporadic uterine leiomyomas suggests that this may be a strong candidate (Ligon and Morton 2001). Several candidate genes encoding important cell signalling pathway members, such as *PIK3CG* (phosphoinositide-3-kinase, catalytic subunit gamma) and *PRKAR2B* (cAMP-dependent protein-kinase regulatory subunit type 2 β). Deletion of the former would reduce PI3K signalling and disrupt the mTOR pathway. This could explain the effects on slowing cell growth of deletions of 7q (Xing et al. 1997; Takahashi et al. 2001a). Conversely, deletion of *PRKAR2B,* which inhibits the activity of cAMP-dependent protein kinase, could increase cell signalling through G-protein coupled pathways. This kinase also localises to the centrosomes, and dissociation is PRKAR2B is required to allow the onset of mitosis (Takahashi et al. 1999).

In addition to the minimal region of overlap observed in 8/9 samples with 7q deletions, two alternative regions of deletion were also observed, both in sample 29M2 (**Figure 6.3**). The first region was a single clone deletion at approximately 100Mb along chromosome 7. This region contains several genes thought to be candidates for the 7q tumour suppressor, including CUTL1, PCOLCE and ORC5L. However, it is also the location of copy

number variation in the human genome (Sebat et al. 2004; Sharp et al. 2005). For this sample no normal DNA was provided by collaborators and so a pooled normal was used. The single clone contains the polymorphic microsatellite marker D7S518. No LOH had been detected at this microsatellite in 29M2, and so it is possible that this single clone deletion is due to a copy number polymorphism.

The larger deletion in this sample spans the region q31.33-q34 and is approximately 17.5Mb long (**Figure 6.3**). A number of genes are encoded within this region, including a subunit of the mitochondrial electron transport chain enzyme NADH dehydrogenase (*NDUFB2*) and the B-Raf proto-oncogene (*BRAF*). The latter appears to be the only gene in this region with any relation to known leiomyoma signalling pathways, being a modulator of receptor tyrosine kinase signalling (Chan et al. 2003). However, the effects of deletion of this gene, when it is normally activated in tumours (Chan et al. 2003), are unknown.

Deletion of this region has been previously reported, along with other rearrangements of 7q34, in uterine leiomyomas (Fan et al. 1990; Vanni et al. 1991). However, it is reported rarely in comparison to the observed deletions of 7q22.

Table 6.1 Summary of chromosome 7 copy number changes observed by 1Mb microarray CGH

	Breakpoint 1[1]		**Breakpoint 2**[1]			
Sample	**Clone**	**Position (Mb)**[2]	**Clone**	**Position (Mb)**[2]	**Length (Mb)**	**Change**
28M1 (1st Change)	ptel	0	RP5-1091E21	55.04	55.04	Del
28M1 (2nd Change)	RP5-1136A10	80.53	RP11-384A20	121.37	40.84	Del
Awaki	RP4-784G16	82.50	RP11-563O5	114.02	31.52	Del
9CR	ptel		ptel		Whole	Del
29M2 (1st Change)[3]	RP11-506M12	99.64	RP11-401L13	102.51	2.87	Del
29M2 (2nd Change)	RP11-420H19	124.83	RP11-282G13	142.31	17.48	Del
38M5	RP11-148A10*	104.08	RP11-264K23	123.71	19.63	Del
38M1	RP4-672O11	103.09	RP11-264K23	123.71	20,62	Del
14M8	RP5-1084H12	91.08	RP11-328M22	112.28	21.20	Del
11M1	RP5-1084H12	91.08	RP11-36B6	130.08	39.00	Del
9M5	RP5-1145A22	97.17	RP11-5N18*	108.00	10.84	Del

*Denotes clones delimiting the smallest region of deletion.

[1]Breakpoint clones are defined as the first clones not considered lost flanking the change.

[2]Positions are defined as the position of the end of the breakpoint clone closest to the change. Positions are from the UCSC genome browser.

[3]This change was unverified by LOH analysis.

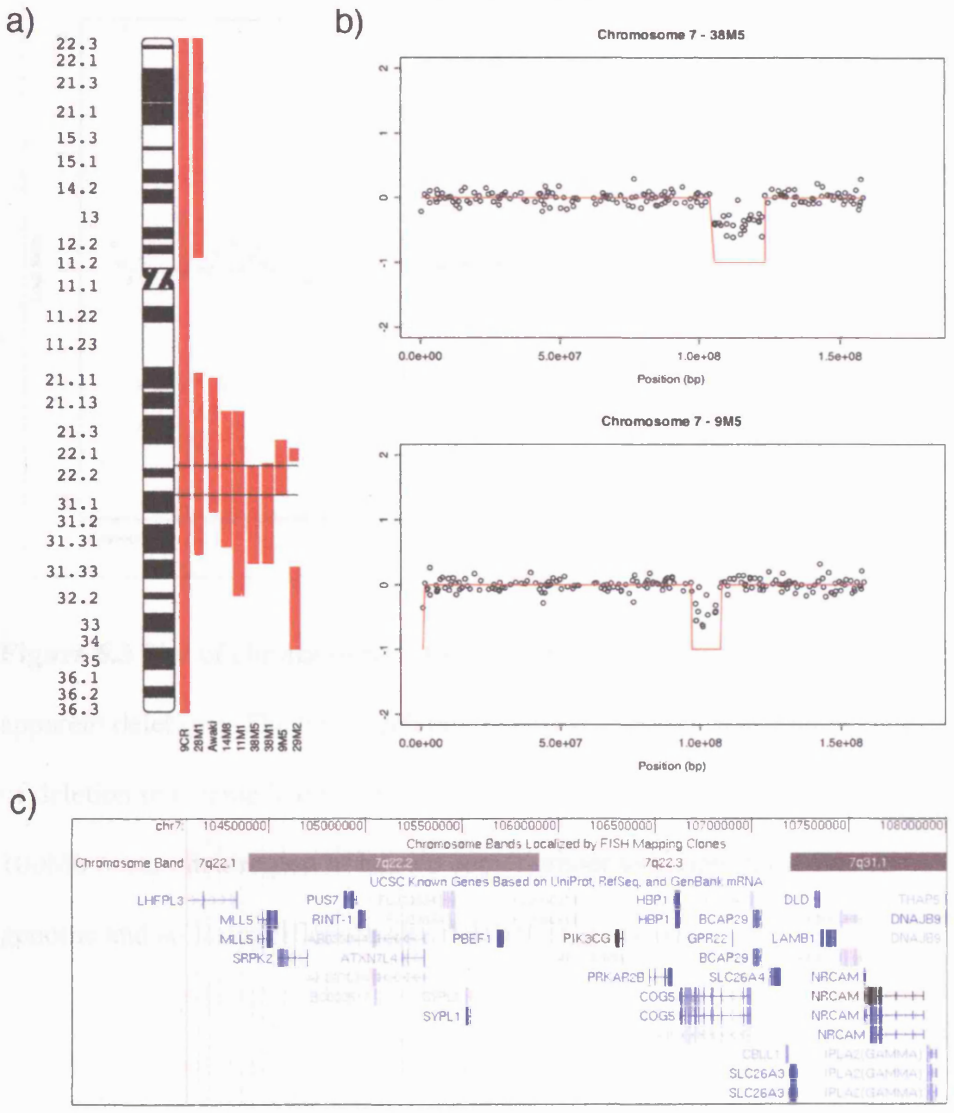

Figure 6.2 Deletions on chromosome 7 in sporadic uterine leiomyomas. (a) A summary of observed chromosome 7 deletions in 8 samples is shown against the chromosome ideogram. (b) The minimum region of overlap, occurring in 7 of the 8 samples, is 3.92Mb and is delimited by the samples 38M5 and 9M5; (c) this region contains approximately 28 known genes.

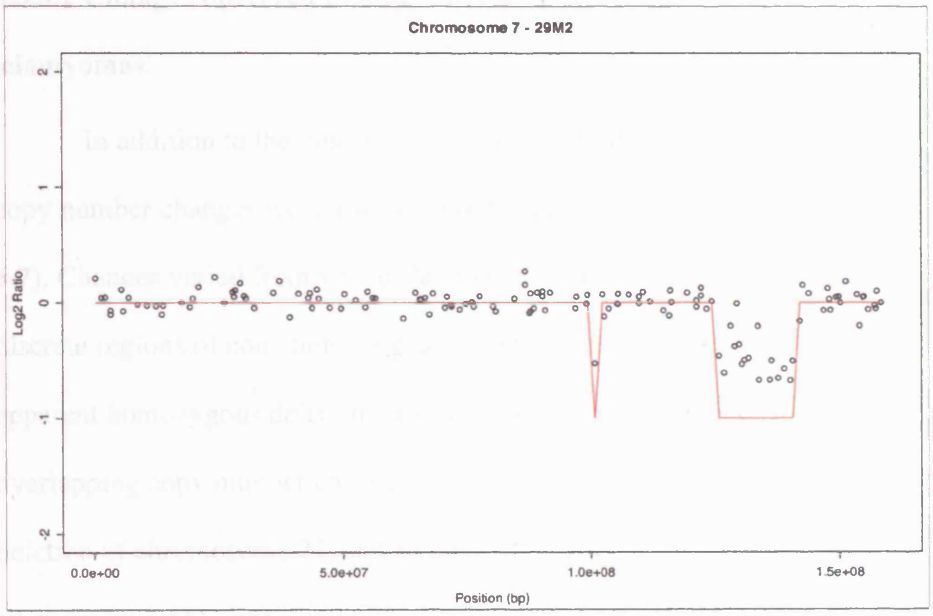

Figure 6.3 Plot of chromosome 7 from sample 29M2. This sample contains 2 apparent deletions. The larger deletion occurs in 7q31.33-q34, a novel region of deletion in uterine leiomyomas. The single clone deletion at approximately 100Mb occurs in a region of known copy number variation in the human genome and so its significance as a deletion is unknown.

6.3.3.2 Changes observed in other chromosomes in sporadic uterine leiomyomas.

In addition to the observed deletions of chromosome 7q, several other copy number changes were also observed (**Table 6.2**, **Figure 6.4 - Figure 6.7**). Changes varied from whole chromosome gains or deletions, to more discrete regions of copy number change, with one sample demonstrating an apparent homozygous deletion on 19q12. Only 3 regions demonstrated overlapping copy number changes: deletion of chromosome 12q21.2-q22, deletion of chromosome 22, and an interstitial deletion on 5p. There was also an apparent 3.5Mb homozygous deletion observed on 19q12 in sample 28M1.

Analysis of these other chromosome changes brought to light limitations of the analysis method (2.13.2). In particular, two changes obvious by eye were not identified, a deletion of chromosome 3 in sample 38M5 (**Figure 6.4**), and a gain of chromosome 19 in sample 51M1 (**Figure 6.6**). In these cases, a call was made by eye, and is indicated in the relevant diagram. Generally, these limitations were only observed where there were a number of changes involving many clones (for example, 51M1), leading to an increased standard deviation, and thus more stringent thresholds for copy number change.

In order to identify novel changes, a search was made for the location and type of each change in the Mitelman database of chromosomal aberrations (Mitelman et al. 2006). 24/27 (89%) of copy number changes observed in this study occurred within or overlapping with previously reported regions of copy number change by karyotyping studies. The three unique changes were the two deletions on 5p and the small gain on chromosome 13.

A number of small copy number changes were identified in this study. These regions were compared to reported regions of copy number polymorphism (CNP) (Sebat et al. 2004; Sharp et al. 2005). One change, on chromosome 5 in sample TB03 0111, mapped to a region containing two deletion and duplication CNPs, and so this change may be due to these CNPs.

Of the remaining small changes, two observed in sample 28M1 are of particular interest: amplification of 21q22.11, and an apparent homozygous deletion of 19q12. While similar changes have been previously reported in these regions in uterine leiomyomas, the deletion of 19q12 was reported as a heterozygous occurrence (Meloni et al. 1992).

The amplified region of chromosome 21 contains a number of potentially interesting genes that could be involved in leiomyoma pathogenesis. There are a number of cytokine receptors, particularly interleukin and interferon receptors. Of perhaps more interest is the cluster of keratin-associated proteins in the region. It has been hypothesised that uterine leiomyomas may form in response to injury, in a similar manner to keloids (Catherino et al. 2004). Keratin expression is upregulated in keloids (Prathiba et al. 2001), and the amplification of keratin-associated proteins in this sample may provide further evidence of a link between the two.

The homozygous deletion of 19q12 does not provide as interesting candidates. Two genes, CCNE1 (Cyclin E1) and UQCRFS1 (Ubiquinol-cytochrome c reductase) catch the eye. The former due to its intrinsic involvement in the cell cycle (Koff et al. 1991), and the latter due to its involvement in mitochondrial metabolism (Duncan et al. 1994). However, the deletion of cyclin E1, which is required to allow a cell to progress from G1 to

S-phase (Koff et al. 1991), would appear to have a detrimental effect on cell growth.

The additional small regions of copy number change also produced potentially interesting candidates. For example, the region of gain on chromosome 13 in sample TB02 0336 contained the MYCBP2 gene, which regulates the Myc proto-oncogene, and also inhibits TSC2, the mutated gene in the Eker rat model of uterine leiomyomas (Murthy et al. 2004).

Balanced translocations involving chromosomes 6p, 12q and 14q are frequent cytogenetic events in uterine leioymomas, involving rearrangements of the high mobility group (HMG) genes on chromosomes 6p and 12q, and RAD51L as a translocation partner on chromosome 14q (Ligon and Morton 2001). This study found a total of 8 changes in 6 samples in each of these chromosomes. This included the frequently reported trisomy 12 (Ligon and Morton 2001), which occurred in sample 51M1, and interstitial gains and deletions in other samples.

Only one of these changes, the deletion of chromosome 14q23.3-24.3 in sample TB03 0560, covered the regions involved in the common translocations. *RAD51L*, which is a translocation partner of *HMGA2* on 12q (Takahashi et al. 2001b), maps to the proximal breakpoint of this deletion (**Figure 6.8**). Therefore, it is likely that a translocation has taken place in this sample, additionally resulting in a loss of some genetic material from the breakpoint on chromosome 14. This deletion also removes a single copy of the *TGFB3* gene encoding TGFβ-3, which is involved in leiomyoma pathogenesis, although it is frequently seen upregulated (Tsibris et al. 2002).

It has been hypothesised that uterine leiomyomas with cytogenetic changes are able to grow independently of oestrogen stimulation (Brosens et al. 1998). Therefore, in order to identify potential candidate genes in the regions of copy number change observed in this study with the potential to allow oestrogen-independent tumour growth, the locations of a number of genes involved in oestrogen biosynthesis and oestrogen signalling were compared to the locations of copy number change. Only one gene, *SPEN* (also known as *MINT*), which encodes a transcriptional regulator involved in a multi-protein complex containing, among others, BRCA1, which inhibits oestrogen signalling (Yang et al. 2005), was identified in regions of copy number change in this study. This gene maps to 1p36, which is deleted in sample 200094A.

The locations of components of other pathways that have been implicated in leiomyoma pathogenesis were also studied, including the progesterone, TGFβ and bFGF pathways. Some genes involved in these pathways did map to the locations of various copy number changes: such as the progestin receptor *PAQR7*, which occurs on the deleted region of 1p (Zhu et al. 2003); and a number of FGF genes on chromosome 8, which were amplified as a part of a whole chromosome gain in one sample, and deleted in another sample. However, the involvement of these genes is purely speculative and could only be confirmed with further refinement of the region, and expression studies of individual genes.

Table 6.2 Summary of all non-7q copy number changes observed in sporadic uterine leiomyomas

		Proximal Breakpoint		Distal Breakpoint			
Chrm	**Sample**	**Clone**	**Position (Mb)**	**Clone**	**Position (Mb)**	**Length (Mb)**	**Change**
1	200094A	pter	0	RP1-118J21	40.00	40.00	Del
3	38M5	RP11-108A8	63.66	pcen	90.60	26.94	Del
5	38M1	RP11-32D12	9.60	RP11-215G15	10.64	1.05	Del
5	200049A	pter	0	RP11-28P24	19.64	19.64	Del
5	200049A	RP11-12D3	90.96	CTD-2332G20	141.85	50.89	Del
5	TB03 0111	RP11-421A17	67.68	RP11-115I6	71.66	3.98	Del
6	200094A	RP11-685G11	105.15	RP11-368P1	142.22	37.07	Del
8	51M1	pter	0	qter	146.27	Whole	Gain
8	28M1	pter	0	CTD-2115H11	43.32	43.32	Del
9	51M1	pter	0	qter	140.27	Whole	Gain
11	200103B	RP11-569N5	68.07	RP11-46D24	79.64	11.56	Del
11	200103B	RP11-56J3	107.61	RP11-485A5	123.30	15.70	Del
12	51M1	pter	0	qter	132.35	Whole	Gain
12	38M5	RP11-362A1	80.92	RP11-74K11	93.05	12.12	Del
12	38M1	RP11-362A1	80.92	RP11-435E3	94.13	13.21	Del
13	TB02 0336	RP11-309H15	72.69	RP11-38E20	77.79	5.10	Gain

		Proximal Breakpoint		Distal Breakpoint			
Chrm	**Sample**	**Clone**	**Position (Mb)**	**Clone**	**Position (Mb)**	**Length (Mb)**	**Change**
14	TB03 0560	RP11-125H8	66.87	RP11-368K8	75.21	8.34	Del
14	Awaki	RP11-98N22	19.73	RP11-159L20	30.16	10.43	Del
14	Awaki	RP11-346L24	49.05	RP11-304L20	54.38	5.33	Gain
14	51M1	pter	0	qter	106.37	Whole	Gain
15	200103B	qcen	17.00	RP11-519G16	43.41	26.41	Del
19	28M1	CTD-2043I16	33.40	CTC-416D1	36.89	3.49	Del (Homo)
19	51M1	pter	0	qter	63.81	63.81	Gain
20	51M1	pter	0	qter	62.44	Whole	Gain
21	28M1	RP11-175P11	29.81	RP1-245P17	34.48	4.68	Gain
22	200103B	pter	0	qter	49.69	Whole	Del
22	Awaki	pter	0	qter	49.69	Whole	Del

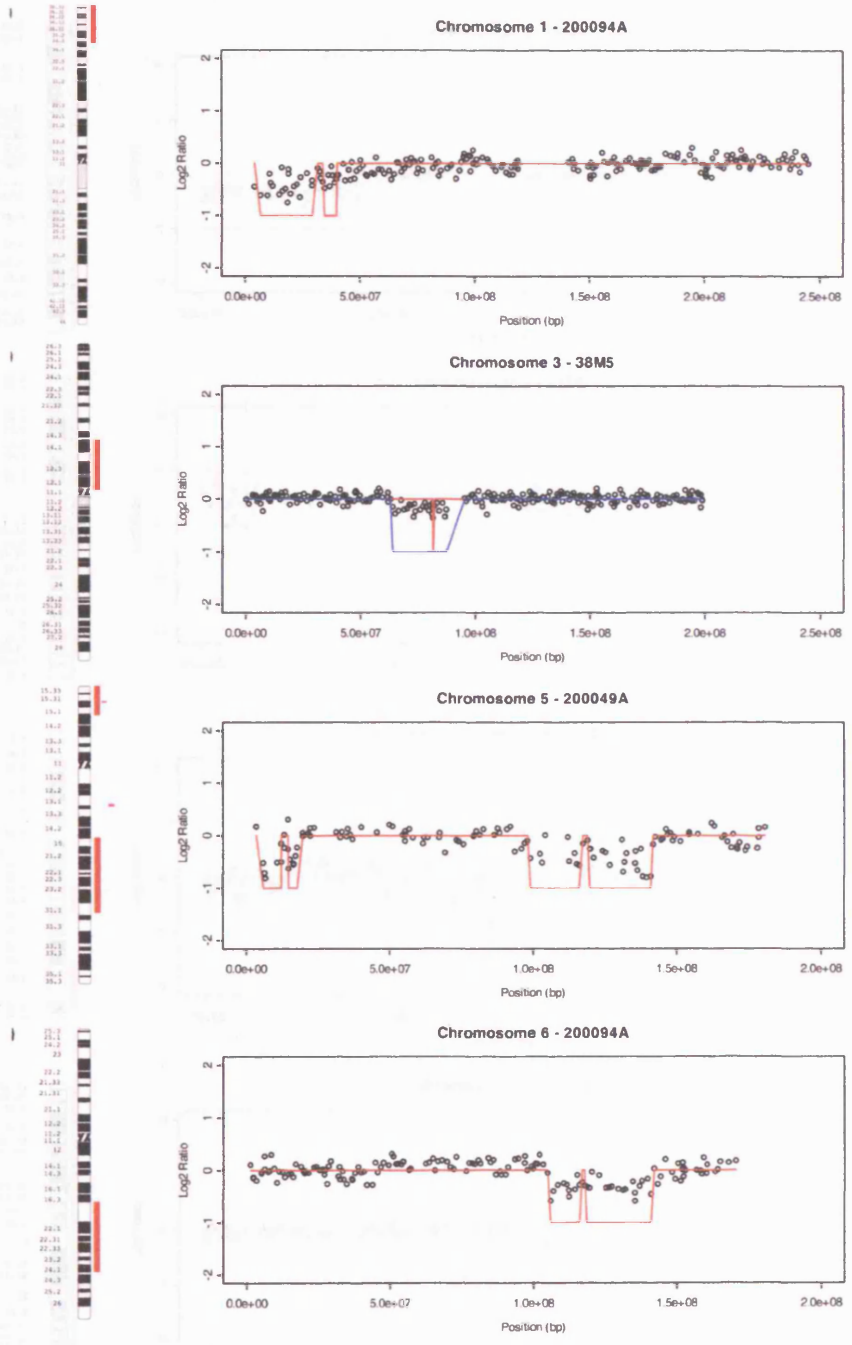

Figure 6.4 Examples of copy number changes – chromosomes 1,3,5,6. The ideogram summarises all observed changes (red bar = deletion, green bar = amplification). The plot shows an example output from one sample with the actual log2 values (black) and the called change (red). If a change has been identified by eye, this is shown as a blue line.

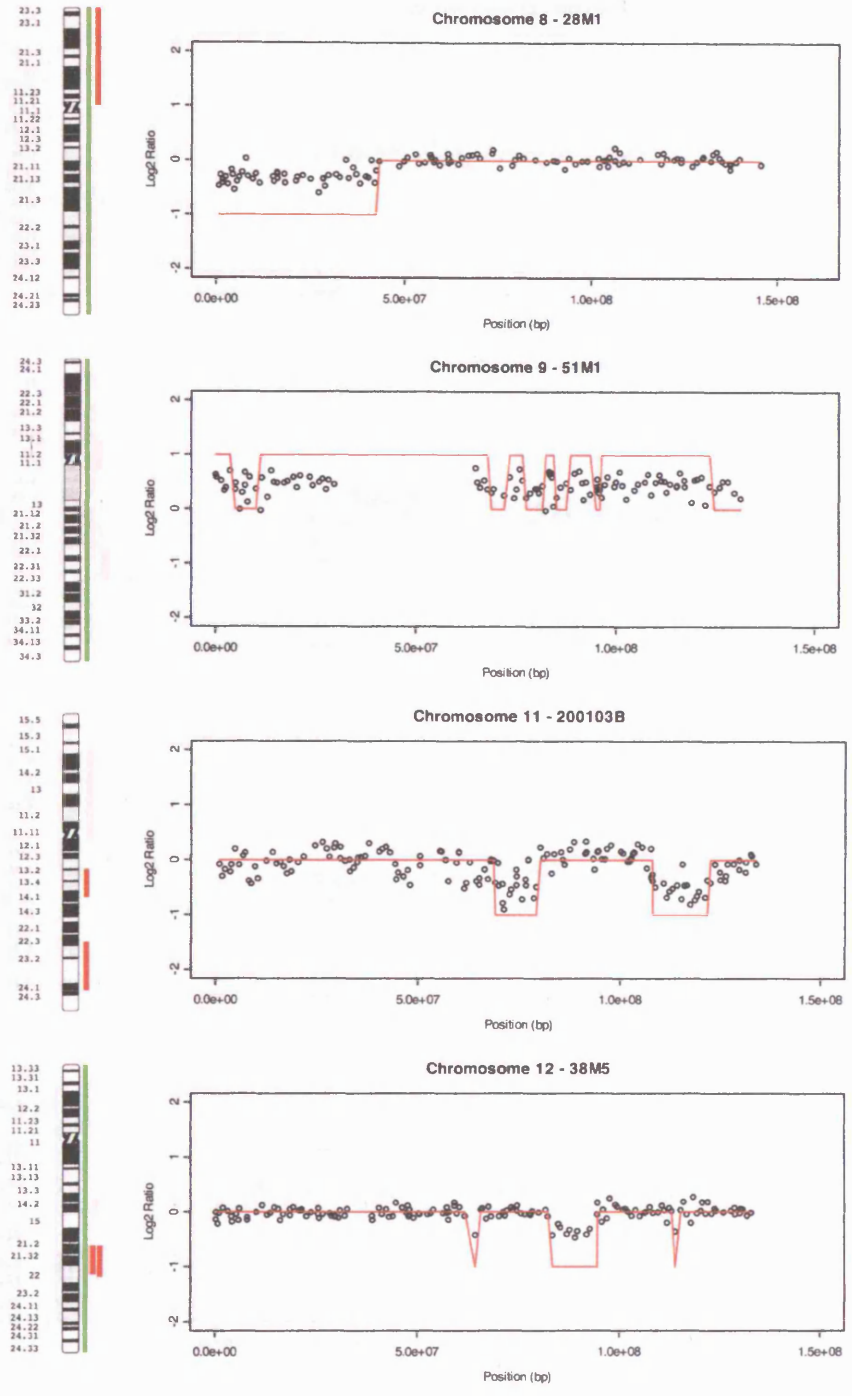

Figure 6.5 Summary of chromosome changes continued - chromosomes, 8,9,11,12.

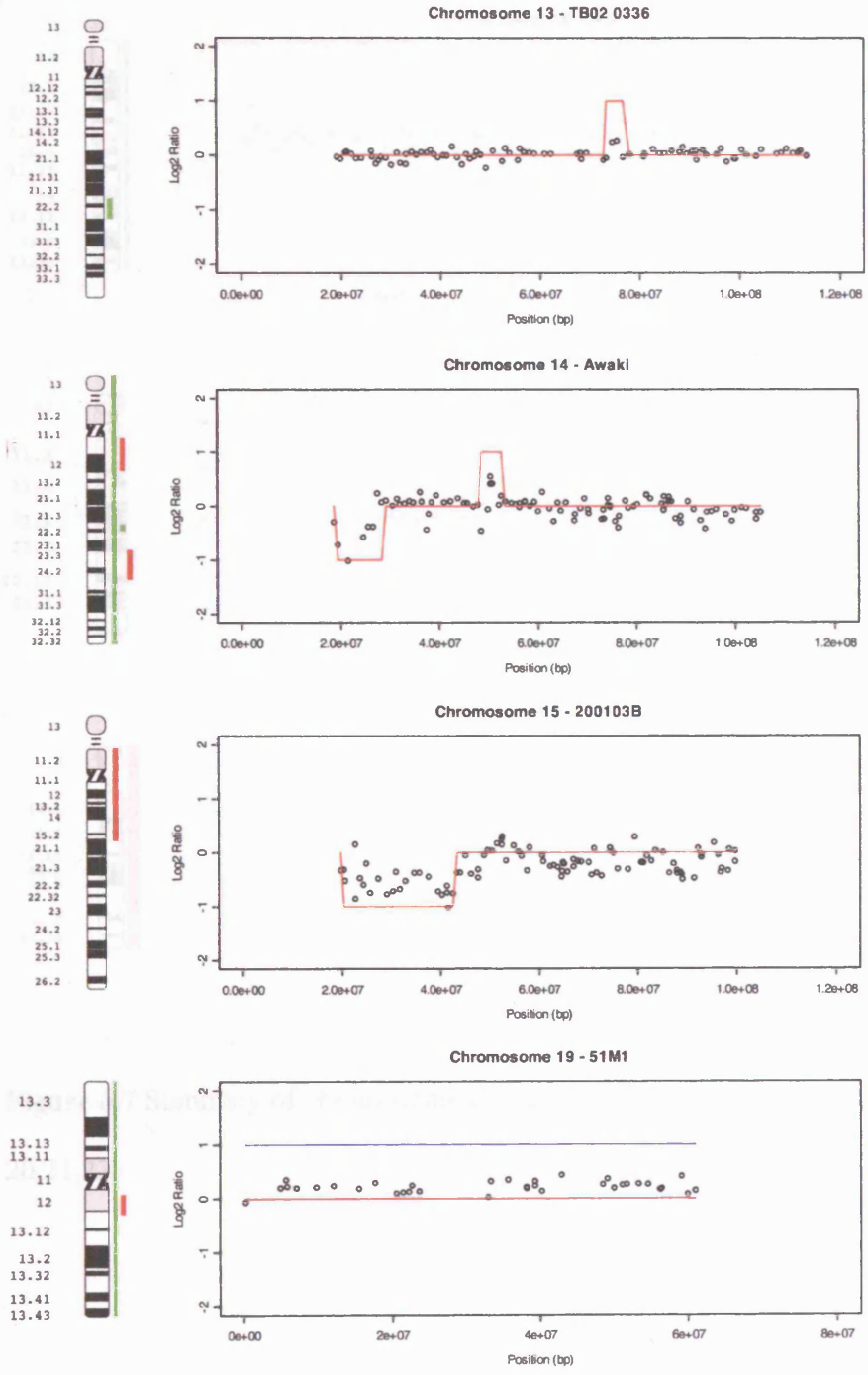

Figure 6.6 Summary of chromosome changes continued – chromosomes 13,14,15,19.

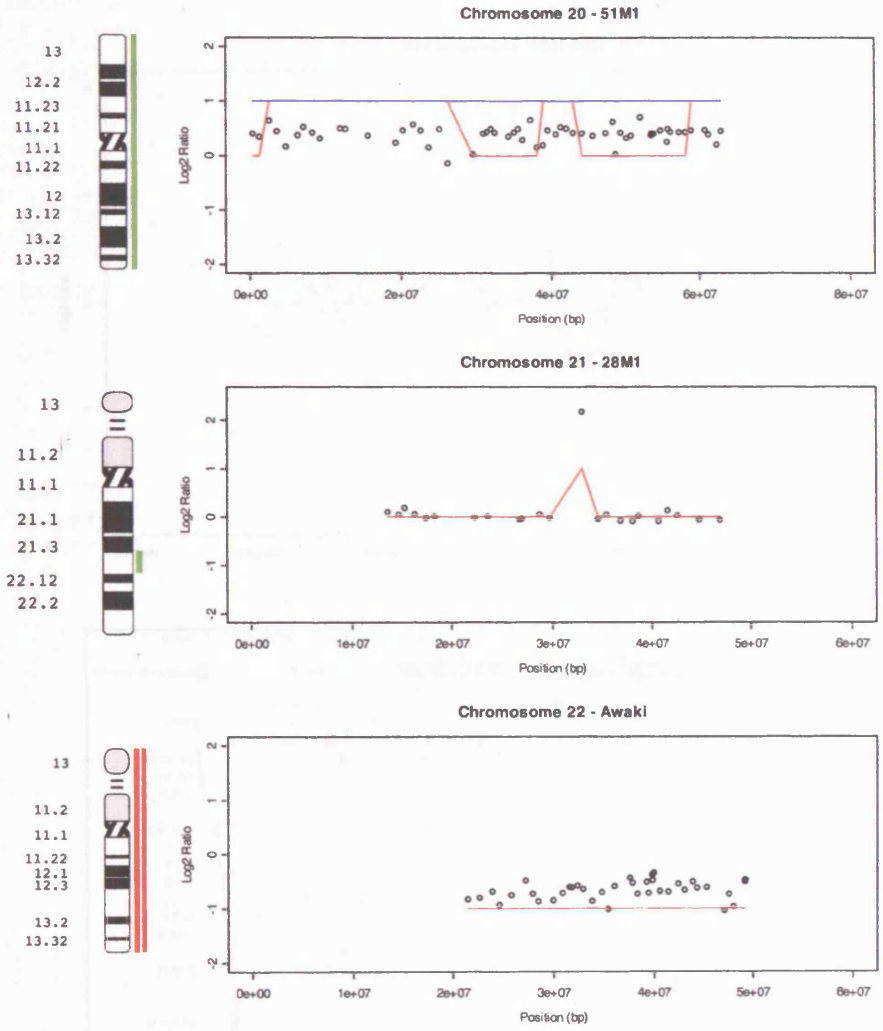

Figure 6.7 Summary of chromosome changes continued – chromosomes 20,21,22.

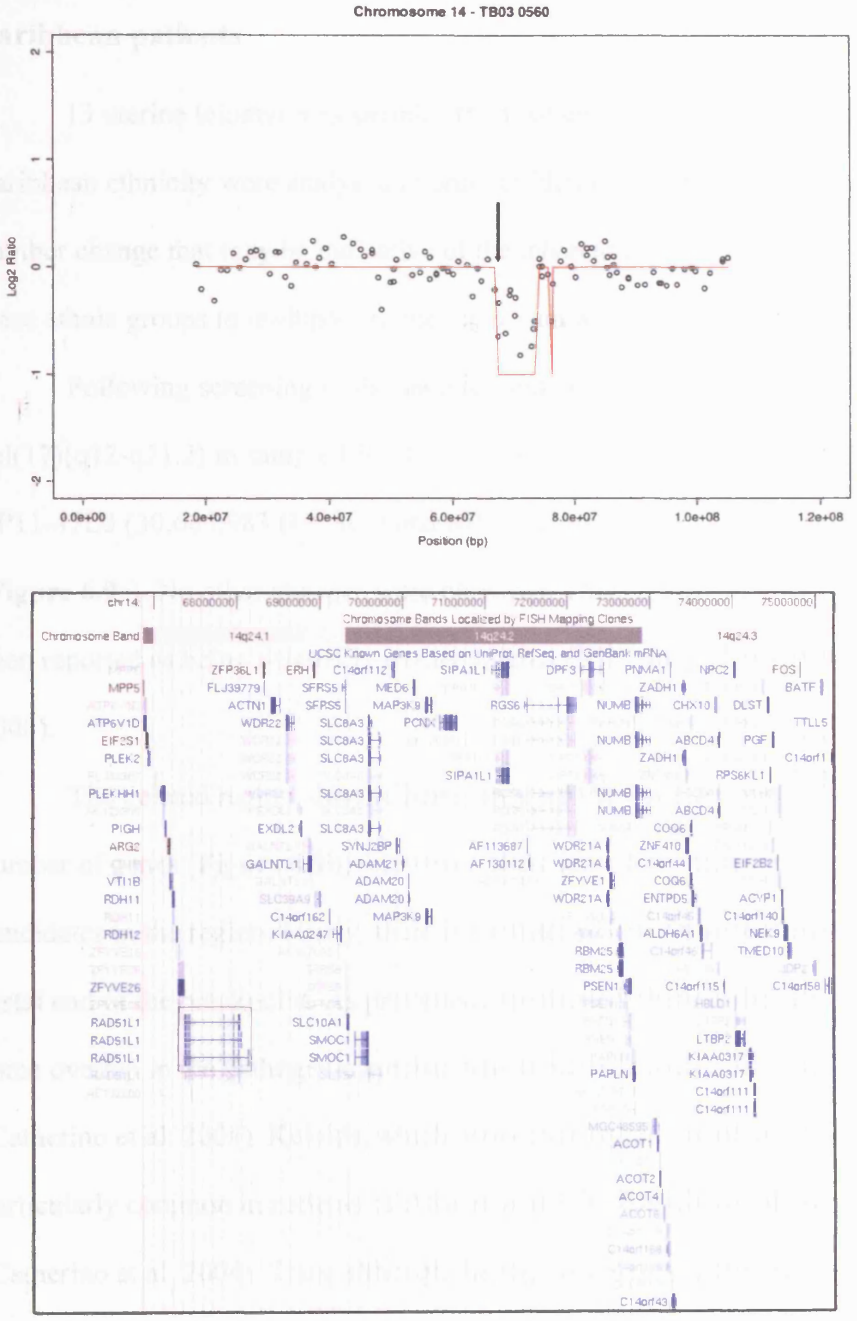

Figure 6.8 Deletion of chromosome 14 in sample TB03 0560. The deletion breakpoint (arrowed) is in the same region as the *RAD51L* gene (boxed) frequently involved in translocations in sporadic uterine leiomyomas.

6.3.4 Analysis of uterine leiomyomas from African and Afro-Caribbean patients

13 uterine leiomyomas samples from patients of African and Afro-Caribbean ethnicity were analysed in order to identify any regions of copy number change that may be indicative of the inherent element predisposing these ethnic groups to multiple uterine leiomyomas.

Following screening of the samples, only one change was identified, del(17)(q12-q21.2) in sample ER F1, a deletion of 6.5Mb flanked by clones RP11-47L3 (30,685,983 (UCSC)) and RP11-156E6 (37,192,545 (UCSC)) (**Figure 6.9**a). No other changes were observed. This region has previously been reported as being deleted in a conventional CGH study (Levy et al. 2000).

The deleted region, despite being only 6.5Mb long, contains a large number of genes (**Figure 6.9**b). However, there are a few interesting candidates in the region. Firstly, there is a cluster of keratin genes towards the distal end of the breakpoint. As previously mentioned, there is thought to be some overlap in the pathogenic mechanisms of keloids and leiomyomas (Catherino et al. 2004). Keloids, which show overexpression of keratins, are particularly common in patients of African and Afro-Caribbean ethnicity (Catherino et al. 2004). Thus, although the region is deleted, the presence of a keratin gene cluster in this region may be significant to leiomyoma pathogenesis.

The second interesting candidate is the *SMARCE1* gene, encoding a protein related to the SWI/SNF chromatin remodelling complex. The product

of this gene has been shown to be required for the transcription of oestrogen responsive genes (Belandia et al. 2002). Finally, 1Mb distal to the region is the BRCA1 tumour suppressor gene, which predisposes to breast cancer. Although no studies have been carried out examining the role of BRCA1 in uterine leiomyomas, the role of this gene in oestrogen signalling could imply some involvement in leiomoyma pathogenesis (Trauernicht and Boyer 2003).

a)

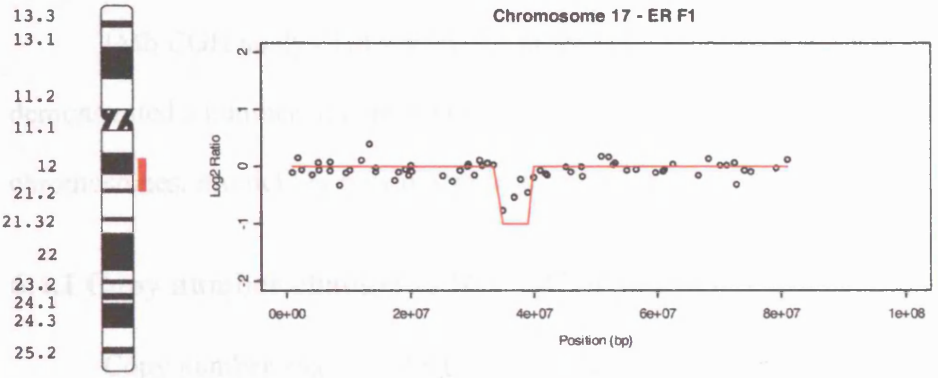

b)

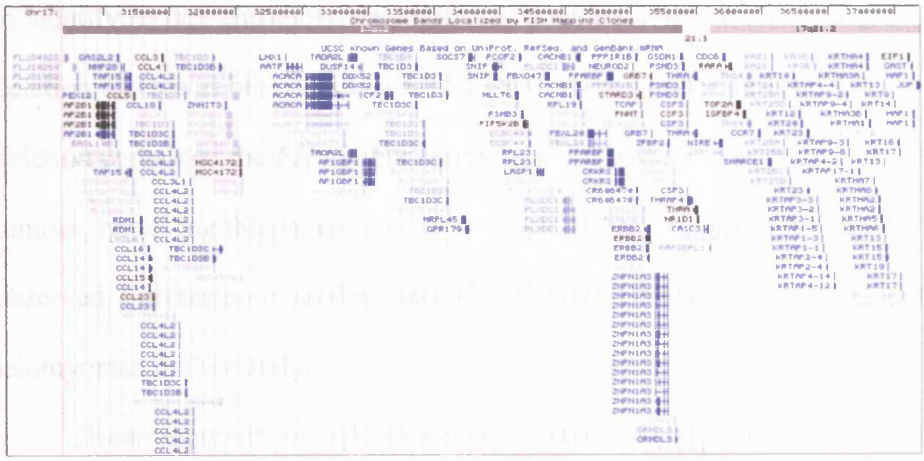

Figure 6.9 del(17)(q12-q21.2) in sample ER F1, a uterine leiomyoma from an Afro-Caribbean patient. A 6.5Mb region is deleted in this sample. No other copy number changes were observed in 12 other tumours of similar origin. b) The UCSC genome browser shows a number of genes within this region that could have the effect of a tumour suppressor.

6.4 Discussion

1Mb CGH analysis of a selection of sporadic uterine leiomyoma demonstrated a number of copy number changes across a wide-distribution of chromosomes, mimicking previous results.

6.4.1 Copy number changes in HLRCC uterine leiomyomas

Copy number analysis of HLRCC leiomyomas was carried out in order to identify further chromosomal regions of potential importance. A single deletion of 1q was observed in a 1/3 HLRCC leiomyoma samples. This deletion contained the *FH* tumour suppressor and was the second 'hit' in this tumour, removing the patient's wildtype copy of *FH*. No other changes were observed. Furthermore, no deletions of 1q42 were observed in sporadic uterine leiomyomas in this study.

Rearrangments of 1q42 in uterine leiomyomas have been previously reported in a number of studies, prior to the discovery of *FH* as the HLRCC tumour suppressor, but they are rare as the sole abnormality, occurring in 3/797 (0.37%) of karyotyped tumours in one study (Dal Cin and Morton 2002). In some cases, rearrangments of 1q42 have been identified in addition to other karyotypic changes, including t(12:14), and del(2)(q31) (Dal Cin and Morton 2002). A further study by Gross *et al* used FISH to examine deletions of the *FH* locus in uterine leiomyomas with rearrangements of 1q42, and found that in 9 /11 tumours, only one copy of *FH* was present, suggesting a role of *FH* in the pathogenesis of those tumours. Again, other karyotypic changes were observed in addition to the rearrangement of 1q42 (Gross et al. 2004).

These results suggest that other karyotypic abnormalities may occur in HLRCC uterine leiomyomas. However, in this study, the potential for discovering these was limited by the very small sample size of tumours tested. Furthermore, a number of additional rearrangements observed in uterine leiomyomas with 1q42 rearrangements were balanced changes, such as translocations and inversions, which cannot be detected by array CGH (Gross et al. 2004). A more thorough study, requiring not just copy number analysis, but also more traditional karyotyping, would give a more thorough overview of additional cytogenetic changes occurring in HLRCC uterine leiomyomas, which may augment the effects of the *FH* tumour suppressor.

6.4.2 Copy number changes in sporadic uterine leiomyomas

Copy number changes appeared as a frequent event in the sporadic uterine leiomyomas. In this study, 9/17 (53%) sporadic leiomyomas, excluding those with knowledge of LOH, exhibited copy number changes. This frequency is higher than the reported frequency of approximately 40% for leiomyomas with karyotype alterations, but may reflect the increased sensistivity of the array CGH method for identifying copy number changes.

6.4.2.1 Chromsome 7q deletions

The role of 7q deletions in leiomyoma pathobiology is confusing. While the frequent deletions observed have lead many to propose a novel tumour suppressor in the deleted region (van der Heijden et al. 1998), studies of the size of tumours with 7q deletions (Rein et al. 1998), their growth behaviour in culture (Xing et al. 1997), and lack of resistance to GnRH analogue treatment (Takahashi et al. 2001a) suggest otherwise. However, the

high frequency of these deletions suggests that there is a role for these deletions in uterine leiomyoma pathobiology.

The minimum region of deletion at 7q22.1 obtained in this Chapter confirms results obtained in the FISH studies of Vanni *et al,* the CGH studies of Levy *et al,* and the LOH study of ven der Heijden *et al* and reduces the minimal region of deletion within the boundaries of the regions observed in these studies (van der Heijden et al. 1998; Vanni et al. 1999; Levy et al. 2000). A number of interesting genes occur in this region that could explain the behaviour of uterine leiomyomas with 7q deletions, including *PIK3CG,* and *PRKAR2B*. However, the minimum regions defined by two LOH-based studies, at markers D7S666 (Ishwad et al. 1997) and D7S2446 (Sell et al. 2005), lie outside of the minimum region defined by this study.

It is possible that the different implied and demonstrated minimal regions of deletion are suggestive of several loci on 7q22 being important for uterine leiomyoma development, a hypothesis that has previously been postulated (Ishwad et al. 1997). However, most studies of 7q deletions aimed at defining the region at the highest resolution have been carried out by LOH analysis, and this presents a number of problems. Firstly, the assumption that LOH of 7q automatically implies deletion is made in many of these studies (van der Heijden et al. 1998; Sell et al. 2005). In this study, one sample, 51M1, demonstrated LOH across a number of markers in the chromosome. However, when this sample was analysed by array-CGH, no changes in copy number were observed. Thus, validation of LOH as a deletion is important.

Secondly, there is a demonstrated unreliability in the method of microsatellite LOH analysis for detecting deletions. The paper by Ishwad *et al*

identified uterine leiomyomas with cytogenetically visible deletions of chromosome 7q, and then analysed these tumours for LOH. The resulting LOH map shows a confusing and inconsistent pattern of loss and retention of heterozygosity, the results suggest a wider minimum region than that suggested by the authors (Ishwad et al. 1997). This confusing pattern of LOH in samples with known deletions suggests that LOH analysis is not a reliable means of their detection. Thus, great care should be taken, where a single marker is observed to have LOH, to validate this result by other methods as much as possible.

An alternative region of deletion was also observed at 7q34 in one sample. Deletion of 7q34 has been previously reported (Fan et al. 1990; Vanni et al. 1991), and it is not inconceivable that leiomyomas with this particular copy number change represent a separate cytogenetic group to those with deletions of 7q22.

6.4.2.2 Other observed copy number changes

Copy number changes affecting other chromosomes were also observed in sporadic leiomyomas in this study. Some of these changes were observed in the same samples as those with 7q deletions and may complement the effects of the deletion. There was some overlap between copy number changes observed in other chromosomes in leiomyomas with and without 7q deletions, and the low number of samples tested means that the significance of any difference in distribution cannot yet be verified. Grouping of other copy number changes was not observed, but again this is probably due to the low

number of samples tested. While a number of interesting regions were identified, no obvious candidate genes were present in these regions.

6.4.3 Copy number changes in African and Afro-Caribbean uterine leiomyomas

While a number of karytoyping studies have been carried out on uterine leiomyomas in general, to date, no study has specifically examined an association between specific karyotypic changes and ethnicity. Here, 13 uterine leiomyomas from patients of African and Afro-Caribbean origin were examined by microarray CGH to identify any specific copy number changes associated with ethnicity. In all the samples, one change was identified, a deletion of 17q12-21.1 in sample ER F1. A small deletion of this region has been previously reported by CGH studies of uterine leiomyomas.

As described above, this region contains several interesting genes, particularly the cluster of keratin genes, which may be important in the increased frequency of uterine leiomyomas in African and Afro-Caribbean patients, and may also be related to increased prevalence of keloids in patients of this ethnicity. However, the presence of only one copy number change in 13 samples does not imply a significant association of this region with ethnic predisposition to uterine leiomyomas. In order to further confirm this association, a far greater number of samples would need to be studied.

It is important to remember that in addition to copy number change, a number of other balanced cytogenetic aberrations occur in leiomyomas, which are undetectable by microarray CGH. A full study of the distribution of karyotypic abnormalities in uterine leiomyoma patients of African/Afro-

Caribbean and Caucasian ethnicity would require karyotyping studies to complement microarray CGH to determine the association of cytogenetic changes beyond copy number changes.

6.4.4 Discussion

The work in this chapter has examined copy number changes in uterine leiomyomas from a variety of backgrounds, including HLRCC, sporadic and Afro-Caribbean leiomyomas. A number of copy number changes have been identified, in particular on chromosome 7q in sporadic leiomyomas, where the region of demonstrated deletion was minimised to 3.92Mb. However, no obvious strong candidate genes for leiomyoma pathobiology have arisen from these regions based on prior knowledge of known pathways of leiomyoma pathogenesis.

The use of high resolution copy-number analysis techniques such as microarray CGH has the potential to identify a number of novel regions of copy number change involved in the pathobiology of uterine leiomyomas. The increased resolution may demonstrate a greater number of copy number changes than have previously been described, and could also implicate many more genes and pathways in leiomyoma pathogenesis.

Other than the region of deletion of chromosome 7q, few other overlapping regions of copy number change were identified. Unfortunately, a very limited quantity of 1Mb arrays was available for this study. An increased number of samples studied would allow potentially more regions to be identified, and, perhaps more importantly, would allow known regions of copy

number change to be refined and potentially important genes in leiomyoma pathogenesis to be identified.

Chapter 7

Construction and validation of a chromosome 7q tiling path genomic microarray

7.1 Introduction

Work in the previous chapter identified a number of deletions of chromosome 7q, as expected from the literature. This initial mapping demonstrated a minimum deleted region of 3.92Mbp. The CGH results were shown to provide more reliable information about deletions than LOH analysis. However, the limited resolution of these arrays means that at least 800kb of sequence was unaccounted for per megabase on the array, and so finer mapping of the deleted region was not possible and small homozygous deletions were likely to be missed. It was, therefore, decided to pursue the novel leiomyoma gene on chromosome 7q by increasing the resolution of the analysis and constructing a tiling-path resolution genomic microarray. This would allow finer mapping of the deleted region, and also potentially allow the identification of homozygous deletions that may harbour the proposed gene. The work in this chapter details the construction and validation of the 7q tiling-path array.

7.2 Materials and Methods

7.2.1 Selection of BAC clones

Three sets of BAC clones were selected for the array: 1067 clones covering chromosome 7q; 554 control clones representing the rest of the genome at approximately 4.5Mb intervals; and 8 clones from *Drosophila melanogaster* as a control for non-specific hybridisation. Specific lists of the clones can be found in Appendix 1.

7.2.1.1 7q Tiling Path Clones

BAC clones mapping to chromosome 7q were used from the "32k" BAC re-array set produced by BACPAC resources (Children's Hospital, Oakland, CA, USA). This set comprises 32,433 BAC clones with an average resolution of 43kb. The clones were selected from the RPCI-11/13 and Caltech-D clone libraries using the fingerprint map of the human genome. They were selected to provide complete genome coverage at high resolution. Selected clones were enriched for those that had end sequence and full sequence data. All selected clones were fingerprinted by Hind III digestion, and overlapping clones were selected on the basis of greater than 3 conserved restriction fragments between clones. Clone localisation was carried out using a combination of end-sequence co-ordinates, fingerprinting and assembly co-ordinates from NCBI release 8 of the human genome (Osoegawa et al. 2001). This library was selected due to its availability as prepared DNA.

Selection of 7q clones was based on mapping data from human genome 15 (hg15). From this data, 1104 clones mapped to 7q, and these clones were amplified and printed. Clone data were updated by the clone

suppliers following the release of hg17. Re-examination of the clones printed on the array showed that of the 1104 clones originally selected, 1067 continued to map to 7q; 19 mapped to different chromosomes and were incorporated into the control set; 12 were un-positioned; and 6 were re-mapped to 7p. A further 15 clones were added to the 7q set from the control set, giving 1082 clones in the final clone set. This set had a median centre to centre clone spacing of 87.1kb, and a resolution (median unique length of sequence per clone) of 57.0kb. A summary of the 7q clone set following re-mapping is shown in Table 7.1 and a list of all the clones amplified and printed on the array can be found in Appendix 1.

Table 7.1 Summary of 7q tiling path clone set

Total number of clones	1,082
Median clone length	164,949bp (Range 18,857-313,512bp)
Total clone length	175,036,319bp
Length of 7q covered by array	97,722,464bp
Chromosome arm coverage	1.79x genome
Total gaps	83
Total gap distance	4,463,104bp
Median gap	27,883bp (Range 5-503,465bp)
Median clone midpoint distance	87,053bp
Median clone overlap	77,831bp (Range 295-221,150bp)
Median unique sequence per clone	56,985bp

[1]Median unique sequence is derived from the 613 clones containing sequence unique to that clone. 469 clones contained no unique sequence.

7.2.1.2 Control Clones

BAC clones for the control set were selected from those used to construct the Sanger Centre's 1Mb resolution microarray used in the previous chapter (Fiegler et al. 2003). 554 clones were picked at approximately 4.5Mb intervals throughout the genome, excluding the Y chromosome and chromosome 7p. The latter was excluded to prevent effects of whole chromosome 7 loss on normalisation. Performance of these clones was assessed by analysis of normal-normal hybridisations to the 1Mb genomic microarray, and information about the clones provided by Nigel Carter's group at the Wellcome Trust Sanger Institute. Clones found to have inconsistent results in hybridisation, or to cross-hybridise in FISH experiments (carried out by Nigel Carter's group), were removed from the control set and replaced with adjacent clones that fulfilled the criteria. DNA for these clones was extracted by Regina Regan at the Wellcome Trust Centre for Human Genetics in Oxford.

In addition to the control clones, 19 of the original 7q were found to map to other chromosomes. These clones were also included in the control set giving a total of 573 clones. The number of control clones per chromosome is shown in **Table 7.2** and a complete list of the clones in the control set can be found in Appendix 1.

Table 7.2 Summary of the control clone set

Total Clones		573	
Median mid-point spacing		4.41Mb	
Chromosome	No. Clones	Chromosome	No. Clones
1	48	13	22
2	41	14	22
3	44	15	19
4	38	16	19
5	37	17	22
6	33	18	18
8[1]	25	19	11
9	23	20	15
10	25	21	7
11	23	22	10
12	25	X	30

[1]No control clones were chosen from 7p

7.2.1.3 Drosophila Clones

In addition to the human clones, eight BAC clones from *Drosophila melanogaster* were selected as a control for non-specific hybridisation (**Table 7.3**). These clones were used as FISH probes on normal human chromosomes, and were found not to map to any point in the genome (**Figure 7.1**). More information about these clones can be found in Appendix 1.

Table 7.3 Drosophila control clones

Clone ID	Drosophila Chromosome mapping	FISH result against human
RP98-10P9	3L-66E4	No hybridisation
RP98-5L4	X	No hybridisation
RP98-38L1	X	No hybridisation
RP98-3G6	3L	No hybridisation
RP98-33N24	X	No hybridisation
RP98-44K7	3L-74C1	No hybridisation
RP98-9C21	3L-9C21	No hybridisation
RP98-7P15	X	No hybridisation

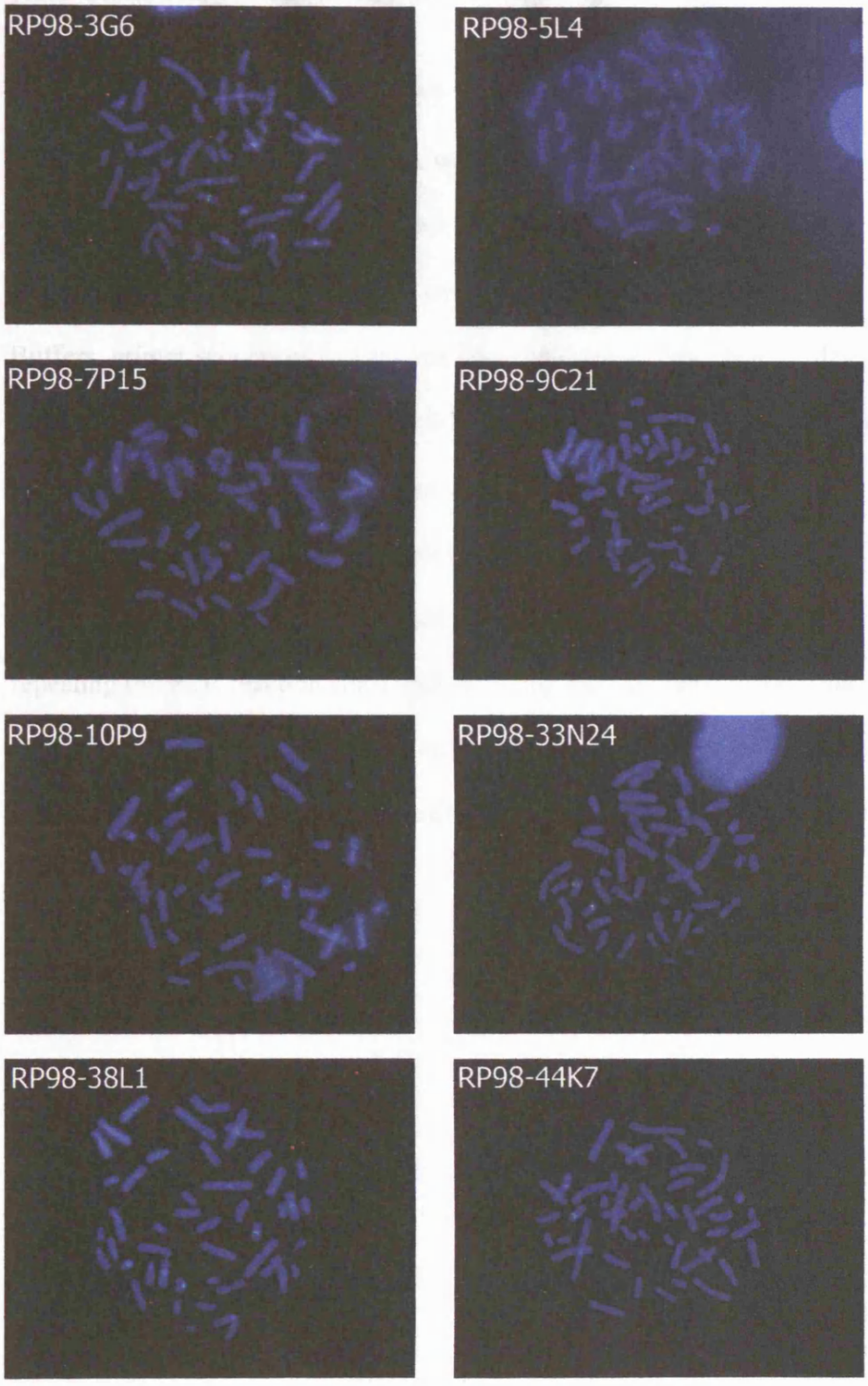

Figure 7.1 Fluorescence in-situ hybridisaton of the control *Drosophila* BAC clones to normal human chromosomes. *Drosophila* BACs, labelled orange, did not hybridise to normal human chromosomes. A 16q specific BAC (green) was included as an experimental control.

7.2.2 Clone Amplification and Array printing

7.2.2.1 Degenerate oligonucleotide primer (DOP) PCR

Amplification of BAC DNA was carried out by three separate DOP-PCR reactions using the three primers designed by Fiegler *et al* to preferentially amplify human DNA over *E.coli* DNA (Fiegler et al. 2003). Buffers, primer sequences and cycling conditions are as described in Materials and Methods (2.3.3). 2.5μl of clone DNA at approximately 1ng/μl was used for each PCR reaction. Amplification was checked by agarose gel electrophoresis and compared to a no-template blank (**Figure 7.2**). Any product detected in this blank implied contamination and necessitated repeating the PCR reaction since contaminating total genomic DNA could dilute the hybridisation ratio of the clone in a hybridisation experiment. PCR products for each DOP primer were then pooled for the aminolinking reaction.

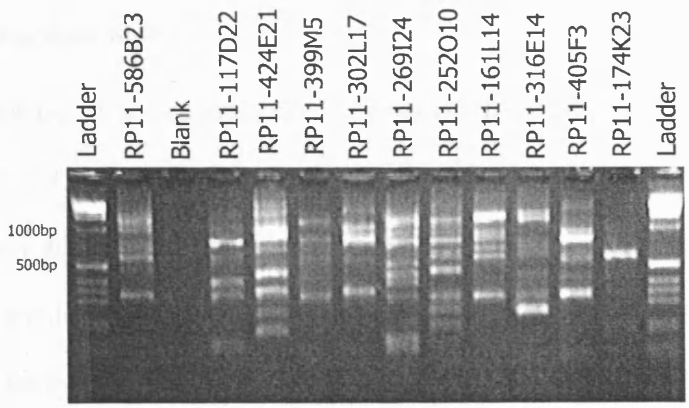

Figure 7.2 Example of DOP1 primer amplified BAC DNA. Amplification produces a distinct pattern of bands for each clone. Equally important is the presence of a blank (Lane 3) indicating no contamination in the PCR reactions.

7.2.2.2 Aminolinking PCR

A further PCR step amplified the pooled DOP-PCR products using a primer with a 5' C-6 aminolink moiety to allow the amplified clone DNA to be covalently attached to the Codelink slides. The protocol and primer sequences are described in materials and methods (2.3.4). As for the DOP-PCR, a no-template control was included, and any contamination witnessed after electrophoresis required a repeat of the PCR.

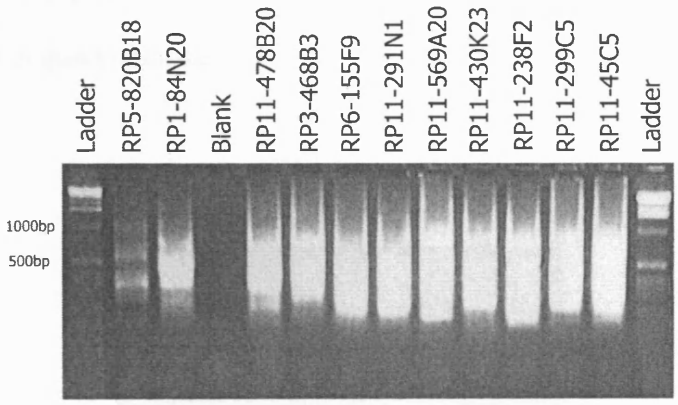

Figure 7.3 Example of a gel following aminolinking PCR. PCR products form a smear of approximately 100-1200bp. The no-template control in lane 4 indicates no contamination of the PCR reaction.

7.2.2.3 Array printing

Array printing was carried out by Cordelia Langford and Oliver Dovey at the Wellcome Trust Sanger Institue as described in Chapter 2 (2.11.1.2). The arrays were printed in 24 blocks of 18 spots by 18 spots. Each block contained a combination of control, 7q and *Drosophila* clones. Within each block, each clone was printed twice, with the upper 9 by 18 spots being the duplicate of the lower 9 by 18 spots (**Figure 7.4**). In addition, each clone was also present in duplicate on another block. Therefore, each clone was printed on the array in quadruplicate.

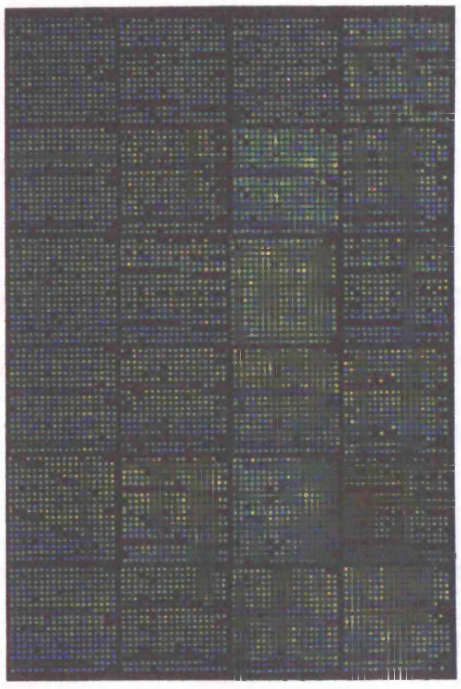

Figure 7.4 Printed layout of the 7q tiling-path array. The array consists of 24 subarray blocks, each containing 324 spots. The top half of each block is the duplicate of the bottom half.

7.3 Array Validation

To ensure the validity of the arrays, and their usefulness for analysis, several stages of validation were carried out. Firstly, test arrays were printed using a small number of the final clone set. Following printing of complete arrays, several normal-normal and sex-mismatched hybridisations were carried out. Finally, hybridisation of samples with known changes was carried out. All three methods of validation ensured the final arrays were robust and producing reliable data.

7.3.1 Test array printing

The first stage of validation involved printing a set of test arrays using amplified DNA from control plates 1 and 2 (192 spots in total). The reasons for this were twofold: to ensure that the amplification and aminolinking methods allowed the DNA to attach to the slide; and to ensure that the blank controls didn't hybridise DNA once printed onto the array.

The array consisted of 192 spots, 188 containing BAC DNA and 4 blanks. Pooled female DNA was labelled and competitively hybridised to the array against itself. The arrays were washed and scanned as previously described (2.11.1).

Visual inspection of the scanned images showed the arrays to be strongly hybridised, with very low background. Furthermore, empty spots printed from the no template PCR reactions showed no evidence of hybridisation above the background (**Figure 7.5**).

The array images were overlaid and quantified using UCSF Spot (Jain et al. 2002) and analysed in Microsoft Excel. A summary of the Cy3 and Cy5 hybridisation signals for BAC and blank spots is shown in **Table 7.4**. Cy3 and Cy5 intensity values for all printed spots were strongly positively correlated, with an R^2=0.916 (**Figure 7.6**) with very few outliers. After lowess correction, the median log2 ratio for each BAC spot was -0.006950494, with a standard deviation of 0.1228517.

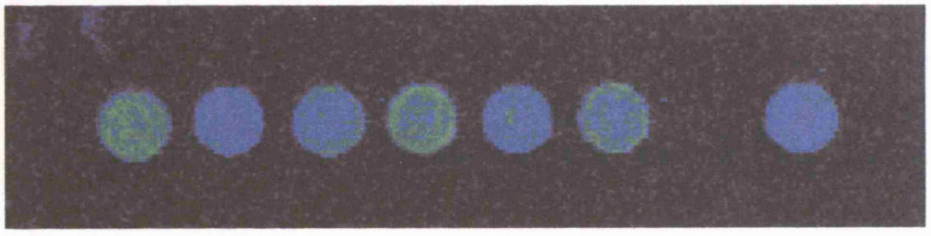

Figure 7.5 Cy5 image of hybridised spots from the test print array. This magnification of a single row containing 7 clone spots and 1 blank spot shows that DNA hybridises evenly to the clone spots, with no hybridisation to the blanks.

Table 7.4 Summary of hybridisation intensities to BAC clone and empty spots on the printing test array. Values are shown as the median, followed by the range of data.

	Cy3		Cy5
BAC clone spots (n=188)	Foreground Intensity	4801.9 (1125.5-13301.5)	9366.4 (1607.8-28908.9)
	Background Intensity	0.065 (0-269)	10.7 (0-101.8)
	Foreground Standard Deviation	597.1 (245.2-1431.1)	633.4 (222.2-2017.3)
Blank spots (n=4)	Spot Intensity	816.4 (639.9-958.0)	398.1 (369.9-505.8)
	Background Intensity	0	0
	Foreground Standard Deviation	160.7 (139.2-203.2)	73.9 (69.9-109.0)

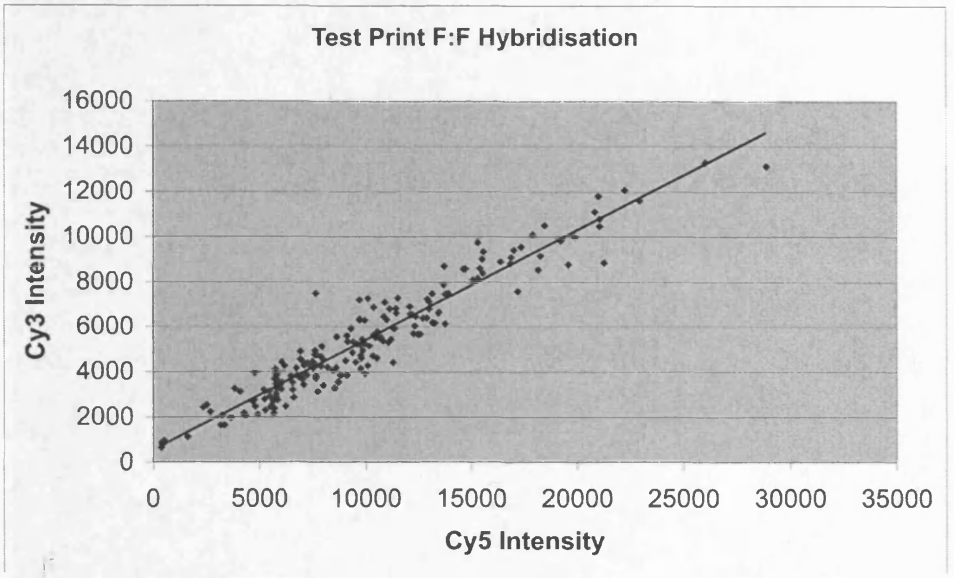

Figure 7.6 Correlation between Cy3 and Cy5 intensity values for the test print array. Values were highly positively correlated with an R^2 value of 0.916.

7.3.2 Normal-Normal hybridisations

The test array printing confirmed that the amplified DNA was attaching satisfactorily to the slide, and that empty positions were not hybridising to samples. As a result, the remaining DNA plates were amplified and full arrays were printed as described in 7.2.2.3. The first stage of validation was to hybridise several slides using 'normal' DNA to ensure that no deleterious hybridisation was occurring.

7.3.2.1 Data analysis considerations

The basic method for analysis of the array data was similar to that involved for the 1Mb array (2.13.2). However, a number of factors needed to be considered given the content of the array. In particular, since the majority

of clones on the array were from chromosome 7q, consideration of normalisation was required. The array was designed with a number of control clones from the other autosomes, and chromosome X to act as a comparison to the ratios observed for the 7q clones. As for the 1Mb CGH array, a lowess normalisation was used for data analysis. Initially, an attempt was made to normalise using only the control clones, however, this was too technically demanding an approach. Therefore, it was decided to normalise using all the clones on the array. Following this, data were adjusted to set the median ratio of the control clones as 0. This meant that copy number changes involving a majority of the clones on the array, such as deletion of the whole arm of 7q, would still be detectable.

The method for calling changes was based on similar principles to the 1Mb array (2.13.2). However, only the clones from the control set (ie non-7q clones) were used to define the thresholds for significant changes. Analysis of the normal-normal hybridisations (7.3.2.2) demonstrated no difference in the spread of data between the 7q clones and the autosomal control clones, so no rescaling of the data was required (**Table 7.5**).

7.3.2.2 Sex match and mismatch

The initial array testing was to ensure that normal-normal hybridisations showed no deleterious effects, and to exclude clones consistently producing unexpected values. 6 hybridisations were carried out: 4 were sex-matched, and 2 were sex-mismatched. Normalised Log2 ratios for each array were obtained as for the 1Mb resolution arrays. Block-lowess normalisation was used and the data for each array was collated.

5 of the 6 hybridisations carried out showed strong hybridisations and tight data on chromosome 7q (**Figure 7.7**). Hybridisation results for chromosome X on the sex-mismatch experiments showed copy number changes of these chromosomes and so demonstrated the ability of the array to detect single-copy chromosome changes (**Figure 7.8**). This demonstrated that no normal contamination was present in the printed, amplified clones.

Results from these hybridisations were also used to exclude clones consistently producing unexpected results. A clone was excluded if it fulfilled one of several criteria:

i) The clone failed to produce a result in >50% of hybridisations.

ii) Unexpected ratios, such as significant loss or gain, were obtained in >50% of hybridisations.

iii) Unexpected ratios occurred as a result of sex-mismatch hybridisations, indicating strong homology with either the X or Y chromosomes. For a clone to be excluded, unexpected ratios would have to occur in both sex-mismatch experiments.

iv) A combination of the above.

In total, 88 clones fulfilled these criteria, all from the 7q set, and were excluded from further analysis. Excluded clones can be found in Appendix 1.

Table 7.5 Median and standard deviations of control and 7q clones in the control experiments

	1095-4 F-M	1242-18 F-F	1095-5 M-F	1095-6 F-F	1238-9 F-F	1095-12 F-F
Control Clones Median (excl X)	-0.0134	0.0026	0.0032	-0.0023	-0.0237	-0.0052
Control clones Standard Deviation	0.0688	0.0418	0.0709	0.0774	0.06680	0.0347
7q Clones Median	0.0060	0.0003	-0.0108	0.0097	0.0063	0.0018
7q Clones Standard Deviation	0.0685	0.0393	0.0691	0.0906	0.0710	0.0393

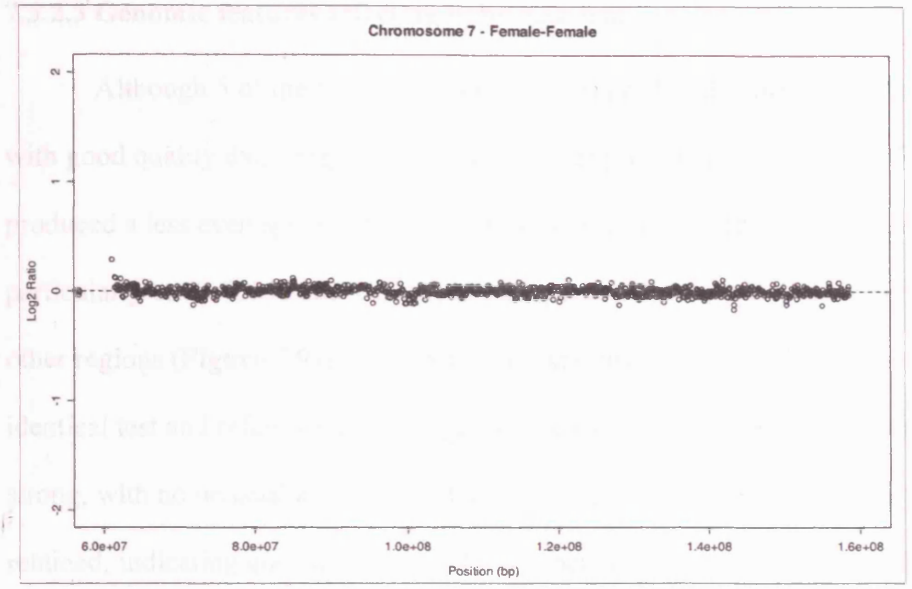

Figure 7.7 Chromosome 7q results of normal-normal hybridisation. A majority of hybridisations produced tight data with little variation around the baseline (Log2 = 0).

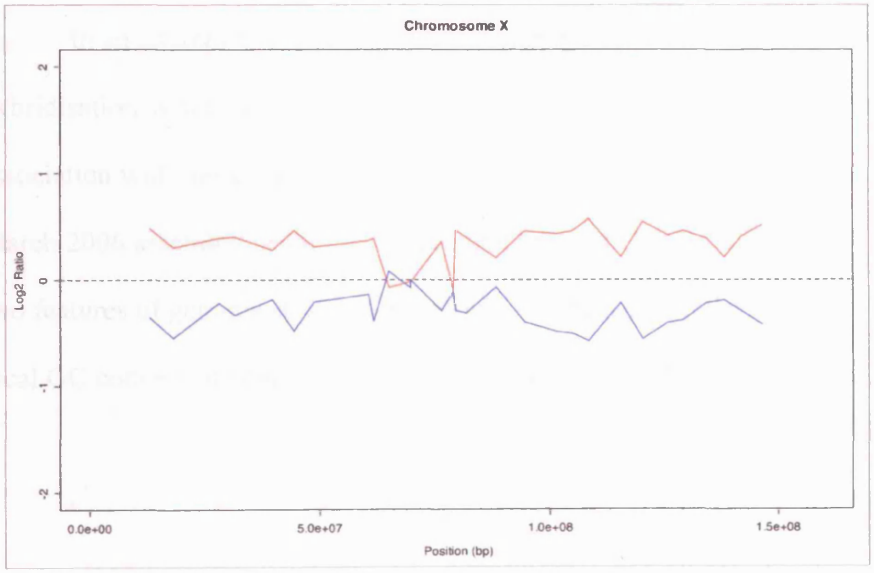

Figure 7.8 Chromosome X results for sex-mismatch hybridisations on the 7q tilepath array. Hybridisations were carried out with a male reference (red) and a female reference (blue). Clear expected differences were observed and were consistent for both hybridisations.

7.3.2.3 Genomic features affecting hybridisation.

Although 5 of the 6 control hybridisations produced expected results, with good quality data (**Figure 7.7**), one of the experimental controls (1095-6) produced a less even spread of data, with certain regions of chromosome 7q, particularly at 60-75Mb and 100Mb, showing a broader spread of data than other regions (**Figure 7.9**a). This particular experiment involved hybridising identical test and reference DNA samples. The hybridisation to the array was strong, with no unusual artefacts, and a large proportion of data points were retained, indicating good agreement of ratios between clones. Furthermore, the standard deviation of data for the control clones was comparable to the other control hybridisations (**Table 7.5**). These regions of broader data spread further appeared in several later experiments, particularly where no deletions were evident.

In an attempt to identify the reasons for this unusual pattern of hybridisation, a number of features of chromosome 7 were investigated for an association with these regions. Following analysis of data obtained from the March 2006 assembly of the UCSC genome browser (Hinrichs et al. 2006), two features of genome structure appeared to associate with these regions: local GC content and density of segmental duplications (**Figure 7.9**b and c).

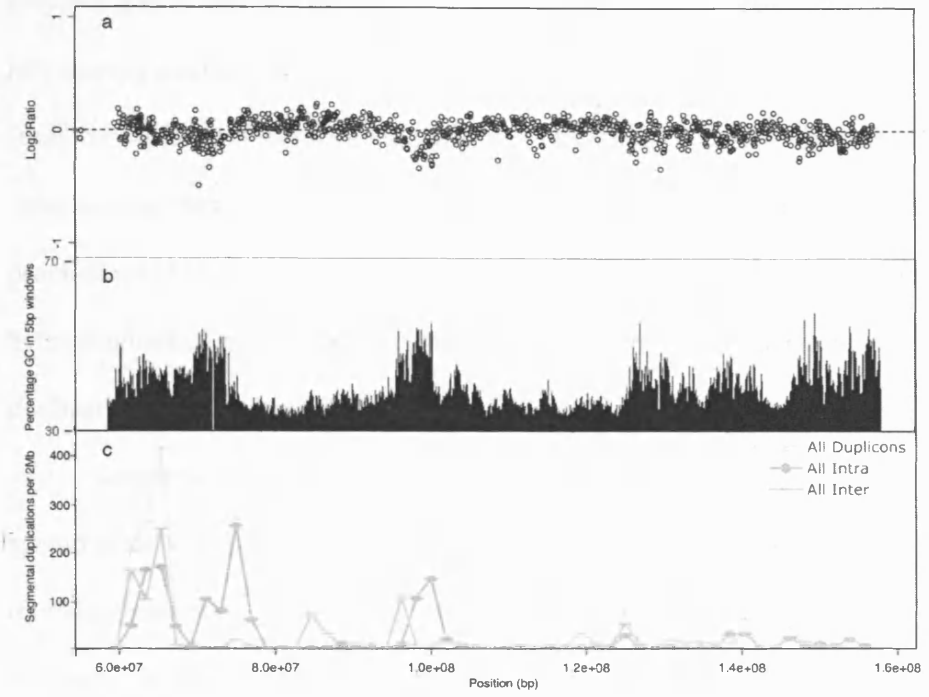

Figure 7.9 Unexpected hybridisation ratios from a female-female hybridisation (a). The unexpected ratios correlate with both an increase in the local GC content (b), and an increase in the frequency of segmental duplications (c).

Segmental duplications are a class of low-copy repeats in the human genome. They range in size from 1-400kb in length and have a very high sequence identity (>90%) between repeats. Unlike other classes of repeating sequences, such as LINEs and SINEs (Long and Short Interspersed Nuclear Elements, eg *Alu* repeats), LTRs (Long Terminal Repeat elements), and satellite repeats; segmental duplications are not blocked by C_0t-1 DNA, due to their low copy number (Strachan and Read 2004). Recently, segmental duplications have been observed to be associated with copy number

polymorphisms between individuals, and so differences between samples may reflect copy number variation between two individuals (Sharp et al. 2005). A study by Locke *et al* examined the effects of segmental duplications on the hybridisation characteristics of BAC microarrays. They found that increased proportions of segmental duplications in a BAC increased the spread of data in hybridisations of normal DNA, compared to BACs with no segmental duplications (Locke et al. 2004).

Regions of increased GC content associate with the regions of greater spread of data. This effect may be due to the effects of increased GC content on the hybridisation dynamics of the DNA. Since G-C pairing in DNA involves 3 hydrogen bonds, compared to the 2 in A-T pairing (Watson and Crick 1953), GC-rich regions have a higher melting temperature (T_m) than AT-rich regions (Strachan and Read 2004).

Since the test and reference DNA samples were identical in this particular experiment, copy number variation was unlikely to be a cause of the broader spread of data, although it was considered an important factor in analysis of results of hybridisations between samples from different individuals. The difference more likely arises from the chemical properties of the Cy3 and Cy5 fluorochromes. An effect has been previously observed (Cox et al. 2004) and it is thought that dye-dye interactions occur between Cy3 and Cy5 result in fluorescence quenching and increased signal variance, particularly for Cy5. In GC-rich regions, a greater concentration of dye would be present, since it is conjugated to dCTP, and so fluorescence quenching is more likely to be observed. Since this quenching affects Cy5 more than Cy3,

the Cy5/Cy3 fluorescence ratio will be skewed to imply reduced copy number of tumour DNA.

It was important to take these regions into account when analysing data from tumours, in order to prevent false calls of copy number change. Since these differences occur infrequently, no permanent alteration to the analysis procedure was deemed necessary. Instead, great care was taken to standardise the experimental technique to minimise variation between arrays. Upon analysis of tumour samples, these regions were treated with care, and any potential changes involving these regions were validated by other experimental techniques, such as LOH analysis using local microsatellites and SNPs.

7.3.3 Known deletion hybridisation

To test the ability of the array to detect copy number polymorphisms, hybridisations were carried out using two leiomyoma cell line samples with known deletions detected on the 1Mb resolution array. The first, F9CR, has a deletion of all of chromosome 7, while the second, Awaki, has an interstitial single-copy deletion of chromosome 7q, and a single copy deletion of chromosome 22.

In both samples, the changes observed on the 1Mb array were also detected on the 7q array. For the Awaki sample, the limits of the interstitial deletion of 7q occurred in the same region to those observed on the 1Mb array. However, the increased resolution of the 7q array gave a more accurate representation of the location of the breakpoints (**Figure 7.10**a). Detection of changes was not perfect, several outlying clones were called as losses, and several clones within the region of deletion were not called deleted. This is an artefact of the higher resolution of the array since many clones will have homology to other chromosomes without copy number changes. In these cases, as for the 1Mb array, such regions were called by eye.

The whole chromosome deletion in F9CR was also identified using the 7q array (**Figure 7.10**b). Again, a number of clones failed to reach a significant level of loss. The distinctive pattern likely resulting from high GC content and dye interaction was also observed in this sample, particularly around 100Mb.

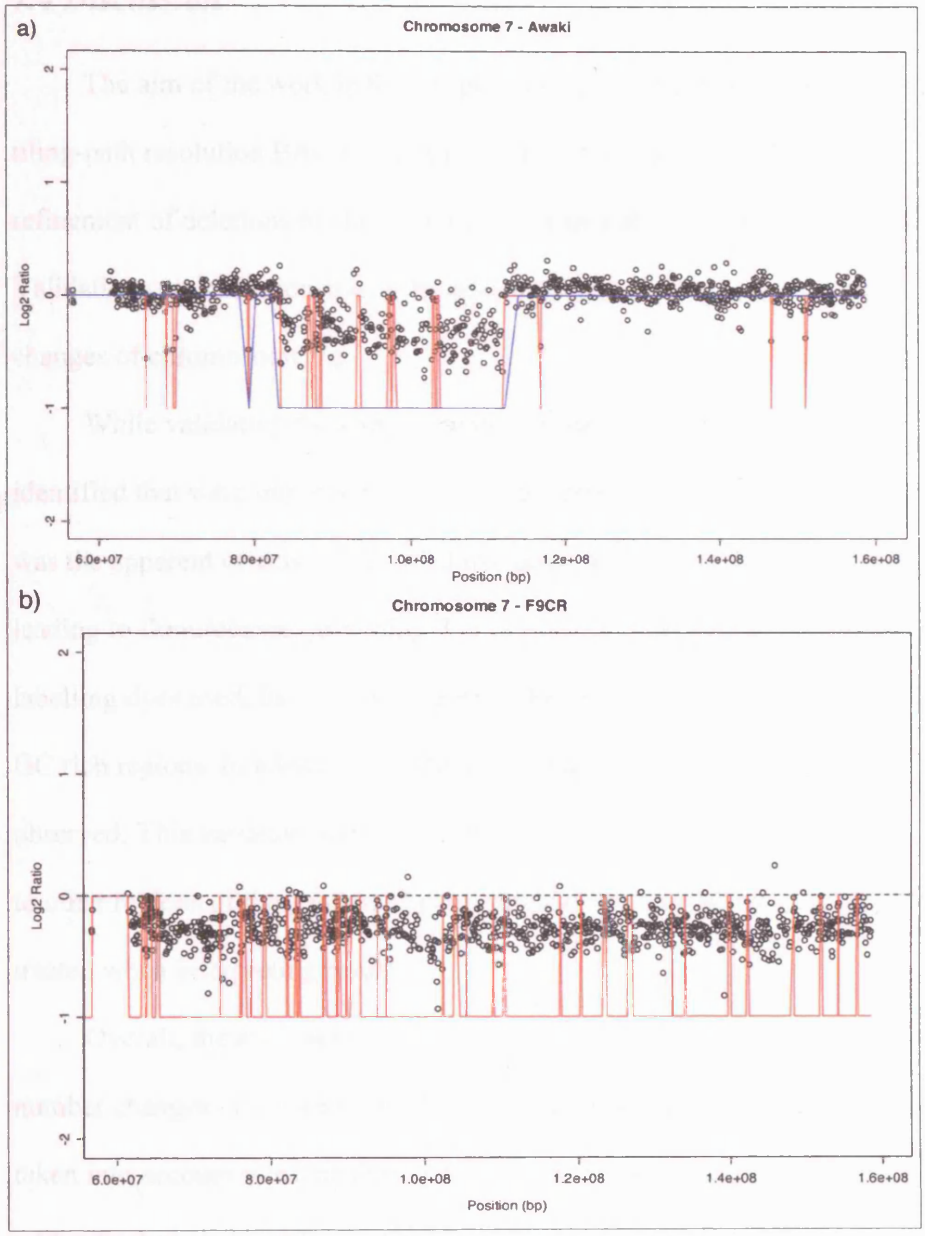

Figure 7.10 Results from hybridisations of known samples. The interstitial deletion detected in the Awaki sample (a – red line) exactly matches the observed deletion using the 1Mb resolution arrays (blue line). Whole chromosome deletion of 7q was detected in F9CR (b).

7.4 Discussion

The aim of the work in this chapter was to construct and validate a tiling-path resolution BAC CGH microarray for the further analysis and refinement of deletions of chromosome 7q in sporadic uterine leiomyomas. Validation results demonstrated the array was able to detect copy number changes of chromosome 7q.

While validating the array a number of features of the array were identified that were important to consider for data analysis. Chief among these was the apparent effects of increased dye concentrations in GC-rich regions leading to fluouresence quenching. For reasons of economy the Cy3 and Cy5 labelling dyes used, but special care was taken in interpreting the results of the GC rich regions. In addition, variation of single clone log2 ratios was also observed. This variation may be due to local clone GC content, or homology to other regions of the genome. Again, single clone changes were carefully treated when interpreting results.

Overall, the array was considered suitable for the detection of copy number changes of chromosome 7q, but with the difficulties described above taken into account when analysing the data, and it was decided to proceed with a further study of 7q deletions in uterine leiomyomas.

Chapter 8

Analysis of Chromosome 7q deletions in sporadic uterine leiomyomata

8.1 Introduction

Having successfully constructed a tiling-path resolution genomic microarray to examine chromosome 7q deletions in sporadic uterine leiomyomas, a larger study was undertaken to examine sporadic leiomyoma samples using this array in order to minimise the critical region of deletion, and thus identify the most likely candidates. Furthermore, the increased resolution would allow the identification of potential homozygous deletions. Potential candidate genes could be further analysed in an attempt to identify the gene.

In addition to identifying the minimal region of deletion, a study was also undertaken to examine the frequency of 7q deletions in uterine leiomyomas in patients of African and Afro-Caribbean ethnicity compared to patients of Caucasian and other ethnicities in order to identify whether there is a different pattern of occurrence of this particular chromosomal aberration.

8.2 Materials and Methods

8.2.1 Selection of samples

DNA samples from all frozen sporadic uterine leiomyomas were used for initial LOH analysis. This included the sample cohorts from: Addenbrookes hospital in Cambridge; the Hammersmith and North Middlesex hospitals in London; and Groote Schuur Hospital in Cape Town, South Africa. In addition, the Finnish samples provided by Lauri Aaltonen with known 7q LOH and used in chapter 6 were also analysed using the arrays. Samples were grouped into four categories of ethnicity: African/Afro-Caribbean; Caucasian; Other, for all other ethnicities where defined; and unknown.

All samples were confirmed as uterine leiomyomas by pathologists at each location and DNA from each of these samples was prepared as described in Chapter 2 (2.2)

8.2.2 Loss of heterozygosity analysis of sporadic uterine leiomyomas

An initial screen of all the leiomyoma samples bar those from Finland, was carried out by loss of heterozygosity (LOH) on 7q as described in Chapter 2 (2.7). Details of the markers used are shown in **Table 8.1**. Markers were chosen to be of greater density in the two regions of 7q deletion observed in Chapter 6. Samples showing LOH were used for subsequent 7q microarray CGH analysis. Where no matched normal DNA was available, samples with a stretch of apparent homozygosity covering at least three consecutive markers were used.

8.2.3 Tiling path microarray CGH analysis

Samples fulfilling the above criteria were used for microarray CGH analysis using the 7q tiling-path microarray. Hybridisation and data analysis were carried out as described in Chapter 2 (2.13.22.11.1) with the adaptations specific for the 7q array described in Chapter 7 (7.3.2.1).

8.2.4 Gene screening

Screening of the 2 genes in the minimal region, *MLL5* and *SRPK2*, was carried out by an initial high resolution melting screen comparing tumour DNA to normal DNA, as described in Chapter 2 (2.5.2). Samples showing differences between the tumour and normal were then sequenced as previously described (2.6). Primer sequences and conditions are shown in **Table 8.2**.

Table 8.1 Markers used for LOH analysis of uterine leiomyomas.

Marker	Chromosome Band	Chromosome Position (From UCSC)	Forward Primer	Reverse Primer	Dye	Size range	PCR program
D7S820	7q21.11	83627317	CCAATATTTGGTGCAATTC	CCTTAAAATCTGAGGTATC	FAM	102	EJ55
D7S527	7q21.3	95453002	CATTGCAAACTCAGGAGATA	TAACAGAGGCATGAAAACCA	HEX	273-297	EJ55
D7S518	7q22.1	101648938	CAGTAGGCAGGGGTGG	GGGTGTGTCTGTGTGACAAC	FAM	179-201	EJ55
D7S1799	7q22.1	103982142	ATGGTATTAGGAGATGGGGC	TTGCATAAGCCAATTTCCAT	TET	175-187	EJ55
D7S2545	7q22.2	104504348	TTTAGTATCTGGNCTTACGG	ACCGTTAAACAGCAGTTTCTA	TET	119-133	AR55
D7S501	7q22.3	106227602	CACCGTTGTGATGGCAGAG	ATTTCTTACCAGGCAGACTGCT	FAM	163-179	EJ55
D7S2420	7q22.3	106677054	CCTGTATGGAGGGCAAACTA	AAATAATGACTGAGGCTCAAAACA	HEX	240-292	EJ55
D7S2459	7q22.3	107118716	AAGAAGTGCATTGAGACTCC	CCGCCTTAGTAAAACCC	TET	140-152	AR55
D7S2456	7q31.1	107470364	CTGGAAATTGACCTGAAACCTT	ACAGGGGTCTCTCACACATATTA	FAM	238-252	AR55
D7S692	7q31.1	108126758	CTGATGATTGCTATAGATATTCATC	TGTAAACACTTTTGTAGAAGAACCT	TET	161-171	EJ55
D7S2418	7q31.1	109765961	AATTGGAAGCAGGTGTATGTG	TCCATAATCGCATGAGTGAT	HEX	166-178	EJ55
D7S471	7q31.1	111824585	AGCAGCTATTATGGAATTGC	CAACATATGCAAGGTGCCTA	HEX	181-199	EJ55
D7S1804	7q32.3	131930139	TTCAAGTGGTTGGGTTCACT	TGGGTCTAGTCCAGTGGTGT	FAM	250-290	EJ55
D7S2202	7q34	139427840	TCTCTTACCCTTTGGGACCT	CTTGCAGATGGCCTAATTGT	HEX	149=169	AR55
D7S2513	7q34	141053887	GCAGCATTATCCTCAACAGC	CACAAATGGCAGCCTTTC	FAM	157-181	EJ55
D7S661	7q35	143232828	TTGGCTGGCCCAGAAC	TGGAGCATGACCTTGGAA	FAM	252-282	AR55

Table 8.2 Primer sequence and conditions for DNA primers for screening MLL5 and SRPK2. All PCR reactions were carried out with 1.5mM $MgCl_2$, 5% DMSO, and 1x LC-Green reagent. Details of the PCR programs can be found in Chapter 2 (2.3.2.1).

Primer Name	Primer Sequence	Product Length	PCR program
MLL5x1F	CTTCATCCCCTCCCCCTCT	468bp	AR55
MLL5x1R	AACTCCCATGGAGACGACAG		
MLL5x2F	TTGGCTGCTTTGTGTGAGTC	223bp	AR55
MLL5x2R	TGGCAGCCATTAAAGAAATAA		
MLL5x3F	TGCCCCAGTGTTTTGGATAC	210bp	AR55
MLL5x3R	CTTCTTCCTACTTTCTAGCTCCAG		
MLL5x4F	TTTGTATAGCCATTATTTTGCTGTAAG	314bp	AR55
MLL5X4R	TTCAAACATGCCGTTTCAAG		
MLL5X5F	TTTAAGTTGCTTGGTTTATATCATTG	362bp	EJ55
MLL5X5R	CAACATTACCAAAGGTTATCAGC		
MLL5X6F	GGAGTACTAAGCTCAAAGTAGGTGCT	233bp	AR55
MLL5x6R	AAAATTACTGGCAATGTTATCAGA		
MLL5x7F	AAACTGTATTGCAAGGGATTTTG	329bp	AR55
MLL5x7R	CAATCAACATTCATCAACAAGG		
MLL5x8F	AAAGATGGAGACGACAATACTTTG	331bp	EJ55
MLL5x8R	AAATTCAGTTCCCTATCCGC		
MLL5x9F	TCTCCTAGTGTCAGCTTTCTTGG	325bp	EJ55
MLL5x9R	GAACTAAGGTCCCACTCCTGG		
MLL5x10F	CCGTAAGTCCAGATACTAAAGCTCA	297bp	EJ55
MLL5x10R	CAATTTTTGGACAAATGATGTATT		
MLL5x11F	TCCTGTAGAGGTAAATACATCATTTG	328bp	EJ55
MLL5x11R	TCACAACATCTAGGTAAAACAGCC		
MLL5x12F	GCCCGGCCTAAAATGTTAAT	225bp	EJ55
MLL5x12R	TGCTCAGATTCCAACACACC		
MLL5x13F	TTTTCCAGGTTGTGTTTGTG	303bp	EJ55
MLL5x13R	TGACAATACCTAAATTATTACAGGGAC		
MLL5x14F	TGGAGTTGCAGCTTAAAATGG	578bp	EJ55
MLL5x14R	TTGTCTGCAATTCTGCAAGG		
MLL5x15F	GGCTGTGTACATGTTGAATTTG	292bp	EJ55
MLL5x15R	AAAAGCCCATGTAAAGGCAG		

MLL5x16F	TTTTCTCCCCATATCCACC	451bp	EJ55
MLL5x16R	GCTGAAACTCCCATAGGATCTG		
MLL5x17F	TTCCATTCGCTTGTATTTTGA	374bp	EJ55
MLL5x17R	CTGTTAGAAAAACAGTTCTTACATTCA		
MLL5x18F	TTCAAGGGAGAATTTGGAATTA	368bp	AR55
MLL5x18R	AGGAATGAGTTGGCATTTGG		
MLL5x19F	AAATGCTTTTGGAATCGGC	304bp	EJ55
MLL5x19R	TGCCTGTTATAAAGCTGTATGTATG		
MLL5x20F	TGGGGTAAAAGTCATAACTGCC	451bp	EJ55
MLL5x20R	TGTTAAAGGAGGGGAAAGAGC		
MLL5x21F	CAGTCTTATTTGGGGAATGG	308bp	EJ55
MLL5x21R	TCACATCTTGGGACTGTTTATTTC		
MLL5x22aF	AATTTTGAAATAAACAGTCCCAAG	426bp	AR55
MLL5x22aR	TGTCAGGTCCCTCAAGTTGG		
MLL5x22bF	CTGAGCCCAACAGCCAAC	413bp	EJ55
MLL5x22bR	AATACATCTAACAATTCCCCTCAG		
MLL5x23F	AAAAGAATGCATTGGTTCTGAC	440bp	EJ55
MLL5x23R	CCTTGGGAGAACAACAAATAGG		
MLL5x24-25F	TTTTCCCAGTAGATCAAAAGCC	558bp	AR55
MLL5x24-25R	AACACTGTTTTAACACCACAAAGC		
MLL5x26F	GAATGTATGTTGCTTTGTGGTG	238bp	EJ55
MLL5x26R	CAGCTTTTCTGCACTCAACC		
MLL5x27aF	AGGATGTTATTTCCTGCCCC	581bp	EJ55
MLL5x27aR	ATTGGCTGGAAGGTTCTGTG		
MLL5x27bF	CACCAAAGCCTCCTTCACAG	481bp	AR55
MLL5x27bR	ACTACGGCAGCAGCAGTTTG		
MLL5x27cF	ACCACAAGCCAGCAAACAG	470bp	EJ55
MLL5x27cR	AGTGGAGGTCCTTGATGAGG		
MLL5x27dF	ATCCACAGGACTCCAAGGTC	625bp	EJ55
MLL5x27dR	AAAATACAACGAAAGAGCACTGG		
SRPK2x1F	GCAGGCAATCTTGGTTGTG	165bp	EJ55
SRPK2x1R	CCTGGTTTGTTTCTTAGCAATG		
SRPK2x2F	CAAATGCATCCATAATGCAAGA	296bp	EJ55
SRPK2x2R	TCCATTCCCCCAACAAATTA		
SRPK2x3F	TGACATCAAGAATGACAAAAGAGA	234bp	EJ55
SRPK2x3R	TCCAGGAAACAAATGCACAA		
SRPK2x4F	CCCAGCCAAACTTGACTTTA	279bp	AR55
SRPK2x4R	CCAATTAGGGATGCTCAACCT		

SRPK2x5F	TTTAAACAGTATTGGTGTTATAATGGG	274bp	EJ55
SRPK2x5R	TTTATGTTGAAGGTGATACAGCAG		
SRPK2x6F	AACTGCCTCACTCCAGGC	371bp	AR55
SRPK2x6R	ATGTTGTTCCCTTCACAACAC		
SRPK2x7F	AACTTTGTACCCTGGCATTG	327bp	EJ55
SRPK2x7R	GCAACTTTGCAAGCTCCC		
SRPK2x8F	CCTACATGAAGGCATGTGTCTG	156bp	EJ55
SRPK2x8R	TTGAACAACTCAATAATAAACGGTC		
SRPK2x9F	ATTGCTATTTGCCATGCTGC	403bp	EJ55
SRPK2x9R	TTGACCTGGCAGAACCCTAC		
SRPK2x10aF	ACAGGGCTTGGCCACTTC	499bp	EJ55
SRPK2x10aR	CGAACATAGACCCTACGTGGA		
SRPK2x10bF	CACTTTCTGCATTTGGCTCA	385bp	AR55
SRPK2x10bR	TTTTACCCCAAAAGCCAAGA		
SRPK2x11-12F	CACATGCAAACCACCTATCC	452bp	AR55
SRPK2x11-12R	GAGTGTGAAAGGAACGAGCC		
SRPK2x13F	AAAAGCTGTTGACTTGGGG	194bp	AR55
SRPK2x13R	TACAGAAGTTCAGGGCTGGC		
SRPK2x14F	TTTATCCCATCCTTCCCTTTG	213bp	AR55
SRPK2x14R	GCAGCTGCTCTTCAGTTTCTG		
SRPK2x15F	CACCGTTTAGGTCCAATGTACT	300bp	AR55
SRPK2x15R	GGAATGCAGATTTGGAGCTT		

8.3 Results

8.3.1 LOH analysis of samples

LOH analysis was carried out on a total of 227 leiomyoma samples from 178 patients. Of these samples, there were 22 leiomyomas from 21 Caucasian patients; 56 leiomyomas from 32 African or Afro-Caribbean patients; 75 leiomyomas from 52 patients of other ethnicity; and 74 leiomyomas from 73 patients of unknown ethnicity.

An example of LOH at one marker is shown in **Figure 8.1**. In total, 14 samples showed LOH of at least one marker, where matched germline DNA was available (**Figure 8.2**). The minimum region of LOH was defined by samples FG103 and FG121, between markers D7S2545 and D7S501, a region of 1.72Mbp. These markers were consecutive in the marker set used, and so no single marker showed LOH in all samples. In addition, 2 samples without matched normal DNA (200173E and 200050A) showed stretches of apparent homozygosity greater than 3 markers long. No evidence of contaminating normal was observed in these samples. One final sample (200062B) showed LOH compared to another leiomyoma sample from the same patient. Therefore, 17/227 (7.5%) of all samples had 7q LOH or indications of LOH. This matched the frequency of LOH observed in the Finnish samples (12/165 (7.3%) of samples). These samples were subsequently analysed by microarray CGH using the 7q tiling-path array.

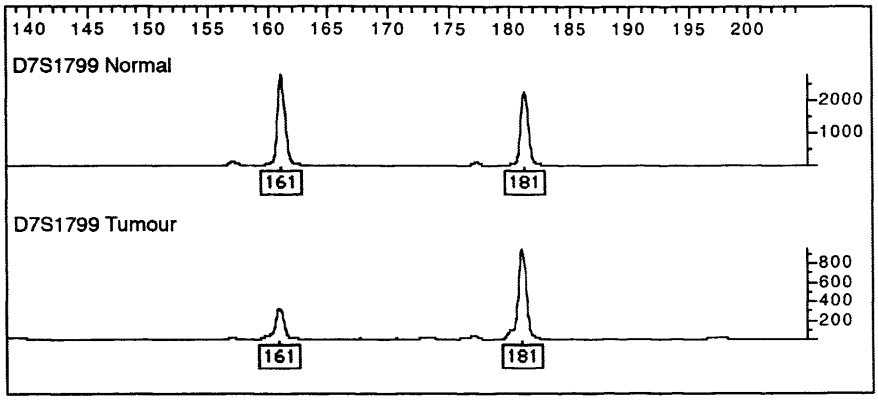

Figure 8.1 Example of LOH at marker D7S1799 in sample FG145 F2. The tumour sample has lost almost all of allele 161. However, a residual peak remains indicating some contamination of normal material.

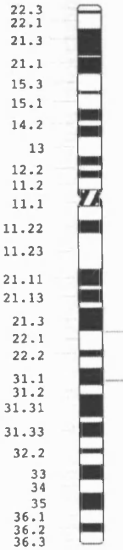

Marker	Positiion	FG129	FG145	FG153	FG156 F1	FG156F2	TB02 0339	TB02 0473	FG21	FG30	FG48	200050A	200062B	200173E	TB03 0358	TB030413	FG103	FG121
D7S820	83627317	NI	NI	NI	NI	NI			NI	NI	NI	NI	NI	NI	NI	NI	NI	NI
D7S527	95453002		-	-	LOH	LOH	LOH	LOH	-	LOH	LOH	LOH	-	NI	NI	LOH	-	LOH
D7S518	101648938	LOH	LOH	LOH	LOH	LOH	LOH	NI	LOH	-	LOH	NI	-	NI	-	LOH	-	LOH
D7S1799	103982142	-	LOH	LOH	LOH	LOH	LOH	LOH	NI	NI	LOH	NI	LOH	NI	LOH	LOH	-	LOH
D7S2545	104504348		LOH	NI	LOH	LOH	LOH	NI	LOH	-	LOH	NI	LOH	NI	LOH	NI	-	LOH
D7S501	106227602		LOH	LOH	LOH	LOH	LOH	LOH	LOH	-	LOH	NI	LOH	NI	LOH	LOH	LOH	-
D7S2420	106677054			LOH	NI	NI		NI	-	-	NI	NI	LOH	NI	LOH	LOH	NI	NI
D7S2459	107118716	-	LOH	NI	NI	NI	LOH	NI	LOH	LOH	LOH	NI	LOH	NI	NI	LOH	NI	NI
D7S2456	107470364	-	LOH	LOH	LOH	LOH	LOH	LOH		LOH	LOH	NI	LOH	NI	LOH	NI	LOH	NI
D7S692	108125758			LOH	LOH	LOH			-	-	NI	-	LOH	NI	-	LOH	LOH	NI
D7S2418	109765961		LOH	-	LOH	LOH	LOH	NI	-	NI	NI	-	LOH	NI	NI	LOH	NI	NI
D7S471	111824585	NI	LOH	-	LOH	LOH	LOH	LOH	-	NI	LOH	NI	LOH	NI	LOH	LOH	-	NI
D7S1804	131930319	LOH	-	-	-	-	-	LOH	-	-	-	-	-	-	-	-	-	NI
D7S2202	139427840		-	NI	-	-	-	NI				-	NI	-	-	-	LOH	NI
D7S2513	141053887	NI	-	NI	-	-	-	LOH	NI	LOH	-	-	-	-		-	LOH	NI
D7S661	143232828	-	-	-	-	-	-	LOH	-	NI	-	-	-	NI	-	-	LOH	NI

Figure 8.2 Summary of sporadic uterine leiomyomas with LOH on chromosome 7q. (LOH) – loss-of-heterozygosity at this marker, (NI) – marker was non-informative; (-) – no LOH was seen at this marker; ( ) – marker not done for this sample. Samples without a normal tissue reference, but with more than 3 consecutive homozygous markers were considered as having LOH. A minimum region of loss was defined by samples FG121 and FG103, between markers D7S2545 and D7S501, a region of 1.73Mbp.

8.3.2 Tiling path resolution microarray CGH

The 17 samples with LOH of 7q and 9 of the 12 Finnish samples with known 7q LOH provided by Lauri Aaltonen were analysed by tiling-path microarray CGH. In addition, the results of the hybridisations of the Awaki and F9CR cell lines used to test the array in the previous chapter were added to the results of the other hybridisations. A further 22 samples with no 7q LOH or regions of homozygosity were analysed to identify small deletions that may occur below the resolution of the microsatellite markers.

Of the samples with 7q LOH, 27/28 showed detectable copy number changes of chromosome 7q (**Figure 8.2**, **Table 8.3**). One experiment, on tumour FG129 F2, failed to produce an adequate hybridisation. Of the 22 samples without 7q LOH that were analysed, only one sample, TB03 0356, showed a discrete deletion of 7q. This deletion occurred in a region that was covered by the markers, although there was no evidence of LOH. The remaining 21 samples with no 7q LOH showed no copy number changes.

A majority of the observed copy number changes were deletions. However one sample, FG103, showed a copy number gain of part of the chromosome arm, followed by deletion of the end of the chromosome arm (Figure 8.3). In addition to this sample, 3 further samples, 29M2, 14M4 and FG30, also had multiple copy number changes, all deletions (**Table 8.3**, **Figure 8.5**). No samples demonstrated changes indicative of homozygous deletion, which was considered if the log2 ratio was less than -1.

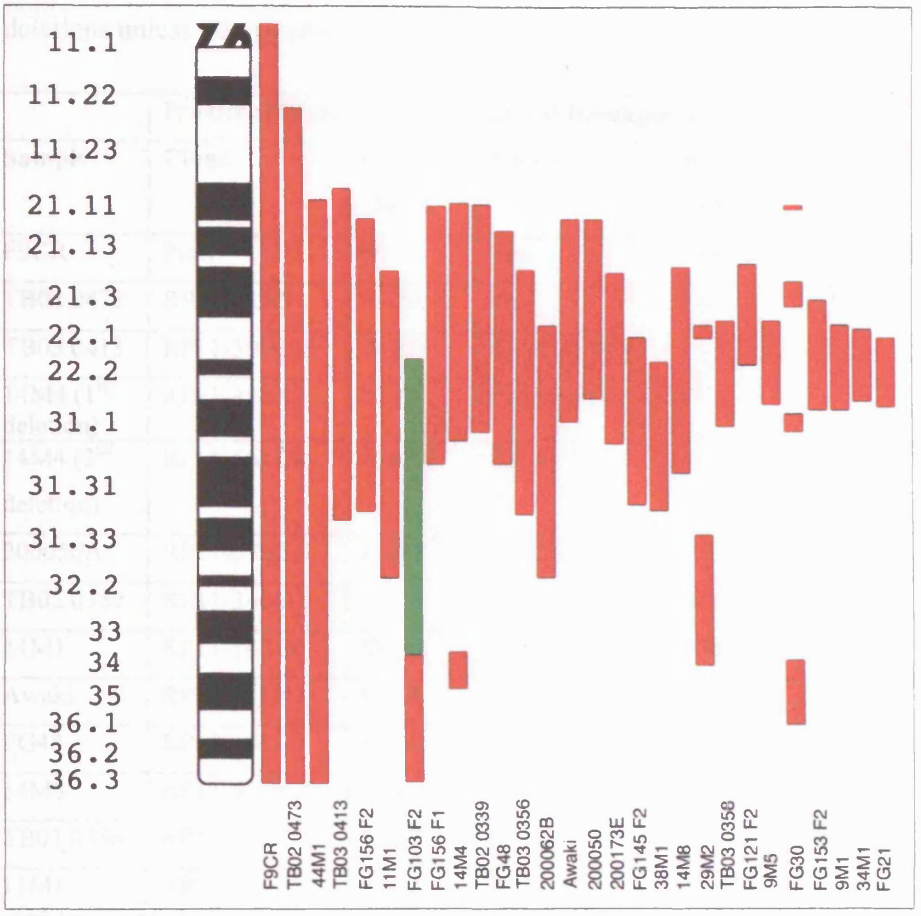

Figure 8.2 Ideogram of copy number changes identified on chromosome 7q in sporadic uterine leiomyomas. Red bars indicate regions of copy number loss, and green bars represent regions of copy number gain.

Table 8.3 Results of chromosome 7q tiling path array CGH. All changes are deletions unless otherwise specified.

	Proximal Breakpoint[1]		**Distal Breakpoint**[1]		
Sample	**Clone**	**Position**[2] **(Mbp)**	**Clone**	**Position**[2] **(Mbp)**	**Size (Mbp)**
F9CR	Pcen	60	pter	158.82	Whole arm
TB02 0473	RP11-32N3	71.70	pter	158.82	87.11
TB03 0413	RP11-390C15	78.80	RP11-618G22	123.74	44.95
14M4 (1st deletion)	RP11-448A3	81.35	RP11-135K23	115.31	33.97
14M4 (2nd deletion)	RP11-561D8	139.33	RP11-177L17	144.29	4.96
200050A	RP11-575G1	81.56	RP11-443I10	107.29	25.73
TB02 0339	RP11-240I3	82.32	RP11-488K2	114.48	32.17
44M1	RP11-142G6	82.64	pter	158.82	76.18
Awaki	RP11-313H6	83.64	RP11-259H24	112.28	28.64
FG48	RP11-493G7	88.06	RP11-398D9	118.63	30.57
14M8	RP11-467N23	92.45	RP11-544C1	110.58	18.13
TB03 0356	RP11-78F12	93.37	RP11-746L19	123.04	29.68
11M1	RP11-78F12	93.37	RP13-750I6	129.75	36.38
200173E	RP11-82B2	94.46	RP11-760I10	115.54	21.08
9M5	RP11-802H13	98.47	RP11-139J13	107.88	9.41
TB03 0358	RP11-694E14	98.66	RP11-786A20	112.88	14.21
34M1	RP11-487B17	99.56	RP11-649H20	107.47	7.91
200062B	RP11-487B17	99.56	RP11-643O2	129.12	29.56
9M1	RP11-443E21	99.80	RP11-18H15	107.98	8.18
FG21	RP11-484K16	100.70	RP11-649H20	107.47	6.77
FG103 F2 (Gain)	RP11-753M2	104.54	RP11-416H18	140.10	35.56
FG103 F2	RP11-661B8**	140.10**	qter	158.82	18.73
FG121 F2	RP11-467N23	92.45	RP11-708P17*	104.78*	12.33

	Proximal Breakpoint[1]		Distal Breakpoint[1]		
Sample	**Clone**	**Position[2] (Mb)**	**Clone**	**Position[2] (Mb)**	**Size (Mb)**
FG156 F1	RP11-39H7	82.01	RP11-417K19	117.94	35.93
FG30 (1st deletion)	RP11-115M02	83.60	RP11-750F10	84.08	0.48
FG30 (2nd deletion)	RP11-82B2	94.46	RP11-321E18	96.92	2.47
FG30 (3rd deletion)	RP11-382F18	111.48	RP11-274E22	113.85	2.37
FG30 (4th deletion)	RP11-661B8**	140.10**	RP11-318D10	149.20	9.11
FG145 F2	RP11-163E9	101.86	RP11-651N9	120.83	18.97
FG153 F2	RP11-610J1	95.93	RP11-206A4	108.24	12.30
FG156 F2	RP11-555E22	86.02	RP11-568I11	126.93	40.92
38M1	RP11-434M1*	104.51*	RP11-746L19	123.04	18.66
29M2 (1st deletion)	RP11-487B17	99.22	RP11-617P22	102.07	2.85
29M2 (2nd deletion)	RP11-519O11	124.95	RP11-203I13**	141.61**	16..66

*Indicates clones delimiting the minimal region of deletion of 7q22.2

**Indicates clones delimiting the minimal region of deletion of 7q34

[1]Breakpoint clones are the first clones not considered deleted, flanking the region of deletion

[2]Positions are defined as the position of the end of the breakpoint clone closest to the deletion. Positions were obtained using the Ensembl and UCSC genome browsers and data from the NCBI clone registry.

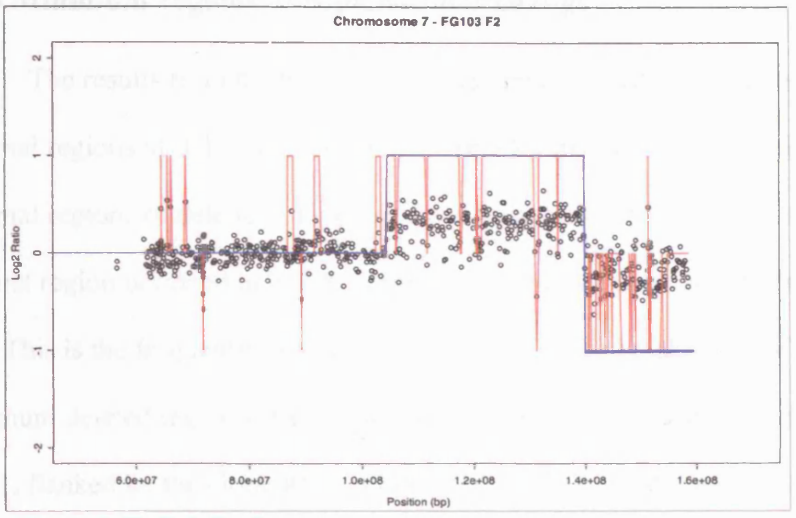

Figure 8.3 Result from sample FG103 showing copy number gain of 7q, followed by a terminal deletion. The red line indicates the call from the R-based analysis program, and the blue line is the called change smoothed by eye. The proximal breakpoint of the amplification is identical to the proximal breakpoint of the minimal region of deletion of 7q22.2, and the distal breakpoint of the amplification is identical to the proximal breakpoint of the minimal region of deletion at 7q34.

8.3.3 Minimum regions of copy number change

The results from the microarray CGH demonstrated a number of minimal regions of deletion in sporadic uterine leiomyomas. In particular, 2 minimal regions of deletion of chromosome 7q were identified. Deletion of the first region occurred in 26/28 samples with detected deletions (**Figure 8.4**). This is the frequently reported region of 7q22. The breakpoints of the minimum deleted region were defined by two samples: proximally by sample 38M1, flanked by the clone RP11-434M1 (104.51kb); and distally by sample FG121, flanked by clone RP11-708P17 (104.78kb). This deletion spans a single clone (RP11-753M2) on the array, a distance of approximately 271kb, and contains only 2 genes: the 3' end of Mixed Lineage Leukaemia gene 5 (*MLL5*); and serine/arginine-specific Protein Kinase 2 (*SRPK2*) (**Figure 8.4**b).

In addition to the observed minimal region of deletion, one final sample gave a further clue to the identity of the involved gene. Sample FG103 was unusual in that it contained an amplification of 7q (Figure 8.3). The breakpoint of this amplification at 7q22 occurred at clone RP11-753M2, the one commonly deleted clone in the minimal region. The proximal end of this clone occurs within the final intron of the *MLL5* gene (**Figure 8.4**b). The potential disruption of a single copy of *MLL5* by this amplification could implicate it as the gene of interest. This assumes that the amplification disrupts the gene in the first place.

The second minimal region of deletion, at 7q34, was detected in 7/28 samples, but was observed discreetly in only 4 samples, and only where more than one copy number change occurred on 7q (**Figure 8.5**). This region was flanked proximally in sample FG30 by clone RP11-661B8 (140.10Mb); and

distally in sample 29M2 by clone RP11-203I13 (141.61Mb), a region of 1.51Mb.

Four other small discrete regions of deletion were observed, all in samples with a deletion involving 7q34 (**Figure 8.2**, **Figure 8.5**a): three deletions, of 0.48, 2.47 and 2.37Mb, in sample FG30; and a 2.85Mb deletion in sample 29M2. These regions are shown in **Figure 8.6**. The deletion in 29M2 was also observed as a single clone deletion by 1Mb resolution CGH in Chapter 6.

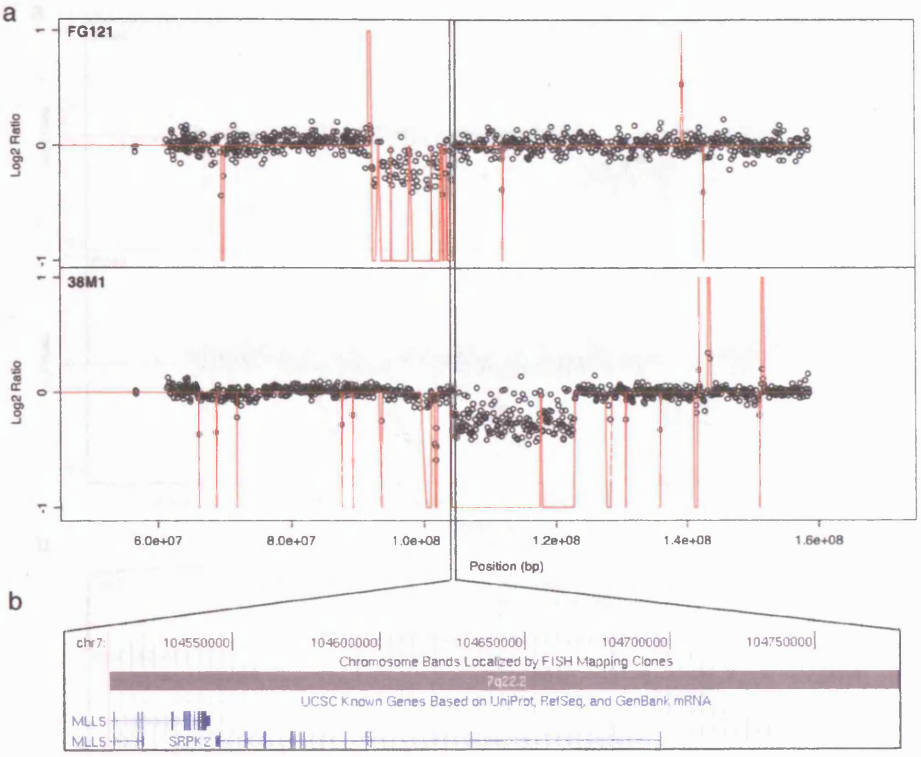

Figure 8.4 a) The minimum region of deletion in 7q22 is defined by samples 38M1 and FG121, occurs in 26/28 samples with 7q deletions. b) This region of deletion spans a single clone (RP11-753M2) and contains one whole gene (*SRPK2*) and the 5' end of another (*MLL5*).

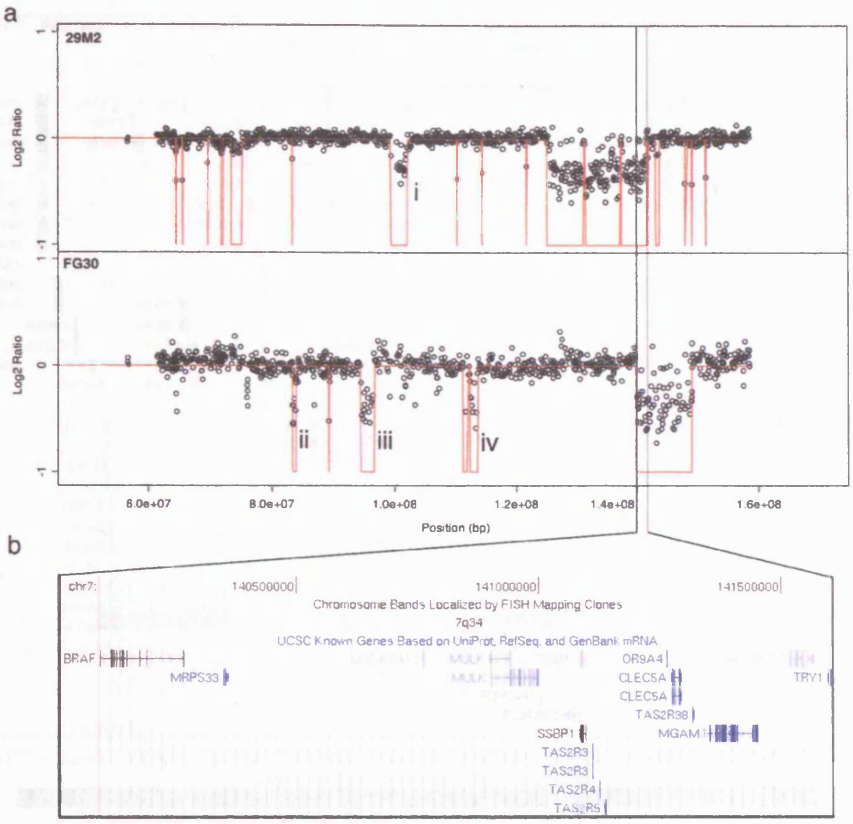

Figure 8.5 a) The minimal region of deletion of 7q34 as defined by samples 29M2 and FG30 spans a region of 1.51Mb. This region (b) contains 16 genes. These two samples demonstrate four further unique regions of deletion (i - iv), more detail of which can be found in (Figure 8.6).

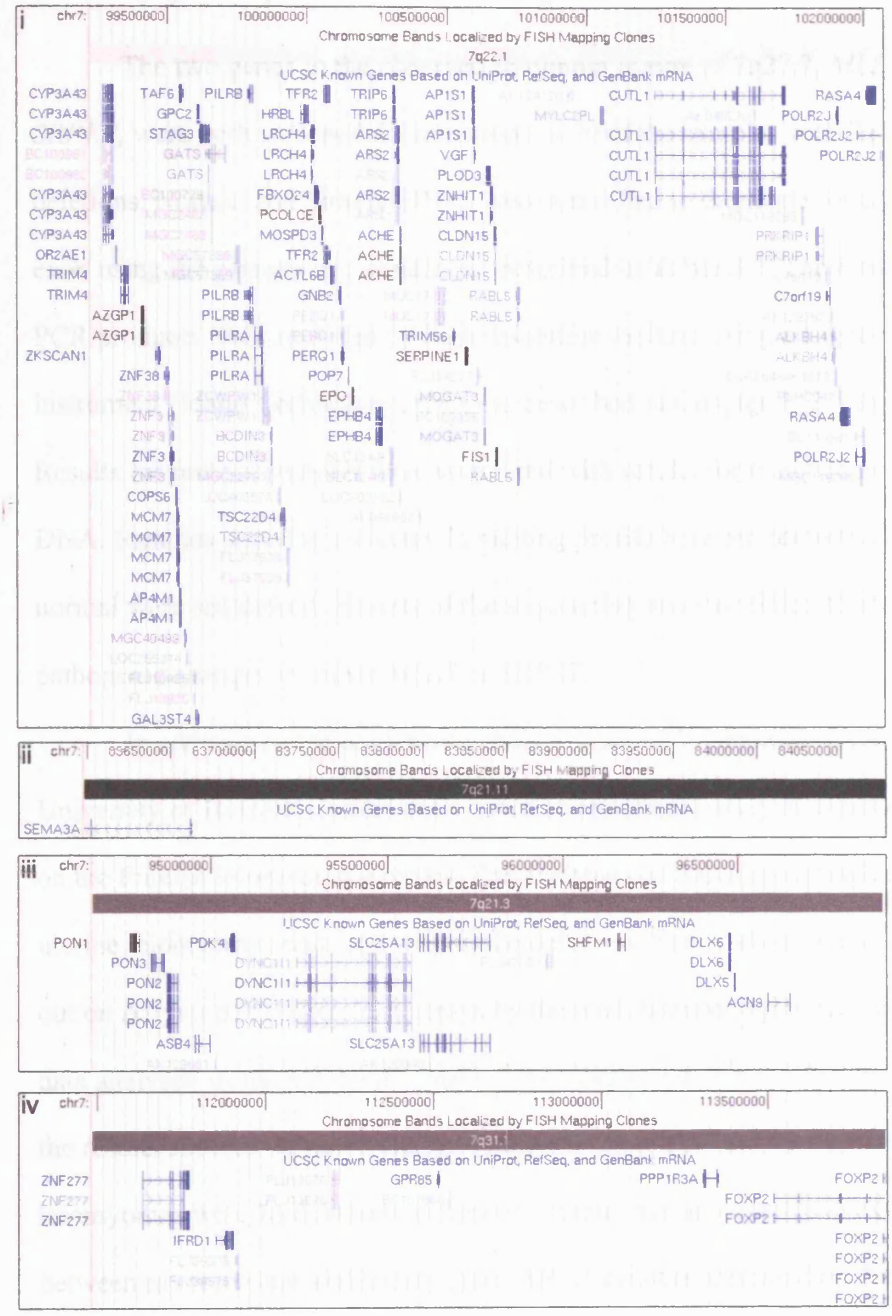

Figure 8.6 Genes in the small regions of deletion in samples 29M2 (i) and FG30 (ii, iii and iv).

8.3.4 Analysis of potential candidate genes

The two genes in the observed minimum region of 7q22.2, *MLL5* and *SRPK2,* were both screened for mutations in 10 of the samples with 7q deletions. Normal and tumour DNAs were amplified in duplicate for each exon using the primers and conditions described in **Table 8.2**. The resulting PCR products were analysed by high resolution melting using a Lightscanner instrument (Idaho Technology, USA) as described in Chapter 2 (2.5.2). Results for tumour samples were compared with results for matched normal DNA. Samples showing a change in melting profile between tumour and normal were sequenced. Results of the sequencing analysis failed to show any pathogenic changes in either *MLL5* or *SRPK2*.

In addition to the sequencing analysis, Sakari Vanharanta at the University of Helsinki carried out a series of expression analysis experiments on the Finnish leiomyoma samples. The analysis compared myometrium with uterine leiomyomas with and without 7q deletions. The analysis was carried out on Affymetrix HG-U133A arrays by the manufacturer's protocol and the data analysed using Affymetrix MAS 5.0 software and dChip 1.3. Analysis of the results showed neither a change in the expression of *SRPK2* between leiomyomas with 7q deletions and those without, nor any change in expression between myometrium and leiomyomas. *MLL5* is not represented on the HG-U133A arrays.

8.3.5 Ethnic distribution of del7q deletions

Disregarding the Finnish and cell line samples, 227 samples were screened for LOH of 7q, and 18 samples were found to have deletions of 7q. Of these, 5 were from patients of African and Afro-Caribbean ethnicity, 2 were from Caucasian patients, 6 were from patients of other (neither African/Afro-Caribbean or Caucasian) ethnicity, and 5 were from patients of unknown ethnicity. Fisher's exact test was used to compare the frequency of 7q deletions in African and Afro-Caribbean patients with that of Caucasian patients, and with that of non-African/Afro-Caribbean patients. Both comparisons showed no significant difference in the frequency of del(7q) between Caucasian and African/Afro-Caribbean patients (p=1, two-tailed Fisher's exact test), or between African/Afro-Caribbean patients and all other patients (p=0.770, two-tailed Fisher's exact test) (**Table 8.4**).

Table 8.4 Distribution of observed LOH by ethnicity

Ethnicity[a]	**Total Samples**	**Samples with del(7q)**	**Proportion with del(7q)**	**Median age of patients with del(7q)**
African/Afro-Caribbean	56	5	8.9%	31
Caucasian	22	2	9.1%	50.5
Other[b]	75	6	8%	47
Unknown	74	5	6.8%	51

[a]Ethnicity self-reported by questionnaire

[b]Includes samples from Asian and mixed-race patients.

8.4 Discussion

Deletions of chromosome 7q are a relatively frequent event in sporadic uterine leiomyomas. They are estimated to occur in approximately 17% of karyotypically abnormal uterine leiomyomas, or 7% of all leiomyomas (Xing et al. 1997). The data in this chapter have demonstrated a frequency by LOH of 7.5%, a result corroborated by the LOH results for the Finnish samples. For most of the samples in this study, LOH was caused by deletion, however, in one case it resulted from copy number gain. Furthermore, one sample with no LOH demonstrated a deletion when analysed by microarray CGH. This may have been indicative of loss of 2 copies from a triploid genome. It may also support the proposal in Chapter 6, questioning the reliability of LOH studies as a reliable means of identifying deleted regions of 7q in leiomyomas, or any tumour. Given that one sample without 7q LOH still showed a deletion, it was possible that other samples with 7q deletions were excluded from CGH analysis because LOH was not observed in these tumours.

The increased resolution of the CGH array used in this study allowed a detailed study of 7q deletions, ultimately demonstrating a minimal region of deletion of ~273kb in 7q22.2. To date, this is the smallest common region of deletion identified, and the two genes in this region are the strongest candidates for the elusive tumour suppressor. Furthermore, several alternative regions of deletion of 7q have been identified, most notably at 7q34, which may provide interesting clues to other pathways involved in leiomyoma tumorigenesis.

8.4.1 *MLL5* or *SRPK2* as the gene associated with uterine leiomyomas on 7q22.2

The minimum region of deletion of 7q22.2 consisted of a single clone deletion, which occurred in 26/28 samples demonstrating 7q deletions. This region contains one complete gene (*SRPK2*) and the 3' end of a second gene (*MLL5*). To date, neither of these genes have been proposed as candidates for the 7q tumour suppressor gene. Unfortunately, sequence analysis of these genes failed to identify any pathogenic changes in the exons of either gene. Therefore, either gene is potentially involved.

Since no coding mutations were identified in either of these two genes, it remains plausible that haploinsufficiency could be an important factor in leiomyoma pathogenesis. With *SRPK2*, the information from expression microarray experiments does not suggest that this is the case. However, no such work has been carried out on *MLL5* and it would be important to examine the expression of this gene with respect to both normal myometrium and uterine leiomyomas without 7q deletions. In order to greater assess the potential role of these two genes, a study of published literature was carried out. In particular, the potential for each gene to act as a tumour suppressor, as has been previously proposed by some groups (Ishwad et al. 1995), or to negatively affect cell growth, as proposed by others (Xing et al. 1997), was assessed.

8.4.1.1 Mixed-lineage leukaemia 5 (*MLL5*)

To date, little work has been carried out on *MLL5*, and only two papers exist devoted exclusively to this protein (Emerling et al. 2002; Deng et al.

2004). However, the work in these papers, and studies of related proteins make this a particularly strong candidate tumour suppressor. *MLL5* is a homolog of the *Drosophila* trihorax gene. Trithorax-family genes modulate transcriptional programs through protein-protein interactions involving PHD and SET domains (Emerling et al. 2002). It was originally identified as a novel gene in a 2.5Mb commonly deleted region of 7q22 in myeloid leukaemia with a high homology to other MLL-family genes (Emerling et al. 2002), the founder member of which, MLL, is involved in recurring translocations with more than 30 partner genes in acute myeloid leukaemia (Armstrong et al. 2002; Emerling et al. 2002).

A functional study carried out by Deng *et al* found that MLL5 is a nuclear protein that forms intranuclear foci. Since MLL5 contains no DNA binding domain, these foci were the result of protein-protein interactions. These foci did not co-localise with other proteins that form intranuclear foci, such as BRCA1, Rad51, Bmi-1 and PCNA. In addition, cells transfected with MLL5 resulted in cell cycle arrest at the G1 phase, implying a role as a potential tumour suppressor (Deng et al. 2004). The related protein MLL-1 has also been shown to form nuclear foci and, interestingly, has been shown to interact with the protein Menin, encoded by the Multiple-endocrine neoplasia 1 gene (*MEN1*) (Yokoyama et al. 2005).

8.4.1.2 Serine/Arginine-specific protein kinase 2

The *SRPK2* gene encodes a serine protein kinase responsible for the phosphorylation of SR proteins, which are involved in spliceosome formation (Wang et al. 1998). Like *MLL5*, little has been specifically published on the function of this protein, but more has been published on the homologous

SRPK1. Both kinases appear to have an important role in spliceosome assembly and disassembly, and overexpression of SRPK2 has been shown to disassemble nuclear speckles, thought to be locations of spliceosomes, containing the SR proteins SF2/ASF and SC35 (Kuroyanagi et al. 1998; Wang et al. 1998).

Both SRPK1 and SRPK2 are localised to the cytoplasm, despite both containing nuclear localisation sequences (Ding et al. 2006). It is thought that they are responsible for the import of SR proteins into the nucleus, since they are imported in a phosphorylation dependent manner (Yun et al. 2003). It has also been shown that SRPK1 and SRPK2 are transported to the nucleus at the G2/M boundary (Ding et al. 2006). The function of this transition is unclear but given that SRPK proteins appear to disassemble spliceosomes when overexpressed (Kuroyanagi et al. 1998; Wang et al. 1998), this transition could allow the disassembly of the spliceosomes prior to chromatin condensation at metaphase. Therefore, loss or reduction of expression or function may lead to a reduction in cell growth.

SRPK2 has also been implicated in viral pathogenesis. Both DNA and RNA viruses have been shown to hijack the cells alternative splicing machinery in order to produce the necessary proteins required for viral replication and packaging (Daub et al. 2002). A recent report demonstrated that increased expression of SRPK2 up-regulated expression of HIV in 293 cells. Pharmacological inhibition of SRPK2 had some effect on reducing HIV expression, but had a more potent effect on Sindbis virus (Fukuhara et al. 2006).

8.4.1.3 Conclusions from the literature

Uterine leiomyomas with deletions of 7q have been shown to be of a similar size, or slightly smaller than leiomyomas with no karyotypic abnormalities (Rein et al. 1991). Furthermore, they have been shown to be as susceptible to GnRH analogue treatment as karyotypically normal tumours (Takahashi et al. 2002). Finally, culture of leiomyoma cells with 7q deletions *in vitro* has shown that these cells grow more slowly than karyotypically normal cells, and are eventually selected out in culture (Xing et al. 1997). Therefore, the significance of 7q deletions in uterine leiomyomas remains unclear. If the involved gene is a tumour suppressor, perhaps loss of function protects the tumour not by conferring sex hormone independence or increasing proliferation, but maybe through immune evasion. From the literature, *MLL5* appears to have a clearer tumour suppressor function (Deng et al. 2004). However, the apparent growth disadvantage *in vitro* would suggest that 7q deletions are detrimental to cell growth, a role that suggest *SRPK2* as a better candidate due to its apparent role in allowing the cell cycle to progress into mitosis (Ding et al. 2006). Therefore, no clear candidate as yet emerges. Unfortunately, time failed to allow studies on the expression of *MLL5* or *SRPK2* using a more sensitive real-time PCR approach. These studies, and other *in vitro* studies of leiomyoma cell lines may help to identify the gene on 7q involved in uterine leiomyoma pathogenesis.

8.4.2 Novel regions of copy number change in 7q imply a distinct cytogenetic group of leiomyomas.

In addition to the frequently reported region of deletion of 7q22.2, further novel deletions of 7q were also observed. The most frequent of these was a deletion of 7q34, observed discretely in 4 samples. Interestingly, these deletions only occurred when at least one other copy number change of 7q was present. One of the limitations of array CGH is its inability to distinguish between individual chromosomes. Thus, it is uncertain whether the observed copy number changes occur on the same chromosome, or on one copy of each chromosome.

A search of the Mitelman database of chromosomal aberrations revealed that deletions of 7q34 have been reported infrequently in sporadic uterine leiomyomas (Mitelman et al. 2006). However, in several cases, inversions of chromosome 7 with a breakpoint in 7q34 have been reported, implying that this region may be a novel region involved in leiomyoma pathogenesis (Pandis et al. 1991). Interestingly, in 2 samples, the proximal breakpoints in the 7q34 deletion were identical, while the proximal breakpoint in a third sample was also very close to this region.

The four other small regions of deletion are found in samples with 7q34 deletions. One of these regions, in sample 29M2, was previously identified as a single clone deletion in the 1Mb resolution CGH array (See Chapter 6). This region (**Figure 8.6**i) contains 2 of the genes previously proposed as candidates for the 7q22 tumour suppressor gene, *PCOLCE (Ligon et al. 2002)*, and *CUTL1 (Zeng et al. 1997)*.

One of the three remaining small novel regions, all observed in sample FG30, contains part of a single gene, *SEMA3A* (**Figure 8.6**ii). This gene encodes the Semaphorin 3A protein, which is responsible for axon guidance in embryonic development (Polleux et al. 2000). It is also involved in vascular morphogenesis. Nonendothelial cells secrete Semaphorin to guide developing blood vessels through tissues by exhibiting a repulsive effect (Serini et al. 2003). Thus loss of expression would allow infiltration of microvessels, increasing tumour vascularity. It would be interesting to see if the original tumour sample from this patient was more vascular than other uterine leiomyomas, which are typically less vascular than the host myometrium (Poncelet et al. 2002; Pollard et al. 2005a).

The remaining two regions contain a number of genes, with a number of interesting candidates (**Figure 8.6**iii and iv). Interesting genes in the 7q21.3 deletion include: *PDK4* (Pyruvate dehydrogenase kinase 4), which modulates glucose metabolism by inhibiton of pyruvate dehydrogenase (Sugden and Holness 2003); and *ASB4*, which is thought to be involved in the degradation of the suppressor of cytokine signalling (SOCS) proteins (Kile et al. 2000). Genes in the 7q31.1 region include: *PPP1R3A* (Protein phosphatase 1 regulatory subunit 3A), polymorphisms of which are associated with diabetes mellitus (Chen et al. 1994); and *IFRD1* (Interferon-related developmental regulator 1), which is thought to be involved in regulating gene activity in response to NGF (Tirone and Shooter 1989).

The high frequency of copy number changes reported in uterine leiomyomas suggests that it is possible that the del(7q34) group of leiomyomas are a distinct cytogenetic group from those with deletions of

7q22.2. Whereas the del(7q22.2) group contain single deletions with the common deleted region at 7q22.2 containing *SRPK2* and *MLL5*, the del(7q34) group contain two deletions, a deletion around 7q34, and a further deletion elsewhere on 7q.

8.4.3 Ethnicity and deletions of chromosome 7q

One part of this study involved studying the ethnic distribution of samples with 7q LOH. Of the 227 leiomyoma samples used in this study, 153 were from patients who had reported their ethnicity. Stratification of the samples revealed a near identical frequency of 7q LOH in Caucasian and African/Afro-Caribbean patients. A comparison of non-African/Afro-Caribbean with African/Afro-Caribbean patients also revealed no change in the frequency of 7q LOH.

The higher frequency and lower age of onset of symptoms of African and Afro-Caribbean women with multiple uterine leiomyomas (Marshall et al. 1997) would seem suggestive of an alternative pathological mechanism of tumour growth and development in these patients. It was expected that this might be reflected by African and Afro-Caribbean women having a different frequency of 7q deletions than women of other ethnicities. However, this was found not to be the case. It was also possible that those African/Afro-Caribbean women with 7q deletions would be of a comparable age to women of other ethnicities with 7q deletions, while those women with the more severe multiple leiomyoma phenotype would be of a younger age and exhibit a distinct pathogenic mechanism. Again, however, this was not the case; the median age of the African/Afro-Caribbean women with leiomyomas with 7q

deletions was 34.5yrs (Range: 31-44), whereas the median age of women of other ethnicities with leiomyomas with 7q deletions was 49yrs (Range: 39-62).

Therefore, this suggests some form of common pathogenic mechanism even in uterine leiomyomas resulting from ethnicity. The mechanism of leiomyoma formation is thought to be an initial transformation of normal myometrial cells into abnormal cells, followed by growth into tumours. Studies of cytogenetic aberrations, particularly of del(7q), has identified karyotypic mosaicism, suggestive of these changes being secondary events in leiomyoma pathogenesis. The identical frequencies of 7q deletions in patients of different ethnicities are perhaps further suggestive of them being secondary aberrations in leiomyomas.

From these results, it can be hypothesised that the differences in the age of onset and frequency of uterine leiomyomas between African/Afro-Caribbean women and women of other ethnicities may be due to the initial event resulting in the transformation of normal myometrial cells into leiomyoma cells. Following this initial event, the tumours follow common paths of leiomyoma pathogenesis, including deletions of chromosome 7q.

8.4.4 Conclusions

The work in this chapter has provided a number of interesting conclusions regarding the pathogenesis of uterine leiomyomas.

i) A 273kb region of 7q22.2 harbours a locus implicated in the pathogenesis of uterine leiomyomas.

ii) *MLL5* and *SRPK2* are equally strong candidates for this gene, given the effects of 7q deletions on uterine leiomyomas observed *in vivo* and *in vitro*.

iii) A cytogenetic subgroup of uterine leiomyomas exists with deletions at 7q34. Leiomyomas with this deletion also contain further deletions of chromosome 7q.

iv) Deletions of 7q occur with an equal frequency in African/Afro-Caribbean women and women of other ethnicities. This could imply that uterine leiomyomas from patients of different ethnicities are initiated through separate mechanisms, resulting in different frequencies of occurrence and age of onset, but ultimately follow converging tumorigenic paths.

Chapter 9

Discussion

9.1 Introduction

Despite their frequency and the huge number of studies that have been carried, the mechanisms by which uterine leiomyomas arise and develop remain poorly understood. The work in this thesis examined several aspects of leiomyoma pathogenesis in inherited, sporadic, and ethnically prevalent tumoura, both at a functional and genetic level. The results from this work have provided further clues to the pathogenic mechanisms involved in uterine leiomyomas and have identified important functional differences between, in particular, sporadic and HLRCC uterine leiomyomas.

9.2 Pathobiology of uterine leiomyomas

9.2.1 HLRCC and sporadic uterine leiomyomas appear to have distinct pathogenesis

The earlier chapters of this thesis compared several features of HLRCC and sporadic uterine leiomyomas. In particular, the frequency of pathogenic *FH* mutations, the occurrence of mtDNA mutations, the potential role of apoptosis, and ultrastructural features of each of these tumour types were examined. The results of each of these studies demonstrated significant differences between the pathogenicity of HLRCC and sporadic uterine leiomyomas.

It appears that the initiating event in HLRCC uterine leiomyoma pathogenesis is loss of the wild-type *FH* allele, either through a second mutation, or through loss of heterozygosity (Alam et al. 2003). This results in loss of FH protein function, which then initiates tumorigenesis through a pseudo-hypoxic pathway (Pollard et al. 2005b). The study of the frequency of *FH* mutations in the sporadic uterine leiomyoma patients (Chapter 3) demonstrated that only 2.8% of these patients had germline *FH* mutations. When the samples were split on the basis of ethnicity, African/Afro-Caribbean patients, despite having a younger age of onset in the study cohort, were found to have no *FH* mutations, although the difference in frequency of *FH* mutations between African/Afro-Caribbean patients and those of other ethnicities, including Caucasian, failed to reach statistical significance.

The lack of *FH* mutations in the germline of sporadic uterine leiomyoma patients, and in their tumours (Barker et al. 2002) implies that a

separate mechanism of initiation occurs in sporadic leiomyomas compared to HLRCC leiomyomas. This finding also has significance for the downstream pathobiology of the two tumour types.

In addition to the initiation of tumorigenesis, other distinctions between the two tumour types have been observed. Pollard *et al* compared the microvessel density of sporadic and HLRCC uterine leiomyomas, and found the latter to be far more vascular, and also noted the expression of VEGF and BNIP3, which are indicative of hypoxic activation. The reduction in vascularity in sporadic leiomyomas, and the lack of VEGF expression implies that hypoxia is not an important pathogenic mechanism of sporadic tumours (Pollard et al. 2005a).

Work in this thesis identified differences in the expression of apoptotic factors, and proliferative markers between HLRCC and sporadic leiomyomas. The results demonstrated increased expression of Bcl-2 and PCNA in both types of tumour compared to myometrium, indicative of increased proliferation and resistance to apoptosis, a result that has described previously (Dixon et al. 2002; Wu et al. 2002). However, HLRCC leiomyomas also demonstrated increased expression of anti-apoptotic Bcl-x and decreased pro-apoptotic Bak, implying that further pathways protecting these cells from apoptosis were involved. In addition, PCNA was significantly more highly expressed in HLRCC leiomyomas than sporadic leiomyomas, indicating a greater level of cell proliferation. These differences are likely to be a result of the involvement of hypoxia in HLRCC pathogenesis, and will be further discussed later.

Ultrastructural studies also revealed differences between HLRCC and sporadic leiomyomas. HLRCC leiomyomas differed in particular in their cellularity and extracellular matrix. Sporadic leiomyomas have an increased extracellular matrix compared to the myometrium, thought to be a result of dysregulated TGFβ-3 signalling (Lee and Nowak 2001). However, HLRCC leiomyomas demonstrated no increase in ECM content compared to the myometrium. This implies that TGFβ-3 signalling does not play a part in the pathogenesis of HLRCC leiomyomas. In addition, the HLRCC leiomyomas were found to be more cellular than their sporadic counterparts, this could be a result of a lack of ECM, allowing the cells to pack more closely together.

Other differences in the ultrastructures of HLRCC and sporadic leiomyomas were observed, including difference in aggregation of intermediate filaments in the cytoplasm, but the significance of these differences were not identified.

The results from Chapters 3 and 4 suggest that HLRCC and sporadic uterine leiomyomas have different pathogenic mechanisms, both in the initial onset of tumorigenesis, and in the pathways that allow tumorigenesis to continue.

9.2.2 Hypoxia and apoptosis resistance in HLRCC uterine leiomyomas

The results from Chapters 4 and 5 gave further clues as to the mechanism of pathogenesis of HLRCC leiomyomas. When *FH* was initially identified as the HLRCC tumour suppressor, several theories of pathogenesis were proposed, including pseudo-hypoxia, apoptosis resistance, anabolic

drive, stress pathway activation, and increased reactive oxygen species, discussd in detail in 1.2.1.1.1.1. The work in this thesis examined two more of these hypotheses. The role of apoptosis was studied by immunohistochemistry, and the production of reactive oxygen species was studied indirectly by examining mtDNA mutations in HLRCC and sporadic leiomyomas.

Constitutive activation of HIF1α in HLRCC tumours leads to a pseudo-hypoxic state, leading to the production of angiogenic factors such as VEGF. A cell exposed to chronic hypoxia will eventually die (Graham et al. 2004). However, in a pseudo-hypoxic state, the cell is still exposed to oxygen, and the highly vascular nature of HLRCC tumours further suggests that a ready supply of oxygen is available (Pollard et al. 2005a). Therefore, alternative mechanisms of oxygen sensing within the cell must override the pro-apoptotic effects of chronic hypoxia. As discussed in Chapter 4, this effect has already been observed in cells expressing constitutively active HIF1α, which demonstrated increased resistance to apoptosis by increased expression of Bcl-x and Bcl-2, and decreased Bak and Bax, when cultured under normoxia (Sasabe et al. 2005). This mimics the results observed *in vivo* in Chapter 4, which demonstrated an increase in Bcl-2 and Bcl-x expression, and decreased Bak expression.

The focus, therefore, is on the alternative mechanism of oxygen sensing that provides a protection from chronic hypoxia-induced apoptosis. One obvious target would be the mitochondrial electron transport chain, which requires oxygen at the last enzyme to mop up electrons used to generate a proton gradient required for ATP synthesis. HIF1α stabilisation has been

shown to require a functioning electron transport chain in some instances (Agani et al. 2000). However, blockage of the Krebs cycle, occurring due to loss of FH function, could lead to reduction, or loss of electron transport chain activity.

Electron transport chain function was indirectly measure in HLRCC leiomyomas by the frequency of mitochondrial DNA mutations, which are indicative of increased ROS (Czarnecka et al. 2006). It was found that the frequency of HLRCC mtDNA mutations was no greater than that observed in sporadic leiomyomas, and only 1/3 tumours showed any mtDNA mutations. Thus it was predicted that the lack of mtDNA mutations implied no increase in ROS, and so a functioning electron transport chain. Therefore, it appears that HLRCC tumours retain electron transport chain activity, possibly through the generation of NADH through other metabolic pathways, such as the pentose phosphate pathway, which produces NADPH (which is readily converted to NADH) without requiring Krebs cycle function (Berg et al. 2002).

This apparently retained function has great significance for HLRCC leiomyoma pathogenesis. Firstly, as mentioned above, HIF1α requires a functioning electron transport chain for stabilisation (Agani et al. 2000). Secondly, the functioning chain could act as a signal to the cell that some molecular oxygen is present, and so promote survival through a hitherto unknown pathway, possibly involving mitochondrial membrane potential.

9.2.3 Pathobiology of sporadic uterine leiomyomas

The major focus on the pathobiology of sporadic uterine leiomyomas looked at genetic changes in these tumours. The functional results examining

apoptosis-related proteins in these tumours concurred with the literature (Dixon et al. 2002; Wu et al. 2002; Kovacs et al. 2003), but did not provide any new insights into apoptosis resistance in leiomyomas.

As discussed above, *FH* mutations do not play a significant role in the pathogenesis of sporadic uterine leiomyomas. Therefore, it was decided to investigate two other types of genetic change in these tumours: copy number changes, with an eventual focus on the frequently deleted region of chromosome 7q; and mutations of the mitochondrial genome.

Results from the mtDNA screen, despite the limitations of the method used, revealed several tumours containing a number of heteroplasmic mutations. Some of these mutations affected the coding region of mtDNA, resulting in missense changes, some of which were predicted to be pathological by Polyphen (Ramensky et al. 2002). The effect of these mutations on leiomyoma pathogenesis was unknown, and further work needs to be done on the physiological effects of these mutations, particularly on mitochondrial metabolism, and subsequently on cell growth.

The high frequency of copy number changes in sporadic uterine leiomyomas is suggestive of an important role in leiomyoma pathobiology (Ligon and Morton 2001). The work in this thesis used microarray CGH to identify copy number changes in sporadic uterine leiomyomas at a higher resolution than previous studies. A large number of copy number changes were observed in these tumours, however, a low number of samples, resulting from limited availability of the microarrays, meant that few recurring copy number changes were observed. As expected, the most frequent of these changes was deletion of 7q22, the minimal region for which was minimised by

these arrays to ~3.8Mb. While this was a larger region than previous LOH-based reports (Ishwad et al. 1997; Sell et al. 2005), it was the smallest minimal region identified by actual demonstration of deletion, rather than implied deletion by LOH.

The frequency of copy number changes identified by microarray CGH was higher than the frequency of reported karyotypic changes in leiomyomas (Ligon and Morton 2001). Therefore, it is likely that the increased resolution of techniques such as array CGH, and more recently copy number analysis using SNP microarrays (LaFramboise et al. 2005), will lead to the identification of novel smaller regions of copy number change in leiomyomas that may be important for leiomyoma pathogenesis. It may also increase the reported frequency of leiomyomas with karyotypic aberrations.

The success of the microarray in minimising the region of deletion lead to the construction of a tiling-path resolution array, which eventually lead to a minimal region of ~273kb at 7q22.2. The actual effect of the 7q22.2 deletion on leiomyoma pathogenesis is still being debated. The frequency of deletion has lead some to suggest that a tumour suppressor is present within the deletion (Ishwad et al. 1995). However, the behaviour of leiomyoma cells with 7q deletions *in vitro* has lead some to propose that deletion of the involved gene may be detrimental to leiomyoma cell growth (Xing et al. 1997). The functions of the two genes within this minimal region, *MLL5* and *SRPK2*, support either of these hypotheses, and so no clear candidate, or mechanism, has yet emerged. It is possible that some, as yet unidentified, genomic feature in this region is responsible for the importance of 7q deletions in uterine leiomyomas.

9.2.4 Factors affecting ethnic prevalence of uterine leiomyomas

As a part of a number of the studies in this thesis, ethnicity was considered, particularly within genetic studies, in order to identify differences or similarities in the tumorigenic pathways of leiomyomas from African/Afro-Caribbean patients, and those of other ethnicities. It was found that *FH* mutations do not appear to play a significant role in this altered prevalence. In addition, the frequency of 7q deletions in leiomyomas of different ethnicities was studied. It was found that deletions of 7q occur with an equal frequency in uterine leiomyomas from African/Afro-Caribbean patients and Caucasian patients. The hypothesis that emerges from this result is that uterine leiomyomas from Caucasian and African/Afro-Caribbean patients follow similar paths of tumorigenesis with regard to karyotypic changes, but the difference in prevalence occurs due to the initial lesion resulting in leiomyoma growth. It would be very interesting to test this hypothesis using other common cytogenetic aberrations that occur in leiomyomas, including t(12;14) and rearrangements of 6p.

9.3 Further work

The results of the studies in this thesis have brought about a number of further questions that could be addressed. Consideration of this further work is presented below.

9.3.1 Chapter 3 – *FH* mutations in HLRCC

The lack of tumour and cell line material for each patient made testing the effects of each mutation more speculative, and the effects of the novel observed mutations remain unclear. In order to test their effects, *in vitro* studies, involving the generation of the mutant cDNA by cloning, and *in vitro* transcription and translation, followed by a functional FH assay, would give a definitive answer to the effects of the novel missense mutants. In addition, fusion of the mutant mitochondrial leader sequences to a reporter protein, such as GFP, would give an answer to the effects of these mutations.

One of the biggest flaws of this study was the lack of 'normal' controls sequenced. Therefore, screening of a panel of normal patients for the novel changes observed would give a better idea of their pathogenicity.

Finally, further screening techniques could be used to get the fullest picture of *FH* mutations in HLRCC. In particular, looking for exon deletions within the gene using techniques such as MAPH and MLPA (Sellner and Taylor 2004) may reveal hitherto missed exon copy number polymorphisms in HLRCC patients.

9.3.2 Chapter 4 – Apoptosis and ultrastructure in sporadic and HLRCC leiomyomas

The results of this study threw up a number of interesting hypotheses regarding the mechanisms of apoptosis resistance in HLRCC uterine leiomyomas, which may extend to HLRCC tumours in general. In particular, the pathways by which HLRCC tumour cells stay alive despite a chronic hypoxia signal, and investigation of alternative pathways of oxygen sensing. The development of an *in vitro* model for HLRCC would be an important first step for these studies. Following this, the role of the electron transport chain in keeping HLRCC cells alive, despite chronic HIF1α stabilisation could be investigated, for example by measuring electron transport chain function, or by assessing the effects of inhibition using specific inhibitors such as rotenone or oligomycin. The results of such a study could have important implications for other tumour types, and could possibly reveal new drug targets.

9.3.3 Chapter 5 – mtDNA mutations in uterine leiomyomas

As for a number of the novel *FH* mutations, the functional effects of mtDNA mutations in uterine leiomyomas were unclear. Therefore, more work would be required to assess their role in tumorigenesis. The difficulties in interpreting the data from the Mitochip array probably means that a number of mutations were missed. Therefore, a more thorough method of mtDNA screening, such as traditional sequencing, would probably be a better option until such time as resequencing array technology can overcome the inherent

difficulties in the technology. This would also allow the mutations observed in Chapter 5 to be confirmed.

9.3.4 Chapter 6 – 1Mb array CGH of uterine leiomyomas

The microarray CGH experiments revealed a number of novel regions of copy number change that could harbour important genes in uterine leiomyoma pathology. There are two chief ways in which this study could be continued: Firstly, through analysis of more tumours by 1Mb CGH to identify more novel regions of interest, and to refine these copy number changes; and secondly, through expression studies to try to correlate changes in expression with regions of copy number change, and so to identify further key players in leiomyoma pathogenesis. The size of the study in this chapter was, unfortunately, limited due to a finite supply of 1Mb arrays.

9.3.5 Chapter 8 – 7q deletions in uterine leiomyomas

The identification of a minimal region of deletion of 7q22.2 in uterine leiomyomas is an important finding. Unfortunately, time limitations prevented further analysis of this region. Therefore, the next step in this study would be to examine both candidates in depth. Quantitative real-time PCR expression studies, which are more sensitive than microarray expression studies, would be an important experiment to carry out initially, followed by protein expression analysis using western blot and immunohistochemistry. In addition, the breakpoints could be properly defined by the use of FISH, or real-time PCR to ensure the minimum region is accurately mapped.

The results from the literature suggested that both genes are potential candidates. However, their suitability as candidates is determined by the role that 7q deletions have *in vivo*. If, as some suggest, deletions of 7q are indicative of a tumour suppressor gene (Ishwad et al. 1995), then *MLL5* is a more suitable candidate. However, if deletions actually inhibit cell growth in some way (Xing et al. 1997), then *SRPK2* emerges as the stronger candidate. Therefore, in order to identify the involved gene on 7q, the role of these deletions on leiomyoma pathogenesis needs to be more thoroughly defined. Additionally, the non-coding DNA of the minimal region may yet harbour a hitherto unknown genetic variant, separate from *MLL5* and *SRPK2* that is actually the important variant.

In addition to the deletion of 7q22.2, a number of other smaller deletions were also observed, particularly at 7q34, and the role of these deletions in leiomyoma pathogenesis requires investigation. Further investigation of the multiple changes observed on 7q in combination with 7q34 deletions would also be required. In particular, identifying whether the changes occur on the same or different copies of chromosome 7.

The role of these novel deletions would be interesting to study. For example, in sample FG30, one of the small deletions contained a single gene, *SEMA3A*, which has a role in guiding vessel formation. To assess the effects of this deletion on the tumour, the vascularity of the original tumour could be studied and quantified. The roles of other novel copy number changes could be assessed in similar ways.

9.4 Future perspectives

The next step in the investigation of uterine leiomyoma pathogenesis is likely to be the implementation of large association studies looking for variants that increase a patient's risk of developing uterine leiomyomas. At least one study is in the process of recruiting patients, the 'finding genes for fibroids' study at Harvard Medical School (http://www.fibroids.net). Recent developments in array-based SNP-typing, plus the publication of the human HapMap have made this a far more viable possibility (2005), allowing simultaneous screening of 500,000+ SNPs on a single array. There are a number of different factors that could be investigated by such a study:

i) Variants increasing the risk of developing uterine leiomyomas.

ii) Variants determining differences in leiomyoma prevalence with ethnicity.

iii) Variants influencing leiomyoma size or location.

One of the biggest difficulties facing such a study would be the recruitment of adequate controls. Cramer and Patel's serial sectioning study of hysterectomy specimens revealed a far higher prevalence of uterine leiomyomas than was originally thought, reporting leiomyomas in 77% of specimens. These were often very small, asymptomatic tumours (Cramer and Patel 1990). If such a high prevalence is representative of the whole population, obtaining true controls whose uteri are free from leiomyomas would require meticulous work and careful selection. Perhaps the best controls for such a study would be post-menopausal patients having hysterectomies for other disorders whose uteri show no evidence of tumours following serial sectioning. However, there may be genetic variants that determine whether

leiomyomas grow to a size that results in morbidity, rather than remain small and asymptomatic. Obtaining controls for that study would be easier.

An association study examining the genetic factors that affect prevalence of leiomyomas in women of different ethnicities would also be a useful study. Again, the high prevalence of leiomyomas in African/Afro-Caribbean women would make the identification of controls very difficult. Again, stratification based on a patients phenotype may be required, comparing patients with few leiomyomas at an older age of onset, with younger patients with more leiomyomas.

However, the results of a carefully designed study should give further insights into leiomyoma pathogenesis that would allow a more complete insight into their pathobiology.

9.5 Conclusions

The pathobiology of uterine leiomyomas is complex for such an apparently basic tumour. The work in this thesis has made an important contribution to the knowledge of uterine leiomyoma pathobiology, particularly in regard to mechanisms of apoptosis resistance in HLRCC leiomyomas, and also copy number changes of chromosome 7q, which could provide a stepping stone to further understanding of a question that is simple to ask, yet difficult to answer: "What causes fibroids?"

Publications directly arising from work in this thesis

Wortham NC, Alam NA, Barclay E, Pollard PJ, Wagner BE, Manek S, Elia G, Tomlinson IPM. (2006) Aberrant expression of apoptosis proteins and ultrastructural observations in uterine leiomyomas from patients with hereditary leiomyomatosis and renal cell carcinoma. Fertil Steril **86**:961-71

Alam NA*, Rowan AJ*, **Wortham, NC***, Pollard **PJ***, Mitchell M, Tyrer JP, et al. Genetic and functional analyses of FH mutations in multiple cutaneous and uterine leiomyomatosis, hereditary leiomyomatosis and renal cancer, and fumarate hydratase deficiency. Hum Mol Genet. 2003 Jun 1;12(11):1241-52.
*denotes joint first authorship

Vanharanta S, **Wortham NC**, Laiho P, Sjoberg J, Aittomaki K, Arola J, et al. 7q deletion mapping and expression profiling in uterine fibroids. Oncogene. 2005 Sep 29;24(43):6545-54.

References

Agani FH, Pichiule P, Chavez JC, LaManna JC (2000) The role of mitochondria in the regulation of hypoxia-inducible factor 1 expression during hypoxia. J Biol Chem 275:35863-35867

Aikhionbare FO, Khan M, Carey D, Okoli J, Go R (2004) Is cumulative frequency of mitochondrial DNA variants a biomarker for colorectal tumor progression? Mol Cancer 3:30

Al-Hendy A, Salama SA (2006a) Catechol-O-methyltransferase polymorphism is associated with increased uterine leiomyoma risk in different ethnic groups. J Soc Gynecol Investig 13:136-144

Al-Hendy A, Salama SA (2006b) Ethnic distribution of estrogen receptor-alpha polymorphism is associated with a higher prevalence of uterine leiomyomas in black Americans. Fertil Steril 86:686-693

Alam NA, Barclay E, Rowan AJ, Tyrer JP, Calonje E, Manek S, Kelsell D, Leigh I, Olpin S, Tomlinson IP (2005a) Clinical features of multiple cutaneous and uterine leiomyomatosis: an underdiagnosed tumor syndrome. Arch Dermatol 141:199-206

Alam NA, Bevan S, Churchman M, Barclay E, Barker K, Jaeger EE, Nelson HM, Healy E, Pembroke AC, Friedmann PS, Dalziel K, Calonje E, Anderson J, August PJ, Davies MG, Felix R, Munro CS, Murdoch M, Rendall J, Kennedy S, Leigh IM, Kelsell DP, Tomlinson IP, Houlston RS (2001) Localization of a gene (MCUL1) for multiple cutaneous leiomyomata and uterine fibroids to chromosome 1q42.3-q43. Am J Hum Genet 68:1264-1269

Alam NA, Olpin S, Leigh IM (2005b) Fumarate hydratase mutations and predisposition to cutaneous leiomyomas, uterine leiomyomas and renal cancer. Br J Dermatol 153:11-17

Alam NA, Rowan AJ, Wortham NC, Pollard PJ, Mitchell M, Tyrer JP, Barclay E, et al. (2003) Genetic and functional analyses of FH mutations in multiple cutaneous and uterine leiomyomatosis, hereditary leiomyomatosis and renal cancer, and fumarate hydratase deficiency. Hum Mol Genet 12:1241-1252

Albertson DG, Pinkel D (2003) Genomic microarrays in human genetic disease and cancer. Hum Mol Genet 12 Spec No 2:R145-152

Alonso A, Martin P, Albarran C, Aquilera B, Garcia O, Guzman A, Oliva H, Sancho M (1997) Detection of somatic mutations in the mitochondrial DNA control region of colorectal and gastric tumors by heteroduplex and single-strand conformation analysis. Electrophoresis 18:682-685

Amant F, Dorfling CM, de Brabanter J, Vandewalle J, Vergote I, Lindeque BG, van Rensburg EJ (2004) A possible role of the cytochrome P450c17alpha gene (CYP17) polymorphism in the pathobiology of uterine leiomyomas from black South African women: a pilot study. Acta Obstet Gynecol Scand 83:234-239

Amant F, Huys E, Geurts-Moespot A, Lindeque BG, Vergote I, Sweep F, Schoenmakers EF (2003) Ethnic variations in uterine leiomyoma biology are not caused by differences in myometrial estrogen receptor alpha levels. J Soc Gynecol Investig 10:105-109

Anderson S, Bankier AT, Barrell BG, de Bruijn MH, Coulson AR, Drouin J, Eperon IC, Nierlich DP, Roe BA, Sanger F, Schreier PH, Smith AJ, Staden R, Young IG (1981) Sequence and organization of the human mitochondrial genome. Nature 290:457-465

Andrews RM, Kubacka I, Chinnery PF, Lightowlers RN, Turnbull DM, Howell N (1999) Reanalysis and revision of the Cambridge reference sequence for human mitochondrial DNA. Nat Genet 23:147

Arici A, Sozen I (2000) Transforming growth factor-beta3 is expressed at high levels in leiomyoma where it stimulates fibronectin expression and cell proliferation. Fertil Steril 73:1006-1011

Arici A, Sozen I (2003) Expression, menstrual cycle-dependent activation, and bimodal mitogenic effect of transforming growth factor-beta1 in human myometrium and leiomyoma. Am J Obstet Gynecol 188:76-83

Armstrong SA, Staunton JE, Silverman LB, Pieters R, den Boer ML, Minden MD, Sallan SE, Lander ES, Golub TR, Korsmeyer SJ (2002) MLL translocations specify a distinct gene expression profile that distinguishes a unique leukemia. Nat Genet 30:41-47

Au KS, Hebert AA, Roach ES, Northrup H (1999) Complete inactivation of the TSC2 gene leads to formation of hamartomas. Am J Hum Genet 65:1790-1795

Baba M, Hong SB, Sharma N, Warren MB, Nickerson ML, Iwamatsu A, Esposito D, Gillette WK, Hopkins RF, 3rd, Hartley JL, Furihata M, Oishi S, Zhen W, Burke TR, Jr., Linehan WM, Schmidt LS, Zbar B (2006) Folliculin encoded by the BHD gene interacts with a binding protein, FNIP1, and AMPK, and is involved in AMPK and mTOR signaling. Proc Natl Acad Sci U S A 103:15552-15557

Badeloe S, van Geel M, van Steensel MA, Bastida J, Ferrando J, Steijlen PM, Frank J, Poblete-Gutierrez P (2006) Diffuse and segmental variants of cutaneous leiomyomatosis: novel mutations in the fumarate hydratase gene and review of the literature. Exp Dermatol 15:735-741

Barbarisi A, Petillo O, Di Lieto A, Melone MA, Margarucci S, Cannas M, Peluso G (2001) 17-beta estradiol elicits an autocrine leiomyoma cell proliferation: evidence for a stimulation of protein kinase-dependent pathway. J Cell Physiol 186:414-424

Barker KT, Bevan S, Wang R, Lu YJ, Flanagan AM, Bridge JA, Fisher C, Finlayson CJ, Shipley J, Houlston RS (2002) Low frequency of somatic mutations in the FH/multiple cutaneous leiomyomatosis gene in sporadic leiomyosarcomas and uterine leiomyomas. Br J Cancer 87:446-448

Battegay EJ, Raines EW, Seifert RA, Bowen-Pope DF, Ross R (1990) TGF-beta induces bimodal proliferation of connective tissue cells via complex control of an autocrine PDGF loop. Cell 63:515-524

Baysal BE, Ferrell RE, Willett-Brozick JE, Lawrence EC, Myssiorek D, Bosch A, van der Mey A, Taschner PE, Rubinstein WS, Myers EN, Richard CW, 3rd, Cornelisse CJ, Devilee P, Devlin B (2000) Mutations in SDHD, a mitochondrial complex II gene, in hereditary paraganglioma. Science 287:848-851

Beckman KB, Ames BN (1999) Endogenous oxidative damage of mtDNA. Mutat Res 424:51-58

Belandia B, Orford RL, Hurst HC, Parker MG (2002) Targeting of SWI/SNF chromatin remodelling complexes to estrogen-responsive genes. Embo J 21:4094-4103

Benassayag C, Leroy MJ, Rigourd V, Robert B, Honore JC, Mignot TM, Vacher-Lavenu MC, Chapron C, Ferre F (1999) Estrogen receptors (ERalpha/ERbeta) in normal and pathological growth of the human myometrium: pregnancy and leiomyoma. Am J Physiol 276:E1112-1118

Berendes U, Kuhner A, Schnyder UW (1971) Segmentary and disseminated lesions in multiple hereditary cutaneous leiomyoma. Humangenetik 13:81-82

Berg JM, Tymoczko JL, Stryer L (2002) Biochemistry. W.H. Freeman & Co., New York

Bianchi MS, Bianchi NO, Bailliet G (1995) Mitochondrial DNA mutations in normal and tumor tissues from breast cancer patients. Cytogenet Cell Genet 71:99-103

Bianchi NO, Bianchi MS, Richard SM (2001) Mitochondrial genome instability in human cancers. Mutat Res 488:9-23

Boehm KD, Daimon M, Gorodeski IG, Sheean LA, Utian WH, Ilan J (1990) Expression of the insulin-like and platelet-derived growth factor genes in human uterine tissues. Mol Reprod Dev 27:93-101

Borrmann L, Wilkening S, Bullerdiek J (2001) The expression of HMGA genes is regulated by their 3'UTR. Oncogene 20:4537-4541

Bourgeron T, Chretien D, Poggi-Bach J, Doonan S, Rabier D, Letouze P, Munnich A, Rotig A, Landrieu P, Rustin P (1994) Mutation of the fumarase gene in two siblings with progressive encephalopathy and fumarase deficiency. J Clin Invest 93:2514-2518

Brandner P, Neis KJ, Diebold P (2000) Hysteroscopic resection of submucous myomas. Contrib Gynecol Obstet 20:81-90

Brandon MC, Lott MT, Nguyen KC, Spolim S, Navathe SB, Baldi P, Wallace DC (2005) MITOMAP: a human mitochondrial genome database--2004 update. Nucleic Acids Res 33:D611-613

Brosens I, Deprest J, Dal Cin P, Van den Berghe H (1998) Clinical significance of cytogenetic abnormalities in uterine myomas. Fertil Steril 69:232-235

Brown NS, Bicknell R (2001) Hypoxia and oxidative stress in breast cancer. Oxidative stress: its effects on the growth, metastatic potential and response to therapy of breast cancer. Breast Cancer Res 3:323-327

Brown TA, Cecconi C, Tkachuk AN, Bustamante C, Clayton DA (2005) Replication of mitochondrial DNA occurs by strand displacement with alternative light-strand origins, not via a strand-coupled mechanism. Genes Dev 19:2466-2476

Bulun SE, Simpson ER, Word RA (1994) Expression of the CYP19 gene and its product aromatase cytochrome P450 in human uterine leiomyoma tissues and cells in culture. J Clin Endocrinol Metab 78:736-743

Burroughs KD, Howe SR, Okubo Y, Fuchs-Young R, LeRoith D, Walker CL (2002) Dysregulation of IGF-I signaling in uterine leiomyoma. J Endocrinol 172:83-93

Buttram VC, Jr. (1986) Uterine leiomyomata--aetiology, symptomatology and management. Prog Clin Biol Res 225:275-296

Buttram VC, Jr., Reiter RC (1981) Uterine leiomyomata: etiology, symptomatology, and management. Fertil Steril 36:433-445

Cai J, Ahmad S, Jiang WG, Huang J, Kontos CD, Boulton M, Ahmed A (2003) Activation of vascular endothelial growth factor receptor-1 sustains angiogenesis and Bcl-2 expression via the phosphatidylinositol 3-kinase pathway in endothelial cells. Diabetes 52:2959-2968

Cai WW, Mao JH, Chow CW, Damani S, Balmain A, Bradley A (2002) Genome-wide detection of chromosomal imbalances in tumors using BAC microarrays. Nat Biotechnol 20:393-396

Candiani GB, Fedele L, Parazzini F, Villa L (1991) Risk of recurrence after myomectomy. Br J Obstet Gynaecol 98:385-389

Canter JA, Kallianpur AR, Parl FF, Millikan RC (2005) Mitochondrial DNA G10398A polymorphism and invasive breast cancer in African-American women. Cancer Res 65:8028-8033

Carelli V, Achilli A, Valentino ML, Rengo C, Semino O, Pala M, Olivieri A, Mattiazzi M, Pallotti F, Carrara F, Zeviani M, Leuzzi V, Carducci C, Valle G, Simionati B, Mendieta L, Salomao S, Belfort R, Jr., Sadun AA, Torroni A (2006) Haplogroup effects and recombination of mitochondrial DNA: novel clues from the analysis of Leber hereditary optic neuropathy pedigrees. Am J Hum Genet 78:564-574

Carvajal-Carmona LG, Alam NA, Pollard PJ, Jones AM, Barclay E, Wortham N, Pignatelli M, Freeman A, Pomplun S, Ellis I, Poulsom R, El-Bahrawy MA, Berney DM, Tomlinson IP (2006) Adult leydig cell tumors of the testis caused by germline fumarate hydratase mutations. J Clin Endocrinol Metab 91:3071-3075

Case JT, Wallace DC (1981) Maternal inheritance of mitochondrial DNA polymorphisms in cultured human fibroblasts. Somatic Cell Genet 7:103-108

Catherino WH, Leppert PC, Stenmark MH, Payson M, Potlog-Nahari C, Nieman LK, Segars JH (2004) Reduced dermatopontin expression is a molecular link between uterine leiomyomas and keloids. Genes Chromosomes Cancer 40:204-217

Chan TL, Zhao W, Leung SY, Yuen ST, Project CG (2003) BRAF and KRAS mutations in colorectal hyperplastic polyps and serrated adenomas. Cancer Res 63:4878-4881

Chandrasekhar Y, Heiner J, Osuamkpe C, Nagamani M (1992) Insulin-like growth factor I and II binding in human myometrium and leiomyomas. Am J Obstet Gynecol 166:64-69

Chandrasekharappa SC, Guru SC, Manickam P, Olufemi SE, Collins FS, Emmert-Buck MR, Debelenko LV, Zhuang Z, Lubensky IA, Liotta LA, Crabtree JS, Wang Y, Roe BA, Weisemann J, Boguski MS, Agarwal SK, Kester MB, Kim YS, Heppner C, Dong Q, Spiegel AM, Burns AL, Marx SJ (1997) Positional cloning of the gene for multiple endocrine neoplasia-type 1. Science 276:404-407

Chatterjee A, Mambo E, Sidransky D (2006) Mitochondrial DNA mutations in human cancer. Oncogene 25:4663-4674

Chegini N, Luo X, Ding L, Ripley D (2003) The expression of Smads and transforming growth factor beta receptors in leiomyoma and

myometrium and the effect of gonadotropin releasing hormone analogue therapy. Mol Cell Endocrinol 209:9-16

Chen CR, Buck GM, Courey NG, Perez KM, Wactawski-Wende J (2001) Risk factors for uterine fibroids among women undergoing tubal sterilization. Am J Epidemiol 153:20-26

Chen W, Erdogan F, Ropers HH, Lenzner S, Ullmann R (2005) CGHPRO -- a comprehensive data analysis tool for array CGH. BMC Bioinformatics 6:85

Chen YH, Hansen L, Chen MX, Bjorbaek C, Vestergaard H, Hansen T, Cohen PT, Pedersen O (1994) Sequence of the human glycogen-associated regulatory subunit of type 1 protein phosphatase and analysis of its coding region and mRNA level in muscle from patients with NIDDM. Diabetes 43:1234-1241

Chomyn A, Attardi G (2003) MtDNA mutations in aging and apoptosis. Biochem Biophys Res Commun 304:519-529

Chuang GS, Martinez-Mir A, Engler DE, Gmyrek RF, Zlotogorski A, Christiano AM (2006a) Multiple cutaneous and uterine leiomyomata resulting from missense mutations in the fumarate hydratase gene. Clin Exp Dermatol 31:118-121

Chuang GS, Martinez-Mir A, Geyer A, Engler DE, Glaser B, Cserhalmi-Friedman PB, Gordon D, Horev L, Lukash B, Herman E, Cid MP, Brenner S, Landau M, Sprecher E, Garcia Muret MP, Christiano AM, Zlotogorski A (2005) Germline fumarate hydratase mutations and evidence for a founder mutation underlying multiple cutaneous and uterine leiomyomata. J Am Acad Dermatol 52:410-416

Chuang LY, Yang CH, Cheng YH, Gu DL, Chang PL, Tsui KH, Chang HW (2006b) V-MitoSNP: visualization of human mitochondrial SNPs. BMC Bioinformatics 7:379

Clamp M, Cuff J, Searle SM, Barton GJ (2004) The Jalview Java alignment editor. Bioinformatics 20:426-427

Clayton DA (1992) Transcription and replication of animal mitochondrial DNAs. Int Rev Cytol 141:217-232

Cleveland WS (1981) LOWESS: A program or smoothing scatterplots by robust locally weighted regression. The American Statistician 35:54

Cochat P, Guibaud P, Garcia Torres R, Roussel B, Guarner V, Larbre F (1988) Diffuse leiomyomatosis in Alport syndrome. J Pediatr 113:339-343

Consortium IH (2005) A haplotype map of the human genome. Nature 437:1299-1320

Coughlin EM, Christensen E, Kunz PL, Krishnamoorthy KS, Walker V, Dennis NR, Chalmers RA, Elpeleg ON, Whelan D, Pollitt RJ, Ramesh V, Mandell R, Shih VE (1998) Molecular analysis and prenatal diagnosis of human fumarase deficiency. Mol Genet Metab 63:254-262

Cox WG, Beaudet MP, Agnew JY, Ruth JL (2004) Possible sources of dye-related signal correlation bias in two-color DNA microarray assays. Anal Biochem 331:243-254

Cramer SF, Patel A (1990) The frequency of uterine leiomyomas. Am J Clin Pathol 94:435-438

Czarnecka AM, Golik P, Bartnik E (2006) Mitochondrial DNA mutations in human neoplasia. J Appl Genet 47:67-78

Dal Cin P, Morton CC (2002) 1q42 approximately q44 is rarely cytogenetically involved in sporadic uterine leiomyomata. Cancer Genet Cytogenet 138:92-93

Dal Cin P, Van den Berghe H, Sciot R, de Wever I (1997) Deletion of the long arm of chromosome 7 in lipoma. Cancer Genet Cytogenet 96:85-86

Daub H, Blencke S, Habenberger P, Kurtenbach A, Dennenmoser J, Wissing J, Ullrich A, Cotten M (2002) Identification of SRPK1 and SRPK2 as the major cellular protein kinases phosphorylating hepatitis B virus core protein. J Virol 76:8124-8137

De Angelis PM, Stokke T, Beigi M, Mjaland O, Clausen OP (2001) Prognostic significance of recurrent chromosomal aberrations detected by comparative genomic hybridization in sporadic colorectal cancer. Int J Colorectal Dis 16:38-45

Deng LW, Chiu I, Strominger JL (2004) MLL 5 protein forms intranuclear foci, and overexpression inhibits cell cycle progression. Proc Natl Acad Sci U S A 101:757-762

Denschlag D, Bentz EK, Hefler L, Pietrowski D, Zeillinger R, Tempfer C, Tong D (2006) Genotype distribution of estrogen receptor-alpha, catechol-O-methyltransferase, and cytochrome P450 17 gene polymorphisms in Caucasian women with uterine leiomyomas. Fertil Steril 85:462-467

Denschlag D, Bettendorf H, Watermann D, Keck C, Tempfer C, Pietrowski D (2005) Polymorphism of the p53 tumor suppressor gene is associated with susceptibility to uterine leiomyoma. Fertil Steril 84:162-166

Deschauer M, Gizatullina Z, Schulze A, Pritsch M, Knoppel C, Knape M, Zierz S, Gellerich FN (2006) Molecular and biochemical investigations in fumarase deficiency. Mol Genet Metab 88:146-152

Di Lieto A, De Falco M, Mansueto G, De Rosa G, Pollio F, Staibano S (2005) Preoperative administration of GnRH-a plus tibolone to premenopausal women with uterine fibroids: evaluation of the clinical response, the immunohistochemical expression of PDGF, bFGF and VEGF and the vascular pattern. Steroids 70:95-102

Ding JH, Zhong XY, Hagopian JC, Cruz MM, Ghosh G, Feramisco J, Adams JA, Fu XD (2006) Regulated cellular partitioning of SR protein-specific kinases in mammalian cells. Mol Biol Cell 17:876-885

Dixon D, Flake GP, Moore AB, He H, Haseman JK, Risinger JI, Lancaster JM, Berchuck A, Barrett JC, Robboy SJ (2002) Cell proliferation and apoptosis in human uterine leiomyomas and myometria. Virchows Arch 441:53-62

Dong Z, Nishiymama J, Yi X, Venkatachalam MA, Denton M, Gu S, Li S, Qiang M (2002) Gene promoter of apoptosis inhibitory protein IAP2: identification of enhancer elements and activation by severe hypoxia. Biochem J 364:413-421

Dong Z, Wang J (2004) Hypoxia selection of death-resistant cells. A role for Bcl-X(L). J Biol Chem 279:9215-9221

Dong Z, Wang JZ, Yu F, Venkatachalam MA (2003) Apoptosis-resistance of hypoxic cells: multiple factors involved and a role for IAP-2. Am J Pathol 163:663-671

Donnez J, Mathieu PE, Bassil S, Smets M, Nisolle M, Berliere M (1996) Laparoscopic myomectomy today. Fibroids: management and treatment: the state of the art. Hum Reprod 11:1837-1840

Donnez J, Schrurs B, Gillerot S, Sandow J, Clerckx F (1989) Treatment of uterine fibroids with implants of gonadotropin-releasing hormone agonist: assessment by hysterography. Fertil Steril 51:947-950

Douwes Dekker PB, Hogendoorn PC, Kuipers-Dijkshoorn N, Prins FA, van Duinen SG, Taschner PE, van der Mey AG, Cornelisse CJ (2003) SDHD mutations in head and neck paragangliomas result in destabilization of complex II in the mitochondrial respiratory chain with loss of enzymatic activity and abnormal mitochondrial morphology. J Pathol 201:480-486

Duncan AM, Anderson L, Duff C, Ozawa T, Suzuki H, Worton R, Rozen R (1994) Assignment of the gene (UQCRFS1) for the Rieske iron-sulfur protein subunit of the mitochondrial cytochrome bc1 complex to the 22q13 and 19q12-q13.1 regions of the human genome. Genomics 21:281-283

Eker R, Mossige J, Johannessen JV, Aars H (1981) Hereditary renal adenomas and adenocarcinomas in rats. Diagn Histopathol 4:99-110

Elson JL, Samuels DC, Turnbull DM, Chinnery PF (2001) Random intracellular drift explains the clonal expansion of mitochondrial DNA mutations with age. Am J Hum Genet 68:802-806

Emerling BM, Bonifas J, Kratz CP, Donovan S, Taylor BR, Green ED, Le Beau MM, Shannon KM (2002) MLL5, a homolog of Drosophila trithorax located within a segment of chromosome band 7q22 implicated in myeloid leukemia. Oncogene 21:4849-4854

Enriquez JA, Chomyn A, Attardi G (1995) MtDNA mutation in MERRF syndrome causes defective aminoacylation of tRNA(Lys) and premature translation termination. Nat Genet 10:47-55

Erlandson R (1994) Diagnostic Transmission Electron Microscopy of Tumors, with Clinicopathological, Immunohistochemical, and Cytogenetic Correlations. Raven Press Ltd, New York

Eyden B (2004) Case for the panel of ultrastructural pathology--uterine leiomyoma. Ultrastruct Pathol 28:115-117

Eyden BP, Hale RJ, Richmond I, Buckley CH (1992) Cytoskeletal filaments in the smooth muscle cells of uterine leiomyomata and myometrium: an ultrastructural and immunohistochemical analysis. Virchows Arch A Pathol Anat Histopathol 420:51-58

Faerstein E, Szklo M, Rosenhein N (2001a) Risk factors for uterine leiomyoma: a practice-based case-control study. I. African-American heritage, reproductive history, body size, and smoking. Am J Epidemiol 153:1-10

Faerstein E, Szklo M, Rosenshein NB (2001b) Risk factors for uterine leiomyoma: a practice-based case-control study. II. Atherogenic risk factors and potential sources of uterine irritation. Am J Epidemiol 153:11-19

Fahling M, Perlewitz A, Doller A, Thiele BJ (2004) Regulation of collagen prolyl 4-hydroxylase and matrix metalloproteinases in fibrosarcoma cells by hypoxia. Comp Biochem Physiol C Toxicol Pharmacol 139:119-126

Fan SX, Sreekantaiah C, Berger CS, Medchill M, Pedron S, Sandberg AA (1990) Cytogenetic findings in nine leiomyomas of the uterus. Cancer Genet Cytogenet 47:179-189

Fayed YM, Tsibris JC, Langenberg PW, Robertson AL, Jr. (1989) Human uterine leiomyoma cells: binding and growth responses to epidermal growth factor, platelet-derived growth factor, and insulin. Lab Invest 60:30-37

Fedele M, Pierantoni GM, Visone R, Fusco A (2006) E2F1 activation is responsible for pituitary adenomas induced by HMGA2 gene overexpression. Cell Div 1:17

Feig LA, Bast RC, Jr., Knapp RC, Cooper GM (1984) Somatic activation of rasK gene in a human ovarian carcinoma. Science 223:698-701

Fiegler H, Carr P, Douglas EJ, Burford DC, Hunt S, Scott CE, Smith J, Vetrie D, Gorman P, Tomlinson IP, Carter NP (2003) DNA microarrays for comparative genomic hybridization based on DOP-PCR amplification of BAC and PAC clones. Genes Chromosomes Cancer 36:361-374

Flake GP, Andersen J, Dixon D (2003) Etiology and pathogenesis of uterine leiomyomas: a review. Environ Health Perspect 111:1037-1054

Fox JL (1996) FBI forensics tries mtDNA. Nat Biotechnol 14:1211

Friedman AJ, Barbieri RL, Doubilet PM, Fine C, Schiff I (1988) A randomized, double-blind trial of a gonadotropin releasing-hormone agonist (leuprolide) with or without medroxyprogesterone acetate in the treatment of leiomyomata uteri. Fertil Steril 49:404-409

Fujimoto J, Hirose R, Ichigo S, Sakaguchi H, Li Y, Tamaya T (1998) Expression of progesterone receptor form A and B mRNAs in uterine leiomyoma. Tumour Biol 19:126-131

Fujimoto J, Hirose R, Sakaguchi H, Tamaya T (2000) Expression of size-polymorphic androgen receptor gene in uterine leiomyoma according to the number of cytosine, adenine, and guanine repeats in androgen receptor alleles. Tumour Biol 21:33-37

Fukuhara T, Hosoya T, Shimizu S, Sumi K, Oshiro T, Yoshinaka Y, Suzuki M, Yamamoto N, Herzenberg LA, Herzenberg LA, Hagiwara M (2006) Utilization of host SR protein kinases and RNA-splicing machinery during viral replication. Proc Natl Acad Sci U S A 103:11329-11333

Gamaley IA, Klyubin IV (1999) Roles of reactive oxygen species: signaling and regulation of cellular functions. Int Rev Cytol 188:203-255

Gao Z, Matsuo H, Nakago S, Kurachi O, Maruo T (2002) p53 Tumor suppressor protein content in human uterine leiomyomas and its down-regulation by 17 beta-estradiol. J Clin Endocrinol Metab 87:3915-3920

Gao Z, Matsuo H, Wang Y, Nakago S, Maruo T (2001) Up-regulation by IGF-I of proliferating cell nuclear antigen and Bcl-2 protein expression in human uterine leiomyoma cells. J Clin Endocrinol Metab 86:5593-5599

Gattas GJ, Quade BJ, Nowak RA, Morton CC (1999) HMGIC expression in human adult and fetal tissues and in uterine leiomyomata. Genes Chromosomes Cancer 25:316-322

Gellera C, Uziel G, Rimoldi M, Zeviani M, Laverda A, Carrara F, DiDonato S (1990) Fumarase deficiency is an autosomal recessive encephalopathy affecting both the mitochondrial and the cytosolic enzymes. Neurology 40:495-499

Gevers W (1984) Protein metabolism of the heart. J Mol Cell Cardiol 16:3-32

Giancotti V, Pani B, D'Andrea P, Berlingieri MT, Di Fiore PP, Fusco A, Vecchio G, Philp R, Crane-Robinson C, Nicolas RH, et al. (1987) Elevated levels of a specific class of nuclear phosphoproteins in cells transformed with v-ras and v-mos oncogenes and by cotransfection with c-myc and polyoma middle T genes. Embo J 6:1981-1987

Glass AR (1989) Endocrine aspects of obesity. Med Clin North Am 73:139-160

Glatstein IZ, Yeh J (1995) Ontogeny of the estrogen receptor in the human fetal uterus. J Clin Endocrinol Metab 80:958-964

Gorman P, Roylance R (2006) Fluorescence in situ hybridization and comparative genomic hybridization. Methods Mol Med 120:269-295

Goto Y, Tsugane K, Tanabe Y, Nonaka I, Horai S (1994) A new point mutation at nucleotide pair 3291 of the mitochondrial tRNA(Leu(UUR)) gene in a patient with mitochondrial myopathy, encephalopathy, lactic acidosis, and stroke-like episodes (MELAS). Biochem Biophys Res Commun 202:1624-1630

Grafstrom E, Egyhazi S, Ringborg U, Hansson J, Platz A (2005) Biallelic deletions in INK4 in cutaneous melanoma are common and associated with decreased survival. Clin Cancer Res 11:2991-2997

Graham RM, Frazier DP, Thompson JW, Haliko S, Li H, Wasserlauf BJ, Spiga MG, Bishopric NH, Webster KA (2004) A unique pathway of cardiac myocyte death caused by hypoxia-acidosis. J Exp Biol 207:3189-3200

Gross KL, Morton CC (2001) Genetics and the development of fibroids. Clin Obstet Gynecol 44:335-349

Gross KL, Neskey DM, Manchanda N, Weremowicz S, Kleinman MS, Nowak RA, Ligon AH, Rogalla P, Drechsler K, Bullerdiek J, Morton CC (2003) HMGA2 expression in uterine leiomyomata and myometrium: quantitative analysis and tissue culture studies. Genes Chromosomes Cancer 38:68-79

Gross KL, Panhuysen CI, Kleinman MS, Goldhammer H, Jones ES, Nassery N, Stewart EA, Morton CC (2004) Involvement of fumarate hydratase in nonsyndromic uterine leiomyomas: genetic linkage analysis and FISH studies. Genes Chromosomes Cancer 41:183-190

Gustafson AW (2002) Paternal inheritance of mitochondrial DNA. N Engl J Med 347:2081-2082; author reply 2081-2082

Hacker NF, Moore JG (1998) Essentials of Obstetrics and Gynaecology. W.B. Saunders, London

Hall KL, Teneriello MG, Taylor RR, Lemon S, Ebina M, Linnoila RI, Norris JH, Park RC, Birrer MJ (1997) Analysis of Ki-ras, p53, and MDM2 genes in uterine leiomyomas and leiomyosarcomas. Gynecol Oncol 65:330-335

Hanahan D, Weinberg RA (2000) The hallmarks of cancer. Cell 100:57-70

Harrison-Woolrych ML, Sharkey AM, Charnock-Jones DS, Smith SK (1995) Localization and quantification of vascular endothelial growth factor messenger ribonucleic acid in human myometrium and leiomyomata. J Clin Endocrinol Metab 80:1853-1858

Havel G, Wedell B, Dahlenfors R, Mark J (1989) Cytogenetic relationship between uterine lipoleiomyomas and typical leiomyomas. Virchows Arch B Cell Pathol Incl Mol Pathol 57:77-79

Heidet L, Dahan K, Zhou J, Xu Z, Cochat P, Gould JD, Leppig KA, Proesmans W, Guyot C, Guillot M, et al. (1995) Deletions of both alpha 5(IV) and alpha 6(IV) collagen genes in Alport syndrome and in Alport syndrome associated with smooth muscle tumours. Hum Mol Genet 4:99-108

Heim S, Nilbert M, Vanni R, Floderus UM, Mandahl N, Liedgren S, Lecca U, Mitelman F (1988) A specific translocation, t(12;14)(q14-15;q23-24), characterizes a subgroup of uterine leiomyomas. Cancer Genet Cytogenet 32:13-17

Higgy NA, Tarnasky HA, Valarche I, Nepveu A, van der Hoorn FA (1997) Cux/CDP homeodomain protein binds to an enhancer in the rat c-mos locus and represses its activity. Biochim Biophys Acta 1351:313-324

Hinrichs AS, Karolchik D, Baertsch R, Barber GP, Bejerano G, Clawson H, Diekhans M, et al. (2006) The UCSC Genome Browser Database: update 2006. Nucleic Acids Res 34:D590-598

Hodges LC, Houston KD, Hunter DS, Fuchs-Young R, Zhang Z, Wineker RC, Walker CL (2002) Transdominant suppression of estrogen receptor

signaling by progesterone receptor ligands in uterine leiomyoma cells. Mol Cell Endocrinol 196:11-20

Holme E, Larsson NG, Oldfors A, Tulinius M, Sahlin P, Stenman G (1993) Multiple symmetric lipomas with high levels of mtDNA with the tRNA(Lys) A-->G(8344) mutation as the only manifestation of disease in a carrier of myoclonus epilepsy and ragged-red fibers (MERRF) syndrome. Am J Hum Genet 52:551-556

Holt IJ, Lorimer HE, Jacobs HT (2000) Coupled leading- and lagging-strand synthesis of mammalian mitochondrial DNA. Cell 100:515-524

Horton TM, Petros JA, Heddi A, Shoffner J, Kaufman AE, Graham SD, Jr., Gramlich T, Wallace DC (1996) Novel mitochondrial DNA deletion found in a renal cell carcinoma. Genes Chromosomes Cancer 15:95-101

Howe SR, Gottardis MM, Everitt JI, Goldsworthy TL, Wolf DC, Walker C (1995) Rodent model of reproductive tract leiomyomata. Establishment and characterization of tumor-derived cell lines. Am J Pathol 146:1568-1579

Hsieh YY, Chang CC, Tsai FJ, Lin CC, Yeh LS, Tsai CH (2004) Tumor necrosis factor-alpha-308 promoter and p53 codon 72 gene polymorphisms in women with leiomyomas. Fertil Steril 82 Suppl 3:1177-1181

Hsieh YY, Chang CC, Tsai FJ, Tsai HD, Yeh LS, Lin CC, Tsai CH (2003) Estrogen receptor thymine-adenine dinucleotide repeat polymorphism is associated with susceptibility to leiomyoma. Fertil Steril 79:96-99

Hsieh YY, Wang YK, Chang CC, Lin CS (2006) Estrogen receptor {alpha}-351 XbaI*G and -397 PvuII*C-related genotypes and alleles are associated with higher susceptibilities of endometriosis and leiomyoma. Mol Hum Reprod

Hu J, Surti U (1991) Subgroups of uterine leiomyomas based on cytogenetic analysis. Hum Pathol 22:1009-1016

Hunter DS, Klotzbucher M, Kugoh H, Cai SL, Mullen JP, Manfioletti G, Fuhrman U, Walker CL (2002) Aberrant expression of HMGA2 in uterine leiomyoma associated with loss of TSC2 tumor suppressor gene function. Cancer Res 62:3766-3772

Ingraham SE, Lynch RA, Surti U, Rutter JL, Buckler AJ, Khan SA, Menon AG, Lepont P (2006) Identification and characterization of novel human transcripts embedded within HMGA2 in t(12;14)(q15;q24.1) uterine leiomyoma. Mutat Res 602:43-53

Isaacs JS, Jung YJ, Mole DR, Lee S, Torres-Cabala C, Chung YL, Merino M, Trepel J, Zbar B, Toro J, Ratcliffe PJ, Linehan WM, Neckers L (2005) HIF overexpression correlates with biallelic loss of fumarate hydratase in renal cancer: novel role of fumarate in regulation of HIF stability. Cancer Cell 8:143-153

Ishwad CS, Ferrell RE, Davare J, Meloni AM, Sandberg AA, Surti U (1995) Molecular and cytogenetic analysis of chromosome 7 in uterine leiomyomas. Genes Chromosomes Cancer 14:51-55

Ishwad CS, Ferrell RE, Hanley K, Davare J, Meloni AM, Sandberg AA, Surti U (1997) Two discrete regions of deletion at 7q in uterine leiomyomas. Genes Chromosomes Cancer 19:156-160

Jain AN, Tokuyasu TA, Snijders AM, Segraves R, Albertson DG, Pinkel D (2002) Fully automatic quantification of microarray image data. Genome Res 12:325-332

Jeronimo C, Nomoto S, Caballero OL, Usadel H, Henrique R, Varzim G, Oliveira J, Lopes C, Fliss MS, Sidransky D (2001) Mitochondrial mutations in early stage prostate cancer and bodily fluids. Oncogene 20:5195-5198

Jonasdottir TJ, Mellersh CS, Moe L, Heggebo R, Gamlem H, Ostrander EA, Lingaas F (2000) Genetic mapping of a naturally occurring hereditary renal cancer syndrome in dogs. Proc Natl Acad Sci U S A 97:4132-4137

Jong K, Marchiori E, Meijer G, Vaart AV, Ylstra B (2004) Breakpoint identification and smoothing of array comparative genomic hybridization data. Bioinformatics 20:3636-3637

Jung F, Weiland U, Johns RA, Ihling C, Dimmeler S (2001) Chronic hypoxia induces apoptosis in cardiac myocytes: a possible role for Bcl-2-like proteins. Biochem Biophys Res Commun 286:419-425

Kaji H, Canaff L, Lebrun JJ, Goltzman D, Hendy GN (2001) Inactivation of menin, a Smad3-interacting protein, blocks transforming growth factor type beta signaling. Proc Natl Acad Sci U S A 98:3837-3842

Kallioniemi OP, Kallioniemi A, Kurisu W, Thor A, Chen LC, Smith HS, Waldman FM, Pinkel D, Gray JW (1992) ERBB2 amplification in breast cancer analyzed by fluorescence in situ hybridization. Proc Natl Acad Sci U S A 89:5321-5325

Kashiwagi H, Uchida K (2000) Genome-wide profiling of gene amplification and deletion in cancer. Hum Cell 13:135-141

Kazmierczak B, Bol S, Wanschura S, Bartnitzke S, Bullerdiek J (1996) PAC clone containing the HMGI(Y) gene spans the breakpoint of a 6p21 translocation in a uterine leiomyoma cell line. Genes Chromosomes Cancer 17:191-193

Kazmierczak B, Hennig Y, Wanschura S, Rogalla P, Bartnitzke S, Van de Ven W, Bullerdiek J (1995) Description of a novel fusion transcript between HMGI-C, a gene encoding for a member of the high mobility group proteins, and the mitochondrial aldehyde dehydrogenase gene. Cancer Res 55:6038-6039

Kelly HA (1906) Operative Gynecology. D. Appleton, New York

Kile BT, Viney EM, Willson TA, Brodnicki TC, Cancilla MR, Herlihy AS, Croker BA, Baca M, Nicola NA, Hilton DJ, Alexander WS (2000) Cloning and characterization of the genes encoding the ankyrin repeat and SOCS box-containing proteins Asb-1, Asb-2, Asb-3 and Asb-4. Gene 258:31-41

King A, Selak MA, Gottlieb E (2006) Succinate dehydrogenase and fumarate hydratase: linking mitochondrial dysfunction and cancer. Oncogene 25:4675-4682

Kirkin V, Joos S, Zornig M (2004) The role of Bcl-2 family members in tumorigenesis. Biochim Biophys Acta 1644:229-249

Kiuru M, Lehtonen R, Arola J, Salovaara R, Jarvinen H, Aittomaki K, Sjoberg J, Visakorpi T, Knuutila S, Isola J, Delahunt B, Herva R, Launonen V, Karhu A, Aaltonen LA (2002) Few FH mutations in sporadic counterparts of tumor types observed in hereditary leiomyomatosis and renal cell cancer families. Cancer Res 62:4554-4557

Kjerulff KH, Guzinski GM, Langenberg PW, Stolley PD, Moye NE, Kazandjian VA (1993) Hysterectomy and race. Obstet Gynecol 82:757-764

Kloepfer HW, Krafchuk J, Derbes V, Burks J (1958) Hereditary multiple leiomyoma of the skin. Am J Hum Genet 10:48-52

Knowles HJ, Harris AL (2001) Hypoxia and oxidative stress in breast cancer. Hypoxia and tumourigenesis. Breast Cancer Res 3:318-322

Koff A, Cross F, Fisher A, Schumacher J, Leguellec K, Philippe M, Roberts JM (1991) Human cyclin E, a new cyclin that interacts with two members of the CDC2 gene family. Cell 66:1217-1228

Kovacs KA, Lengyel F, Kornyei JL, Vertes Z, Szabo I, Sumegi B, Vertes M (2003) Differential expression of Akt/protein kinase B, Bcl-2 and Bax proteins in human leiomyoma and myometrium. J Steroid Biochem Mol Biol 87:233-240

Kovacs KA, Lengyel F, Vertes Z, Kornyei JL, Gocze PM, Sumegi B, Szabo I, Vertes M (2006) Phosphorylation of PTEN (phosphatase and tensin homologue deleted on chromosome ten) protein is enhanced in human fibromyomatous uteri. J Steroid Biochem Mol Biol

Kurachi O, Matsuo H, Samoto T, Maruo T (2001) Tumor necrosis factor-alpha expression in human uterine leiomyoma and its down-regulation by progesterone. J Clin Endocrinol Metab 86:2275-2280

Kurose K, Mine N, Doi D, Ota Y, Yoneyama K, Konishi H, Araki T, Emi M (2000) Novel gene fusion of COX6C at 8q22-23 to HMGIC at 12q15 in a uterine leiomyoma. Genes Chromosomes Cancer 27:303-307

Kuroyanagi N, Onogi H, Wakabayashi T, Hagiwara M (1998) Novel SR-protein-specific kinase, SRPK2, disassembles nuclear speckles. Biochem Biophys Res Commun 242:357-364

LaFramboise T, Weir BA, Zhao X, Beroukhim R, Li C, Harrington D, Sellers WR, Meyerson M (2005) Allele-specific amplification in cancer revealed by SNP array analysis. PLoS Comput Biol 1:e65

Langer S, Geigl JB, Ehnle S, Gangnus R, Speicher MR (2005) Live cell catapulting and recultivation does not change the karyotype of HCT116 tumor cells. Cancer Genet Cytogenet 161:174-177

Launonen V, Vierimaa O, Kiuru M, Isola J, Roth S, Pukkala E, Sistonen P, Herva R, Aaltonen LA (2001) Inherited susceptibility to uterine leiomyomas and renal cell cancer. Proc Natl Acad Sci U S A 98:3387-3392

Lee BS, Nowak RA (2001) Human leiomyoma smooth muscle cells show increased expression of transforming growth factor-beta 3 (TGF beta 3) and altered responses to the antiproliferative effects of TGF beta. J Clin Endocrinol Metab 86:913-920

Lehmann U, Kreipe H (2001) Real-time PCR analysis of DNA and RNA extracted from formalin-fixed and paraffin-embedded biopsies. Methods 25:409-418

Leppert PC, Baginski T, Prupas C, Catherino WH, Pletcher S, Segars JH (2004) Comparative ultrastructure of collagen fibrils in uterine leiomyomas and normal myometrium. Fertil Steril 82 Suppl 3:1182-1187

Levy B, Mukherjee T, Hirschhorn K (2000) Molecular cytogenetic analysis of uterine leiomyoma and leiomyosarcoma by comparative genomic hybridization. Cancer Genet Cytogenet 121:1-8

Lightowlers RN, Chinnery PF, Turnbull DM, Howell N (1997) Mammalian mitochondrial genetics: heredity, heteroplasmy and disease. Trends Genet 13:450-455

Ligon AH, Morton CC (2001) Leiomyomata: heritability and cytogenetic studies. Hum Reprod Update 7:8-14

Ligon AH, Scott IC, Takahara K, Greenspan DS, Morton CC (2002) PCOLCE deletion and expression analyses in uterine leiomyomata. Cancer Genet Cytogenet 137:133-137

Linder D, Gartler SM (1965) Glucose-6-phosphate dehydrogenase mosaicism: utilization as a cell marker in the study of leiomyomas. Science 150:67-69

Lingaas F, Comstock KE, Kirkness EF, Sorensen A, Aarskaug T, Hitte C, Nickerson ML, Moe L, Schmidt LS, Thomas R, Breen M, Galibert F, Zbar B, Ostrander EA (2003) A mutation in the canine BHD gene is associated with hereditary multifocal renal cystadenocarcinoma and

nodular dermatofibrosis in the German Shepherd dog. Hum Mol Genet 12:3043-3053

Linnartz B, Anglmayer R, Zanssen S (2004) Comprehensive scanning of somatic mitochondrial DNA alterations in acute leukemia developing from myelodysplastic syndromes. Cancer Res 64:1966-1971

Liu VW, Shi HH, Cheung AN, Chiu PM, Leung TW, Nagley P, Wong LC, Ngan HY (2001) High incidence of somatic mitochondrial DNA mutations in human ovarian carcinomas. Cancer Res 61:5998-6001

Liu W, Wang DR, Cao YL (2004) TGF-beta: a fibrotic factor in wound scarring and a potential target for anti-scarring gene therapy. Curr Gene Ther 4:123-136

Locke DP, Segraves R, Nicholls RD, Schwartz S, Pinkel D, Albertson DG, Eichler EE (2004) BAC microarray analysis of 15q11-q13 rearrangements and the impact of segmental duplications. J Med Genet 41:175-182

Lum JJ, DeBerardinis RJ, Thompson CB (2005) Autophagy in metazoans: cell survival in the land of plenty. Nat Rev Mol Cell Biol 6:439-448

Luo X, Ding L, Xu J, Chegini N (2005) Gene expression profiling of leiomyoma and myometrial smooth muscle cells in response to transforming growth factor-beta. Endocrinology 146:1097-1118

MacMahon B, Trichopoulos D, Cole P, Brown J (1982) Cigarette smoking and urinary estrogens. N Engl J Med 307:1062-1065

Maitra A, Cohen Y, Gillespie SE, Mambo E, Fukushima N, Hoque MO, Shah N, Goggins M, Califano J, Sidransky D, Chakravarti A (2004) The Human MitoChip: a high-throughput sequencing microarray for mitochondrial mutation detection. Genome Res 14:812-819

Malhi RS, Breece KE, Shook BA, Kaestle FA, Chatters JC, Hackenberger S, Smith DG (2004) Patterns of mtDNA diversity in northwestern North America. Hum Biol 76:33-54

Man PY, Turnbull DM, Chinnery PF (2002) Leber hereditary optic neuropathy. J Med Genet 39:162-169

Mandahl N, Heim S, Arheden K, Rydholm A, Willen H, Mitelman F (1988) Three major cytogenetic subgroups can be identified among chromosomally abnormal solitary lipomas. Hum Genet 79:203-208

Mangrulkar RS, Ono M, Ishikawa M, Takashima S, Klagsbrun M, Nowak RA (1995) Isolation and characterization of heparin-binding growth factors in human leiomyomas and normal myometrium. Biol Reprod 53:636-646

Marshall LM, Spiegelman D, Barbieri RL, Goldman MB, Manson JE, Colditz GA, Willett WC, Hunter DJ (1997) Variation in the incidence of uterine leiomyoma among premenopausal women by age and race. Obstet Gynecol 90:967-973

Marshall LM, Spiegelman D, Goldman MB, Manson JE, Colditz GA, Barbieri RL, Stampfer MJ, Hunter DJ (1998) A prospective study of reproductive factors and oral contraceptive use in relation to the risk of uterine leiomyomata. Fertil Steril 70:432-439

Martin Negrier ML, Coquet M, Moretto BT, Lacut JY, Dupon M, Bloch B, Lestienne P, Vital C (1998) Partial triplication of mtDNA in maternally transmitted diabetes mellitus and deafness. Am J Hum Genet 63:1227-1232

Martinez-Mir A, Glaser B, Chuang GS, Horev L, Waldman A, Engler DE, Gordon D, Spelman LJ, Hatzibougias I, Green J, Christiano AM, Zlotogorski A (2003) Germline fumarate hydratase mutations in families with multiple cutaneous and uterine leiomyomata. J Invest Dermatol 121:741-744

Marugo M, Centonze M, Bernasconi D, Fazzuoli L, Berta S, Giordano G (1989) Estrogen and progesterone receptors in uterine leiomyomas. Acta Obstet Gynecol Scand 68:731-735

Maruo T, Matsuo H, Shimomura Y, Kurachi O, Gao Z, Nakago S, Yamada T, Chen W, Wang J (2003) Effects of progesterone on growth factor expression in human uterine leiomyoma. Steroids 68:817-824

Maruo T, Ohara N, Wang J, Matsuo H (2004) Sex steroidal regulation of uterine leiomyoma growth and apoptosis. Hum Reprod Update 10:207-220

Massart F, Becherini L, Gennari L, Facchini V, Genazzani AR, Brandi ML (2001) Genotype distribution of estrogen receptor-alpha gene polymorphisms in Italian women with surgical uterine leiomyomas. Fertil Steril 75:567-570

Matsuo H, Kurachi O, Shimomura Y, Samoto T, Maruo T (1999) Molecular bases for the actions of ovarian sex steroids in the regulation of proliferation and apoptosis of human uterine leiomyoma. Oncology 57 Suppl 2:49-58

Matsuo H, Maruo T, Samoto T (1997) Increased expression of Bcl-2 protein in human uterine leiomyoma and its up-regulation by progesterone. J Clin Endocrinol Metab 82:293-299

McKeeby JL, Li X, Zhuang Z, Vortmeyer AO, Huang S, Pirner M, Skarulis MC, James-Newton L, Marx SJ, Lubensky IA (2001) Multiple leiomyomas of the esophagus, lung, and uterus in multiple endocrine neoplasia type 1. Am J Pathol 159:1121-1127

Meek DW (2004) The p53 response to DNA damage. DNA Repair (Amst) 3:1049-1056

Meloni AM, Surti U, Contento AM, Davare J, Sandberg AA (1992) Uterine leiomyomas: cytogenetic and histologic profile. Obstet Gynecol 80:209-217

Mendoza AE, Young R, Orkin SH, Collins T (1990) Increased platelet-derived growth factor A-chain expression in human uterine smooth muscle cells during the physiologic hypertrophy of pregnancy. Proc Natl Acad Sci U S A 87:2177-2181

Mine N, Kurose K, Konishi H, Araki T, Nagai H, Emi M (2001) Fusion of a sequence from HEI10 (14q11) to the HMGIC gene at 12q15 in a uterine leiomyoma. Jpn J Cancer Res 92:135-139

Mitelman F, Johansson B, Mertens F (2006) Mitelman Database of Chromosomal Aberrations in Cancer. Vol. 2006

Mizuno K, Hayashi T, Peyton DH, Bachinger HP (2004) Hydroxylation-induced stabilization of the collagen triple helix. Acetyl-(glycyl-4(R)-hydroxyprolyl-4(R)-hydroxyprolyl)(10)-NH(2) forms a highly stable triple helix. J Biol Chem 279:38072-38078

Moon NS, Rong Zeng W, Premdas P, Santaguida M, Berube G, Nepveu A (2002) Expression of N-terminally truncated isoforms of CDP/CUX is increased in human uterine leiomyomas. Int J Cancer 100:429-432

Moore SD, Herrick SR, Ince TA, Kleinman MS, Cin PD, Morton CC, Quade BJ (2004) Uterine leiomyomata with t(10;17) disrupt the histone acetyltransferase MORF. Cancer Res 64:5570-5577

Mulholland PJ, Fiegler H, Mazzanti C, Gorman P, Sasieni P, Adams J, Jones TA, Babbage JW, Vatcheva R, Ichimura K, East P, Poullikas C, Collins VP, Carter NP, Tomlinson IP, Sheer D (2006) Genomic profiling identifies discrete deletions associated with translocations in glioblastoma multiforme. Cell Cycle 5:783-791

Murphy AA, Morales AJ, Kettel LM, Yen SS (1995) Regression of uterine leiomyomata to the antiprogesterone RU486: dose-response effect. Fertil Steril 64:187-190

Murphy LJ, Murphy LC, Friesen HG (1987) Estrogen induces insulin-like growth factor-I expression in the rat uterus. Mol Endocrinol 1:445-450

Murthy V, Han S, Beauchamp RL, Smith N, Haddad LA, Ito N, Ramesh V (2004) Pam and its ortholog highwire interact with and may negatively regulate the TSC1.TSC2 complex. J Biol Chem 279:1351-1358

Myllyharju J (2003) Prolyl 4-hydroxylases, the key enzymes of collagen biosynthesis. Matrix Biol 22:15-24

Nickerson ML, Warren MB, Toro JR, Matrosova V, Glenn G, Turner ML, Duray P, Merino M, Choyke P, Pavlovich CP, Sharma N, Walther M, Munroe D, Hill R, Maher E, Greenberg C, Lerman MI, Linehan WM, Zbar B, Schmidt LS (2002) Mutations in a novel gene lead to kidney tumors, lung wall defects, and benign tumors of the hair follicle in patients with the Birt-Hogg-Dube syndrome. Cancer Cell 2:157-164

Nilbert M, Heim S, Mandahl N, Floderus UM, Willen H, Akerman M, Mitelman F (1988) Ring formation and structural rearrangements of chromosome 1 as secondary changes in uterine leiomyomas with t(12;14)(q14-15;q23-24). Cancer Genet Cytogenet 36:183-190

Nishi H, Nakada T, Hokamura M, Osakabe Y, Itokazu O, Huang LE, Isaka K (2004) Hypoxia-inducible factor-1 transactivates transforming growth factor-beta3 in trophoblast. Endocrinology 145:4113-4118

Nisolle M, Gillerot S, Casanas-Roux F, Squifflet J, Berliere M, Donnez J (1999) Immunohistochemical study of the proliferation index, oestrogen receptors and progesterone receptors A and B in

leiomyomata and normal myometrium during the menstrual cycle and under gonadotrophin-releasing hormone agonist therapy. Hum Reprod 14:2844-2850

Nor JE, Christensen J, Mooney DJ, Polverini PJ (1999) Vascular endothelial growth factor (VEGF)-mediated angiogenesis is associated with enhanced endothelial cell survival and induction of Bcl-2 expression. Am J Pathol 154:375-384

Osoegawa K, Mammoser AG, Wu C, Frengen E, Zeng C, Catanese JJ, de Jong PJ (2001) A bacterial artificial chromosome library for sequencing the complete human genome. Genome Res 11:483-496

Ozisik YY, Meloni AM, Surti U, Davare J, Sandberg AA (1992) Inversion (X)(p22q13) in a uterine leiomyoma. Cancer Genet Cytogenet 61:131-133

Palman C, Bowen-Pope DF, Brooks JJ (1992) Platelet-derived growth factor receptor (beta-subunit) immunoreactivity in soft tissue tumors. Lab Invest 66:108-115

Pandis N, Heim S, Bardi G, Flodeerus UM, Willen H, Mandahl N, Mitelman F (1991) Chromosome analysis of 96 uterine leiomyomas. Cancer Genet Cytogenet 55:11-18

Paramio JM, Jorcano JL (2002) Beyond structure: do intermediate filaments modulate cell signalling? Bioessays 24:836-844

Parr RL, Maki J, Reguly B, Dakubo GD, Aguirre A, Wittock R, Robinson K, Jakupciak JP, Thayer RE (2006) The pseudo-mitochondrial genome influences mistakes in heteroplasmy interpretation. BMC Genomics 7:185

Patrikis MI, Bryan EJ, Thomas NA, Rice GE, Quinn MA, Baker MS, Campbell IG (2003) Mutation analysis of CDP, TP53, and KRAS in uterine leiomyomas. Mol Carcinog 37:61-64

Penta JS, Johnson FM, Wachsman JT, Copeland WC (2001) Mitochondrial DNA in human malignancy. Mutat Res 488:119-133

Petit MM, Schoenmakers EF, Huysmans C, Geurts JM, Mandahl N, Van de Ven WJ (1999) LHFP, a novel translocation partner gene of HMGIC in a lipoma, is a member of a new family of LHFP-like genes. Genomics 57:438-441

Petros JA, Baumann AK, Ruiz-Pesini E, Amin MB, Sun CQ, Hall J, Lim S, Issa MM, Flanders WD, Hosseini SH, Marshall FF, Wallace DC (2005) mtDNA mutations increase tumorigenicity in prostate cancer. Proc Natl Acad Sci U S A 102:719-724

Pettersen EF, Goddard TD, Huang CC, Couch GS, Greenblatt DM, Meng EC, Ferrin TE (2004) UCSF Chimera--a visualization system for exploratory research and analysis. J Comput Chem 25:1605-1612

Phelan JP (1995) Myomas and pregnancy. Obstet Gynecol Clin North Am 22:801-805

Phillips TM, Gibson JB, Ellison DA (2006) Fumarate hydratase deficiency in monozygotic twins. Pediatr Neurol 35:150-153

Pithukpakorn M, Wei MH, Toure O, Steinbach PJ, Glenn GM, Zbar B, Linehan WM, Toro JR (2006) Fumarate hydratase enzyme activity in lymphoblastoid cells and fibroblasts of individuals in families with hereditary leiomyomatosis and renal cell cancer. J Med Genet 43:755-762

Pokras R, Hufnagel VG (1988) Hysterectomy in the United States, 1965-84. Am J Public Health 78:852-853

Pollack JR, Perou CM, Alizadeh AA, Eisen MB, Pergamenschikov A, Williams CF, Jeffrey SS, Botstein D, Brown PO (1999) Genome-wide analysis of DNA copy-number changes using cDNA microarrays. Nat Genet 23:41-46

Pollard P, Wortham N, Barclay E, Alam A, Elia G, Manek S, Poulsom R, Tomlinson I (2005a) Evidence of increased microvessel density and activation of the hypoxia pathway in tumours from the hereditary leiomyomatosis and renal cell cancer syndrome. J Pathol 205:41-49

Pollard PJ, Briere JJ, Alam NA, Barwell J, Barclay E, Wortham NC, Hunt T, Mitchell M, Olpin S, Moat SJ, Hargreaves IP, Heales SJ, Chung YL, Griffiths JR, Dalgleish A, McGrath JA, Gleeson MJ, Hodgson SV, Poulsom R, Rustin P, Tomlinson IP (2005b) Accumulation of Krebs cycle intermediates and over-expression of HIF1{alpha} in tumours which result from germline FH and SDH mutations. Hum Mol Genet 14:2231-2239

Pollard PJ, Briere JJ, Alam NA, Barwell J, Barclay E, Wortham NC, Hunt T, Mitchell M, Olpin S, Moat SJ, Hargreaves IP, Heales SJ, Chung YL, Griffiths JR, Dalgleish A, McGrath JA, Gleeson MJ, Hodgson SV, Poulsom R, Rustin P, Tomlinson IP (2005c) Accumulation of Krebs cycle intermediates and over-expression of HIF1alpha in tumours which result from germline FH and SDH mutations. Hum Mol Genet 14:2231-2239

Pollard PJ, Wortham NC, Tomlinson IP (2003) The TCA cycle and tumorigenesis: the examples of fumarate hydratase and succinate dehydrogenase. Ann Med 35:632-639

Polleux F, Morrow T, Ghosh A (2000) Semaphorin 3A is a chemoattractant for cortical apical dendrites. Nature 404:567-573

Polyak K, Li Y, Zhu H, Lengauer C, Willson JK, Markowitz SD, Trush MA, Kinzler KW, Vogelstein B (1998) Somatic mutations of the mitochondrial genome in human colorectal tumours. Nat Genet 20:291-293

Poncelet C, Madelenat P, Feldmann G, Walker F, Darai E (2002) Expression of von Willebrand's factor, CD34, CD31, and vascular endothelial growth factor in uterine leiomyomas. Fertil Steril 78:581-586

Prathiba V, Rao KS, Gupta PD (2001) Altered expression of keratins during abnormal wound healing in human skin. Cytobios 104:43-51

Quade BJ, Weremowicz S, Neskey DM, Vanni R, Ladd C, Dal Cin P, Morton CC (2003) Fusion transcripts involving HMGA2 are not a common molecular mechanism in uterine leiomyomata with rearrangements in 12q15. Cancer Res 63:1351-1358

Rakha EA, Green AR, Powe DG, Roylance R, Ellis IO (2006) Chromosome 16 tumor-suppressor genes in breast cancer. Genes Chromosomes Cancer 45:527-535

Ramensky V, Bork P, Sunyaev S (2002) Human non-synonymous SNPs: server and survey. Nucleic Acids Res 30:3894-3900

Rein MS, Friedman AJ, Barbieri RL, Pavelka K, Fletcher JA, Morton CC (1991) Cytogenetic abnormalities in uterine leiomyomata. Obstet Gynecol 77:923-926

Rein MS, Powell WL, Walters FC, Weremowicz S, Cantor RM, Barbieri RL, Morton CC (1998) Cytogenetic abnormalities in uterine myomas are associated with myoma size. Mol Hum Reprod 4:83-86

Richards PA, Richards PD, Tiltman AJ (1998) The ultrastructure of fibromyomatous myometrium and its relationship to infertility. Hum Reprod Update 4:520-525

Roise D, Schatz G (1988) Mitochondrial presequences. J Biol Chem 263:4509-4511

Rose IA (1997) Restructuring the active site of fumarase for the fumarate to malate reaction. Biochemistry 36:12346-12354

Rose IA, Weaver TM (2004) The role of the allosteric B site in the fumarase reaction. Proc Natl Acad Sci U S A 101:3393-3397

Ross R, Raines EW, Bowen-Pope DF (1986a) The biology of platelet-derived growth factor. Cell 46:155-169

Ross RK, Pike MC, Vessey MP, Bull D, Yeates D, Casagrande JT (1986b) Risk factors for uterine fibroids: reduced risk associated with oral contraceptives. Br Med J (Clin Res Ed) 293:359-362

Rozen S, Skaletsky H (2000) Primer3 on the WWW for general users and for biologist programmers. Methods Mol Biol 132:365-386

Rudner EJ, Schwartz OD, Grekin JN (1964) Multiple Cutaneous Leiomyoma in Identical Twins. Arch Dermatol 90:81-82

Rustin P, Bourgeron T, Parfait B, Chretien D, Munnich A, Rotig A (1997) Inborn errors of the Krebs cycle: a group of unusual mitochondrial diseases in human. Biochim Biophys Acta 1361:185-197

Sadan O, van Iddekinge B, Savage N, Robinson M, Zakut H (1988) Ethnic variation in estrogen and progesterone receptor concentration in leiomyoma and normal myometrium. Gynecol Endocrinol 2:275-282

Sadan O, van Iddekinge B, van Gelderen CJ, Savage N, Becker PJ, van der Walt LA, Robinson M (1987) Oestrogen and progesterone receptor concentrations in leiomyoma and normal myometrium. Ann Clin Biochem 24 (Pt 3):263-267

Saito E, Okamoto A, Saito M, Shinozaki H, Takakura S, Yanaihara N, Ochiai K, Tanaka T (2005) Genes associated with the genesis of leiomyoma

of the uterus in a commonly deleted chromosomal region at 7q22. Oncol Rep 13:469-472

Salas A, Yao YG, Macaulay V, Vega A, Carracedo A, Bandelt HJ (2005) A critical reassessment of the role of mitochondria in tumorigenesis. PLoS Med 2:e296

Samadi AR, Lee NC, Flanders WD, Boring JR, 3rd, Parris EB (1996) Risk factors for self-reported uterine fibroids: a case-control study. Am J Public Health 86:858-862

Samonte RV, Eichler EE (2002) Segmental duplications and the evolution of the primate genome. Nat Rev Genet 3:65-72

Sargent MS, Weremowicz S, Rein MS, Morton CC (1994) Translocations in 7q22 define a critical region in uterine leiomyomata. Cancer Genet Cytogenet 77:65-68

Sasabe E, Tatemoto Y, Li D, Yamamoto T, Osaki T (2005) Mechanism of HIF-1alpha-dependent suppression of hypoxia-induced apoptosis in squamous cell carcinoma cells. Cancer Sci 96:394-402

Schoenmakers EF, Huysmans C, Van de Ven WJ (1999) Allelic knockout of novel splice variants of human recombination repair gene RAD51B in t(12;14) uterine leiomyomas. Cancer Res 59:19-23

Schoenmakers EF, Wanschura S, Mols R, Bullerdiek J, Van den Berghe H, Van de Ven WJ (1995) Recurrent rearrangements in the high mobility group protein gene, HMGI-C, in benign mesenchymal tumours. Nat Genet 10:436-444

Sebat J, Lakshmi B, Troge J, Alexander J, Young J, Lundin P, Maner S, Massa H, Walker M, Chi M, Navin N, Lucito R, Healy J, Hicks J, Ye K, Reiner A, Gilliam TC, Trask B, Patterson N, Zetterberg A, Wigler M (2004) Large-scale copy number polymorphism in the human genome. Science 305:525-528

Selak MA, Armour SM, MacKenzie ED, Boulahbel H, Watson DG, Mansfield KD, Pan Y, Simon MC, Thompson CB, Gottlieb E (2005) Succinate links TCA cycle dysfunction to oncogenesis by inhibiting HIF-alpha prolyl hydroxylase. Cancer Cell 7:77-85

Sell SM, Tullis C, Stracner D, Song CY, Gewin J (2005) Minimal interval defined on 7q in uterine leiomyoma. Cancer Genet Cytogenet 157:67-69

Sellner LN, Taylor GR (2004) MLPA and MAPH: new techniques for detection of gene deletions. Hum Mutat 23:413-419

Serini G, Valdembri D, Zanivan S, Morterra G, Burkhardt C, Caccavari F, Zammataro L, Primo L, Tamagnone L, Logan M, Tessier-Lavigne M, Taniguchi M, Puschel AW, Bussolino F (2003) Class 3 semaphorins control vascular morphogenesis by inhibiting integrin function. Nature 424:391-397

Sharp AJ, Locke DP, McGrath SD, Cheng Z, Bailey JA, Vallente RU, Pertz LM, Clark RA, Schwartz S, Segraves R, Oseroff VV, Albertson DG, Pinkel D, Eichler EE (2005) Segmental duplications and copy-number variation in the human genome. Am J Hum Genet 77:78-88

Sherry ST, Ward MH, Kholodov M, Baker J, Phan L, Smigielski EM, Sirotkin K (2001) dbSNP: the NCBI database of genetic variation. Nucleic Acids Res 29:308-311

Shimomura Y, Matsuo H, Samoto T, Maruo T (1998) Up-regulation by progesterone of proliferating cell nuclear antigen and epidermal growth factor expression in human uterine leiomyoma. J Clin Endocrinol Metab 83:2192-2198

Shozu M, Murakami K, Segawa T, Kasai T, Inoue M (2003) Successful treatment of a symptomatic uterine leiomyoma in a perimenopausal woman with a nonsteroidal aromatase inhibitor. Fertil Steril 79:628-631

Shozu M, Sumitani H, Segawa T, Yang HJ, Murakami K, Inoue M (2001) Inhibition of in situ expression of aromatase P450 in leiomyoma of the uterus by leuprorelin acetate. J Clin Endocrinol Metab 86:5405-5411

Shozu M, Sumitani H, Segawa T, Yang HJ, Murakami K, Kasai T, Inoue M (2002) Overexpression of aromatase P450 in leiomyoma tissue is driven primarily through promoter I.4 of the aromatase P450 gene (CYP19). J Clin Endocrinol Metab 87:2540-2548

Shushan A, Rojansky N, Laufer N, Klein BY, Shlomai Z, Levitzki R, Hartzstark Z, Ben-Bassat H (2004) The AG1478 tyrosine kinase

inhibitor is an effective suppressor of leiomyoma cell growth. Hum Reprod 19:1957-1967

Smith SJ (2000) Uterine fibroid embolization. Am Fam Physician 61:3601-3607, 3611-3602

Solovyev V, Kosarev P, Seledsov I, Vorobyev D (2006) Automatic annotation of eukaryotic genes, pseudogenes and promoters. Genome Biol 7 Suppl 1:S10 11-12

Stewart EA (2001a) Uterine Fibroids. Lancet 357:293-298

Stewart EA (2001b) Uterine fibroids. Lancet 357:293-298

Stewart EA, Nowak RA (1998) New concepts in the treatment of uterine leiomyomas. Obstet Gynecol 92:624-627

Strachan T, Read AP (2004) Human Molecular Genetics. Garland Science, London

Sugden MC, Holness MJ (2003) Recent advances in mechanisms regulating glucose oxidation at the level of the pyruvate dehydrogenase complex by PDKs. Am J Physiol Endocrinol Metab 284:E855-862

Sumitani H, Shozu M, Segawa T, Murakami K, Yang HJ, Shimada K, Inoue M (2000) In situ estrogen synthesized by aromatase P450 in uterine leiomyoma cells promotes cell growth probably via an autocrine/intracrine mechanism. Endocrinology 141:3852-3861

Sutovsky P, Van Leyen K, McCauley T, Day BN, Sutovsky M (2004) Degradation of paternal mitochondria after fertilization: implications for heteroplasmy, assisted reproductive technologies and mtDNA inheritance. Reprod Biomed Online 8:24-33

Takahashi K, Kawamura N, Ishiko O, Ogita S (2002) Shrinkage effect of gonadotropin releasing hormone agonist treatment on uterine leiomyomas and t(12;14). Int J Oncol 20:279-283

Takahashi K, Kawamura N, Tsujimura A, Ichimura T, Ito F, Ishiko O, Ogita S (2001a) Association of the shrinkage of uterine leiomyoma treated with GnRH agonist and deletion of long arm of chromosome 7. Int J Oncol 18:1259-1263

Takahashi M, Shibata H, Shimakawa M, Miyamoto M, Mukai H, Ono Y (1999) Characterization of a novel giant scaffolding protein, CG-NAP,

that anchors multiple signaling enzymes to centrosome and the golgi apparatus. J Biol Chem 274:17267-17274

Takahashi T, Nagai N, Oda H, Ohama K, Kamada N, Miyagawa K (2001b) Evidence for RAD51L1/HMGIC fusion in the pathogenesis of uterine leiomyoma. Genes Chromosomes Cancer 30:196-201

Tallini G, Vanni R, Manfioletti G, Kazmierczak B, Faa G, Pauwels P, Bullerdiek J, Giancotti V, Van Den Berghe H, Dal Cin P (2000) HMGI-C and HMGI(Y) immunoreactivity correlates with cytogenetic abnormalities in lipomas, pulmonary chondroid hamartomas, endometrial polyps, and uterine leiomyomas and is compatible with rearrangement of the HMGI-C and HMGI(Y) genes. Lab Invest 80:359-369

Tatusova TA, Madden TL (1999) BLAST 2 Sequences, a new tool for comparing protein and nucleotide sequences. FEMS Microbiol Lett 174:247-250

Taylor RW, Turnbull DM (2005) Mitochondrial DNA mutations in human disease. Nat Rev Genet 6:389-402

Team RDC (2006) R: A Language and Environment for Statistical Computing. R Foundation for Statistical Computing, Vienna, Austria

Telenius H, Pelmear AH, Tunnacliffe A, Carter NP, Behmel A, Ferguson-Smith MA, Nordenskjold M, Pfragner R, Ponder BA (1992) Cytogenetic analysis by chromosome painting using DOP-PCR amplified flow-sorted chromosomes. Genes Chromosomes Cancer 4:257-263

Thompson JD, Higgins DG, Gibson TJ (1994) CLUSTAL W: improving the sensitivity of progressive multiple sequence alignment through sequence weighting, position-specific gap penalties and weight matrix choice. Nucleic Acids Res 22:4673-4680

Tiltman AJ (1985) The effect of progestins on the mitotic activity of uterine fibromyomas. Int J Gynecol Pathol 4:89-96

Tirone F, Shooter EM (1989) Early gene regulation by nerve growth factor in PC12 cells: induction of an interferon-related gene. Proc Natl Acad Sci U S A 86:2088-2092

Tomlinson IP, Alam NA, Rowan AJ, Barclay E, Jaeger EE, Kelsell D, Leigh I, et al. (2002) Germline mutations in FH predispose to dominantly inherited uterine fibroids, skin leiomyomata and papillary renal cell cancer. Nat Genet 30:406-410

Toro JR, Nickerson ML, Wei MH, Warren MB, Glenn GM, Turner ML, Stewart L, Duray P, Tourre O, Sharma N, Choyke P, Stratton P, Merino M, Walther MM, Linehan WM, Schmidt LS, Zbar B (2003) Mutations in the fumarate hydratase gene cause hereditary leiomyomatosis and renal cell cancer in families in North America. Am J Hum Genet 73:95-106

Torroni A, Huoponen K, Francalacci P, Petrozzi M, Morelli L, Scozzari R, Obinu D, Savontaus ML, Wallace DC (1996) Classification of European mtDNAs from an analysis of three European populations. Genetics 144:1835-1850

Trauernicht AM, Boyer TG (2003) BRCA1 and estrogen signaling in breast cancer. Breast Dis 18:11-20

Treloar SA, Martin NG, Dennerstein L, Raphael B, Heath AC (1992) Pathways to hysterectomy: insights from longitudinal twin research. Am J Obstet Gynecol 167:82-88

Trisciuoglio D, Iervolino A, Zupi G, Del Bufalo D (2005) Involvement of PI3K and MAPK signaling in bcl-2-induced vascular endothelial growth factor expression in melanoma cells. Mol Biol Cell 16:4153-4162

Tsibris JC, Segars J, Coppola D, Mane S, Wilbanks GD, O'Brien WF, Spellacy WN (2002) Insights from gene arrays on the development and growth regulation of uterine leiomyomata. Fertil Steril 78:114-121

Turc-Carel C, Dal Cin P, Boghosian L, Terk-Zakarian J, Sandberg AA (1988) Consistent breakpoints in region 14q22-q24 in uterine leiomyoma. Cancer Genet Cytogenet 32:25-31

van der Heijden O, Chiu HC, Park TC, Takahashi H, LiVolsi VA, Risinger JI, Barrett JC, Berchuck A, Evans AC, Behbakht K, Menzin AW, Liu PC, Benjamin I, Morgan MA, King SA, Rubin SC, Boyd J (1998) Allelotype analysis of uterine leiomyoma: localization of a potential

tumor suppressor gene to a 4-cM region of chromosome 7q. Mol Carcinog 23:243-247

Vanni R, Lecca U, Faa G (1991) Uterine leiomyoma cytogenetics II. Report of forty cases. Cancer Genet Cytogenet 53:247-256

Vanni R, Schoenmakers EF, Andria M (1999) Deletion 7q in uterine leiomyoma: fluorescence in situ hybridization characterization on primary cytogenetic preparations. Cancer Genet Cytogenet 113:183-187

Varol A, Stapleton K, Roscioli T (2006) The syndrome of hereditary leiomyomatosis and renal cell cancer (HLRCC): The clinical features of an individual with a fumarate hydratase gene mutation. Australas J Dermatol 47:274-276

Viville B, Charnock-Jones DS, Sharkey AM, Wetzka B, Smith SK (1997) Distribution of the A and B forms of the progesterone receptor messenger ribonucleic acid and protein in uterine leiomyomata and adjacent myometrium. Hum Reprod 12:815-822

Walker CL, Hunter D, Everitt JI (2003) Uterine leiomyoma in the Eker rat: a unique model for important diseases of women. Genes Chromosomes Cancer 38:349-356

Walker CL, Stewart EA (2005) Uterine fibroids: the elephant in the room. Science 308:1589-1592

Walker RH, Reed WB (1972) Genetic cutaneous disorders with gynecologic tumors. Trans Pac Coast Obstet Gynecol Soc 40:30-37

Wallace DC, Brown MD, Lott MT (1999) Mitochondrial DNA variation in human evolution and disease. Gene 238:211-230

Wang HY, Lin W, Dyck JA, Yeakley JM, Songyang Z, Cantley LC, Fu XD (1998) SRPK2: a differentially expressed SR protein-specific kinase involved in mediating the interaction and localization of pre-mRNA splicing factors in mammalian cells. J Cell Biol 140:737-750

Watanabe K, Ogura G, Suzuki T (2003) Leiomyoblastoma of the uterus: an immunohistochemical and electron microscopic study of distinctive tumours with immature smooth muscle cell differentiation mimicking fetal uterine myocytes. Histopathology 42:379-386

Watson JD, Crick FH (1953) The structure of DNA. Cold Spring Harb Symp Quant Biol 18:123-131

Watters JJ, Chun TY, Kim YN, Bertics PJ, Gorski J (2000) Estrogen modulation of prolactin gene expression requires an intact mitogen-activated protein kinase signal transduction pathway in cultured rat pituitary cells. Mol Endocrinol 14:1872-1881

Weaver T, Banaszak L (1996) Crystallographic studies of the catalytic and a second site in fumarase C from Escherichia coli. Biochemistry 35:13955-13965

Weaver T, Lees M, Banaszak L (1997) Mutations of fumarase that distinguish between the active site and a nearby dicarboxylic acid binding site. Protein Sci 6:834-842

Weaver TM (2000) The pi-helix translates structure into function. Protein Sci 9:201-206

Weaver TM, Levitt DG, Donnelly MI, Stevens PP, Banaszak LJ (1995) The multisubunit active site of fumarase C from Escherichia coli. Nat Struct Biol 2:654-662

Wei J, Chiriboga L, Mizuguchi M, Yee H, Mittal K (2005) Expression profile of tuberin and some potential tumorigenic factors in 60 patients with uterine leiomyomata. Mod Pathol 18:179-188

Wei JJ, Chiriboga L, Arslan AA, Melamed J, Yee H, Mittal K (2006a) Ethnic differences in expression of the dysregulated proteins in uterine leiomyomata. Hum Reprod 21:57-67

Wei MH, Toure O, Glenn GM, Pithukpakorn M, Neckers L, Stolle C, Choyke P, Grubb R, Middelton L, Turner ML, Walther MM, Merino MJ, Zbar B, Linehan WM, Toro JR (2006b) Novel mutations in FH and expansion of the spectrum of phenotypes expressed in families with hereditary leiomyomatosis and renal cell cancer. J Med Genet 43:18-27

Wilkinson N, Rollason TP (2001) Recent advances in the pathology of smooth muscle tumours of the uterus. Histopathology 39:331-341

Wittwer CT, Reed GH, Gundry CN, Vandersteen JG, Pryor RJ (2003) High-resolution genotyping by amplicon melting analysis using LCGreen. Clin Chem 49:853-860

Wood T (1986) Physiological functions of the pentose phosphate pathway. Cell Biochem Funct 4:241-247

Wu X, Blanck A, Olovsson M, Henriksen R, Lindblom B (2002) Expression of Bcl-2, Bcl-x, Mcl-1, Bax and Bak in human uterine leiomyomas and myometrium during the menstrual cycle and after menopause. J Steroid Biochem Mol Biol 80:77-83

Xing YP, Powell WL, Morton CC (1997) The del(7q) subgroup in uterine leiomyomata: genetic and biologic characteristics. Further evidence for the secondary nature of cytogenetic abnormalities in the pathobiology of uterine leiomyomata. Cancer Genet Cytogenet 98:69-74

Yang L, Cao Z, Li F, Post DE, Van Meir EG, Zhong H, Wood WC (2004) Tumor-specific gene expression using the survivin promoter is further increased by hypoxia. Gene Ther 11:1215-1223

Yang X, Li J, Qin H, Yang H, Li J, Zhou P, Liang Y, Han H (2005) Mint represses transactivation of the type II collagen gene enhancer through interaction with alpha A-crystallin-binding protein 1. J Biol Chem 280:18710-18716

Yang YH, Dudoit S, Luu P, Lin DM, Peng V, Ngai J, Speed TP (2002) Normalization for cDNA microarray data: a robust composite method addressing single and multiple slide systematic variation. Nucleic Acids Res 30:e15

Yeung RS, Xiao GH, Everitt JI, Jin F, Walker CL (1995) Allelic loss at the tuberous sclerosis 2 locus in spontaneous tumors in the Eker rat. Mol Carcinog 14:28-36

Yeung RS, Xiao GH, Jin F, Lee WC, Testa JR, Knudson AG (1994) Predisposition to renal carcinoma in the Eker rat is determined by germ-line mutation of the tuberous sclerosis 2 (TSC2) gene. Proc Natl Acad Sci U S A 91:11413-11416

Ylisaukko-oja SK, Cybulski C, Lehtonen R, Kiuru M, Matyjasik J, Szymanska A, Szymanska-Pasternak J, Dyrskjot L, Butzow R, Orntoft TF, Launonen V, Lubinski J, Aaltonen LA (2006) Germline fumarate hydratase mutations in patients with ovarian mucinous cystadenoma. Eur J Hum Genet 14:880-883

Yokoyama A, Somervaille TC, Smith KS, Rozenblatt-Rosen O, Meyerson M, Cleary ML (2005) The menin tumor suppressor protein is an essential oncogenic cofactor for MLL-associated leukemogenesis. Cell 123:207-218

Yun CY, Velazquez-Dones AL, Lyman SK, Fu XD (2003) Phosphorylation-dependent and -independent nuclear import of RS domain-containing splicing factors and regulators. J Biol Chem 278:18050-18055

Zaslawski R, Surowiak P, Dziegiel P, Pretnik L, Zabel M (2001) Analysis of the expression of estrogen and progesteron receptors, and of PCNA and Ki67 proliferation antigens, in uterine myomata cells in relation to the phase of the menstrual cycle. Med Sci Monit 7:908-913

Zeng WR, Scherer SW, Koutsilieris M, Huizenga JJ, Filteau F, Tsui LC, Nepveu A (1997) Loss of heterozygosity and reduced expression of the CUTL1 gene in uterine leiomyomas. Oncogene 14:2355-2365

Zhang ZL, Zhang Y, Zhou JH (2005) [Expression of bcl-2 and bax protein in uterine leiomyosarcomas and leiomyomas]. Zhong Nan Da Xue Xue Bao Yi Xue Ban 30:183-186

Zhou J, Mochizuki T, Smeets H, Antignac C, Laurila P, de Paepe A, Tryggvason K, Reeders ST (1993) Deletion of the paired alpha 5(IV) and alpha 6(IV) collagen genes in inherited smooth muscle tumors. Science 261:1167-1169

Zhou S, Kassauei K, Cutler DJ, Kennedy GC, Sidransky D, Maitra A, Califano J (2006) An oligonucleotide microarray for high-throughput sequencing of the mitochondrial genome. J Mol Diagn 8:476-482

Zhu Y, Bond J, Thomas P (2003) Identification, classification, and partial characterization of genes in humans and other vertebrates homologous to a fish membrane progestin receptor. Proc Natl Acad Sci U S A 100:2237-2242

Appendix 1

BAC clones used in the chromosome 7q genomic microarray

A1.1 Control Clones

554 BAC clones were selected at approximately 5 megabase intervals from the set of clones selected by Fiegler *et al* for the 1Mb resolution genomic microaray (Fiegler et al. 2003). Clones were selected on the basis of previous experiments using the 1Mb genomic microarray. Clones consistently producing unexpected results were removed and adjacent alternatives selected. These clones were selected to act as a whole genome normalisation control. DNA for these clones was extracted by Regina Regan at the Wellcome Trust centre for Human Genetics in Oxford. Clones producing unexpected hybridisations in the final array are highlighted in yellow.

Clone Name	Chromosome	Start	End	Midpoint Position	Clone Size
RP3-438L4	1	6734038	6860851	6797444.5	126813
RP4-575L21	1	9762410	9856831	9809620.5	94421
RP4-560M15	1	14820829	14955897	14888363	135068
RP1-184J9	1	22483929	22584879	22534404	100950
RP4-669K10	1	28332168	28467987	28400077.5	135819
RP11-114B7	1	32528048	32700923	32614485.5	172875
RP4-731G4	1	36258282	36397220	36327751	138938
RP1-118J21	1	40071667	40238162	40154914.5	166495
RP11-428D12	1	48503255	48688954	48596104.5	185699
RP11-117D22	1	53095140	53274113	53184626.5	178973
RP11-5P4	1	62780646	62959676	62870161	179030

RP4-547N15	1	66824623	66955867	66890245	131244
RP11-175G14	1	71539699	71706962	71623330.5	167263
RP11-297N6	1	75462153	75643352	75552752.5	181199
RP11-398N17	1	81943890	82121042	82032466	177152
RP4-722L13	1	85384438	85479558	85431998	95120
RP11-298P9	1	89861338	90022603	89941970.5	161265
RP11-14O19	1	95126453	95304425	95215439	177972
RP11-260K3	1	99189373	99354410	99271891.5	165037
RP11-202K23	1	101884899	102025519	101955209	140620
RP5-916A15	1	106115383	106239985	106177684	124602
RP11-20F20	1	108740654	108905960	108823307	165306
RP5-831G13	1	109116674	109232785	109174729.5	116111
RP4-663N10	1	114959020	115136085	115047552.5	177065
RP4-610L12	1	118706067	118826176	118766121.5	120109
RP4-706A17	1	143505085	143626363	143565724	121278
RP11-216N14	1	150463354	150613519	150538436.5	150165
RP11-172I6	1	152857449	152909842	152883645.5	52393
RP11-430G6	1	159642370	159818401	159730385.5	176031
RP4-702J19	1	164681223	164781866	164731544.5	100643
RP3-433G19	1	171402964	171464845	171433904.5	61881
RP11-163L4	1	174289185	174469501	174379343	180316
RP11-71D4	1	179149277	179299768	179224522.5	150491
RP11-108M21	1	183696640	183867278	183781959	170638
RP11-3B17	1	187174084	187325974	187250029	151890
RP11-552K17	1	192685962	192837310	192761636	151348
RP11-469A15	1	196748763	196914264	196831513.5	165501
RP11-383G10	1	201436746	201617779	201527262.5	181033

RP5-879K22	1	207161851	207299528	207230689.5	137677
RP11-438G15	1	212236238	212440909	212338573.5	204671
RP11-492K2	1	216023276	216223712	216123494	200436
RP11-105I12	1	220324315	220505567	220414941	181252
RP11-99J16	1	227364296	227563459	227463877.5	199163
RP5-940F7	1	232351444	232515453	232433448.5	164009
RP11-553N16	1	238232307	238376273	238304290	143966
RP11-438H8	1	243994883	244162295	244078589	167412
RP11-292A20	2	4443265	4601782	4522523.5	158517
RP11-413M20	2	27530765	27726644	27628704.5	195879
RP11-288C18	2	36948031	37131949	37039990	183918
RP11-299C5	2	42438000	42622949	42530474.5	184949
RP11-27C22	2	45998023	46189235	46093629	191212
RP11-335O22	2	52297470	52477417	52387443.5	179947
RP11-152O18	2	55771556	55938781	55855168.5	167225
RP11-422B1	2	58197781	58322040	58259910.5	124259
RP11-52F10	2	62699704	62846957	62773330.5	147253
RP11-304A15	2	68964455	69128448	69046451.5	163993
RP11-343N14	2	72351544	72532758	72442151	181214
RP11-9O10	2	78038303	78192922	78115612.5	154619
RP11-294I20	2	89043591	89209246	89126418.5	165655
RP11-542D13	2	97710653	97941078	97825865.5	230425
RP11-30G7	2	100355304	100530412	100442858	175108
RP11-350B7	2	105105221	105287572	105196396.5	182351
RP11-528G9	2	110363698	110539320	110451509	175622
RP11-412A2	2	115983908	116126580	116055244	142672
RP11-19E11	2	119472589	119622682	119547635.5	150093

RP11-207G14	2	129826704	129989789	129908246.5	163085
RP11-1L22	2	133192012	133371737	133281874.5	179725
RP11-279M2	2	141694696	141869885	141782290.5	175189
RP11-207O14	2	146897423	147081828	146989625.5	184405
RP11-329H24	2	150455875	150656782	150556328.5	200907
RP11-266L10	2	155783329	155962516	155872922.5	179187
RP11-440P12	2	161852242	162042452	161947347	190210
RP11-5J4	2	164341415	164503712	164422563.5	162297
RP11-551O2	2	170052584	170193044	170122814	140460
RP11-176L20	2	172373348	172540036	172456692	166688
RP4-745K6	2	177126136	177217628	177171882	91492
RP11-391P1	2	180577822	180756826	180667324	179004
RP11-29E4	2	186051834	186257023	186154428.5	205189
RP11-172N20	2	189111537	189281464	189196500.5	169927
RP11-363G3	2	194026091	194196561	194111326	170470
RP11-347P5	2	196794111	197009289	196901700	215178
RP11-329O10	2	203573149	203736110	203654629.5	162961
RP11-470J24	2	207080568	207279068	207179818	198500
RP11-560C24	2	213416750	213602967	213509858.5	186217
RP11-307A11	2	217317794	217482271	217400032.5	164477
RP11-444B5	2	221590943	221767798	221679370.5	176855
RP11-551D18	2	224273832	224403384	224338608	129552
RP11-95E11	3	3151017	3321810	3236413.5	170793
RP11-129J10	3	5044648	5197799	5121223.5	153151
RP11-163D23	3	12607628	12752839	12680233.5	145211
RP11-80D24	3	17198216	17362120	17280168	163904
RP11-16E8	3	21449056	21617033	21533044.5	167977

RP11-421F9	3	25322783	25426788	25374785.5	104005
RP11-69K20	3	30150307	30322389	30236348	172082
RP11-524O15	3	32325331	32522440	32423885.5	197109
RP11-129K12	3	36705146	36874417	36789781.5	169271
RP4-613B23	3	42444041	42629201	42536621	185160
RP11-88B8	3	47702308	47891600	47796954	189292
RP11-89F17	3	51272113	51440611	51356362	168498
RP11-58O15	3	55485886	55677395	55581640.5	191509
RP11-170K19	3	59581144	59755752	59668448	174608
RP11-108A8	3	63134788	63276188	63205488	141400
RP11-152N21	3	69124542	69282193	69203367.5	157651
RP11-252O10	3	73186876	73335038	73260957	148162
RP11-442C9	3	81370437	81532918	81451677.5	162481
RP11-474M18	3	84346772	84524804	84435788	178032
RP11-12A13	3	95891701	96049008	95970354.5	157307
RP11-121C1	3	100289280	100344133	100316706.5	54853
RP11-115B22	3	105613784	105769982	105691883	156198
RP11-561O4	3	108071506	108263827	108167666.5	192321
RP11-402J7	3	112541586	112738134	112639860	196548
RP11-58D2	3	116078196	116228489	116153342.5	150293
RP11-295B8	3	119474842	119621371	119548106.5	146529
RP11-299J3	3	123285258	123456636	123370947	171378
RP11-71H17	3	125709391	125875461	125792426	166070
RP11-129J11	3	131256145	131415278	131335711.5	159133
RP11-91K8	3	134417031	134570680	134493855.5	153649
RP11-197K1	3	137505672	137686933	137596302.5	181261
RP11-397E9	3	140070644	140250349	140160496.5	179705

RP11-165M11	3	144645061	144830491	144737776	185430
RP11-21M4	3	147509084	147650355	147579719.5	141271
RP11-251C9	3	151899193	152078689	151988941	179496
RP11-117L15	3	156440983	156608976	156524979.5	167993
CTD-2049J23	3	160880530	161037608	160959069	157078
RP11-491K7	3	166828293	166999550	166913921.5	171257
RP11-3K16	3	170648661	170851376	170750018.5	202715
RP11-163H6	3	173100478	173267359	173183918.5	166881
RP11-71G7	3	177604260	177768984	177686622	164724
RP11-682A21	3	180212677	180368586	180290631.5	155909
RP11-445C21	3	182217326	182390040	182303683	172714
RP11-252K11	3	197315053	197479187	197397120	164134
RP3-323A24	4	2644489	2700384	2672436.5	55895
RP11-168E17	4	11509028	11670803	11589915.5	161775
RP11-441O12	4	18107264	18293016	18200140	185752
RP11-406E22	4	22991214	23141025	23066119.5	149811
RP11-390C19	4	29460286	29637752	29549019	177466
RP11-135M12	4	35365058	35558567	35461812.5	193509
RP11-213G21	4	38333901	38515731	38424816	181830
RP11-354H17	4	41201012	41383758	41292385	182746
RP11-100N21	4	47419175	47587351	47503263	168176
RP11-18M17	4	54201059	54359963	54280511	158904
RP11-738E22	4	57589610	57805706	57697658	216096
RP11-340A13	4	59788461	59961559	59875010	173098
RP11-204H9	4	65123062	65288065	65205563.5	165003
RP11-1J11	4	72420936	72587412	72504174	166476
RP11-224D4	4	77956327	78117137	78036732	160810

RP11-377G16	4	81489983	81684140	81587061.5	194157
RP11-107G7	4	88905288	89077149	88991218.5	171861
RP11-115D19	4	90928929	91098412	91013670.5	169483
RP11-16I17	4	94836626	95012134	94924380	175508
RP11-242D9	4	98796646	99007208	98901927	210562
RP11-13F20	4	101684333	101845851	101765092	161518
RP11-122B24	4	105462123	105623074	105542598.5	160951
RP11-109F18	4	108812660	108970859	108891759.5	158199
RP11-402J6	4	113751654	113953271	113852462.5	201617
RP11-100C9	4	120062268	120241680	120151974	179412
RP11-15O17	4	126528468	126693514	126610991	165046
RP11-209D20	4	130174860	130369188	130272024	194328
RP11-335K21	4	134545830	134725170	134635500	179340
RP11-425J20	4	138619496	138796522	138708009	177026
RP11-141I1	4	144001065	144155358	144078211.5	154293
RP11-425A23	4	149001370	149198594	149099982	197224
RP11-64M20	4	151778069	151965491	151871780	187422
RP11-27G13	4	156620582	156798785	156709683.5	178203
RP11-171N4	4	157912091	158086952	157999521.5	174861
RP11-440L13	4	168193229	168367049	168280139	173820
RP11-119J20	4	173588498	173758054	173673276	169556
RP11-287F9	4	176695234	176916111	176805672.5	220877
RP11-396I22	4	181563401	181770189	181666795	206788
RP11-228F3	4	186219769	186387681	186303725	167912
RP11-121L11	5	3405732	3576991	3491361.5	171259
RP11-114M17	5	6495614	6688370	6591992	192756
RP11-215G15	5	10624443	10804444	10714443.5	180001

RP11-269G2	5	13197866	13354720	13276293	156854
RP11-19O2	5	16173373	16338191	16255782	164818
RP11-46C20	5	27450982	27605795	27528388.5	154813
RP11-53L13	5	32706750	32880188	32793469	173438
RP11-7M4	5	36952938	37141434	37047186	188496
RP11-274J22	5	41626760	41793769	41710264.5	167009
RP4-592P18	5	51018605	51167212	51092908.5	148607
RP11-506H20	5	54497449	54698853	54598151	201404
RP11-16B11	5	59275673	59425673	59350673	150000
RP11-18K15	5	63260284	63433944	63347114	173660
RP11-421A17	5	67432932	67611836	67522384	178904
RP11-399M5	5	73128988	73317911	73223449.5	188923
CTC-1347N9	5	73875863	74044548	73960205.5	168685
RP11-538B23	5	79939288	80085749	80012518.5	146461
RP11-463C5	5	82573059	82745846	82659452.5	172787
RP11-302L17	5	89567617	89731589	89649603	163972
CTC-1366N20	5	94530747	94666121	94598434	135374
RP11-195A20	5	98957041	99114398	99035719.5	157357
RP11-528K12	5	102995361	103193051	103094206	197690
RP11-276O18	5	109352836	109509336	109431086	156500
RP11-467F22	5	112491785	112698521	112595153	206736
RP11-321G16	5	118274416	118447293	118360854.5	172877
RP11-48C14	5	124182286	124353907	124268096.5	171621
CTC-1352M6	5	127600154	127762073	127681113.5	161919
RP1-241C15	5	131368738	131580952	131474845	212214
RP11-114H21	5	135742954	135919021	135830987.5	176067
RP1-98O22	5	137715529	137836260	137775894.5	120731

CTD-2185H17	5	142508071	142745792	142626931.5	237721
CTB-1176I15	5	147872964	147929136	147901050	56172
CTB-1013H5	5	149410404	149497218	149453811	86814
CTC-1263A14	5	154420715	154524576	154472645.5	103861
CTC-1279E3	5	159198172	159281832	159240002	83660
RP11-170P5	5	165680688	165844015	165762351.5	163327
RP11-420L4	5	168985026	169142475	169063750.5	157449
RP11-15N12	6	3337049	3516147	3426598	179098
RP11-320C15	6	6692138	6850876	6771507	158738
RP3-365E2	6	14490663	14628392	14559527.5	137729
RP11-408C8	6	18892364	19085810	18989087	193446
RP11-204E9	6	21466595	21653117	21559856	186522
RP11-289G11	6	25437140	25631948	25534544	194808
RP11-150A6	6	29275623	29450291	29362957	174668
RP3-468B3	6	33769697	33906582	33838139.5	136885
RP3-350J21	6	38883787	39022618	38953202.5	138831
RP11-501I18	6	42709208	42849343	42779275.5	140135
RP11-334H12	6	48718029	48886789	48802409	168760
RP3-341E18	6	52889365	52981922	52935643.5	92557
RP11-199A24	6	58503657	58682040	58592848.5	178383
RP3-324B8	6	66770251	66915033	66842642	144782
RP11-111D8	6	72050748	72235703	72143225.5	184955
RP11-343P23	6	77517433	77681806	77599619.5	164373
RP11-379B8	6	82396598	82583994	82490296	187396
RP11-106G15	6	88179481	88349676	88264578.5	170195
RP1-154G14	6	91144723	91245716	91195219.5	100993
RP11-572N15	6	96215454	96396616	96306035	181162

RP1-167P23	6	101293237	101434643	101363940	141406
RP3-454N4	6	105931842	106046929	105989385.5	115087
RP1-71D21	6	110558902	110677884	110618393	118982
RP1-230I3	6	118569617	118681380	118625498.5	111763
RP1-84N20	6	125282636	125434684	125358660	152048
RP11-593A16	6	130125822	130298637	130212229.5	172815
RP11-323N12	6	135426583	135611804	135519193.5	185221
RP11-368P1	6	142115804	142254889	142185346.5	139085
RP11-545I5	6	145958830	146159631	146059230.5	200801
RP3-443C4	6	152007969	152101913	152054941	93944
RP11-266C7	6	158158294	158354215	158256254.5	195921
RP11-300M24	6	164974796	165158137	165066466.5	183341
CTB-57H24	6	170456322	170561549	170508935.5	105227
RP11-172O13	7	5448528	5590890	5519709	142362
RP11-505D17	7	7691571	7869931	7780751	178360
RP5-855F16	7	10648774	10744118	10696446	95344
RP11-512E16	7	13852390	14023199	13937794.5	170809
RP11-486P11	7	19740880	19929817	19835348.5	188937
RP11-343P21	7	24231396	24400925	24316160.5	169529
RP4-596O9	7	28201516	28345393	28273454.5	143877
RP11-179B11	7	33885182	34034436	33959809	149254
RP11-571N3	7	45697110	45864440	45780775	167330
RP4-756H11	7	65407869	65542912	65475390.5	135043
RP11-156A14	7	67306381	67464348	67385364.5	157967
RP11-450O3	7	71834041	72029592	71931816.5	195551
RP4-799O8	7	75950356	76121892	76036124	171536
RP5-1136A10	7	80148213	80288468	80218340.5	140255

RP11-313H6	7	83231894	83395664	83313779	163770
RP11-212B1	7	86666503	86814646	86740574.5	148143
RP5-998H4	7	88431567	88556269	88493918	124702
RP5-1099C19	7	91733496	91850768	91792132	117272
RP4-550A13	7	98465321	98544836	98505078.5	79515
RP5-1059M17	7	100735998	100909966	100822982	173968
RP11-374M7	7	116081375	116235248	116158311.5	153873
RP11-88K4	7	136015635	136168619	136092127	152984
RP5-1173P7	7	140076153	140242117	140159135	165964
RP4-721B17	7	143536315	143643109	143589712	106794
RP11-302C22	7	146768222	146943332	146855777	175110
RP11-19N21	8	16209078	16383596	16296337	174518
RP11-667P13	8	19608613	19660956	19634784.5	52343
RP11-177H13	8	22871911	23051255	22961583	179344
RP11-473A17	8	30682363	30862460	30772411.5	180097
RP11-51K12	8	40122856	40271044	40196950	148188
RP11-567J20	8	49071182	49246550	49158866	175368
RP11-11C20	8	52337416	52481168	52409292	143752
RP11-342K10	8	57478832	57662499	57570665.5	183667
RP3-491L6	8	61479259	61554406	61516832.5	75147
RP11-366K18	8	66739606	66904686	66822146	165080
RP11-351E7	8	73059447	73238151	73148799	178704
RP11-48D4	8	77430450	77594059	77512254.5	163609
RP11-62E9	8	81464963	81656320	81560641.5	191357
RP5-1098O20	8	90547005	90666572	90606788.5	119567
RP11-320N21	8	95578454	95777663	95678058.5	199209
RP11-21E8	8	101895464	102075830	101985647	180366

RP11-132E3	8	104817649	105002116	104909882.5	184467
RP11-115M13	8	108579701	108736971	108658336	157270
RP11-11A18	8	113091472	113259535	113175503.5	168063
RP11-455I9	8	118789437	118973003	118881220	183566
RP11-96B2	8	123125490	123297613	123211551.5	172123
RP11-17E16	8	130164147	130303786	130233966.5	139639
RP11-45B19	8	135192573	135355179	135273876	162606
RP11-172M18	8	138922576	139068480	138995528	145904
CTC-489D14	8	145662838	145767796	145715317	104958
RP11-19G1	9	9932073	10130653	10031363	198580
RP11-413D24	9	13729563	13912972	13821267.5	183409
RP11-503K16	9	18579957	18743122	18661539.5	163165
RP11-33K8	9	24090707	24243454	24167080.5	152747
RP11-264J11	9	28670843	28840515	28755679	169672
RP11-265B8	9	65119518	65307680	65213599	188162
RP11-71A24	9	69188839	69357940	69273389.5	169101
RP11-174K23	9	74875373	75056851	74966112	181478
RP11-384P5	9	76523026	76704628	76613827	181602
RP11-40C6	9	83573764	83740617	83657190.5	166853
RP11-8B23	9	85977930	86146744	86062337	168814
RP11-333I7	9	90635179	90810468	90722823.5	175289
RP11-23J9	9	93498478	93663909	93581193.5	165431
RP11-96L7	9	95300677	95476573	95388625	175896
RP11-75J9	9	97899288	98058418	97978853	159130
RP11-287A8	9	101601630	101774553	101688091.5	172923
RP11-470J20	9	106331849	106509763	106420806	177914
RP11-78H18	9	111021219	111179918	111100568.5	158699

RP11-58C3	9	112325822	112495168	112410495	169346
RP11-360A18	9	116149987	116332280	116241133.5	182293
RP11-101K10	9	120541770	120704608	120623189	162838
RP11-545E17	9	124915364	125082027	124998695.5	166663
RP11-295G24	9	128975111	129184321	129079716	209210
RP11-298K24	10	6387907	6586872	6487389.5	198965
RP11-730A19	10	13168712	13364914	13266813	196202
RP11-37P5	10	16149169	16307032	16228100.5	157863
RP11-129O7	10	25251193	25417053	25334123	165860
RP11-207K8	10	29951571	30125165	30038368	173594
RP11-22G4	10	34581983	34749229	34665606	167246
RP11-38B21	10	44319977	44479480	44399728.5	159503
RP11-534N5	10	45880691	46088516	45984603.5	207825
RP11-47O13	10	53120747	53291835	53206291	171088
RP11-430K23	10	56932219	57104585	57018402	172366
RP11-166B18	10	62124592	62291417	62208004.5	166825
RP11-161L14	10	67034063	67184024	67109043.5	149961
RP11-816P15	10	70892063	71090978	70991520.5	198915
RP11-506B4	10	75947886	76118719	76033302.5	170833
RP11-90J7	10	79910369	80067437	79988903	157068
RP11-20E23	10	82620395	82789946	82705170.5	169551
RP11-165M8	10	89673152	89836182	89754667	163030
RP11-80H5	10	91456500	91604895	91530697.5	148395
RP11-162K11	10	95915414	96065358	95990386	149944
RP11-19C6	10	99761532	99922766	99842149	161234
RP11-724N1	10	104793687	104954739	104874213	161052
RP11-478K18	10	109431987	109629942	109530964.5	197955

RP11-426E5	10	114001336	114197992	114099664	196656
RP11-264E18	10	129972701	130134744	130053722.5	162043
RP11-206L19	11	11764177	11910857	11837517	146680
RP11-4B7	11	16709495	16884205	16796850	174710
RP11-121C18	11	21648954	21829680	21739317	180726
RP11-406D1	11	27967439	28140995	28054217	173556
RP11-163K24	11	62765180	62915180	62840180	150000
RP5-1083G3	11	31858329	31983998	31921163.5	125669
RP11-31I23	11	34842421	35018652	34930536.5	176231
RP11-194C13	11	36752876	36935109	36843992.5	182233
RP11-220C23	11	41011253	41172121	41091687	160868
RP11-12C11	11	44954201	45121167	45037684	166966
RP11-131J4	11	55331941	55500242	55416091.5	168301
RP11-399J13	11	65057551	65245484	65151517.5	187933
RP11-569N5	11	68565746	68772008	68668877	206262
RP11-598K3	11	70851736	71024499	70938117.5	172763
RP11-512I24	11	71141644	71334855	71238249.5	193211
RP11-179A16	11	81847029	81988303	81917666	141274
RP11-291N1	11	91502319	91708399	91605359	206080
RP11-349I16	11	94545261	94706664	94625962.5	161403
RP11-45C5	11	100674260	100828417	100751338.5	154157
RP11-725J15	11	102782437	102849564	102816000.5	67127
RP11-569A20	11	106612629	106780908	106696768.5	168279
RP11-241D13	11	108069316	108250858	108160087	181542
RP11-10N17	11	125016509	125174951	125095730	158442
RP11-264F23	12	4183840	4350675	4267257.5	166835
RP11-277E18	12	7927138	7998956	7963047	71818

RP11-144O23	12	10853956	11027690	10940823	173734
RP11-328P13	12	19289723	19425674	19357698.5	135951
RP11-230B21	12	28632872	28783457	28708164.5	150585
RP11-333D23	12	38630437	38800069	38715253	169632
RP11-510P12	12	42925574	43054923	42990248.5	129349
RP11-493L12	12	47292778	47484823	47388800.5	192045
RP11-152A18	12	49510213	49689943	49600078	179730
RP11-112N23	12	50448120	50629221	50538670.5	181101
RP11-183H16	12	56269874	56438367	56354120.5	168493
RP11-290I21	12	64284724	64436391	64360557.5	151667
RP11-444B24	12	68171312	68362272	68266792	190960
RP11-566J10	12	76518277	76702092	76610184.5	183815
RP11-202G24	12	77933796	78069040	78001418	135244
RP11-362A1	12	82235777	82382759	82309268	146982
RP11-202H2	12	86931689	87094934	87013311.5	163245
RP11-239F20	12	91781777	91959053	91870415	177276
RP11-410A13	12	95890010	96038191	95964100.5	148181
RP1-261P5	12	112399736	112537419	112468577.5	137683
RP11-497G19	12	116785783	116936893	116861338	151110
RP11-18C24	12	120696111	120833352	120764731.5	137241
RP11-178A2	12	128823421	129014458	128918939.5	191037
RP11-110K8	13	21014693	21193824	21104258.5	179131
RP11-570F6	13	25930592	26097378	26013985	166786
RP11-218E6	13	28869843	29040462	28955152.5	170619
RP11-87G1	13	32881076	33063992	32972534	182916
RP11-131P10	13	37835914	37989889	37912901.5	153975
RP11-117I13	13	42194047	42339827	42266937	145780

RP11-264F20	13	46587555	46737915	46662735	150360
RP11-40A8	13	50367155	50510478	50438816.5	143323
RP11-478B20	13	55410925	55582814	55496869.5	171889
RP11-310K10	13	60757818	60921048	60839433	163230
RP11-424E21	13	65332707	65500164	65416435.5	167457
RP11-370A2	13	68219446	68373244	68296345	153798
RP11-309H15	13	72645530	72815984	72730757	170454
RP11-52L5	13	77993552	78150853	78072202.5	157301
RP11-120L14	13	83805114	83963196	83884155	158082
RP11-275J18	13	88514869	88681377	88598123	166508
RP11-632L2	13	92538397	92719963	92629180	181566
RP11-383H17	13	97306800	97505793	97406296.5	198993
RP11-564N10	13	101357326	101546021	101451673.5	188695
RP11-232K22	13	106566054	106746872	106656463	180818
RP11-480K16	13	112064534	112246895	112155714.5	182361
RP11-84C10	14	19303764	19461742	19382753	157978
RP11-144C18	14	25481639	25665288	25573463.5	183649
RP11-159L20	14	29078484	29245614	29162049	167130
RP11-259K15	14	34533893	34699018	34616455.5	165125
RP11-34O18	14	38289308	38458298	38373803	168990
RP11-134J10	14	42208900	42373413	42291156.5	164513
RP11-346L24	14	47799905	47971249	47885577	171344
RP11-262M8	14	50687246	50885062	50786154	197816
RP11-108M12	14	55377186	55543671	55460428.5	166485
RP11-62H20	14	58256276	58421210	58338743	164934
RP11-544I20	14	62262466	62420889	62341677.5	158423
RP11-226F19	14	67330230	67496508	67413369	166278

RP4-816G1	14	70097161	70228291	70162726	131130
RP11-316E14	14	73306343	73509352	73407847.5	203009
RP11-463C8	14	75573588	75753918	75663753	180330
RP11-114N19	14	79418008	79578366	79498187	160358
RP11-203D9	14	82773865	82921435	82847650	147570
RP11-2E15	14	85754128	85906871	85830499.5	152743
RP11-79J20	14	87739152	87907321	87823236.5	168169
RP11-298I23	14	93822042	93987822	93904932	165780
RP11-68I8	14	96755903	96931901	96843902	175998
RP11-73M18	14	102137566	102303182	102220374	165616
RP11-289D12	15	20230681	20409344	20320012.5	178663
RP11-142M24	15	24237601	24416992	24327296.5	179391
RP11-164K24	15	29000750	29159519	29080134.5	158769
RP11-70A1	15	34492228	34652252	34572240	160024
RP11-164J13	15	40191009	40336241	40263625	145232
RP11-519G16	15	43204847	43405649	43305248	200802
RP11-232J12	15	51370999	51528040	51449519.5	157041
RP11-178D12	15	53203690	53354822	53279256	151132
RP11-169M2	15	60509763	60687245	60598504	177482
RP11-321F6	15	64420512	64630680	64525596	210168
RP11-2I17	15	69931377	70102499	70016938	171122
RP11-78M2	15	74288711	74436014	74362362.5	147303
RP11-127F21	15	80974294	81145086	81059690	170792
RP11-133L19	15	84972397	85149035	85060716	176638
RP3-443N8	15	88547365	88627956	88587660.5	80591
RP11-34L4	15	92789758	92955983	92872870.5	166225
RP11-262P8	15	96822948	97001148	96912048	178200

RP11-14C10	15	99606717	99811390	99709053.5	204673
RP11-433P17	16	3352717	3532227	3442472	179510
RP11-518I8	16	5501064	5704568	5602816	203504
RP11-148F10	16	7992941	8180436	8086688.5	187495
RP11-489O1	16	15431773	15593312	15512542.5	161539
RP5-973M2	16	21924160	22037720	21980940	113560
CTD-2515A14	16	24657417	24876429	24766923	219012
RP11-74E23	16	29641806	29821555	29731680.5	179749
RP11-523L20	16	47637620	47785040	47711330	147420
RP11-424K7	16	50797985	50973961	50885973	175976
RP11-357N13	16	53608406	53806822	53707614	198416
RP11-405F3	16	57356486	57508641	57432563.5	152155
RP11-157H19	16	61536303	61704456	61620379.5	168153
RP11-229O3	16	64639732	64793319	64716525.5	153587
RP11-76H6	16	68130660	68312309	68221484.5	181649
RP11-311C24	16	69342826	69509651	69426238.5	166825
RP5-991G20	16	72494571	72635883	72565227	141312
RP11-281J9	16	77615449	77787782	77701615.5	172333
RP11-2L4	16	82302795	82461010	82381902.5	158215
RP11-478M13	16	85563108	85723221	85643164.5	160113
RP11-4F24	17	1568827	1779994	1674410.5	211167
RP11-104O19	17	4005140	4173973	4089556.5	168833
RP11-144K9	17	6898009	7008780	6953394.5	110771
RP11-12H18	17	8411033	8576675	8493854	165642
RP11-388F14	17	13213933	13419102	13316517.5	205169
RP11-385D13	17	15323659	15512500	15418079.5	188841
RP5-836L9	17	19977261	20098081	20037671	120820

RP11-104I20	17	27899018	28089346	27994182	190328
RP1-29G21	17	31107106	31248368	31177737	141262
RP11-115K3	17	35797540	35979164	35888352	181624
RP11-390P24	17	37460666	37635985	37548325.5	175319
RP5-1110E20	17	38891937	39028958	38960447.5	137021
RP5-905N1	17	41837623	41932374	41884998.5	94751
RP11-374N3	17	43716793	43751400	43734096.5	34607
RP11-81K2	17	47741447	47929515	47835481	188068
RP11-429O1	17	50831753	51016056	50923904.5	184303
RP11-372K20	17	53099732	53255181	53177456.5	155449
RP11-19F16	17	55603555	55747849	55675702	144294
RP11-332H18	17	59644799	59834154	59739476.5	189355
RP11-89H15	17	62459662	62614325	62536993.5	154663
RP11-238F2	17	69147559	69296184	69221871.5	148625
RP11-155C2	17	72409645	72586956	72498300.5	177311
RP11-313F15	17	79131187	79302492	79216839.5	171305
RP11-324G2	18	168428	340445	254436.5	172017
RP11-502P1	18	3863228	4046694	3954961	183466
RP11-146G7	18	6752911	6933647	6843279	180736
RP11-99M10	18	10436606	10587118	10511862	150512
RP11-17J14	18	20658424	20815606	20737015	157182
RP11-526I8	18	24374624	24565006	24469815	190382
RP11-413I9	18	29891111	30049089	29970100	157978
RP11-383C19	18	33969157	34136044	34052600.5	166887
RP11-25C13	18	37123788	37291079	37207433.5	167291
RP11-463D17	18	42850560	43042716	42946638	192156
RP11-141E12	18	46659813	46821973	46740893	162160

RP11-1E21	18	48908822	49077297	48993059.5	168475
RP11-397A16	18	53079547	53282112	53180829.5	202565
RP11-350K6	18	56501246	56683540	56592393	182294
RP11-28F1	18	60692611	60849700	60771155.5	157089
RP11-430H7	18	68387071	68563596	68475333.5	176525
RP11-118I2	18	75238962	75410506	75324734	171544
RP11-16L7	18	75542665	75651403	75597034	108738
RP11-269I24	18	131243135	131396939	131320037	153804
CTC-546C11	19	295393	475000	385196.5	179607
CTB-1025J19	19	7064590	7214590	7139590	150000
CTB-1187L3	19	15400042	15553105	15476573.5	153063
RP11-26D24	19	21329374	21488498	21408936	159124
RP11-359H18	19	23539218	23716516	23627867	177298
CTD-2043I16	19	33277317	33383462	33330389.5	106145
CTD-2525J15	19	41994480	42183965	42089222.5	189485
RP11-15A1	19	49030102	49190855	49110478.5	160753
RP11-2J15	19	51650034	51819357	51734695.5	169323
RP11-423F16	19	56300117	56487777	56393947	187660
RP5-1060P11	19	59906569	59990304	59948436.5	83735
RP11-394L10	19	60898594	61072653	60985623.5	174059
CTD-3138B18	19	63340054	63500905	63420479.5	160851
RP4-686C3	20	2441323	2600594	2520958.5	159271
RP4-811H13	20	9197701	9340955	9269328	143254
RP11-526K24	20	13564713	13774030	13669371.5	209317
RP5-1096J16	20	20143748	20240131	20191939.5	96383
RP5-1025A1	20	24936530	25109994	25023262	173464
RP1-310O13	20	31173458	31336433	31254945.5	162975

RP5-1161H23	20	34112722	34254763	34183742.5	142041
RP4-633O20	20	37039719	37136178	37087948.5	96459
RP1-232N11	20	41885784	41997424	41941604	111640
RP3-337O18	20	45094666	45180745	45137705.5	86079
RP4-791K14	20	48587999	48743316	48665657.5	155317
RP4-724E16	20	52766526	52895396	52830961	128870
RP5-1167H4	20	55541473	55677165	55609319	135692
RP4-719C8	20	58788624	58939608	58864116	150984
RP5-1107C24	20	61099667	61221648	61160657.5	121981
RP1-270M7	21	15134622	15379650	15257136	245028
RP11-258A5	21	22151924	22333706	22242815	181782
RP11-15H6	21	26643245	26798260	26720752.5	155015
RP1-245P17	21	34482485	34601463	34541974	118978
RP11-164E1	21	38599546	38738905	38669225.5	139359
RP11-113F1	21	42528815	42710796	42619805.5	181981
CTA-221G9	22	23874371	23991534	23932952.5	117163
RP3-353E16	22	26491834	26717291	26604562.5	225457
RP1-127L4	22	30829975	30927214	30878594.5	97239
CTA-221H1	22	32879027	32927801	32903414	48774
CTA-445C9	22	36033386	36125793	36079589.5	92407
RP11-12M9	22	39614662	39790948	39702805	176286
RP3-437M21	22	41430046	41517447	41473746.5	87401
RP3-398C22	22	44312892	44441800	44377346	128908
RP5-925J7	22	47573681	47672127	47622904	98446
RP1-122K4	23	13107070	13307215	13207142.5	200145
RP11-421K1	23	18257078	18448395	18352736.5	191317
RP11-37E19	23	28220640	28306944	28263792	86304

RP5-1147O16	23	31639277	31771566	31705421.5	132289
RP11-469E19	23	39714763	39904047	39809405	189284
RP5-1158E12	23	44467859	44631729	44549794	163870
RP11-576P23	23	48815725	48982820	48899272.5	167095
RP13-34C21	23	60584706	60779286	60681996	194580
RP11-284B18	23	61667590	61836491	61752040.5	168901
RP11-523P2	23	69685582	69880502	69783042	194920
RP11-159L8	23	76407107	76573916	76490511.5	166809
RP5-1156N12	23	79543649	79690008	79616828.5	146359
RP5-1109K10	23	81885385	81995148	81940266.5	109763
RP13-166C10	23	88331157	88482056	88406606.5	150899
RP11-274M8	23	94499022	94658413	94578717.5	159391
RP11-230E14	23	101644461	101803008	101723734.5	158547
RP5-820B18	23	105067893	105195945	105131919	128052
RP5-914P14	23	108481901	108637275	108559588	155374
RP6-155F9	23	115573778	115696451	115635114.5	122673
RP1-181N1	23	120342878	120469351	120406114.5	126473
RP6-109P7	23	125880539	126039266	125959902.5	158727
RP5-965E19	23	129301158	129460507	129380832.5	159349
RP1-20J23	23	134389225	134526335	134457780	137110
RP11-518F7	23	138317108	138482486	138399797	165378
RP11-390O24	23	142033283	142211890	142122586.5	178607
RP5-937E21	23	146524468	146636027	146580247.5	111559
RP11-54I20	23	150291840	150471039	150381439.5	179199

A.2 7q BAC clones

1082 BAC clones for chromosome 7q were selected from the BAC 32k rearray produced by BACPAC resources at the Oakland Children's Hospital, Oakland, CA, USA. The whole genome set was purchased as a series of prepared BAC DNA, and 7q clones were selected and amplified by DOP-PCR. Clones producing unexpected hybridisation on the final array are highlighted in yellow.

Clone Name	Chromosome	Start	End	Mid point	Length
RP11-764P14	1	21980519	22120000	22050259.5	139481
RP11-15K14	1	57593750	57638814	57616282	45064
RP11-104J19	1	83571016	83648391	83609703.5	77375
RP11-340I6	1	234896179	234971851	234934015	75672
CTD-2017N4	2	41341791	41399901	41370846	58110
RP11-454E16	2	119825056	119892019	119858537.5	66963
RP11-612G11	3	4525274	4659725	4592499.5	134451
RP13-866K15	3	106807531	106871559	106839545	64028
RP11-767K21	4	118488401	118600000	118544200.5	111599
RP11-692I6	4	135439967	135517137	135478552	77170
RP11-637I24	4	164311751	164344833	164328292	33082
RP11-659F13	6	88922418	88986995	88954706.5	64577
RP11-172O13	7	5499542	5668701	5584121.5	169159
RP11-505D17	7	7741405	7930339	7835872	188934
RP11-172C5	7	19278897	19354440	19316668.5	75543
RP11-486P11	7	19813021	19987132	19900076.5	174111
RP11-343P21	7	24296329	24465905	24381117	169576

RP11-818A14	7	25880205	25942006	25911105.5	61801
CTD-2004J10	7	56624162	56759445	56691803.5	135283
RP11-1298L14	7	56629051	56839676	56734363.5	210625
RP11-410M8	7	60902367	61068300	60985333.5	165933
RP11-533E18	7	60900893	61085935	60993414	185042
RP13-621P11	7	61053523	61082414	61067968.5	28891
RP11-34I22	7	61420370	61604430	61512400	184060
CTD-2420F24	7	61537065	61566295	61551680	29230
RP11-112O15	7	61604424	61762853	61683638.5	158429
CTD-2229D8	7	61747424	61884692	61816058	137268
RP11-288C22	7	61941236	62121831	62031533.5	180595
RP11-373D7	7	62042085	62168633	62105359	126548
RP11-445O5	7	62099056	62346012	62222534	246956
RP11-560L17	7	62176597	62328847	62252722	152250
CTD-2005N23	7	62196113	62316194	62256153.5	120081
RP11-73B2	7	62196113	62316194	62256153.5	120081
RP11-1162A20	7	62176597	62346012	62261304.5	169415
RP11-1268A5	7	62176597	62346012	62261304.5	169415
RP11-555G16	7	62415501	62581198	62498349.5	165697
RP11-618G11	7	62406872	62591309	62499090.5	184437
RP11-331L17	7	62441180	62623260	62532220	182080
RP11-802G15	7	62547503	62724726	62636114.5	177223
RP11-500H11	7	62623261	62781464	62702362.5	158203
CTD-2143G24	7	62848012	62981658	62914835	133646
RP11-726L22	7	62920373	63118752	63019562.5	198379
RP11-585N1	7	62993350	63165317	63079333.5	171967
RP11-584F18	7	63068804	63235110	63151957	166306

RP11-725P15	7	63104011	63302395	63203203	198384
RP11-561O12	7	63247581	63440908	63344244.5	193327
RP11-149J7	7	63392493	63565761	63479127	173268
RP11-417K4	7	63426208	63611584	63518896	185376
RP11-416N13	7	63488050	63693966	63591008	205916
RP11-263F16	7	63564798	63693966	63629382	129168
RP11-493I14	7	63598125	63815665	63706895	217540
RP11-637E4	7	63687614	63863547	63775580.5	175933
RP11-808P5	7	63780000	63970285	63875142.5	190285
RP11-466B18	7	63863813	64024115	63943964	160302
RP11-225E12	7	63874986	64036736	63955861	161750
RP11-12L22	7	63912609	64073410	63993009.5	160801
CTD-2090P17	7	64015538	64115462	64065500	99924
RP13-650L9	7	64014519	64157106	64085812.5	142587
RP13-887C2	7	64097646	64225895	64161770.5	128249
RP11-350C17	7	64099891	64274606	64187248.5	174715
RP11-328P23	7	64150188	64225895	64188041.5	75707
RP13-244O17	7	64107525	64294312	64200918.5	186787
CTD-2288I20	7	64149128	64292262	64220695	143134
RP11-521O10	7	64150188	64300275	64225231.5	150087
RP11-746P2	7	64150188	64321567	64235877.5	171379
RP13-929L15	7	64199976	64321567	64260771.5	121591
RP13-680C23	7	64210249	64393129	64301689	182880
RP11-667F9	7	64291470	64343664	64317567	52194
RP13-626B11	7	64384198	64495088	64439643	110890
RP11-124K5	7	64424689	64515187	64469938	90498
RP11-551F1	7	64429612	64556370	64492991	126758

RP11-445F7	7	64429612	64595091	64512351.5	165479
RP11-146A10	7	64465603	64565479	64515541	99876
RP13-171N4	7	64429612	64625953	64527782.5	196341
RP13-157F18	7	64419123	64648950	64534036.5	229827
RP11-96H22	7	64454792	64623450	64539121	168658
RP11-465L14	7	64427093	64665343	64546218	238250
RP11-522D19	7	64429612	64665343	64547477.5	235731
RP11-479O9	7	64535967	64728195	64632081	192228
RP11-265G24	7	64610556	64821321	64715938.5	210765
RP11-567L18	7	64610556	64821321	64715938.5	210765
RP11-376L15	7	64779110	64942870	64860990	163760
RP11-636K11	7	64855188	65025393	64940290.5	170205
RP11-732N17	7	64855188	65035288	64945238	180100
RP11-763P10	7	64985190	65200253	65092721.5	215063
RP11-318B19	7	65150900	65353464	65252182	202564
RP11-618F10	7	65335959	65504079	65420019	168120
RP11-350A24	7	65484475	65663813	65574144	179338
RP11-217F24	7	65541083	65647129	65594106	106046
RP11-701N9	7	65614342	65726526	65670434	112184
RP11-605M5	7	65598163	65801440	65699801.5	203277
CTD-2140O19	7	65720032	65896612	65808322	176580
RP11-6C21	7	65798928	65980537	65889732.5	181609
RP11-325K1	7	65843310	66015941	65929625.5	172631
RP11-368E23	7	65960958	66164635	66062796.5	203677
RP13-500P23	7	66032848	66189383	66111115.5	156535
RP11-243C20	7	66140699	66322463	66231581	181764
CTD-2011L15	7	66151160	66335601	66243380.5	184441

RP13-936H15	7	66310518	66465758	66388138	155240
RP13-628N2	7	66413722	66554741	66484231.5	141019
RP13-827M24	7	66461278	66583218	66522248	121940
RP13-829H10	7	66507264	66552207	66529735.5	44943
RP13-525L9	7	66507264	66621396	66564330	114132
RP11-522A22	7	66459386	66704367	66581876.5	244981
RP11-446P8	7	66682329	66883765	66783047	201436
CTD-2337G16	7	66806739	66907490	66857114.5	100751
RP11-752D15	7	66878330	67028660	66953495	150330
RP11-793E12	7	66951340	67179746	67065543	228406
RP11-339E23	7	67159505	67350483	67254994	190978
RP11-754N7	7	67205052	67392557	67298804.5	187505
RP11-156A14	7	67357045	67519496	67438270.5	162451
RP11-156A14	7	67357045	67519496	67438270.5	162451
RP11-151E8	7	67483110	67618584	67550847	135474
RP11-521N10	7	67618585	67782919	67700752	164334
RP11-535N23	7	67749005	67918785	67833895	169780
RP11-594G14	7	67748165	67957400	67852782.5	209235
RP11-547J3	7	68017401	68190260	68103830.5	172859
RP11-752M2	7	68110519	68224668	68167593.5	114149
RP11-790K18	7	68250971	68447376	68349173.5	196405
RP11-561G6	7	68383831	68540830	68462330.5	156999
RP11-617P15	7	68407458	68591111	68499284.5	183653
RP11-818D5	7	68443565	68658171	68550868	214606
RP11-358I11	7	68566820	68809142	68687981	242322
RP11-170H15	7	68659462	68813002	68736232	153540
RP11-232F14	7	68767880	68924046	68845963	156166

RP11-309P19	7	68920563	69060225	68990394	139662
RP11-138M21	7	69006585	69147184	69076884.5	140599
RP11-801B4	7	69087377	69273898	69180637.5	186521
RP11-180J15	7	69219215	69423175	69321195	203960
RP11-689B18	7	69439915	69661929	69550922	222014
RP11-366L17	7	69634002	69682830	69658416	48828
RP11-575M4	7	69630435	69817986	69724210.5	187551
RP11-803O5	7	69752965	69958239	69855602	205274
RP11-492O3	7	69938062	70140768	70039415	202706
RP11-330E10	7	70072482	70284888	70178685	212406
RP11-786A1	7	70193724	70322667	70258195.5	128943
RP11-237L22	7	70280835	70454588	70367711.5	173753
RP11-332E12	7	70444428	70616535	70530481.5	172107
RP11-421B22	7	70568140	70756211	70662175.5	188071
RP11-395G21	7	70678115	70881857	70779986	203742
RP11-460F3	7	70816056	71008669	70912362.5	192613
RP11-90B1	7	70888200	71032684	70960442	144484
RP11-694L3	7	70940726	71116177	71028451.5	175451
RP11-53M13	7	71011779	71177768	71094773.5	165989
RP11-746H3	7	71014000	71179901	71096950.5	165901
RP11-751G4	7	71039330	71177768	71108549	138438
RP11-642F10	7	71011779	71258401	71135090	246622
RP11-542O11	7	71171643	71321909	71246776	150266
CTD-2018O17	7	71225446	71351669	71288557.5	126223
RP11-359E24	7	71302680	71489145	71395912.5	186465
RP11-32N3	7	71351670	71506334	71429002	154664
RP11-576G4	7	71403999	71559889	71481944	155890

RP11-35P20	7	71464807	71637730	71551268.5	172923
RP11-213A22	7	71489180	71640842	71565011	151662
RP11-519I5	7	71528854	71684059	71606456.5	155205
RP11-795J4	7	71590803	71782008	71686405.5	191205
RP11-78P11	7	71673466	71832562	71753014	159096
RP11-762B10	7	71778705	71969666	71874185.5	190961
RP11-313P13	7	71778705	71971622	71875163.5	192917
RP11-1328G23	7	71766538	71996821	71881679.5	230283
CTD-2143B9	7	71821081	71971622	71896351.5	150541
RP11-780K20	7	71843425	72034679	71939052	191254
RP11-548E9	7	71881953	72060659	71971306	178706
RP11-728E18	7	71963625	72133505	72048565	169880
RP11-367N11	7	71963826	72164463	72064144.5	200637
RP11-334D20	7	72032613	72301047	72166830	268434
RP11-288I2	7	72141187	72319733	72230460	178546
RP11-101D2	7	72259198	72436625	72347911.5	177427
RP11-667P12	7	72242381	72480257	72361319	237876
RP11-552B12	7	72329400	72504915	72417157.5	175515
RP11-590H3	7	72415294	72585074	72500184	169780
RP11-737E18	7	72415294	72675576	72545435	260282
RP11-100D10	7	72519572	72682330	72600951	162758
RP11-307G22	7	72570957	72789866	72680411.5	218909
RP11-11I22	7	72611015	72811598	72711306.5	200583
RP13-568O8	7	72771565	72927656	72849610.5	156091
RP11-644H24	7	72839800	73004869	72922334.5	165069
RP11-356N2	7	72874739	73045496	72960117.5	170757
RP11-100C23	7	72929705	73136892	73033298.5	207187

RP11-41F22	7	72970758	73109172	73039965	138414
RP11-331N10	7	72981346	73134408	73057877	153062
RP11-422O1	7	73141937	73264896	73203416.5	122959
RP11-329B5	7	73174290	73340724	73257507	166434
RP11-189A5	7	73233795	73429688	73331741.5	195893
RP11-196F10	7	73317260	73482782	73400021	165522
RP11-137E8	7	73389370	73574238	73481804	184868
RP11-583G15	7	73411006	73559231	73485118.5	148225
RP11-659G13	7	73411006	73588349	73499677.5	177343
RP11-180C6	7	73413479	73588349	73500914	174870
RP11-91L7	7	73413479	73588349	73500914	174870
RP11-1328E4	7	73487707	73707365	73597536	219658
RP11-813J7	7	73530488	73707365	73618926.5	176877
RP11-259J2	7	73597589	73763640	73680614.5	166051
RP11-681A16	7	73645740	73812663	73729201.5	166923
CTD-2285H13	7	73708037	73829266	73768651.5	121229
RP11-774J17	7	73774411	73946646	73860528.5	172235
RP11-1254M14	7	73825432	74015866	73920649	190434
RP11-219M8	7	73861902	74050724	73956313	188822
RP11-502I24	7	73946647	74100113	74023380	153466
RP11-567F24	7	73958192	74100113	74029152.5	141921
CTD-2104I4	7	74108701	74157258	74132979.5	48557
RP11-119P19	7	74596259	74710216	74653237.5	113957
RP11-613J9	7	74620669	74847736	74734202.5	227067
RP11-279K6	7	74689304	74870225	74779764.5	180921
RP11-99J9	7	74771608	74952654	74862131	181046
RP11-429B10	7	74900077	75062475	74981276	162398

RP11-812L15	7	74966957	75152692	75059824.5	185735
CTD-2032H20	7	75072873	75254057	75163465	181184
RP11-379D10	7	75164883	75317803	75241343	152920
RP11-229D13	7	75221960	75388533	75305246.5	166573
RP11-7A21	7	75330292	75498794	75414543	168502
RP11-351A5	7	75695279	75770021	75732650	74742
RP11-122A5	7	75767576	75949027	75858301.5	181451
RP11-398O10	7	75919802	76088478	76004140	168676
RP11-683I19	7	75954043	76144650	76049346.5	190607
RP11-85K14	7	76026292	76203167	76114729.5	176875
RP11-409L7	7	76048273	76183097	76115685	134824
RP11-506L7	7	76117750	76319174	76218462	201424
RP11-672F22	7	76242931	76418754	76330842.5	175823
RP11-467H10	7	76297379	76493929	76395654	196550
RP11-275G11	7	76491236	76674207	76582721.5	182971
RP11-764I16	7	76517399	76680579	76598989	163180
RP11-533K2	7	76587420	76774091	76680755.5	186671
RP11-176J13	7	76758870	76923102	76840986	164232
RP11-229J1	7	76838579	76996855	76917717	158276
RP11-98O12	7	76946486	77120129	77033307.5	173643
RP11-604I6	7	77039517	77218346	77128931.5	178829
RP11-86C23	7	77081758	77213123	77147440.5	131365
RP11-446O8	7	77122663	77364719	77243691	242056
RP11-157F12	7	77326058	77508779	77417418.5	182721
RP11-294I7	7	77399856	77591743	77495799.5	191887
CTD-2242M21	7	77524430	77631633	77578031.5	107203
RP11-567K8	7	77505194	77686751	77595972.5	181557

RP11-538D15	7	77505194	77705500	77605347	200306
RP11-634B10	7	77574029	77772382	77673205.5	198353
RP11-788P16	7	77614347	77783217	77698782	168870
RP11-144P23	7	77652773	77789143	77720958	136370
RP11-290P2	7	77721708	77939218	77830463	217510
RP11-130I20	7	77862948	78029856	77946402	166908
RP11-210G8	7	77993295	78153755	78073525	160460
RP11-758O19	7	78187961	78375276	78281618.5	187315
RP13-486L4	7	78267846	78476649	78372247.5	208803
RP11-718N3	7	78348835	78520898	78434866.5	172063
RP11-390C15	7	78439299	78597845	78518572	158546
RP11-561D14	7	78464150	78617873	78541011.5	153723
RP11-638G10	7	78597846	78762614	78680230	164768
RP11-472I2	7	78727275	78907495	78817385	180220
RP11-757A2	7	78844612	79035883	78940247.5	191271
RP11-327P19	7	78917558	79094083	79005820.5	176525
RP11-566B4	7	79027204	79206634	79116919	179430
RP11-500G1	7	79098073	79275458	79186765.5	177385
RP11-317H18	7	79173130	79335517	79254323.5	162387
RP11-176M5	7	79315596	79449943	79382769.5	134347
RP11-469I3	7	79370782	79514484	79442633	143702
RP11-421P24	7	79405990	79589008	79497499	183018
RP11-512J17	7	79477517	79628729	79553123	151212
RP11-284B4	7	79628730	79766963	79697846.5	138233
RP11-331E13	7	79663018	79824856	79743937	161838
RP11-764E4	7	79764065	79966743	79865404	202678
RP11-563A3	7	79924739	80139245	80031992	214506

RP11-501A18	7	80102558	80259014	80180786	156456
RP11-520A8	7	80254235	80411748	80332991.5	157513
RP11-633A20	7	80366424	80563242	80464833	196818
RP11-223F3	7	80486344	80657055	80571699.5	170711
RP11-665G16	7	80525983	80724425	80625204	198442
RP11-211K16	7	80568191	80718612	80643401.5	150421
RP11-284I24	7	80716396	80893900	80805148	177504
RP11-295A1	7	80827692	81001334	80914513	173642
RP11-24F4	7	80961854	81140390	81051122	178536
RP11-448A3	7	80965735	81157984	81061859.5	192249
RP11-522D24	7	81047718	81223527	81135622.5	175809
RP11-575G1	7	81230368	81424378	81327373	194010
RP11-459E23	7	81390339	81547805	81469072	157466
RP11-556B13	7	81515961	81670637	81593299	154676
RP11-560N24	7	81626840	81804831	81715835.5	177991
RP11-39H7	7	81794174	82009417	81901795.5	215243
RP11-789I4	7	81940351	82140185	82040268	199834
RP11-56M7	7	82010714	82169871	82090292.5	159157
RP11-562O3	7	82011240	82219036	82115138	207796
RP11-240I3	7	82140186	82315457	82227821.5	175271
CTD-2085L13	7	82246720	82355800	82301260	109080
RP11-261H1	7	82264155	82423339	82343747	159184
RP11-785F16	7	82293334	82472163	82382748.5	178829
RP11-796P2	7	82387322	82578005	82482663.5	190683
RP11-142G6	7	82471135	82637070	82554102.5	165935
RP11-772C17	7	82588795	82767188	82677991.5	178393
RP11-592A12	7	82726787	82905118	82815952.5	178331

RP11-750H24	7	82840903	83012166	82926534.5	171263
RP11-514G1	7	82923829	83111542	83017685.5	187713
RP11-456A9	7	83020089	83204224	83112156.5	184135
RP11-398N16	7	83133933	83293271	83213602	159338
RP11-794C5	7	83218908	83433600	83326254	214692
RP11-115M2	7	83253404	83404554	83328979	151150
RP11-488O20	7	83265657	83467392	83366524.5	201735
RP11-166I21	7	83312072	83467392	83389732	155320
RP11-663J4	7	83348114	83550882	83449498	202768
CTD-2010O4	7	83377432	83524652	83451042	147220
RP11-98M4	7	83460861	83610655	83535758	149794
RP11-343P19	7	83451737	83630396	83541066.5	178659
RP11-572C2	7	83536658	83693553	83615105.5	156895
RP11-674G6	7	83692641	83847856	83770248.5	155215
RP11-600K18	7	83774675	83978080	83876377.5	203405
RP13-959M22	7	83805221	83971740	83888480.5	166519
RP11-750F10	7	83876589	84052732	83964660.5	176143
RP11-746J12	7	83922250	84120361	84021305.5	198111
RP11-299O9	7	84000647	84171912	84086279.5	171265
RP11-765N7	7	84179139	84344811	84261975	165672
RP11-617F3	7	84237140	84424961	84331050.5	187821
RP11-343D5	7	84250600	84448204	84349402	197604
RP11-270A23	7	84319911	84498431	84409171	178520
RP11-269B15	7	84376350	84536300	84456325	159950
RP11-683E23	7	84389905	84573523	84481714	183618
RP11-349O5	7	84406854	84587182	84497018	180328
RP11-533L22	7	84537359	84707351	84622355	169992

RP11-706L16	7	84649308	84780969	84715138.5	131661
RP11-278A21	7	84799599	84966567	84883083	166968
RP11-695L4	7	84870411	85035793	84953102	165382
CTD-2023H7	7	84953468	85053534	85003501	100066
CTD-2083K15	7	84975040	85084144	85029592	109104
RP13-535J21	7	85011183	85151554	85081368.5	140371
CTD-2265E6	7	85032482	85136294	85084388	103812
RP13-483O24	7	85070497	85245896	85158196.5	175399
CTD-2651D18	7	85092011	85291211	85191611	199200
RP11-729A18	7	85222295	85384466	85303380.5	162171
RP11-561F17	7	85339868	85495476	85417672	155608
RP11-435O7	7	85441441	85605530	85523485.5	164089
RP11-555E22	7	85639303	85833284	85736293.5	193981
RP11-287O4	7	85757083	85922055	85839569	164972
RP11-669A8	7	85912822	86085650	85999236	172828
RP11-449H8	7	86021997	86206087	86114042	184090
RP11-811P13	7	86054671	86277736	86166203.5	223065
RP11-543E17	7	86284097	86475852	86379974.5	191755
RP11-69L24	7	86363255	86527064	86445159.5	163809
RP11-488M3	7	86380556	86563553	86472054.5	182997
RP11-310P19	7	86389443	86563553	86476498	174110
RP11-575C11	7	86499469	86666561	86583015	167092
RP11-127F1	7	86659102	86811423	86735262.5	152321
RP11-537J16	7	86702498	86857403	86779950.5	154905
RP11-103N4	7	86822603	86990346	86906474.5	167743
RP11-784B3	7	86855425	87078303	86966864	222878
RP11-513N8	7	86954450	87124028	87039239	169578

RP11-542G18	7	87051502	87252322	87151912	200820
RP11-803P20	7	87240760	87430447	87335603.5	189687
RP11-315D17	7	87378607	87564718	87471662.5	186111
RP11-815D20	7	87509173	87695944	87602558.5	186771
RP11-462N5	7	87558480	87714977	87636728.5	156497
RP11-470G18	7	87731845	87945648	87838746.5	213803
RP11-174I14	7	87804935	87968364	87886649.5	163429
RP11-493G7	7	87866824	88062333	87964578.5	195509
RP11-766E9	7	87891721	88084221	87987971	192500
RP13-577C5	7	87965641	88142802	88054221.5	177161
RP11-772C5	7	88044311	88193159	88118735	148848
RP13-220C18	7	88044311	88222389	88133350	178078
RP13-359O15	7	88072176	88246113	88159144.5	173937
RP11-209B4	7	88127207	88264152	88195679.5	136945
RP11-1279M16	7	88127207	88305425	88216316	178218
RP11-756A17	7	88257143	88441998	88349570.5	184855
RP11-82D15	7	88328564	88515266	88421915	186702
RP11-693A17	7	88352275	88564392	88458333.5	212117
CTD-2326K17	7	88444568	88547502	88496035	102934
RP11-702P9	7	88497523	88650479	88574001	152956
RP11-279D8	7	88514554	88670815	88592684.5	156261
RP11-732C21	7	88505913	88700714	88603313.5	194801
RP11-192O9	7	88589450	88741028	88665239	151578
RP11-360F3	7	88650481	88804737	88727609	154256
RP11-624I3	7	88766086	88945296	88855691	179210
RP11-734C11	7	88797827	88974504	88886165.5	176677
RP11-404B16	7	88947165	89104685	89025925	157520

RP11-12D1	7	89068064	89257523	89162793.5	189459
RP11-584M11	7	89143108	89317970	89230539	174862
RP11-451O5	7	89241989	89425049	89333519	183060
RP13-560A13	7	89275939	89432393	89354166	156454
RP11-454K3	7	89297229	89468333	89382781	171104
RP11-660C12	7	89297622	89473971	89385796.5	176349
CTD-2038A8	7	89364926	89511319	89438122.5	146393
RP11-248A17	7	89380390	89509445	89444917.5	129055
RP11-544P11	7	89476556	89655603	89566079.5	179047
RP11-594G22	7	89578340	89731552	89654946	153212
RP11-573O6	7	89647357	89850441	89748899	203084
RP11-717E22	7	89764787	89985650	89875218.5	220863
RP13-508F18	7	89899361	90068993	89984177	169632
RP11-298J7	7	90006176	90144413	90075294.5	138237
RP11-553F2	7	90006176	90176583	90091379.5	170407
RP11-98J8	7	90083990	90269903	90176946.5	185913
RP11-215P16	7	90123930	90278380	90201155	154450
RP11-342C19	7	90234101	90383349	90308725	149248
RP11-291D21	7	90278381	90416651	90347516	138270
RP11-337D7	7	90496685	90694000	90595342.5	197315
RP11-646C11	7	90563861	90757345	90660603	193484
RP11-658E10	7	90598652	90816097	90707374.5	217445
RP11-332H6	7	90745616	90928607	90837111.5	182991
CTD-2333B13	7	90776867	90900353	90838610	123486
RP11-568M21	7	90772084	90975471	90873777.5	203387
RP11-225G3	7	90913043	91109788	91011415.5	196745
RP11-62D6	7	90964659	91126591	91045625	161932

RP11-806O14	7	91040071	91237927	91138999	197856
RP11-623E20	7	91226541	91352826	91289683.5	126285
RP11-371H19	7	91245408	91406462	91325935	161054
RP11-291G20	7	91388974	91592980	91490977	204006
RP11-339M3	7	91514274	91724132	91619203	209858
RP11-736O1	7	91608735	91777185	91692960	168450
RP11-606J5	7	91681581	91860158	91770869.5	178577
RP11-82E23	7	91781912	91951988	91866950	170076
RP11-514K1	7	91885885	92105262	91995573.5	219377
RP11-332M5	7	91975364	92160167	92067765.5	184803
RP11-467N23	7	92075268	92260660	92167964	185392
CTD-2260H18	7	92197467	92346033	92271750	148566
RP11-335L6	7	92283061	92490798	92386929.5	207737
RP11-773N18	7	92450337	92659473	92554905	209136
RP11-269A13	7	92648735	92786012	92717373.5	137277
RP11-309L13	7	92672117	92853228	92762672.5	181111
RP11-471H1	7	92784568	92947529	92866048.5	162961
RP11-78F12	7	92983772	93174165	93078968.5	190393
RP11-461H15	7	93150129	93326095	93238112	175966
RP11-470G15	7	93492602	93648187	93570394.5	155585
RP11-57C4	7	93647739	93812420	93730079.5	164681
CTD-2130O12	7	93794436	93909780	93852108	115344
RP11-648L18	7	93852006	94002009	93927007.5	150003
RP11-367L3	7	93845994	94038039	93942016.5	192045
RP11-564F14	7	94016109	94188079	94102094	171970
RP11-619A2	7	94149723	94338293	94244008	188570
RP11-82B2	7	94282577	94456401	94369489	173824

RP11-601D18	7	94463006	94606231	94534618.5	143225
RP11-48F16	7	94548068	94709169	94628618.5	161101
RP11-674B12	7	94665835	94887039	94776437	221204
RP11-84F19	7	94820970	94990548	94905759	169578
RP11-95A10	7	94927842	95117170	95022506	189328
RP11-295J1	7	94990549	95170265	95080407	179716
RP11-574B19	7	95033117	95233192	95133154.5	200075
RP11-769F19	7	95189210	95370254	95279732	181044
RP11-94N6	7	95370026	95523366	95446696	153340
RP11-814L20	7	95463854	95630339	95547096.5	166485
RP11-413E12	7	95589287	95787884	95688585.5	198597
RP11-610J1	7	95752181	95933693	95842937	181512
RP11-418K11	7	95920483	96080682	96000582.5	160199
RP11-94N7	7	96020619	96192101	96106360	171482
RP11-2N22	7	96190805	96367434	96279119.5	176629
RP11-63H9	7	96347104	96519179	96433141.5	172075
RP11-800O14	7	96410124	96616120	96513122	205996
RP11-184F2	7	96596782	96746120	96671451	149338
RP11-321E18	7	96721430	96934470	96827950	213040
RP11-312C19	7	96833385	96981453	96907419	148068
RP11-743C24	7	96960514	97146716	97053615	186202
RP11-380G21	7	97120935	97292680	97206807.5	171745
RP11-526I4	7	97259838	97409099	97334468.5	149261
RP11-212K3	7	97371530	97535201	97453365.5	163671
RP11-52E8	7	97477080	97644254	97560667	167174
RP11-65E17	7	97504820	97710179	97607499.5	205359
RP11-723A10	7	97563681	97676851	97620266	113170

RP11-473H4	7	97726720	97900477	97813598.5	173757
RP11-470P14	7	97838856	98018471	97928663.5	179615
RP11-112P23	7	97974638	98128898	98051768	154260
RP11-802H13	7	98094101	98277304	98185702.5	183203
RP11-412N23	7	98181856	98313174	98247515	131318
RP11-1358J4	7	98265318	98454943	98360130.5	189625
RP11-694E14	7	98277414	98460689	98369051.5	183275
RP13-1013E23	7	98469549	98615253	98542401	145704
RP11-140D10	7	98464223	98651132	98557677.5	186909
RP11-112I13	7	98592779	98772235	98682507	179456
RP11-717M24	7	98778305	98979264	98878784.5	200959
RP11-757A13	7	98913558	99107604	99010581	194046
RP11-543L21	7	99079251	99262630	99170940.5	183379
RP11-487B17	7	99216953	99367271	99292112	150318
RP11-494B20	7	99318239	99367271	99342755	49032
RP11-443E21	7	99375909	99604363	99490136	228454
RP11-758P17	7	99562676	99758064	99660370	195388
RP11-44M6	7	99680294	99845417	99762855.5	165123
RP11-344K24	7	99807154	100007486	99907320	200332
RP11-336D7	7	99861727	100040000	99950863.5	178273
RP11-126L15	7	100007608	100172069	100089838.5	164461
RP13-650G11	7	100070310	100189539	100129924.5	119229
RP11-395B7	7	100199486	100338967	100269226.5	139481
RP11-279E13	7	100246271	100411890	100329080.5	165619
RP11-484K16	7	100285732	100510453	100398092.5	224721
RP11-554O7	7	100397851	100560929	100479390	163078
RP11-151L12	7	100422282	100605109	100513695.5	182827

RP11-132A1	7	100467644	100677365	100572504.5	209721
RP11-596H8	7	100688380	100850921	100769650.5	162541
RP11-277D15	7	100803715	100970467	100887091	166752
RP11-692F19	7	100866930	101060211	100963570.5	193281
RP11-962B9	7	101011690	101197426	101104558	185736
RP11-177B2	7	101057565	101228116	101142840.5	170551
RP11-703F10	7	101222556	101402062	101312309	179506
RP11-396D9	7	101286517	101478869	101382693	192352
RP11-765M9	7	101399535	101581563	101490549	182028
RP11-163E9	7	101494175	101666161	101580168	171986
RP11-342G18	7	101574440	101889820	101732130	315380
RP13-771B7	7	101730411	101830616	101780513.5	100205
RP13-944M22	7	101730411	101908605	101819508	178194
RP13-874J16	7	101749448	101908605	101829026.5	159157
RP11-1385F10	7	101730411	101928015	101829213	197604
RP11-676J21	7	101808025	101908605	101858315	100580
RP11-792E22	7	101776746	101969901	101873323.5	193155
RP11-694M1	7	101900000	102081147	101990573.5	181147
RP11-617P22	7	102057995	102281705	102169850	223710
RP11-226H9	7	102285195	102447467	102366331	162272
RP11-203D11	7	102372859	102558921	102465890	186062
RP11-779F24	7	102501181	102707747	102604464	206566
RP11-186B5	7	102633570	102813087	102723328.5	179517
RP11-424G13	7	102734623	102936339	102835481	201716
RP11-510M19	7	102844684	103048153	102946418.5	203469
RP11-574B15	7	102969618	103162771	103066194.5	193153
RP11-689F3	7	103096409	103268595	103182502	172186

RP11-815A11	7	103212352	103366689	103289520.5	154337
RP11-36J11	7	103305533	103460117	103382825	154584
RP11-451J3	7	103333988	103527366	103430677	193378
RP11-172N10	7	103509244	103679659	103594451.5	170415
RP11-150H24	7	103587014	103779432	103683223	192418
RP11-148A10	7	103737568	103889393	103813480.5	151825
RP11-640M20	7	103826865	104029888	103928376.5	203023
RP11-612L3	7	103867654	104055303	103961478.5	187649
RP11-203P23	7	104016454	104190717	104103585.5	174263
RP11-437M1	7	104113486	104314735	104214110.5	201249
RP11-753M2	7	104347813	104543037	104445425	195224
RP11-764M5	7	104462730	104611313	104537021.5	148583
RP11-708P17	7	104553819	104706452	104630135.5	152633
CTD-2305F9	7	104694931	104808189	104751560	113258
RP11-96B13	7	104762663	104914797	104838730	152134
RP11-752M11	7	104876692	105080591	104978641.5	203899
RP11-735J9	7	105040118	105181650	105110884	141532
CTD-2060N15	7	105147091	105299944	105223517.5	152853
RP11-193P5	7	105214647	105360515	105287581	145868
RP11-532G4	7	105239746	105409310	105324528	169564
CTD-2014M11	7	105360514	105490493	105425503.5	129979
RP11-22N19	7	105395309	105566071	105480690	170762
CTD-2026C17	7	105443947	105649531	105546739	205584
RP11-620K1	7	105476052	105669998	105573025	193946
RP11-621C24	7	105561634	105756778	105659206	195144
RP11-17I10	7	105597335	105756723	105677029	159388
RP11-610G5	7	105627919	105822108	105725013.5	194189

RP11-768J5	7	105707392	105893141	105800266.5	185749
RP11-687D7	7	105856379	106011089	105933734	154710
RP11-375A10	7	105908031	106085619	105996825	177588
RP11-523G16	7	106082845	106267131	106174988	184286
RP11-258L19	7	106182920	106346360	106264640	163440
RP11-262G16	7	106267416	106466411	106366913.5	198995
RP11-762B6	7	106403391	106572650	106488020.5	169259
RP11-454I21	7	106529757	106716110	106622933.5	186353
RP11-158F24	7	106558882	106701295	106630088.5	142413
RP11-764B12	7	106655311	106830949	106743130	175638
RP11-1N16	7	106706672	106862550	106784611	155878
CTD-2315O16	7	106790439	106928106	106859272.5	137667
RP11-467F9	7	106843265	107018037	106930651	174772
RP11-516H16	7	106883096	107044176	106963636	161080
RP11-149B12	7	106977329	107168961	107073145	191632
RP11-443I10	7	107091051	107287631	107189341	196580
RP11-698M9	7	107153601	107347972	107250786.5	194371
RP11-708I9	7	107269200	107432552	107350876	163352
RP11-649H20	7	107281569	107471191	107376380	189622
RP11-590J14	7	107380601	107605147	107492874	224546
CTD-2182E11	7	107634902	107720250	107677576	85348
RP11-139J13	7	107706571	107838229	107772400	131658
RP11-18H15	7	107779927	107931476	107855701.5	151549
RP11-152F20	7	107846683	108007125	107926904	160442
RP11-206A4	7	107931477	108068358	107999917.5	136881
RP11-372G6	7	108060421	108240355	108150388	179934
RP11-393L14	7	108161412	108338244	108249828	176832

RP11-461P5	7	108189573	108370997	108280285	181424
RP11-698J23	7	108350169	108517595	108433882	167426
RP11-21G9	7	108400570	108575544	108488057	174974
RP11-90N13	7	108530568	108684654	108607611	154086
RP11-325I9	7	108643780	108831936	108737858	188156
RP11-328M14	7	108820205	109013485	108916845	193280
RP11-718D16	7	108955016	109121654	109038335	166638
RP11-515I13	7	109112115	109306191	109209153	194076
RP11-347P13	7	109179037	109385816	109282426.5	206779
RP11-110B16	7	109277103	109446394	109361748.5	169291
RP11-331K20	7	109393071	109581136	109487103.5	188065
RP11-64F12	7	109447938	109609486	109528712	161548
RP11-762D9	7	109546885	109700091	109623488	153206
RP11-639F12	7	109697013	109844116	109770564.5	147103
RP11-647L12	7	109813087	109961656	109887371.5	148569
RP11-312H11	7	109972971	110126699	110049835	153728
RP11-495O8	7	110057541	110233163	110145352	175622
RP11-452K21	7	110202859	110381728	110292293.5	178869
CTD-2105K8	7	110286481	110450495	110368488	164014
RP11-645L13	7	110438906	110612834	110525870	173928
RP11-544C1	7	110584343	110770763	110677553	186420
RP11-86H8	7	110743496	110904224	110823860	160728
RP11-80H21	7	110818942	110975163	110897052.5	156221
RP11-124K17	7	110911401	111107805	111009603	196404
RP11-260P7	7	110992649	111176054	111084351.5	183405
RP11-382F18	7	111103847	111282168	111193007.5	178321
RP11-92J13	7	111233618	111401092	111317355	167474

RP11-153L5	7	111381724	111555750	111468737	174026
RP11-315F18	7	111477314	111657880	111567597	180566
CTD-2252G20	7	111594788	111707124	111650956	112336
RP11-397O20	7	111662670	111826800	111744735	164130
RP11-674F20	7	111753987	111945379	111849683	191392
RP11-184K23	7	111823857	111982641	111903249	158784
RP11-259H24	7	112084438	112269456	112176947	185018
RP11-467K21	7	112178105	112362579	112270342	184474
RP11-638L12	7	112276571	112444564	112360567.5	167993
RP11-335D17	7	112316394	112538487	112427440.5	222093
RP11-698G17	7	112415340	112602267	112508803.5	186927
RP11-703P11	7	112530662	112684795	112607728.5	154133
RP11-786A20	7	112652900	112835444	112744172	182544
RP11-697C1	7	112782654	112948201	112865427.5	165547
RP11-158E8	7	112849253	113037563	112943408	188310
RP11-687A7	7	113037268	113224986	113131127	187718
RP11-43J7	7	113055027	113211379	113133203	156352
RP11-658L17	7	113290825	113405020	113347922.5	114195
RP11-433L10	7	113296351	113457471	113376911	161120
CTD-2023N18	7	113377670	113525513	113451591.5	147843
RP11-160G23	7	113445564	113619447	113532505.5	173883
RP11-53I2	7	113525514	113725786	113625650	200272
RP11-274E22	7	113661493	113812671	113737082	151178
RP11-664F19	7	113813391	114004005	113908698	190614
RP11-663I18	7	113925921	114091366	114008643.5	165445
CTD-2340L2	7	114002799	114106349	114054574	103550
RP11-78C11	7	114102146	114261695	114181920.5	159549

RP11-695F7	7	114157882	114340254	114249068	182372
RP11-488K2	7	114301749	114505070	114403409.5	203321
RP11-103A1	7	114409017	114573150	114491083.5	164133
RP11-17G24	7	114564920	114729171	114647045.5	164251
RP11-192B3	7	114680458	114834129	114757293.5	153671
RP11-164A15	7	114782264	114945318	114863791	163054
RP11-458K10	7	114911858	115128416	115020137	216558
RP11-22K23	7	115048848	115198394	115123621	149546
RP11-135K23	7	115121645	115268164	115194904.5	146519
RP11-242J21	7	115209498	115393576	115301537	184078
RP11-760I10	7	115347661	115546310	115446985.5	198649
RP11-299N2	7	115491977	115652311	115572144	160334
RP11-413C23	7	115527476	115699897	115613686.5	172421
RP11-146P12	7	115573634	115751056	115662345	177422
RP11-691L23	7	115573634	115795471	115684552.5	221837
RP11-367L24	7	115650414	115795471	115722942.5	145057
RP11-730H9	7	115738660	115915208	115826934	176548
RP11-153D24	7	115833131	115996125	115914628	162994
RP11-95I20	7	115892918	116062671	115977794.5	169753
RP11-564A14	7	116008685	116243417	116126051	234732
RP11-706D4	7	116202831	116372147	116287489	169316
CTD-2163N8	7	116270185	116392319	116331252	122134
RP11-326M1	7	116343485	116545962	116444723.5	202477
CTD-2125N8	7	116435263	116567597	116501430	132334
RP11-644B4	7	116551115	116741704	116646409.5	190589
RP11-182C8	7	116723712	116877465	116800588.5	153753
RP11-514N9	7	116773499	116967352	116870425.5	193853

RP11-702P18	7	116934463	117153925	117044194	219462
RP11-69A8	7	117035127	117189569	117112348	154442
RP11-99N14	7	117175814	117334302	117255058	158488
RP11-797I7	7	117287504	117459764	117373634	172260
RP11-318O5	7	117449808	117606964	117528386	157156
RP11-110G3	7	117487407	117635500	117561453.5	148093
CTD-2002E16	7	117603751	117737780	117670765.5	134029
RP11-417K19	7	117716364	117894543	117805453.5	178179
RP11-808J6	7	117894544	118095729	117995136.5	201185
RP11-631C5	7	117946858	118117624	118032241	170766
RP11-747E15	7	117999639	118205979	118102809	206340
RP11-533K11	7	118137291	118333313	118235302	196022
RP11-304F13	7	118351102	118507350	118429226	156248
RP11-105B19	7	118436021	118613318	118524669.5	177297
RP11-418E22	7	118478492	118660097	118569294.5	181605
RP11-398D9	7	118633456	118794921	118714188.5	161465
RP11-447A2	7	118660098	118876217	118768157.5	216119
CTD-2009D17	7	118807484	118960176	118883830	152692
RP11-722I21	7	118834912	119022260	118928586	187348
RP11-642D23	7	118876218	119078218	118977218	202000
RP11-328J2	7	118950995	119115211	119033103	164216
RP11-542G3	7	119045589	119250062	119147825.5	204473
RP11-227H8	7	119179120	119370570	119274845	191450
RP11-317F8	7	119277466	119480228	119378847	202762
RP11-2C10	7	119508230	119671077	119589653.5	162847
RP11-683J21	7	119670108	119853467	119761787.5	183359
CTD-2006F7	7	119728155	119850608	119789381.5	122453

RP11-367A17	7	119738869	119911447	119825158	172578
RP11-693C16	7	119876610	120089138	119982874	212528
RP11-291E13	7	120020363	120180087	120100225	159724
RP11-506L11	7	120189575	120398461	120294018	208886
RP11-69L14	7	120343110	120529807	120436458.5	186697
RP11-23L15	7	120428649	120571228	120499938.5	142579
RP11-583P4	7	120503933	120659306	120581619.5	155373
RP11-636H22	7	120645216	120849013	120747114.5	203797
RP11-651N9	7	120834002	120991323	120912662.5	157321
RP11-716D15	7	120902171	121089051	120995611	186880
RP11-217B9	7	120951567	121119054	121035310.5	167487
RP11-269L1	7	121005972	121176604	121091288	170632
RP11-407M2	7	121044165	121238797	121141481	194632
RP11-384A20	7	121121491	121279437	121200464	157946
RP11-367M11	7	121097893	121337847	121217870	239954
RP11-179C1	7	121295532	121470253	121382892.5	174721
RP11-95F4	7	121397679	121554961	121476320	157282
RP11-12H16	7	121483708	121654613	121569160.5	170905
RP11-197A20	7	121604983	121787109	121696046	182126
RP11-350G10	7	121738662	121919382	121829022	180720
RP11-770I13	7	121790162	121971603	121880882.5	181441
RP11-805P19	7	121895552	122088724	121992138	193172
RP11-633J6	7	122023294	122212582	122117938	189288
RP11-61D3	7	122192244	122345539	122268891.5	153295
RP11-605K13	7	122297358	122480789	122389073.5	183431
RP11-588I9	7	122473376	122666511	122569943.5	193135
RP11-15L19	7	122509495	122694782	122602138.5	185287

RP11-674K13	7	122540790	122704085	122622437.5	163295
RP11-598C13	7	122681563	122853927	122767745	172364
RP11-746L19	7	122849569	123052370	122950969.5	202801
RP11-143J10	7	122924300	123080213	123002256.5	155913
RP11-601G11	7	123057049	123202774	123129911.5	145725
RP11-592J18	7	123138761	123318372	123228566.5	179611
RP11-345L15	7	123169643	123384384	123277013.5	214741
RP11-805E14	7	123397083	123591888	123494485.5	194805
RP11-618G22	7	123551327	123683137	123617232	131810
RP11-726A19	7	123647606	123855205	123751405.5	207599
RP11-379L24	7	123766218	123941478	123853848	175260
RP11-324E14	7	123865174	124025089	123945131.5	159915
RP11-661D8	7	123984966	124164118	124074542	179152
RP11-550C15	7	124069636	124227519	124148577.5	157883
RP11-415O10	7	124203910	124357946	124280928	154036
RP11-3B12	7	124307960	124484070	124396015	176110
RP11-272G19	7	124407397	124583300	124495348.5	175903
RP11-420H19	7	124485201	124668576	124576888.5	183375
RP11-119C8	7	124568858	124707041	124637949.5	138183
RP11-818I12	7	124562285	124750079	124656182	187794
RP11-807H17	7	124638725	124801647	124720186	162922
RP11-732N22	7	124640207	124847850	124744028.5	207643
RP11-210B22	7	124793577	124938633	124866105	145056
RP11-519O11	7	124948922	125127005	125037963.5	178083
RP11-610F5	7	125047576	125192091	125119833.5	144515
RP11-398N23	7	125150998	125351170	125251084	200172
RP11-791P8	7	125369486	125529388	125449437	159902

RP11-346L18	7	125465104	125629770	125547437	164666
RP11-510O20	7	125577084	125770941	125674012.5	193857
RP11-105E3	7	125666080	125834115	125750097.5	168035
RP11-432H11	7	125775702	125957492	125866597	181790
RP11-475H14	7	125937229	126119121	126028175	181892
CTD-2100M22	7	126070577	126201513	126136045	130936
RP11-16K22	7	126120350	126265569	126192959.5	145219
RP11-309K22	7	126120350	126265569	126192959.5	145219
RP11-290P11	7	126129088	126292020	126210554	162932
RP11-641M11	7	126187314	126368364	126277839	181050
RP11-715K19	7	126238527	126419176	126328851.5	180649
RP11-329O5	7	126388390	126541276	126464833	152886
RP11-562D24	7	126512334	126701134	126606734	188800
RP11-619D12	7	126600073	126797107	126698590	197034
RP11-568I11	7	126737158	126951836	126844497	214678
RP11-531B18	7	126883462	127104347	126993904.5	220885
RP11-348K6	7	127054946	127264956	127159951	210010
RP11-809F9	7	127205070	127371393	127288231.5	166323
RP11-475K8	7	127285757	127458115	127371936	172358
RP11-640G20	7	127416566	127619167	127517866.5	202601
RP11-282F23	7	127455621	127619168	127537394.5	163547
RP11-155G14	7	127564262	127729340	127646801	165078
RP11-636E12	7	127564296	127741861	127653078.5	177565
RP11-79D5	7	127655629	127814781	127735205	159152
RP11-683N8	7	127701088	127904595	127802841.5	203507
RP11-338L6	7	127774677	127950852	127862764.5	176175
RP11-526K5	7	127830025	128033552	127931788.5	203527

RP11-66F23	7	127950853	128145770	128048311.5	194917
RP11-638M14	7	128006656	128189702	128098179	183046
CTD-2036B8	7	128187799	128349949	128268874	162150
RP11-198N5	7	128310207	128468642	128389424.5	158435
RP11-396H10	7	128339444	128562653	128451048.5	223209
RP11-69C1	7	128511843	128667708	128589775.5	155865
RP11-126N23	7	128656991	128834751	128745871	177760
RP11-448A19	7	128787761	128997928	128892844.5	210167
CTD-2107H2	7	128979960	129157258	129068609	177298
CTD-2353O2	7	129085218	129216171	129150694.5	130953
RP11-643O2	7	129119357	129296428	129207892.5	177071
RP11-306G20	7	129167640	129352442	129260041	184802
RP11-710I21	7	129338473	129518049	129428261	179576
RP11-190G13	7	129413444	129583846	129498645	170402
RP11-2E11	7	129578386	129745580	129661983	167194
RP13-554J11	7	129652384	129744784	129698584	92400
RP11-584H16	7	129702778	129798422	129750600	95644
RP11-537A1	7	129745642	129869408	129807525	123766
RP13-750I6	7	129746887	129889663	129818275	142776
CTD-2214L23	7	129860793	130003621	129932207	142828
RP11-36B6	7	129882101	130056512	129969306.5	174411
RP11-161B24	7	130010308	130168946	130089627	158638
RP11-449I7	7	130045387	130217438	130131412.5	172051
RP11-288L5	7	130145565	130336488	130241026.5	190923
RP11-375L14	7	130266296	130434915	130350605.5	168619
RP11-420J2	7	130388405	130564845	130476625	176440
RP11-692A14	7	130496055	130632752	130564403.5	136697

RP11-14M12	7	130488687	130643566	130566126.5	154879
RP11-145E16	7	130597244	130756297	130676770.5	159053
RP11-180C16	7	130632753	130787253	130710003	154500
RP13-668E23	7	130680558	130841957	130761257.5	161399
CTD-2063A19	7	130841956	130898507	130870231.5	56551
CTD-2007A16	7	130841962	130973584	130907773	131622
RP11-193I17	7	130931500	131118684	131025092	187184
RP11-19B3	7	131030855	131194206	131112530.5	163351
RP11-805M23	7	131166329	131379118	131272723.5	212789
RP11-195M5	7	131252256	131439080	131345668	186824
RP11-348A15	7	131374719	131525870	131450294.5	151151
RP11-24E10	7	131484326	131662166	131573246	177840
RP11-44F19	7	131566704	131737474	131652089	170770
RP11-540B11	7	131603386	131788183	131695784.5	184797
CTD-2234G19	7	131697489	131800637	131749063	103148
RP11-29A12	7	131702292	131861777	131782034.5	159485
RP11-545C1	7	131861778	132061711	131961744.5	199933
CTD-2225B7	7	131967961	132072125	132020043	104164
RP11-734G16	7	132041731	132216707	132129219	174976
RP11-67O6	7	132155853	132328525	132242189	172672
RP11-105M19	7	132274731	132439011	132356871	164280
RP11-435P4	7	132307829	132496405	132402117	188576
CTD-2265P2	7	132430629	132544364	132487496.5	113735
RP11-104L14	7	132499530	132687690	132593610	188160
RP11-25J16	7	132607054	132795898	132701476	188844
RP11-108H23	7	132752166	132919188	132835677	167022
RP11-118J20	7	132856117	133077899	132967008	221782

RP11-237E23	7	132901984	133053289	132977636.5	151305
CTD-2019H7	7	133001258	133174930	133088094	173672
RP11-641M23	7	133110274	133314244	133212259	203970
RP11-4G15	7	133213460	133359005	133286232.5	145545
RP11-16K7	7	133328686	133493650	133411168	164964
RP11-98D12	7	133357500	133529727	133443613.5	172227
RP11-651P9	7	133533353	133701682	133617517.5	168329
RP11-599C9	7	133567032	133761936	133664484	194904
RP11-69H23	7	133632921	133791741	133712331	158820
RP11-73K10	7	133719760	133885847	133802803.5	166087
RP11-792L21	7	133734311	133920574	133827442.5	186263
RP13-728L15	7	133847795	133993959	133920877	146164
RP11-221G19	7	133893049	134036379	133964714	143330
RP11-615F13	7	133922665	134127976	134025320.5	205311
RP11-248K17	7	133965367	134136822	134051094.5	171455
RP11-597L4	7	134074495	134248828	134161661.5	174333
RP11-814N17	7	134235619	134446899	134341259	211280
RP11-260N14	7	134295876	134456240	134376058	160364
RP11-161C4	7	134364499	134546349	134455424	181850
RP11-166D1	7	134511355	134680583	134595969	169228
RP11-140I14	7	134546627	134697486	134622056.5	150859
RP11-706J21	7	134622360	134783209	134702784.5	160849
RP11-649J7	7	134640000	134799096	134719548	159096
RP11-14I1	7	134733289	134896863	134815076	163574
RP11-577P14	7	134826046	134999449	134912747.5	173403
RP11-663H22	7	134931508	135119715	135025611.5	188207
RP11-24I23	7	135046341	135198644	135122492.5	152303

RP11-473G8	7	135125392	135308607	135216999.5	183215
RP11-277F10	7	135295894	135461727	135378810.5	165833
RP11-116N1	7	135314168	135484458	135399313	170290
RP11-607B22	7	135442680	135637665	135540172.5	194985
RP11-811K22	7	135589552	135786273	135687912.5	196721
RP11-733N14	7	135631263	135806424	135718843.5	175161
RP11-324O17	7	135676027	135895729	135785878	219702
RP11-798E5	7	135822074	136037994	135930034	215920
RP11-661I6	7	135887746	136074343	135981044.5	186597
RP11-486O1	7	135907641	136099418	136003529.5	191777
RP11-346J1	7	136040699	136212996	136126847.5	172297
RP11-322H10	7	136075865	136244939	136160402	169074
RP11-708B14	7	136087221	136265690	136176455.5	178469
RP11-294C9	7	136205587	136373210	136289398.5	167623
RP11-107J16	7	136288920	136463723	136376321.5	174803
RP11-777L18	7	136439969	136612770	136526369.5	172801
RP11-805B10	7	136515507	136711418	136613462.5	195911
RP11-19L13	7	136667159	136821404	136744281.5	154245
RP11-115N3	7	136761627	136914342	136837984.5	152715
RP11-360I15	7	136770095	136973982	136872038.5	203887
RP11-390H20	7	136833582	137011020	136922301	177438
RP11-29B3	7	136957814	137110063	137033938.5	152249
CTD-2002C18	7	137093304	137207181	137150242.5	113877
RP11-83I11	7	137074710	137281029	137177869.5	206319
RP11-20M11	7	137168702	137322726	137245714	154024
RP11-183I20	7	137253723	137392056	137322889.5	138333
RP11-175F11	7	137341566	137490372	137415969	148806

RP11-289F17	7	137365966	137542971	137454468.5	177005
RP11-512K22	7	137419716	137631607	137525661.5	211891
RP11-663A4	7	137535434	137722903	137629168.5	187469
RP11-559C14	7	137708060	137885149	137796604.5	177089
RP11-355D18	7	137927743	138131368	138029555.5	203625
RP11-737E2	7	138095648	138286187	138190917.5	190539
RP11-600E3	7	138153618	138329432	138241525	175814
RP11-787G19	7	138332910	138507966	138420438	175056
RP11-373E1	7	138318449	138533002	138425725.5	214553
RP11-634H22	7	138436289	138614761	138525525	178472
RP11-413B4	7	138537272	138713176	138625224	175904
RP11-1172G19	7	138533003	138728029	138630516	195026
RP13-912P9	7	138634783	138782279	138708531	147496
RP11-202L12	7	138640547	138803809	138722178	163262
RP11-693A14	7	138651930	138803809	138727869.5	151879
RP13-820B19	7	138886360	139026544	138956452	140184
RP11-236H5	7	138936589	139090239	139013414	153650
RP11-265A15	7	138937718	139105508	139021613	167790
CTD-2105E24	7	138967429	139126997	139047213	159568
RP11-65A18	7	138985502	139147510	139066506	162008
RP11-758F21	7	139020010	139213908	139116959	193898
RP11-101M4	7	139093460	139263870	139178665	170410
RP11-812N19	7	139245520	139415953	139330736.5	170433
RP11-561D8	7	139331785	139521722	139426753.5	189937
RP11-795E24	7	139479689	139617245	139548467	137556
RP11-723C11	7	139589728	139760648	139675188	170920
RP11-788O6	7	139694523	139880060	139787291.5	185537

RP11-661B8	7	139703996	139872708	139788352	168712
RP11-304K20	7	139845406	140055499	139950452.5	210093
RP11-416H18	7	139900744	140090590	139995667	189846
RP11-447A24	7	140066850	140232631	140149740.5	165781
RP11-793D16	7	140054475	140251563	140153019	197088
RP11-186O24	7	140205233	140367684	140286458.5	162451
RP11-657G24	7	140255824	140451548	140353686	195724
RP11-313O20	7	140360091	140527038	140443564.5	166947
RP11-471G1	7	140462195	140641230	140551712.5	179035
RP11-118A19	7	140511823	140653667	140582745	141844
RP11-717H20	7	140617638	140774510	140696074	156872
RP11-155M10	7	140700133	140863676	140781904.5	163543
RP11-120E14	7	140812955	140961603	140887279	148648
RP11-693F16	7	140851580	141019431	140935505.5	167851
RP11-64M15	7	140983746	141135677	141059711.5	151931
RP11-17D6	7	141000038	141163390	141081714	163352
RP11-1353A4	7	141000038	141194658	141097348	194620
RP13-581E15	7	141085851	141248158	141167004.5	162307
RP11-10L5	7	141289326	141430453	141359889.5	141127
RP11-786A19	7	141367324	141547420	141457372	180096
RP11-714J22	7	141429528	141610636	141520082	181108
RP11-143G2	7	141536842	141691318	141614080	154476
RP11-203I13	7	141610138	141782205	141696171.5	172067
RP11-325O4	7	141638863	141840748	141739805.5	201885
RP11-453N21	7	141750162	141919082	141834622	168920
RP11-114B6	7	141813913	141973680	141893796.5	159767
CTD-2087C12	7	141887557	142030287	141958922	142730

RP11-114L10	7	141931613	142123518	142027565.5	191905
RP11-368I15	7	142045199	142239842	142142520.5	194643
RP11-78G15	7	142067625	142240972	142154298.5	173347
RP11-18B22	7	142252023	142432885	142342454	180862
RP11-556I13	7	142402113	142561955	142482034	159842
RP11-202L22	7	142516580	142669655	142593117.5	153075
RP11-811J9	7	142598468	142802162	142700315	203694
RP11-119F21	7	142704281	142763109	142733695	58828
RP11-165B5	7	142740171	142769533	142754852	29362
RP11-407F8	7	142967914	143186365	143077139.5	218451
RP11-137A1	7	143095419	143267019	143181219	171600
RP11-703N5	7	143182512	143354063	143268287.5	171551
RP11-634O11	7	143317949	143356258	143337103.5	38309
RP11-466J6	7	143317195	143511372	143414283.5	194177
RP11-714J20	7	143471913	143646353	143559133	174440
RP11-340G20	7	143652126	143846769	143749447.5	194643
RP11-136L16	7	143675486	143835792	143755639	160306
RP11-353H9	7	143806339	143954406	143880372.5	148067
RP11-466N22	7	143863302	144056081	143959691.5	192779
RP11-621J17	7	144003818	144192912	144098365	189094
RP11-747D17	7	144110019	144269719	144189869	159700
RP11-409M7	7	144165741	144322766	144244253.5	157025
RP11-37M18	7	144267725	144436499	144352112	168774
RP11-177L17	7	144289468	144441284	144365376	151816
RP11-597H23	7	144312586	144497195	144404890.5	184609
RP11-185G4	7	144381491	144529157	144455324	147666
RP11-252P1	7	144492756	144644877	144568816.5	152121

RP11-679O8	7	144534763	144701553	144618158	166790
RP11-158G24	7	144633984	144785573	144709778.5	151589
RP11-599M4	7	144701554	144863493	144782523.5	161939
RP11-266G14	7	144777237	144933173	144855205	155936
RP11-204B17	7	144837454	144994137	144915795.5	156683
RP11-107N5	7	145047033	145207126	145127079.5	160093
RP11-711K12	7	145126903	145295731	145211317	168828
RP11-48E17	7	145178445	145322952	145250698.5	144507
RP11-593N14	7	145248588	145439519	145344053.5	190931
RP11-178F1	7	145412559	145588197	145500378	175638
RP11-6J19	7	145530487	145678627	145604557	148140
RP11-328C18	7	145590883	145754644	145672763.5	163761
RP11-141D5	7	145721003	145894012	145807507.5	173009
RP11-161H9	7	145804753	145979323	145892038	174570
RP11-739B3	7	146076031	146277183	146176607	201152
RP11-620C13	7	146198804	146395379	146297091.5	196575
RP11-643A21	7	146381733	146533429	146457581	151696
RP11-699J3	7	146487826	146647058	146567442	159232
RP11-162A9	7	146593600	146755135	146674367.5	161535
RP11-773G19	7	146724436	146880186	146802311	155750
RP11-284J17	7	146833262	147024350	146928806	191088
RP11-564O4	7	146958966	147139262	147049114	180296
RP11-99G19	7	147107321	147284112	147195716.5	176791
RP11-79K23	7	147191958	147343032	147267495	151074
CTD-2025B7	7	147323173	147488874	147406023.5	165701
RP11-89P11	7	147485335	147638644	147561989.5	153309
RP11-765I1	7	147532537	147724448	147628492.5	191911

RP11-323L17	7	147622223	147844328	147733275.5	222105
RP11-801N1	7	147808606	148034588	147921597	225982
CTD-2415L21	7	147928119	148125855	148026987	197736
RP11-185C24	7	147944912	148122806	148033859	177894
RP11-794E21	7	148300593	148469198	148384895.5	168605
RP11-279B9	7	148375225	148520704	148447964.5	145479
RP11-603M10	7	148461442	148664636	148563039	203194
RP11-749O22	7	148499421	148690806	148595113.5	191385
RP11-478H20	7	148761390	148943299	148852344.5	181909
RP11-263O17	7	148862483	149037741	148950112	175258
CTD-2140I24	7	148984195	149122596	149053395.5	138401
RP11-474L2	7	149018936	149117281	149068108.5	98345
RP11-586O9	7	148998753	149157307	149078030	158554
RP11-318D10	7	149011517	149157307	149084412	145790
RP11-728K20	7	149020484	149169295	149094889.5	148811
RP11-473L10	7	149106042	149247375	149176708.5	141333
RP11-544F18	7	149146769	149368311	149257540	221542
RP11-676P18	7	149340017	149499017	149419517	159000
RP11-620K21	7	149417269	149605924	149511596.5	188655
RP11-7P1	7	149638777	149808332	149723554.5	169555
RP11-64C23	7	149763561	149941148	149852354.5	177587
RP11-126M15	7	149807794	150002372	149905083	194578
RP11-684M7	7	149924997	150090017	150007507	165020
RP11-445P2	7	149962182	150275694	150118938	313512
RP11-119F18	7	150172852	150350523	150261687.5	177671
RP11-552G14	7	150219969	150440807	150330388	220838
RP11-717G15	7	150297453	150468061	150382757	170608

RP11-428M3	7	150360689	150605358	150483023.5	244669
RP11-193C16	7	150468062	150675792	150571927	207730
RP11-60D3	7	150586755	150756902	150671828.5	170147
RP11-113A18	7	150709360	150875049	150792204.5	165689
RP11-639C15	7	150803631	150979651	150891641	176020
RP11-381K9	7	150910300	151092509	151001404.5	182209
RP11-796I2	7	150959344	151131820	151045582	172476
RP11-146E20	7	151134086	151294605	151214345.5	160519
RP11-137O21	7	151211236	151395090	151303163	183854
RP11-343L6	7	151253666	151420996	151337331	167330
RP11-208G20	7	151365120	151531931	151448525.5	166811
RP13-507K23	7	151370060	151540322	151455191	170262
RP11-658C6	7	151482865	151649593	151566229	166728
RP11-170E21	7	151593007	151792433	151692720	199426
RP11-1211F5	7	151593007	151805654	151699330.5	212647
RP11-31J9	7	151753465	151895564	151824514.5	142099
RP11-364L19	7	151753465	151900946	151827205.5	147481
RP11-452J20	7	151744858	151951495	151848176.5	206637
RP11-753N9	7	151791192	152030326	151910759	239134
RP11-1137J16	7	151953981	152115488	152034734.5	161507
RP11-399E23	7	152057131	152236516	152146823.5	179385
RP11-349M19	7	152200048	152401585	152300816.5	201537
RP11-715L6	7	152327290	152513240	152420265	185950
RP11-26I6	7	152438821	152598400	152518610.5	159579
RP11-103E18	7	152480190	152641769	152560979.5	161579
RP11-138K3	7	152574934	152741364	152658149	166430
RP11-794I22	7	152617487	152836204	152726845.5	218717

RP11-354C19	7	152783136	152936999	152860067.5	153863
RP11-737G12	7	152783236	153002753	152892994.5	219517
RP11-135F23	7	152872498	153054474	152963486	181976
RP11-732N20	7	153035961	153190158	153113059.5	154197
RP11-30J12	7	153036456	153195879	153116167.5	159423
RP11-564B10	7	153161824	153322470	153242147	160646
RP13-620M21	7	153220028	153397424	153308726	177396
RP13-862B20	7	153379129	153511918	153445523.5	132789
RP13-500D13	7	153402959	153549213	153476086	146254
RP11-389I18	7	153418445	153586933	153502689	168488
RP11-79K9	7	153441322	153586968	153514145	145646
RP11-641O17	7	153437393	153619711	153528552	182318
RP11-446O21	7	153437393	153626868	153532130.5	189475
RP11-422E4	7	153511919	153706971	153609445	195052
RP11-232A2	7	153816356	153965944	153891150	149588
RP11-476H24	7	153933858	154141084	154037471	207226
RP11-51M20	7	154155007	154319485	154237246	164478
RP11-448D3	7	154155214	154356493	154255853.5	201279
RP11-799A21	7	154155214	154376481	154265847.5	221267
RP11-295N1	7	154208705	154415465	154312085	206760
RP11-317A13	7	154265817	154458618	154362217.5	192801
RP11-279O22	7	154298853	154449825	154374339	150972
RP11-1430O6	7	154341891	154504352	154423121.5	162461
RP13-553J3	7	154366740	154483393	154425066.5	116653
RP13-559G12	7	154396881	154482253	154439567	85372
CTD-2014I17	7	154651263	154792424	154721843.5	141161
RP11-60D5	7	154729457	154893855	154811656	164398

RP11-61K21	7	154729921	154901700	154815810.5	171779
RP11-265E13	7	154761099	154935115	154848107	174016
RP11-69O3	7	155000392	155154956	155077674	154564
RP11-451N23	7	155091298	155274533	155182915.5	183235
RP11-134M1	7	155248338	155411612	155329975	163274
RP11-264P5	7	155371524	155542400	155456962	170876
RP11-459H7	7	155514709	155739542	155627125.5	224833
RP11-691F21	7	155658864	155839469	155749166.5	180605
RP11-728F9	7	155846192	156008086	155927139	161894
RP11-133G9	7	155881752	156086853	155984302.5	205101
RP11-776L17	7	155922117	156121832	156021974.5	199715
CTD-2008L1	7	155979854	156120116	156049985	140262
RP11-693K11	7	156058580	156225616	156142098	167036
RP11-798G13	7	156203928	156352462	156278195	148534
RP11-333G1	7	156256187	156451285	156353736	195098
RP11-51L24	7	156336152	156484531	156410341.5	148379
RP13-508B4	7	156451286	156610548	156530917	159262
RP11-80N17	7	156587049	156681068	156634058.5	94019
RP11-527G9	7	156587049	156748116	156667582.5	161067
RP11-172F22	7	156568073	156782288	156675180.5	214215
RP11-637M7	7	156660000	156877064	156768532	217064
RP11-732K4	7	156791707	156979406	156885556.5	187699
RP11-666K15	7	156882549	157089996	156986272.5	207447
RP11-815G4	7	156999684	157238725	157119204.5	239041
RP11-50D7	7	157105012	157315334	157210173	210322
RP11-452C13	7	157103817	157328557	157216187	224740
CTD-2041J20	7	157203152	157325773	157264462.5	122621

RP13-965C1	7	157203152	157350018	157276585	146866
RP11-599B11	7	157422158	157552466	157487312	130308
RP11-711A5	7	157430294	157585876	157508085	155582
RP11-683I4	7	157507520	157585876	157546698	78356
RP11-434G15	7	157485044	157663102	157574073	178058
RP11-744K13	7	157575793	157760598	157668195.5	184805
RP13-967I21	7	157760858	157800439	157780648.5	39581
RP13-613J3	7	157763325	157865942	157814633.5	102617
RP11-582J15	7	157825922	157983696	157904809	157774
RP11-106C11	7	157933821	158104642	158019231.5	170821
RP11-240J1	7	158077275	158252830	158165052.5	175555
RP11-664B5	7	158211184	158402685	158306934.5	191501
CTD-2031M22	7	158343036	158377124	158360080	34088
RP11-129F1	7	158343036	158493889	158418462.5	150853
RP11-133J16	7	158343435	158496543	158419989	153108
RP11-83D3	7	158413174	158594317	158503745.5	181143
RP13-1052O2	7	158466998	158612807	158539902.5	145809
CTD-2319F20	7	158498002	158624831	158561416.5	126829
RP11-455I9	8	119194110	119373058	119283584	178948
RP11-455I9	8	119194110	119373058	119283584	178948
RP11-167H17	11	28573327	28607450	28590388.5	34123
RP11-439P15	12	13717255	13919901	13818578	202646
RP13-839K18	12	39645817	39775948	39710882.5	130131
RP11-41P11	14	62953734	62995830	62974782	42096
RP11-611C24	16	7700099	7794509	7747304	94410
RP11-297H14	16	32404379	32439725	32422052	35346
RP11-20L17	19	32534541	32639571	32587056	105030

CTD-2276I11	-	0	0	0	0
RP11-252I21	-	0	0	0	0
RP11-253J2	-	0	0	0	0
RP11-256G7	-	0	0	0	0
RP11-274A2	-	0	0	0	0
RP11-435D24	-	0	0	0	0
RP11-470I21	-	0	0	0	0
RP11-522C18	-	0	0	0	0
RP11-574E17	-	0	0	0	0
RP11-753N11	-	0	0	0	0

A.3 Drosophila background hybridisation controls

Eight BAC clones from *Drosophila melanogaster* were selected as background hybridisation controls. These clones were purchased from the BACPAC resource centre at Oakland Children's Hospital, Oakland, CA, USA. Clones were hybridised to normal human chromosomes by Fluroescnce in-situ hybridisation (FISH) and found not to hybridise to human chromosomes.

Clone ID	Drosophila Chromosome mapping	FISH result against human
RP98-10P9	3L-66E4	No hybridisation
RP98-5L4	X	No hybridisation
RP98-38L1	X	No hybridisation
RP98-3G6	3L	No hybridisation
RP98-33N24	X	No hybridisation
RP98-44K7	3L-74C1	No hybridisation
RP98-9C21	3L-9C21	No hybridisation
RP98-7P15	X	No hybridisation